

Behavior of Corrugated Metal Panels for use as Storm Shutters

**By
Alexander Borges Irizarry**

**Dissertation submitted in partial fulfillment of the requirements for the degree
of**

**DOCTOR OF PHILOSOPHY
in
CIVIL ENGINEERING**

**UNIVERSITY OF PUERTO RICO
MAYAGÜEZ CAMPUS
2009**

Approved by:

**Ricardo R. López, Ph.D.
President, Graduate Committee**

Date

**Luis A. Godoy, Ph.D.
Member, Graduate Committee**

Date

**Raúl E. Zapata López, Ph.D.
Member, Graduate Committee**

Date

**Alí Saffar, Ph.D.
Member, Graduate Committee**

Date

**Luis A. Montejo, Ph.D.
Representative of Graduate Studies**

Date

**Ismael Pagán Trinidad, MSCE.
Chairman of the Department**

Date

Abstract

This investigation presents a study of the nonlinear dynamics of thin-walled folded plate structures under the localized impact of a rigid object. The research emerges in the context of the structural design and assessment of storm shutters used to protect windows and doors during hurricanes. The development of a testing facility for storm shutter panels and test results are introduced as a fundamental source of information for the proposed analytical approach. Two impact tests were carried out to validate the functionality of the testing facility. The tests consisted in the evaluation of two specimens subjected to the impact of a 2'x 4" piece of wood. For both tests, the impacted panels suffered a permanent deformation and a failure at the lower support was achieved when some of the clips or connectors were lost.

Numerical analyses were carried out using the general purpose finite element code ABAQUS. Models simulated the interaction of contact of windborne debris traveling at a specific velocity against the shutters. As a result, a nonlinear dynamics response was computed leading to plastic deformations of the shutters. The obtained permanent deformation values were compared with the ones measured from the specimens evaluated in the testing facility.

Parameters like geometrical configuration of panels, materials, boundary conditions, impact location and missile velocity were evaluated to determine the most detrimental behavior of the storm shutter assembly by means of parametric studies. A nonlinear behavior was obtained for all the studied parameters. For missile velocities greater than 25 mph, the

maximum displacement of the impacted panel exceeded 3 inches. Therefore, elements to be protected by storm shutter panels can be damaged due to the contact produced by the impacted panel. The results showed that the edge rotation of the panels was reduced when different boundary conditions and a larger number of panels were used in the assembly.

Three zones of maximum stresses were identified to occur in the impact panel. The maximum stresses were generated at each zone following a sequence of occurrence which varied according to the rigidity of the system. Failure of the material was not achieved in any case.

Resumen

Esta investigación presenta el estudio del comportamiento no lineal en placas delgadas sometidas a cargas de impacto causados por objetos de mayor rigidez. La misma surge como contexto del diseño y análisis de paneles de tormenteras utilizados como elementos de protección de puertas y ventanas durante el impacto de huracanes. Se desarrollaron facilidades para la realización de pruebas en paneles de tormenteras. Los resultados de las pruebas experimentales fueron utilizados como base para el desarrollo de estudios analíticos. Dos pruebas de impacto fueron realizadas con el propósito de validar la funcionalidad de las facilidades de prueba. Las pruebas consistieron en la evaluación de dos muestras sometidas al impacto de un pedazo de madera de dimensiones 2" x 4". En ambas pruebas, los paneles impactados resultaron con deformaciones permanentes. Una falla del soporte inferior del sistema fue registrada cuando varios conectores se desprendieron del sistema.

Simulaciones que recrean el impacto de proyectiles viajando a diferentes velocidades contra el sistema de tormenteras fueron realizadas utilizando el programa de computadoras ABAQUS. Basado en los resultados obtenidos, deformaciones permanentes y grandes desplazamientos demuestran el comportamiento no lineal del sistema. Los valores de deformaciones permanentes obtenidos se compararon con los valores medidos de las muestras utilizadas en las pruebas.

Parámetros tales como: configuración geométrica de los paneles, materiales, condiciones de borde, localización de impacto y velocidad del proyectil fueron evaluados con el propósito de establecer las condiciones mas criticas a las cuales el sistema pudiese

estar sometido a través de un estudio de parámetros. Para velocidades de misil mayores a 25 millas por hora, el desplazamiento máximo del panel impactado excedió las tres (3) pulgadas. Por lo tanto, elementos a ser protegidos por los paneles pueden sufrir daños debido al contacto producido con el panel impactado. Los resultados muestran que las rotaciones en los bordes de los paneles fueron reducidas cuando diferentes condiciones de borde y un número mayor de paneles fue utilizado en el sistema.

Tres zonas principales de máximos esfuerzos fueron identificadas a ser desarrolladas en el panel bajo impacto. Los esfuerzos máximos fueron generados en cada una de las zonas siguiendo una secuencia que varía de acuerdo a la rigidez del sistema. En ninguno de los casos se registró alguna falla del material.

Acknowledgements

First of all, I would like to express my thanks to God my heavenly Father, for giving me the strength to reach my goals no matter the obstacles in my life. I would like to express my deepest gratitude to my academic and research advisor Dr. Ricardo López for his guidance and constant support while conducting and completing this work. I would also like to thank Dr. Luis Godoy for his continuous encouragement and his expertise. In addition, I want to thank Dr. Raul Zapata and Dr. Ali Saffar for serving on my advisory committee, as well as for their generous advice.

Many thanks to all the people I have come to know in the Civil Engineering Department, whose friendship and companionship I will always enjoy. I owe my sincere appreciation to my family and relatives who have supported and encouraged me over the years. I especially want to thank my wife Licia and my children Alexander Jr. and Valeria for being my inspiration and unconditional support during my studies. Finally, I want to extend my profound appreciation to my beloved parents for their love, affection, and invaluable support during my life and studies.

I want to recognize that part of this project was funded by the Federal Emergency Management Agency (FEMA) under Section 404 Hazard Mitigation Grant Program, FEMA 1068-DR-PR. The project was given the number PR 0007.

Table of Contents

| | |
|---|-----|
| ABSTRACT | ii |
| RESUMEN | iv |
| ACKNOWLEDGEMENTS | vi |
| TABLE OF CONTENTS | vii |
| LIST OF TABLES | x |
| LIST OF FIGURES..... | xii |
| CHAPTER I INTRODUCTION..... | 1 |
| 1.1 Introduction | 1 |
| 1.2 Scope and Objectives..... | 2 |
| 1.3 Justification | 3 |
| 1.4 Previous Works | 4 |
| 1.5 Work Description | 7 |
| 1.5.1 Development of Testing Facility | 7 |
| 1.5.2 Analytical Part | 10 |
| 1.6 Summary of Procedure | 10 |
| 1.6.1 Experimental Phase | 11 |
| 1.6.2 Analytical Phase..... | 11 |
| 1.7 Contents of this Study | 12 |
| CHAPTER II PRESSURE SETUP..... | 14 |
| 2.1 Introduction..... | 14 |
| 2.2 Design Criteria..... | 14 |
| 2.3 Design Loads..... | 15 |
| 2.4 Pressure Setup Components..... | 17 |
| 2.4.1 Rigid Frame..... | 17 |
| 2.4.2 Load Transfer System..... | 21 |
| CHAPTER III IMPACT SETUP..... | 25 |
| 3.1 Introduction..... | 25 |
| 3.2 Impact Test Devices..... | 26 |

| | | |
|---|--|-----------|
| 3.3 | Calibration Values for Air Cannon Device | 31 |
| 3.4 | Impact Setup Performance..... | 32 |
| 3.4.1 | Test 1: One Supported Edge | 33 |
| 3.4.2 | Test 2: Unsupported Edges | 36 |
| CHAPTER IV GUIDELINES FOR TESTING AND APPROVAL OF STORM | | |
| | SHUTTERS AND PANELS | 39 |
| 4.1 | Introduction..... | 39 |
| 4.2 | Proposed guidelines for testing and approval of storm protection | 40 |
| CHAPTER V ANALITICAL STUDY OF STORM SHUTTERS BEHAVIOR DUE TO | | |
| | IMPACT LOADS..... | 46 |
| 5.1 | Introduction | 46 |
| 5.2 | Definition of Storm Shutter System..... | 47 |
| 5.2.1 | Panel Material..... | 47 |
| 5.2.2 | Boundary Conditions..... | 50 |
| 5.2.3 | Cross Section..... | 52 |
| 5.2.4 | Contact Interactions..... | 52 |
| 5.2.5 | Windborne Definition..... | 55 |
| 5.3 | Model Generation..... | 56 |
| 5.3.1 | Model Assembly..... | 56 |
| 5.3.2 | Meshing..... | 60 |
| 5.3.2.1 | Frequency Analysis..... | 63 |
| 5.3.2.2 | Convergence Analysis..... | 66 |
| 5.3.3 | Shell Finite Elements..... | 74 |
| 5.4 | Model Validation | 80 |
| 5.5 | Discussion of Results | 82 |
| CHAPTER VI PARAMETRIC STUDY OF STORM SHUTTERS DUE TO | | |
| | IMPACT LOADS | 86 |
| 6.1 | Introduction..... | 86 |
| 6.2 | Parametric Study..... | 87 |
| 6.2.1 | Base Case Model..... | 87 |

| | | |
|--|---|-----|
| 6.2.2 | Effect of Panel Material..... | 89 |
| 6.2.3 | Effect of Geometrical Configuration | 105 |
| 6.2.3.1 | Cross Sections..... | 106 |
| 6.2.3.2 | Number of Panels..... | 117 |
| 6.2.4 | Effect of Boundary Conditions..... | 126 |
| 6.2.5 | Effect of Missile Velocity..... | 136 |
| 6.2.6 | Effect of Impact Location | 146 |
| 6.3 | Discussion of Results | 150 |
| CHAPTER VII SUMMARY, CONCLUSIONS AND RECOMMENDATIONS | | 155 |
| 7.1 | Introduction | 155 |
| 7.2 | Storm Shutter Testing Facilities..... | 156 |
| 7.3 | Modeling of Storm Shutter Panels..... | 157 |
| 7.4 | Parametric Study..... | 160 |
| 7.5 | Recommendations..... | 162 |
| REFERENCES..... | | 164 |
| APPENDIX A: STORM SHUTTER PROFILES..... | | 169 |

List of Tables

| | | |
|------------|--|-----|
| Table 2-1: | Test loads based on the building code..... | 16 |
| Table 3-1: | Storm Shutter Systems..... | 32 |
| Table 4-1: | Test loads, based on ASCE Standard, ASCE (2006)..... | 44 |
| Table 4-2: | Repetitive Pressure Loading..... | 45 |
| Table 5-1: | Mechanical and physical properties for aluminum panels..... | 48 |
| Table 5-2: | Windborne Debris or Missile properties..... | 56 |
| Table 5-3: | Partitions used on part related to shutter panel..... | 59 |
| Table 5-4: | Proportionality factors for a damped system..... | 65 |
| Table 5-5: | Summary of values obtained from the convergence analysis..... | 73 |
| Table 5-6: | Shell Finite Elements..... | 75 |
| Table 5-7: | Summary of values obtained for different shell elements..... | 78 |
| Table 5-8: | Maximum strain values obtained for different kinematics formulation..... | 79 |
| Table 6-1: | Description of Base Case model..... | 88 |
| Table 6-2: | Mechanical and physical properties of typical materials used in the storm panels fabrication..... | 90 |
| Table 6-3: | Proportionality factors for damped systems in the evaluation of panel materials..... | 93 |
| Table 6-4: | Maximum and permanent deformation obtained varying the panel's material..... | 97 |
| Table 6-5: | Maximum Von Mises stresses acting at different zones of the impact panel. Values obtained for different panel materials..... | 104 |
| Table 6-6: | Cross sections used on the parametric study..... | 109 |
| Table 6-7: | Proportionality factors for damped systems in the evaluation of panel cross sections..... | 109 |
| Table 6-8: | Maximum and permanent deformation obtained varying the panel cross section..... | 112 |
| Table 6-9: | Maximum Von Mises stresses acting at different zones of the | |

| | | |
|-------------|---|-----|
| | impact panel. Values obtained for different panel cross sections..... | 117 |
| Table 6-10: | Maximum and permanent deformation obtained varying the number of panels in the assembly..... | 121 |
| Table 6-11: | Maximum Von Mises stresses acting at different zones of the impact panel. Values obtained for different number of panels in the assembly..... | 126 |
| Table 6-12: | Maximum and permanent deformation obtained varying the type of the upper support..... | 132 |
| Table 6-13: | Maximum Von Mises stresses acting at different zones of the impact panel. Values obtained for different type of upper edge supports..... | 137 |
| Table 6-14: | Maximum and permanent deformation obtained varying the missile velocity..... | 140 |
| Table 6-15: | Maximum Von Mises stresses acting at different zones of the impact panel. Values obtained for different missile velocities | 147 |

List of Figures

| | | |
|--------------|--|----|
| Figure 1-1: | Pressure setup: Steel Rigid Frame..... | 8 |
| Figure 1-2: | Proposed Air Cannon..... | 9 |
| Figure 2-1: | Pressure Setup: Steel Rigid Frame..... | 18 |
| Figure 2-2: | Horizontal beams and concrete blocks..... | 18 |
| Figure 2-3: | Vertical setting position for horizontal beams..... | 19 |
| Figure 2-4: | Intermediate support adapted to an existing reaction frame..... | 20 |
| Figure 2-5: | Final Assembly: Rigid frame with four shutter panels attached..... | 21 |
| Figure 2-6: | Load Transfer System: Principal Components..... | 22 |
| Figure 2-7: | Final Assembly: Load Transfer System..... | 23 |
| Figure 2-8: | Secondary Frame..... | 24 |
| Figure 2-9: | Steel Wheels Connection..... | 24 |
| Figure 3-1: | Air Cannon Device..... | 26 |
| Figure 3-2: | Elastomeric Pad attached at the end of the Large Missile..... | 27 |
| Figure 3-3: | Valve Distribution..... | 28 |
| Figure 3-4: | Liquid Dial Gage..... | 29 |
| Figure 3-5: | Liquid Dial Gage location and valve distribution layout..... | 29 |
| Figure 3-6: | Frame and Table Support Dimensions..... | 30 |
| Figure 3-7: | Rigid Frame and Table Support..... | 30 |
| Figure 3-8: | Calibration Testing Results..... | 31 |
| Figure 3-9: | Radar Gun used for Missile Velocity Measures..... | 32 |
| Figure 3-10: | Lateral support only at one edge..... | 34 |
| Figure 3-11: | Permanent deformation at middle span..... | 34 |
| Figure 3-12: | Rotation and lost of clips due to impact..... | 35 |
| Figure 3-13: | Lost of upper edge restrain due to impact..... | 36 |
| Figure 3-14: | No Lateral support at both panel edges..... | 36 |
| Figure 3-15: | Permanent deformation at middle span..... | 38 |
| Figure 5-1: | Aluminum 3003-H14 Stress-Strain Curve..... | 49 |
| Figure 5-2: | Typical Storm Shutters Assembly..... | 50 |

| | | |
|--------------|--|----|
| Figure 5-3: | Typical lower edge attachments devices: (a) metal clips (b) wing nuts and washers..... | 51 |
| Figure 5-4: | Cross section “CST#1” of shutter panels used on Test 1..... | 52 |
| Figure 5-5: | Contact pair between missile and panel..... | 53 |
| Figure 5-6: | Contact pair between panels..... | 54 |
| Figure 5-7: | Contact pair between header and panels..... | 54 |
| Figure 5-8: | Missile used on Test 1..... | 55 |
| Figure 5-9: | Screen showing in ABAQUS the part related to shutter panel..... | 57 |
| Figure 5-10: | Part related to missile..... | 57 |
| Figure 5-11: | Part related to top header walls..... | 58 |
| Figure 5-12: | Partitions on the part related to shutter panel..... | 58 |
| Figure 5-13: | Instances used in the model..... | 60 |
| Figure 5-14: | Example of Finite Element Mesh..... | 61 |
| Figure 5-15: | Initial missile location from impact zone..... | 62 |
| Figure 5-16: | Seeds generation along instance edges..... | 63 |
| Figure 5-17: | Effect of critical damping in main panel displacements..... | 66 |
| Figure 5-18: | Model meshes used on Case #1..... | 67 |
| Figure 5-19: | Model meshes used on Case #2..... | 68 |
| Figure 5-20: | Model meshes used on Case #3..... | 69 |
| Figure 5-21: | Model meshes used on Case #4..... | 70 |
| Figure 5-22: | Model meshes used on Case #5..... | 71 |
| Figure 5-23: | Missile displacement obtained in Case #1..... | 71 |
| Figure 5-24: | Impact Simulation Sequence..... | 72 |
| Figure 5-25: | Convergence Analysis Results for Five Cases..... | 72 |
| Figure 5-26: | Maximum deformation vs. number of elements..... | 74 |
| Figure 5-27: | Main panel displacement for different shell elements..... | 78 |
| Figure 5-28: | Three panel’s model..... | 81 |
| Figure 5-29: | Main panel deformation for two and three panel’s model..... | 82 |
| Figure 6-1: | Cross section used in Base Case model..... | 89 |
| Figure 6-2: | Aluminum 3003-H14 Stress-Strain Curve..... | 90 |

| | | |
|--------------|---|-----|
| Figure 6-3: | Aluminum 3004-H34 Stress-Strain Curve..... | 91 |
| Figure 6-4: | Aluminum 5052-H32 Stress-Strain Curve..... | 91 |
| Figure 6-5: | Aluminum 6063-T6 Stress Strain-Curve..... | 92 |
| Figure 6-6: | Galvanized Steel, ASTM A446, Gr. 40 Stress-Strain Curve..... | 92 |
| Figure 6-7: | Maximum and permanent deformation for Aluminum Alloy 3003-H14..... | 94 |
| Figure 6-8: | Maximum and permanent deformation for Aluminum Alloy 3004-H34..... | 94 |
| Figure 6-9: | Maximum and permanent deformation for Aluminum Alloy 5052-H32..... | 95 |
| Figure 6-10: | Maximum and permanent deformation for Aluminum Alloy 6063-T6..... | 95 |
| Figure 6-11: | Maximum and permanent deformation for Galvanized Steel, ASTM A446, Gr. 40..... | 96 |
| Figure 6-12: | Maximum and permanent deformations of impact panel obtained for different materials..... | 96 |
| Figure 6-13: | High stress level zones on the impact panel..... | 98 |
| Figure 6-14: | Maximum Von Mises stresses for Aluminum Alloy 3003-H14 acting at (a) impact zone (b) top ridge and (c) lower edge connection..... | 99 |
| Figure 6-15: | Maximum Von Mises stresses for Aluminum Alloy 3004 H34 acting at (a) impact zone (b) top ridge and (c) lower edge connection..... | 100 |
| Figure 6-16: | Maximum Von Mises stresses for Aluminum Alloy 5052 H32 acting at (a) impact zone (b) top ridge and (c) lower edge connection..... | 101 |
| Figure 6-17: | Maximum Von Mises stresses for Aluminum Alloy 6063 T6 acting at (a) impact zone (b) top ridge and (c) lower edge connection..... | 102 |
| Figure 6-18: | Maximum Von Mises stresses for Aluminum Galvanized ASTM A446, Gr. 40 acting at (a) impact zone (b) top ridge and (c) lower edge connection..... | 103 |
| Figure 6-19: | Equipment used in the storm shutter panel's fabrication..... | 106 |
| Figure 6-20: | Variation of twenty seven (27) cross sections of shutter panels..... | 107 |
| Figure 6-21: | Cross Section CS#1..... | 108 |
| Figure 6-22: | Cross Section CS#2..... | 108 |
| Figure 6-23: | Cross Section CS#3..... | 108 |
| Figure 6-24: | Cross Section CS#4..... | 108 |

| | | |
|--------------|--|-----|
| Figure 6-25: | Maximum and permanent deformation for CS#1..... | 110 |
| Figure 6-26: | Maximum and permanent deformation for CS#2..... | 110 |
| Figure 6-27: | Maximum and permanent deformation for CS#3..... | 111 |
| Figure 6-28: | Maximum and permanent deformation for CS#4..... | 111 |
| Figure 6-29: | Maximum and permanent deformations of impact panel obtained for different cross sections..... | 112 |
| Figure 6-30: | Maximum Von Mises stresses for CS #1 acting at (a) impact zone (b) top ridge and (c) lower edge connection..... | 113 |
| Figure 6-31: | Maximum Von Mises stresses for CS #2 acting at (a) impact zone (b) top ridge and (c) lower edge connection..... | 114 |
| Figure 6-32: | Maximum Von Mises stresses for CS #3 acting at (a) impact zone (b) top ridge and (c) lower edge connection..... | 115 |
| Figure 6-33: | Maximum Von Mises stresses for CS #4 acting at (a) impact zone (b) top ridge and (c) lower edge connection..... | 116 |
| Figure 6-34: | Storm shutter model defined with: (a) two panels (b) three panels (c) five panels | 118 |
| Figure 6-35: | Maximum and permanent deformation using two panels..... | 119 |
| Figure 6-36: | Maximum and permanent deformation using three panels..... | 120 |
| Figure 6-37: | Maximum and permanent deformation using five panels | 120 |
| Figure 6-38: | Maximum and permanent deformation varying the number of panels..... | 121 |
| Figure 6-39: | Reduction of the upper edge rotation of the impacted panel due to the contact with the third panel | 122 |
| Figure 6-40: | Maximum Von Mises stresses for a two panel's model acting at (a) impact zone (b) top ridge and (c) lower edge connection | 123 |
| Figure 6-41: | Maximum Von Mises stresses for a three panel's model acting at (a) impact zone (b) top ridge and (c) lower edge connection..... | 124 |
| Figure 6-42: | Maximum Von Mises stresses for a five panel's model acting at (a) impact zone (b) top ridge and (c) lower edge connection | 125 |
| Figure 6-43: | Typical top headers (a) cross sections (b) dimensions | 128 |
| Figure 6-44: | Top Header model | 129 |

| | | |
|--------------|--|-----|
| Figure 6-45: | Maximum and permanent deformation of the impact panel when its top edge was supported by a roller connection | 130 |
| Figure 6-46: | Maximum and permanent deformation of the impact panel when its top edge was supported by a the top header | 131 |
| Figure 6-47: | Maximum and permanent deformation of the impact panel when its top edge was supported by a pinned connection..... | 131 |
| Figure 6-48: | Maximum and permanent deformation varying the type of the top edge support | 132 |
| Figure 6-49: | Panel edge rotation inside the top header: (a) zero rotation previous to the applied load, $t = 0.0$ sec. (b) panel rotation constrained by the contact with the inside walls of the top header, maximum rotation at $t=0.027$ sec | 133 |
| Figure 6-50: | Maximum Von Mises stresses for a top roller support model acting at (a) impact zone (b) top ridge and (c) lower edge connection | 134 |
| Figure 6-51: | Maximum Von Mises stresses for a top header model acting at (b) impact zone (b) top ridge and (c) lower edge connection | 135 |
| Figure 6-52: | Maximum Von Mises stresses for a top pinned support model acting at (a) impact zone (b) top ridge and (c) lower edge connection | 136 |
| Figure 6-53: | Maximum and permanent deformation of the impact panels with a missile velocity of 25 mph | 138 |
| Figure 6-54: | Maximum and permanent deformation of the impact panels with a missile velocity of 34.1 mph | 139 |
| Figure 6-55: | Maximum and permanent deformation of the impact panels with a missile velocity of 50 mph | 139 |
| Figure 6-56: | Maximum and permanent deformation of the impact panels with a missile velocity of 75 mph | 140 |
| Figure 6-57: | Maximum and permanent deformation of the impact panel varying the missile velocity | 141 |
| Figure 6-58: | Main panel lost the edge support provided by the adjacent panel for 75 mph missile velocity | 141 |

| | | |
|--------------|--|-----|
| Figure 6-59: | An excessive deformation of the main panel avoids any possible failure of the panel material..... | 142 |
| Figure 6-60: | Maximum Von Mises stresses for a missile velocity of 25 mph acting at (a) impact zone (b) top ridge and (c) lower edge connection..... | 143 |
| Figure 6-61: | Maximum Von Mises stresses for a missile velocity of 34.1 mph acting at (a) impact zone (b) top ridge and (c) lower edge connection..... | 144 |
| Figure 6-62: | Maximum Von Mises stresses for a missile velocity of 50 mph acting at (a) impact zone (b) top ridge and (c) lower edge connection..... | 145 |
| Figure 6-63: | Maximum Von Mises stresses for a missile velocity of 75 mph acting at (a) impact zone (b) top ridge and (c) lower edge connection..... | 146 |
| Figure 6-64: | Impact missile over the hill at 0.001 sec | 149 |
| Figure 6-65: | Impact missile over the hill at 0.004 sec | 149 |
| Figure 6-66: | Impact missile over the hill at 0.008 sec | 150 |
| Figure 6-67: | Impact missile over the hill at 0.013 sec | 150 |
| Figure 6-68: | Impact missile over the hill at 0.022 sec | 151 |

Chapter I

Introduction

1.1 Introduction

Every year, we experience the threats of hurricanes that move near the island of Puerto Rico in the Caribbean area. Historically, these atmospheric phenomena have been a cause of concern at least once every five years, leaving heavily damaged areas and several deaths behind it. Recent events such as hurricanes Hugo (1989), Marilyn (1995), Hortense (1996), Georges (1998), and Jeanne (2004) are just reminders of how vulnerable we are and of how imperative is the need to be prepared against hurricanes and storms.

The integrity of any structure depends on the structural and deformation capacity of its individual areas (walls and roof). Damage usually starts with breakage of weak elements such as doors and windows. These components need additional protection to prevent further damages to the interior of the structure, which could lead to a possible complete loss of the property and could endanger lives. Typical hurricane protection available in Puerto Rico includes shutters of different types and materials. Current regulations in Puerto Rico (ARPE, 1999) require that shutters installed meet the requirements of the Puerto Rico Building Code (ICBO, 1997) in order to preserve the integrity of the structure under hurricane conditions. The basic requirement of the code is that shutters withstand the specified wind pressure at the height they are installed.

Of the shutters available in Puerto Rico some products have been tested and already comply with regulations from other regions of the United States such as Miami Dade County in the State of Florida (SFBC, 1994). These regulations may or may not comply with the Puerto Rico Building Code (ICBO, 1997). Others shutters had been tested to secure some degree of safety but without following an established testing program. As a result of this lack of a valid certification standard in Puerto Rico the consumer may end up selecting a product that may not fully protect their home.

Formal analytical testing of the capacity of storm shutters made of corrugated metal is difficult because of the nonlinearity of deformation and because of the lack of knowledge of the behavior of such panels subjected to impact loads. Our approach is to obtain suitable analytical solutions for the behavior of storm shutter panels exposed to impact loads.

In order to establish a formal certification process that ensures the public is getting a safe product, a valid testing program needs to be created. This project develops the guidelines for creating a certification program for storm protection shutters. In addition, an analytical study can be used to evaluate the nonlinear behavior of shutter under impact loads. The current study will be limited to the corrugated storm shutter type.

1.2 Scope and Objectives

1. To establish guidelines for testing storm protection shutters. These guidelines will include the development of tests for uniform static pressure in tension and compression, as well as for cycles of pressure in compression - tension and impact loads. Testing equipment was designed to comply with this objective.

2. To study the nonlinear behavior of storm shutter protection under impact loads (corrugated type) using an existing computer program. A model that describes this behavior was created. This model can be used to predict the behavior of the shutters during the design process, or for evaluations purposes.
3. To develop models that will help future designers to study the most detrimental behavior of shutters before they are fabricated.

1.3 Justification

Due to the fact that in Puerto Rico a complete testing program for certifying storm shutters protection has not been developed, the creation of guidelines for such a program is essential. These guidelines will give to the manufacturer scientific orientation to develop their products. As a result the consumer will benefit from safer products with higher quality and the manufacturer will benefit from a more profound knowledge of shutter behavior that will shorten the design cycle.

The establishment of guidelines requires the storm shutter to be tested under realistic circumstances. To comply with this, the installation of specimens needs to be in accordance with the manufacturers recommendations. Also appropriate testing equipment has to be developed. The construction of testing setup for the project will give the opportunity to establish a local testing laboratory at the Civil Engineering Department laboratories of the University of Puerto Rico at Mayagüez. Funding for construction of the setup was obtained from the Federal Emergency Management Agency and University of Puerto Rico at Mayagüez; from now on, FEMA and UPRM.

The testing setup will provide scientific data about support conditions, stability, and other relevant factors that influence the storm shutter behavior under loads. Actually, access to data concerning those topics is severely limited.

Extensive evaluations of building damage in windstorms have shown that windborne debris must be considered during the design of the structure protection (Minor, 2005). Windborne debris has been established as a principal cause for the breaking of the building envelope during hurricanes and tornadoes. As part of test equipment, an air cannon was developed to test the effect of impacts on a storm shutter. The results obtained of the tests were used to develop a model that can describe the behavior of the specimens.

1.4 Previous Works

The Dade County Building Code Compliance Office in Miami, Florida, has developed a series of protocols oriented to the testing of storm shutters (e.g., Dade County, 1994a, 1994b, 1994c). The Protocols include: definitions related to materials, test equipment and loads; requirements for test facilities, testing procedures and format for developing test reports. These protocols are based on the South Florida Building Code (SFBC, 1994) specifications.

As established by Dade County, some local organizations have developed a document that is used as a simple guide for the installation of hurricane protection products in Puerto Rico (e.g., CIAPR, et al., 1996). The organizations involved in this effort are Colegio de Ingenieros y Agrimensores de Puerto Rico, Defensa Civil Estatal de Puerto Rico (presently known as Agencia Estatal para Manejo de Emergencias, AEME) and FEMA. The guide

present descriptions, materials, performance and installation of hurricane protection as shutters and panels.

Behr and Minor (1994) concluded that windborne debris was a major factor in damage in South Florida during Hurricane Andrew. Sparks (1994) attributed most of the damage to the building envelope of residences to windborne debris. Finally, major investigations following Hurricane Andrew highlighted windborne debris as the major cause of damage (Dade County, 1992; FEMA, 1992; WERC, 1992).

The subject of protection from windborne debris was brought to the American Society of Testing Materials, ASTM, on April 1993, for the purpose of developing standards (Hattis, 2006). The ASTM Subcommittee E06.51 established a research group under the co-chairmanship of Hattis (1996). This group was divided into two Working Groups. Working Group A, under the chairmanship of Hattis, addressed the performance of exterior walls fenestration assemblies in hurricane environment. They worked with the development of standard test method for performance of exterior windows, curtain walls, doors and storm shutters impacted by missiles and exposed to cyclic differential pressures. The test method impacts fenestration with a variety of missiles propelled at velocities representative of the velocities of debris in hurricanes, and then subjects them to a sequence of pressure cycles representatives of wind gust in hurricanes. The impact apparatus may include an air cannon, slingshot, or any other apparatus capable of delivering the missiles as specified.

Working Group B was assigned to work with a rank ordering of fenestration assemblies and components in terms of their impact energy resistance. They were responsible for the development of standards for evaluation of fenestration components and

assemblies for resistance to impact energies. The impact apparatus used was a pendulum that delivered different impact energies as a function of the height of its drop.

Minor (et al., 1972) observed that windows are traditionally designed for wind pressures, but the breakage from impact by windborne debris was the most common failure mechanism during hurricanes. He identified roof gravel as the principal form of small debris that can be carried into all elevations of buildings facades. Similarly, in residential areas, Minor (1994) concluded that the most prevalent type of windborne debris was timber from wood frame houses. Individual timbers were observed to have penetrated walls and roof during tornadoes. These observations led to the selection of a 2" x 4" timber as representative object for use in defining impact criteria for tornadoes (and now during hurricanes) protection in residences.

It was observed by many investigators in South Florida that roofing tile was the most prevalent type of windborne debris. Roofing tile was selected initially by the Dade County Building Code Committee as the design missile for the debris impact standard for the South Florida Building Code. However, it was difficult to propel a tile, in the same orientation and the same speed as part of a standard test. For that reason, the Building Code Committee (SFBC, 1994) ultimately recommended for use in design a 9 pounds timber plank, with cross-section dimensions of 2" x 4" as a representative object for use.

Rodríguez (1995) realized experimental and analytical work with shutter systems as part of a private consulting study for a shutter company. During the experimental part, he found that shutters tend to slip between them when uniform static load in tension was applied. As a result of this behavior the element changes its geometry causing a significant

reduction in the strength of the system. Therefore, a stability problem in shutter is present when uniform static load in tension is applied to it.

1.5 Work Description

This study is divided in two principal parts. The first part is the development of a testing facility for storm shutter panels. All the testing components were designed such that storm shutters could be tested according to the proposed guidelines for testing. The second part is an analytical study of the behavior of shutters subjected to impact. For this general purpose finite element software is used to create models which represent the tested specimens. In addition, a parametric study was used to analyze the most detrimental behavior of storm shutter panels.

1.5.1 Development of Testing Facility

The testing procedures were performed on the same setup. The setup consists of a steel frame capable of sustaining the applied loads with minimum displacement. The restriction on displacement (maximum displacement ≤ 0.1 inches) was established such that the measurements obtained on the specimens could not be affected.

The Puerto Rico Building Code (PRBC, 1987) is used to establish the magnitudes for the different loads that will be applied to the frame. Based on these loads the frame elements are designed using the Load and Resistance Factor Design (LRFD), (AISC, 1994), to select the appropriate steel section for columns and beams.

The frame has been designed to test different types and sizes of specimens. A maximum area of 10' x 15' was established for testing. Based on this pre-established covering area, the size of the frame was determined to be 15' x 15' as shown on Figure 1. An hydraulic actuator will be used to apply the load to the specimens. The type of loads proposed includes: the application of uniform static pressure (compression and tension) and cycles of pressure.

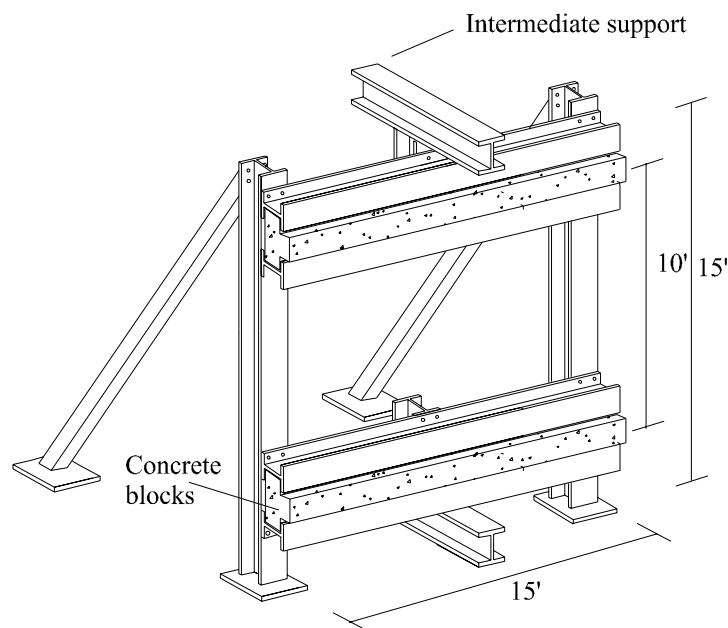


Figure 1.1 Pressure Setup: Steel Rigid Frame

A steel plate is connected to the actuator in such a way that the applied load will be approximately uniform. The uniformity of the load will be facilitated by the use of air bags between the steel plate and the specimen. Deformation of specimens at critical points and other locations was measured using LVDT's.

As mentioned before, an air cannon was developed to study the effect of windborne debris to shutters as shown in Figure 1.2. Special PVC tubes are the principal components of the system. These PVC tubes will be used to store about eight cubic feet of pressurized air which will be released instantaneously toward the cannon section of the system.

The air cannon is able to shoot two different kinds of missiles:

- a. Large missiles - consist of a 9 pound, 2" x 4" piece of wood. The shooting is made through the four inches diameter tube. The length of missile is based on the density of the wood. Typical length values range between 7' to 9'.
- b. Small missiles - a cluster of gravel. The shooting is made through a two inches diameter tube.

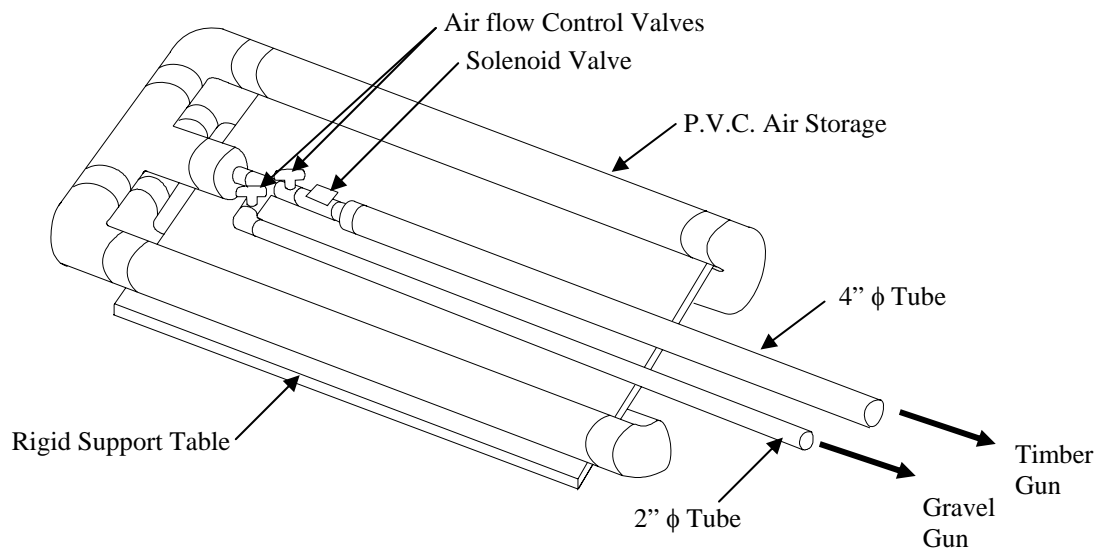


Figure 1.2 Proposed air cannon

The air cannon system was mounted on a rigid support table. The support table is able to position the air cannon at different heights from the ground and maintain it fixed during the tests.

1.5.2 Analytical Part

The finite element program ABAQUS, was used for the creation of the model used in simulation of the impact load test. The objective of the simulation was to study the structural behavior of a typical assembly of storm shutter panels and the interaction of contact produced by the missile traveling at a specific velocity against it.

Using some experimental data obtained during the calibration process of the setup and analytical results obtained from the simulation, a simple method that can represent the effect of impact loads was formulated. The material properties used in the method correspond to corrugate aluminum shutters. The span length was limited to 7' (typical window size). Other variables considered were boundary conditions, cross section geometry of panels and dimensions. The objective was to obtain an approximate displacement measure of the shutter when it was impacted by the large missile. The definition and velocity of the missile are established in the guidelines.

1.6 Summary of the Procedure

The procedures to accomplish the objectives of this research are detailed in the following sections:

1.6.1 Experimental Phase

1. Design and build a steel frame able to sustain the highest wind load that is established in the Puerto Rico Building Code (PRBC, 1987). The type and size for the frame elements are selected in accordance with the Load and Resistance Factor Design (LFRD), (AISC, 1994). The frame will be connected using bolts such to make it very simple to assemble and disassemble. Perforated columns and bolts will permit the testing of different sizes of storm shutters.
2. Design the connection for the actuator such it is placed at a height of 7' - 6" from the ground. This height is exactly the middle height of the frame.
3. Design and build an air cannon that is able to propel a missile against the shutters.
4. Build the air cannon support.
5. Determine the air pressure necessary to obtain the desired missile velocity test.
6. Validation of set up.
7. Sample test.

1.6.2 Analytical Phase

1. Develop a model that simulates the shutter behavior under impact loads using Finite Element Method. For this, a general purpose finite element code ABAQUS was used.
2. Validation of model.

3. Develop a series of models to perform a parametric study to obtain the most detrimental behavior of a typical storm shutter panels.
4. Conclusions and recommendations.

1.7 Contents of this Study

In Chapter II, the development of a pressure setup used as one of the testing devices of the proposed storm shutter testing facility is described. Also the testing loads in compliance to the Puerto Rico Building Code (PRBC, 1987) are calculated. Chapter III presents the design and construction of the second testing device, the impact setup. The process of validation for the device through performing of two impact tests is described. The obtained results are discussed and used as validation values to the subsequent analysis.

The first draft of guidelines developed for testing and approval of storm protection shutter and panels in Puerto Rico (Borges, 1997) is presented in Chapter IV. The guidelines are defined according to the local products and procedures used in the construction industry.

Chapter V describes the different steps required to develop a computer simulation that represent the behavior of a storm shutter panels to the missile impact. Starting with defining the most relevant parameters of storm shutter panels, up to the complete analysis of analytical models using a general purposed finite element code ABAQUS is presented. In addition, a modeling criterion is defined based on the performing of a convergence analysis and a comparative study of different type of finite elements.

In Chapter VI the most critical behavior of storm shutter panels is presents by means of a parametric study. The creation of different models as the proposed parameters are

incorporated into a base model is described. A series of descriptive tables with the obtained results are presented such that the response of the panels to the proposed changes is appreciated. Finally, Chapter VII presents the conclusions of the current research.

Chapter II

Pressure Setup

2.1 Introduction

The research described in this thesis includes experimental and analytical work. This chapter is concerned with the experimental setup built to test the storm shutters under uniform pressure (Borges, et al., 2006). The first step to establish the design criteria for the pressure setup is to define the physical parameters used for window installation in residential construction. The parameters under consideration were width, height and the number of window units installed as a single panel. The geometrical configuration for the pressure setup was established such that typical shutter systems can be tested. The local building code was used to obtain the maximum loads applied to the system during a test. This chapter describes the design and construction of the pressure setup and all related components.

2.2 Design criteria

Typically local residential areas consist of single family dwelling units with no more than two levels. In the majority of the cases the exterior walls are constructed in reinforced concrete and concrete blocks. Therefore, concrete represent the typical base material in which the storm shutter assemblies are attached to the structures.

Each residential unit shows their unique architectural design. Therefore, different sizes and configurations of windows are used in residential buildings. Typically, the

predominant window configuration is two window units forming one panel. The typical window dimensions for this arrangement were 5'-0" height by 2'-6" wide, resulting in an opening wall of 5'-0" height by 5'-0" wide. However, some residences included in their design the use of glass panels. These elements show a greater opening wall area than the typical window.

Based on this information an opening area of 10'-0" height by 15'-0" wide has been specified as the maximum area to be provided by the pressure setup in order to perform the testing program described in Chapter IV.

2.3 Design loads

FEMA (1998) proposed the development of the first testing laboratory for storm shutter systems in Puerto Rico. The facilities are located at the Structure Laboratory of the Civil Engineering and Surveying Department of the University of Puerto Rico at Mayagüez. At that moment "Reglamento Número 7" of the Puerto Rico Planning Board (PRBC, 1987) was the official building construction code used in Puerto Rico. Based in this building code the suggested design loads were used in the design of the pressure setup components. According to this code, the wind load pressure P , is calculated as

$$P = qCqKI \quad (2.1)$$

where q is the basic wind pressure, Cq is the pressure coefficient, K is the lightweight elements factor, and I is the importance factor.

As this study is concerned with the protection of residential structures the following parameters were established as prevalent conditions for the design of the pressure setup.

1. Enclosed structures were considered thus C_q value is 1.2 for pressure loads.
2. Corner or edge elements were considered thus C_q value is 2.0 for suction loads.

Table 2-1 shows the variation of wind loads as the height of the structure is increased. It was noticed that in typical terrain residences the wall height varies from 8 to 10 feet. In the case of two level residences the height of walls varies from 18 to 20 feet. Therefore, the design loads used for the pressure setup design were the specified values for structures in which their height above the ground elevation varies from 0 to 20 feet.

Table 2-1. Test loads based on the building code, (PRBC, 1987).

| Height from ground elevation, (ft) | Basic pressure (q) lb/ft ² | K | Pressure coef. (C _q) | | Importance factor I | Load | | Connections lb/ft ² |
|------------------------------------|---------------------------------------|-----|----------------------------------|---------|---------------------|-----------------------------|----------------------------|--------------------------------|
| | | | Pressure | Suction | | Pressure lb/ft ² | Suction lb/ft ² | |
| 0 - 20 | 30 | 1.3 | 1.2 | 2 | 1 | 46.8 | 78.0 | 97.5 |
| | | | | | 1.15 | 53.8 | 89.7 | 112.1 |
| 20 - 40 | 33 | 1.3 | 1.2 | 2 | 1 | 51.5 | 85.8 | 107.3 |
| | | | | | 1.15 | 59.2 | 98.7 | 123.3 |
| 40 - 60 | 39 | 1.3 | 1.2 | 2 | 1 | 60.8 | 101.4 | 126.8 |
| | | | | | 1.15 | 70.0 | 116.6 | 145.8 |
| 60 - 100 | 42 | 1.3 | 1.2 | 2 | 1 | 65.5 | 109.2 | 136.5 |
| | | | | | 1.15 | 75.3 | 125.6 | 157.0 |
| 100 - 150 | 48 | 1.3 | 1.2 | 2 | 1 | 74.9 | 124.8 | 156.0 |
| | | | | | 1.15 | 86.1 | 143.5 | 179.4 |
| 150 - 200 | 51 | 1.3 | 1.2 | 2 | 1 | 79.6 | 132.6 | 165.8 |
| | | | | | 1.15 | 91.5 | 152.5 | 190.6 |
| 200 - 300 | 57 | 1.3 | 1.2 | 2 | 1 | 88.9 | 148.2 | 185.3 |
| | | | | | 1.15 | 102.3 | 170.4 | 213.0 |
| 300 - 400 | 62 | 1.3 | 1.2 | 2 | 1 | 96.7 | 161.2 | 201.5 |
| | | | | | 1.15 | 111.2 | 185.4 | 231.7 |

Note: Dotted area denotes the minimum wind loads used in the design of the pressure setup components.

2.4 Pressure Setup Components

All the testing procedures are performed on the same setup. The setup consists of a steel frame capable of sustaining the applied loads with minimum displacement of the support. The restriction on displacement was established such that the measurements obtained on the specimens will not be affected. The steel elements in which the specimens can be attached were designed for a maximum displacement value of 0.1 inch.

2.4.1 Rigid Frame

As mentioned before, the frame has been designed to test different types and sizes of specimens. A system of panels or storm shutters covering a possible maximum area of 10' x 15' was established for testing. Figure 2-1 shows the selected dimensions for the frame based on the pre-established covering area. The size of the frame was determined to be 15' x 15'.

As mentioned earlier, concrete has become the most used material in the construction of residential buildings. Figure 2-2 shows that the horizontal elements of the frame will support the material (concrete, wood) where the panel connections are attached. Special concrete blocks were designed for this purpose. The objective is to provide a more realistic behavior for testing by allowing the shutters to be connected as typically suggested by manufacture.

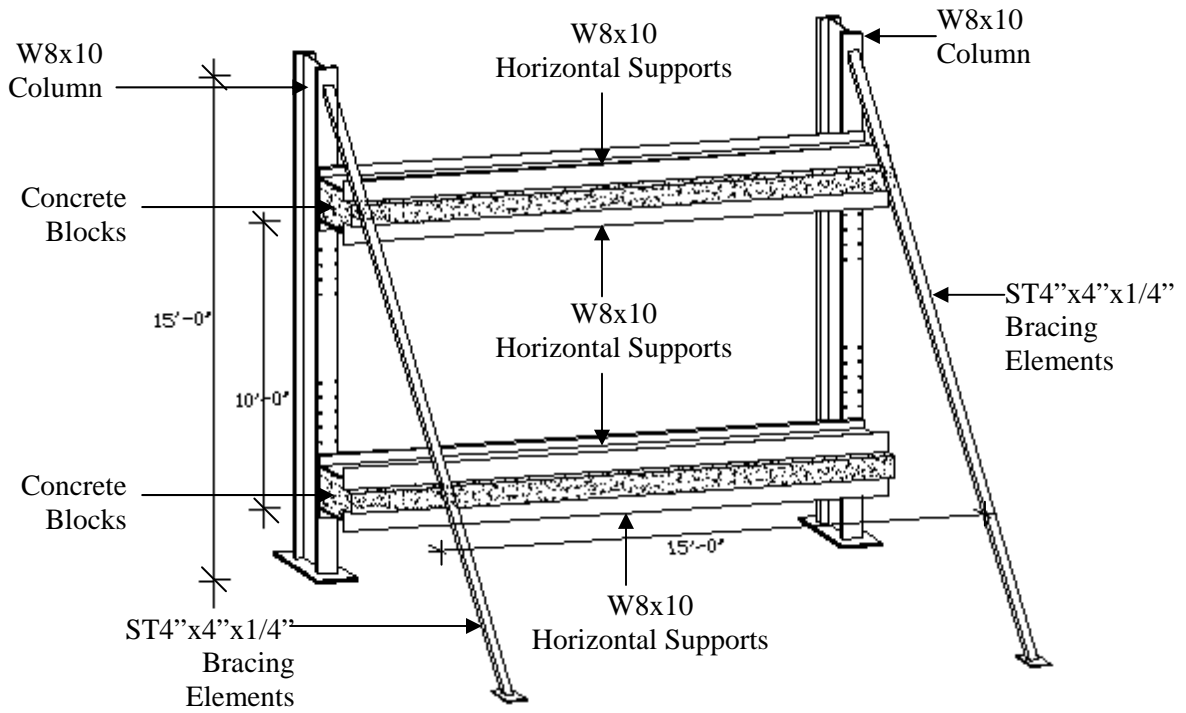


Figure 2-1. Pressure Setup: Steel Rigid Frame

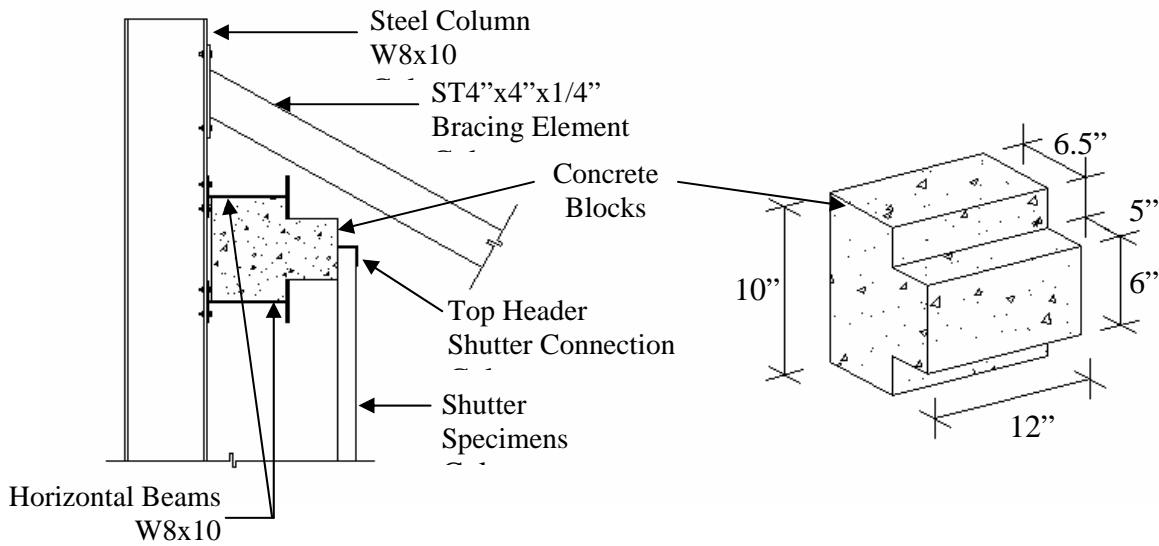


Figure 2-2. Horizontal beams and concrete blocks

The horizontal elements can be moved vertically, such that different span length specimens can be placed on the system according to the panel to be tested as shown in Figure 2-3. The capability of movement is provided by standards holes realized at the frame column flanges. High strength bolt connection provides a simple way to establish the desired location for the horizontal beams.

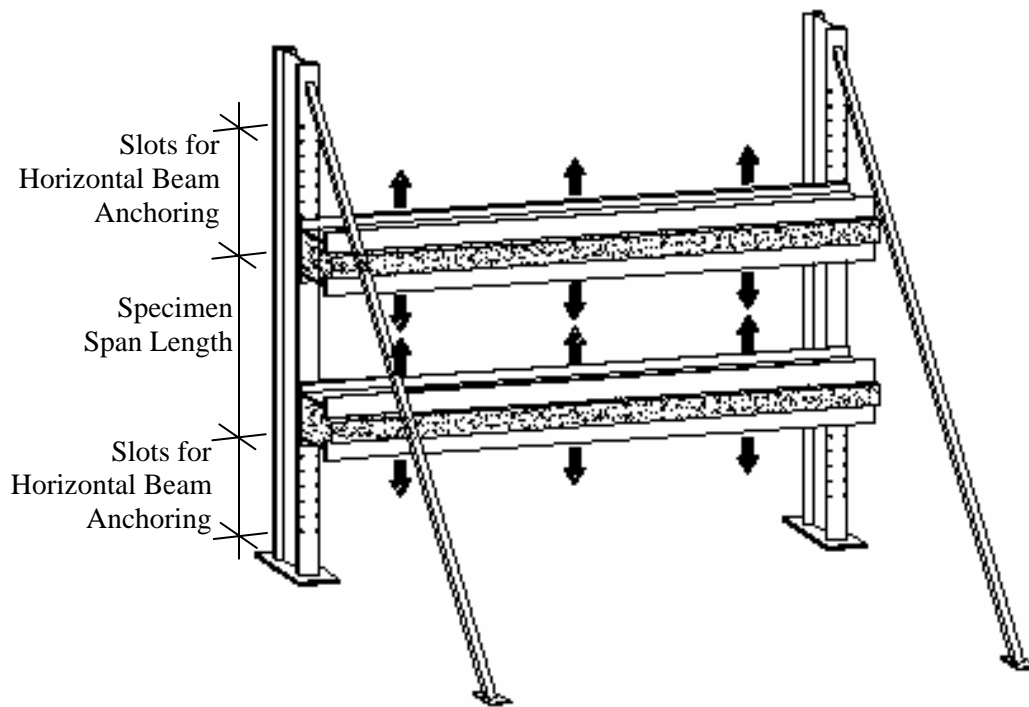


Figure 2-3. Vertical setting position for horizontal beams

The beam deflection and the use of lightweight section were the principal criteria for sizing the elements of the frame. For this reason an intermediate support for the beams was necessary to obtain a more economical section and control the system displacement. The intermediate support consists of two vertical elements which were perforated and positioned

in the setup such that those holes and the ones of the columns will be aligned. This way the beams of the rigid frame will have an additional bolt connection at its mid span. Figure 2-4 shows how the two sections were adapted to an existing reaction frame at the Structure Laboratory. Finally, steel W 8x10 sections (AISC, 1994) were selected in the design of the main frame and the mentioned supports as shown in Figure 2-5.

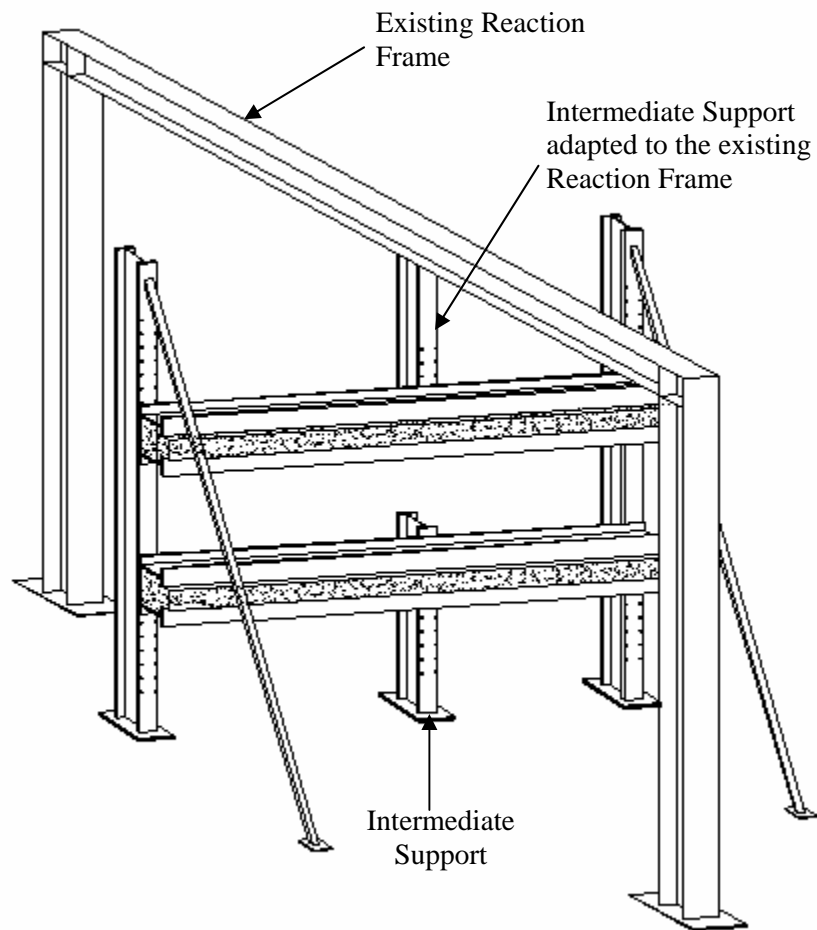


Figure 2-4. Intermediate support adapted to an existing reaction frame



Figure 2-5. Final Assembly: Rigid frame with four shutter panels attached

2.4.2 Load Transfer System

The wind load effects over the specimens are simulated using an hydraulic actuator. To spread the loads a special system is attached to the actuator such the applied load is modified from a concentrated load to a uniform load. The direction of the applied load depends on the location of the hydraulic actuator and the load transfer system.

The load transfer system consists of: steel beams, steel plates and air bags. The beam deflection was the principal criteria for sizing the elements. Beams W 10 x 12 were selected. The beams were connected using bolts forming a principal frame as shown in Figure 2-6. Steel plates were attached to the frame such that a solid surface was obtained. The formed

surface area is approximately the same as the area of the specimens. Considering that the load transfer system and the specimens do not have the same rigidity, the deformation of the surfaces (the one created by the steel plates and the one created by the specimens) are not the same. For this reason, it is necessary to add another component to the system such the surface deformation on both sides is not affected. Air bags present the perfect media to transfer the load between surfaces avoiding the effect of different rigidities. The final assembly for the load transfer system is shown in Figure 2-7.

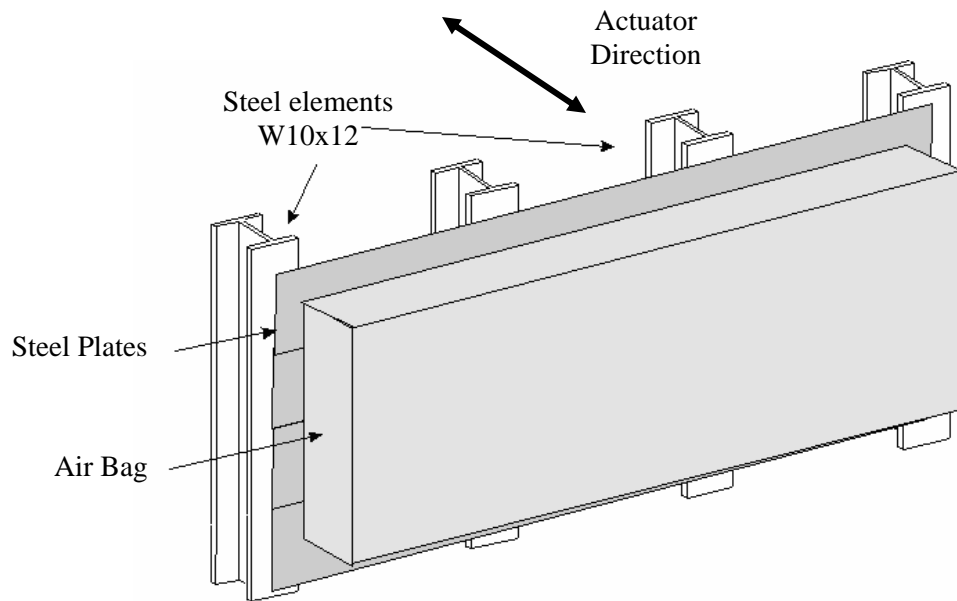


Figure 2-6. Load Transfer System: Principal Components

Additional steel elements were necessary to provide a vertical support to the load transfer system during operations. The transfer load system is too heavy to be supported by the hydraulic actuator. Therefore, a secondary frame that could be responsible for the vertical support of the load transfer system was installed.



Figure 2-8. Secondary Frame



Figure 2-9. Steel Wheels Connection

Chapter III

Impact Setup

3.1 Introduction

One of the most dangerous agents during the passing of a hurricane are the windborne debris. They could produce serious damage to storm shutters and to the elements protected by them. Windborne debris are considered a critical design factor for above-ground shelters, schools, and hospitals, where the protection of people is the primary concern (McDonald, 1976). In modern urban areas, windows and architectural glazing systems of tall buildings are among the structures which are most vulnerable to windborne debris. Minor (1994) illustrated the serious windows damage caused by windborne debris in severe storms. Recently, Wills (et al., 2002) reported on the significant glazing damage to one of the Asia's tallest buildings, Central Plaza, Hong Kong, during Typhoon York, in September 1999. Therefore, the behavior of storm shutters to impacting objects is very critical to the structural integrity. They must be studied and standardized.

This chapter describes the design and construction of the impact setup and its components. The impact device must be able to shoot windstorm debris called missiles such that impact debris events can be simulated.

3.2 Impact Test Devices

The impact setup consists of two main parts. The first part is an air cannon capable of shooting large or small missiles against the specimens. The second is a support table-car that will support and move the air cannon at the testing area. The specimens are installed at the main frame designed for the pressure setup as discussed in Chapter II.

The air cannon consists of an assembly of six (6) inches diameter P.V.C. pipes for air storage as shown in Figure 3-1. These pipes were connected imperviously such that they will retain injected air at their interior. The pipes shall be able to sustain high levels of air pressure to at least 150 psi. Therefore, all elements of the air cannon were designed to be air pressure resistant. The designed configuration can storage a total of eight cubic feet of air. This air volume is enough to provide the pushing force of the missile to be shot at a given velocity of impact. A special hose connector was installed such that an external air compressor will provide the air into the pipes.



Figure 3-1. Air Cannon Device

As mentioned earlier, two types of missiles are used in the air cannon. The first type of missile is called small missiles. Small missiles consist of aggregated (gravel) weighing approximately 0.0044 pounds (2 grams) with a nominal diameter range between 0.5 inches to 0.75 inches. They are located at the interior of a two (2") inches P.V.C. pipe. The second missile is called large missile. A large missile consists of a 2"x 4" timber plank weighing approximately 9 pounds. Its length will vary between 7' to 9' based on the density of the wood. It is located at the interior of a four (4") inches P.V.C. pipe. For large missiles an elastomeric pad is connected at its end as shown in Figure 3-2. The pad serves as a seal that minimizes the loss of air pressure during the shot. In addition some grease is applied to the interior of the pipe to minimize the friction that will be generated due to the contact of both materials affecting the missile velocity.

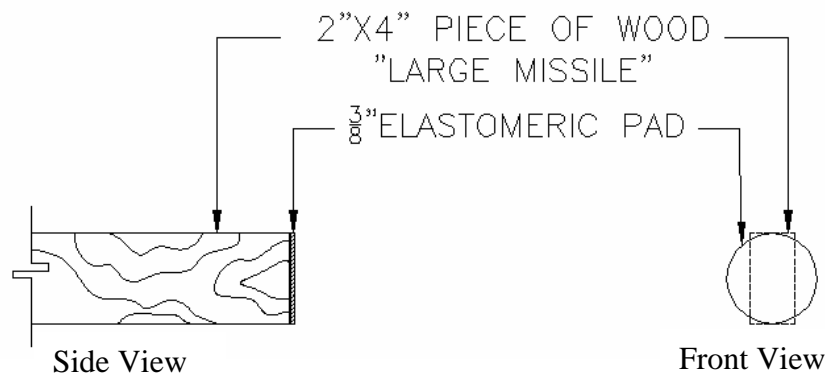


Figure 3-2. Elastomeric Pad attached at the end of the Large Missile

A solenoid valve controls the sudden air flow. This solenoid valve is activated manually by an electronic switch when the air determined internal pressure is reached producing the impact missile velocity established for the test. The kind of missile to be shot

(timber or gravel) through the air cannon will be controlled by the use of two balls valves.

The valve distribution for the system is shown on Figure 3-3.

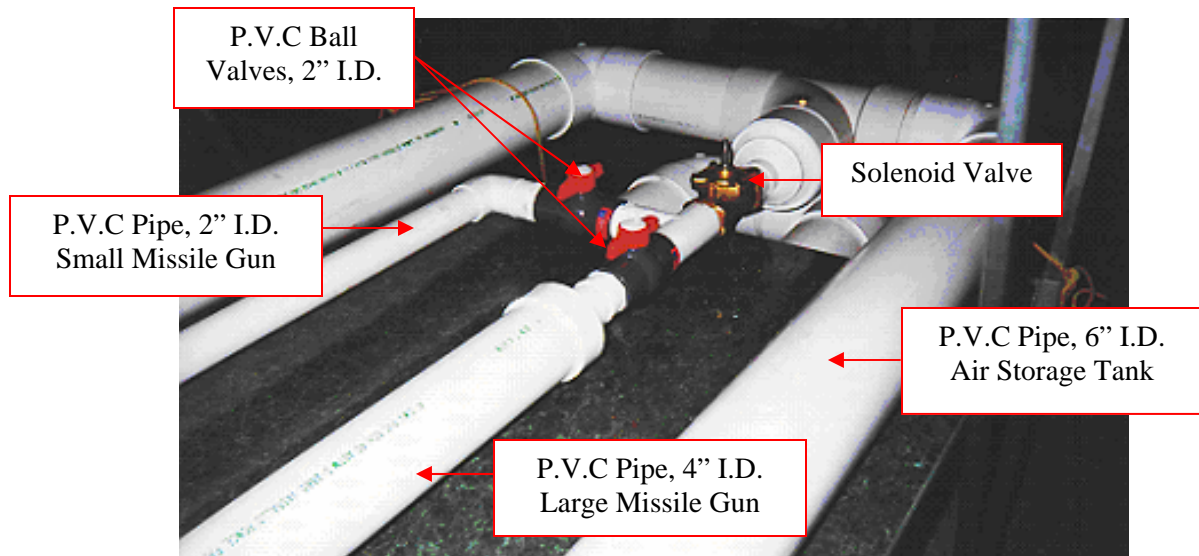


Figure 3-3. Valve Distribution

The air pressure must be measured all the time during a test as shown in Figure 3-4. For this reason a liquid dial gage was installed at the air cannon tank. It is located previous to the solenoid valve according to the valve distribution as shown in Figure 3-5. The liquid dial gage will indicate the specific pressure present at the moment that the shooting must be done.

For the air cannon system a rigid support table was designed. The support table must be able to sustain the weight of the system, position the air cannon at different heights from the ground and maintain it fixed during the tests. It consists of a steel tube rigid frame. Figure 3-6 shows the rigid frame dimensions that were required for the system. The support table was designed such that its elements can be disconnected for storage or replacement.



Figure 3-4. Liquid Dial Gage

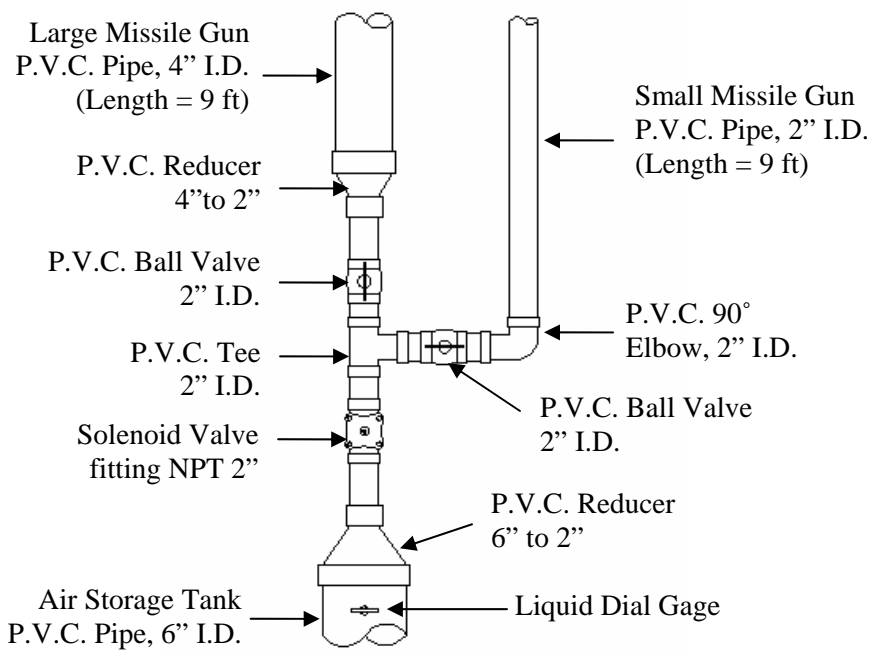


Figure 3-5. Liquid Dial Gage location and valve distribution layout

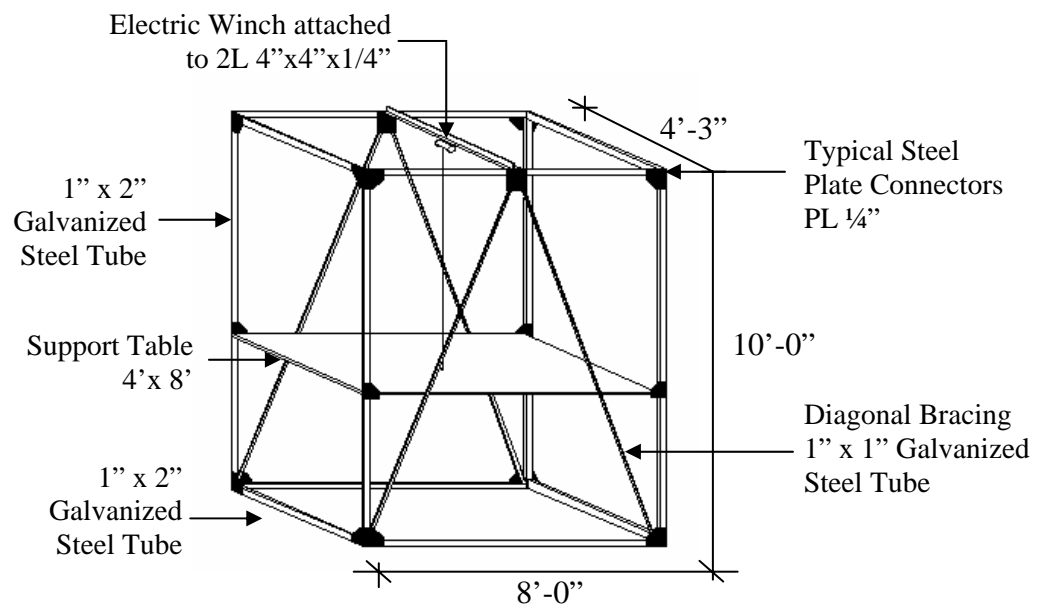


Figure 3-6. Frame and Table Support Dimensions

Considering the dimensions and weight of the system, the frame is attached to four wheels to facilitate its movement to the required position of the air cannon. The final rigid frame assembly is shown in Figure 3-7.



Figure 3-7. Rigid Frame and Table Support

3.3 Calibration Values for Air Cannon Device

As part of the calibration process an infiltration test was performed. This test established the performance of the air cannon joints under compressed air pressure. The results were satisfactory since no loss of pressure was detected at any time and pressure ranges tested up to 78 psi. Once this test was performed the next step was to establish the air pressure needed to obtain the required missile velocity. For this purpose, a series of missile shots were performed to obtain the relationship between the required air pressure injected in the air cannon and the corresponding exiting missile velocity. Figure 3-8 shows the results for the calibration test. A 9-pound 2" x 4" piece of wood defined as the large missile was used for each trial. A radar gun model Stalker Sport by Radar Sales was used to measure the missile velocity during the test as shown in Figure 3-9.

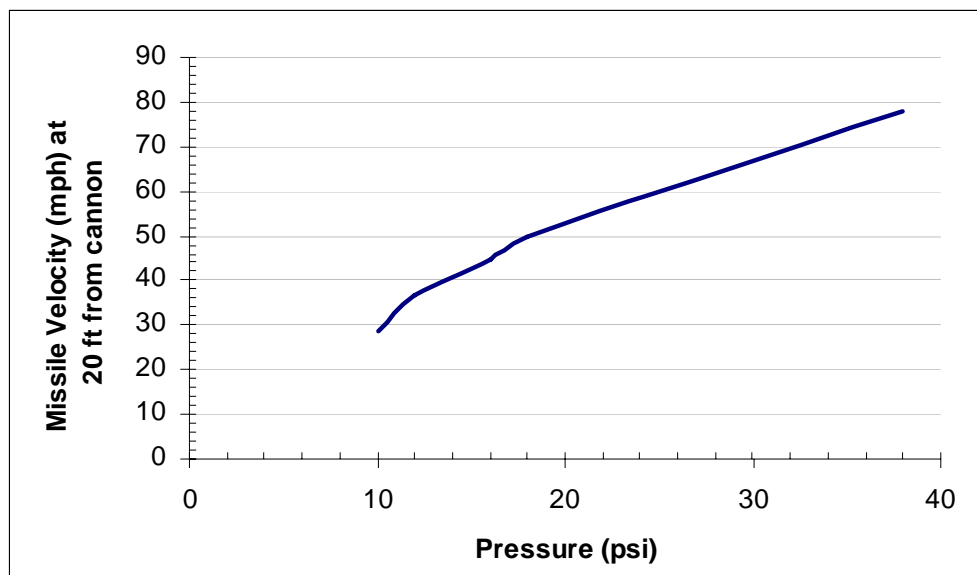


Figure 3-8. Calibration Testing Results



Figure 3-9. Radar Gun used for Missile Velocity Measures

3.4 Impact Setup Performance

Two tests were carried out to validate the functionality of the impact setup. The tests were done on a typical storm shutter panel system installed on the pressure setup main frame. The air cannon was located twenty feet in front of the system. The impact occurred at the center of the panel system. Table 3-1 shows the storm shutter systems used for the both tests.

Table 3-1. Storm Shutters Systems

| Parameter | Description |
|-----------------------|-------------------------|
| Material | Aluminum |
| Thickness | 0.063" |
| Height | 2" |
| Span | 7' - 2" |
| Number of panels | 3 - 5 |
| Cover area* | 18 - 30 ft ² |
| End Support Condition | Clips** |

* Area to be protected ** Two or three clips per sheet

Two sets were tested in which the main difference between those sets was the shutter arrangement of each sheet in the system. One of the tests was allowing the shutter panel to be supported on one edge of the neighboring panel and the second set was not allowing this kind of lateral support. The details of these two types of testing are presented next.

3.4.1 Test 1: One Supported Edge

The storm shutter system was assembled such that each sheet provided some support to the adjacent sheet. One edge of each sheet was placed over the previous sheet as shown in Figure 3-10. This was the first test to measure the behavior of the storm shutters under impact loads. The target missile velocity for this test was 50.0 mph using an air cannon pressure of 18.0 psi. However, the velocity obtained during the test was 51.7 mph. It is important to recognize that the missile used was a new one. Although, the new missile had the same specifications as the one used in the calibration process of the air cannon, any imperfection or slight difference in its weight were factors that can affect the velocity of the missile. For that reason a higher velocity was obtained using the required air pressure. The impact location was at the middle span of the center sheet.

The results for this test were the following:

- a) At middle span the permanent deformation was approximately of 6 ½ inches as shown in Figure 3-11. That means that under real condition the impact load would damage the protected fenestration which is typically located 1½ to 3 inches from the shutter.

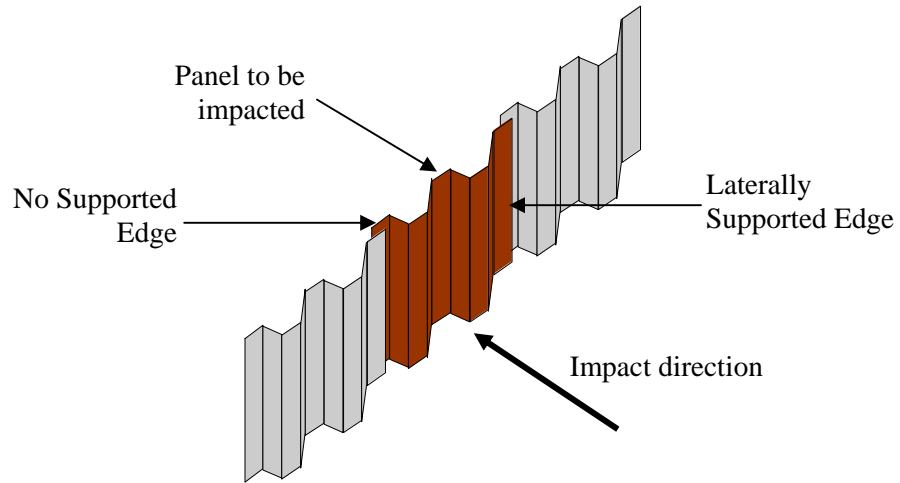


Figure 3-10. Lateral support only at one edge



Figure 3-11. Permanent deformation at middle span

- b) The impacted sheet lost the clips that were attached at its lower end. The clip deformation was too large so it could not be used again as shown in Figure 3-12.
- c) Other clips of the system lost their original position. The clips rotated approximately 45° (clockwise) as shown in Figure 3-12.
- d) The impacted sheet lost its encasing with the top channel as shown in Figure 3-11 and 3-13. Each sheet is encased with a channel that acts as top support of the system.
- e) A torsional deformation occurred because one edge support was more rigid than the other. As one edge was able to have essentially free displacement, the restriction provided by the edge supported produced a torsional effect on the sheet.



Figure 3-12. Rotation and lost of clips due to impact



Figure 3-13. Lost of upper edge restraint due to impact

3.4.2 Test 2: Unsupported Edges

A 2" x 4" x 9' with 9 lb of weight timber missile was shot at a speed of 52 mph. This second test was performed using three sheets. As the impacted sheet did not have any lateral support from the others (as it was in the first test), the use of three sheets was enough as shown in Figure 3-14. This case represents a condition of wrong panel installation.

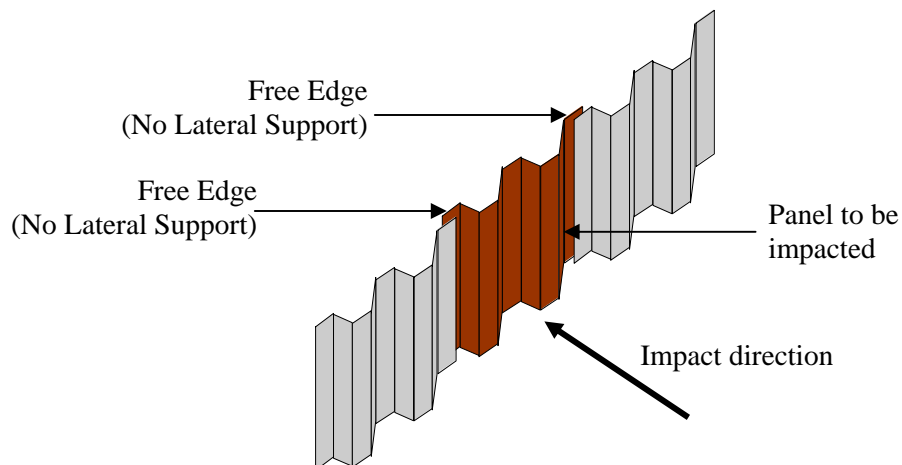


Figure 3-14. No lateral support at both panel edges

The manufacturer suggests the sequence of installation of panel used in the previous test. As the first test, the use of clips connectors at the lower end of panels was used to secure panels to the setup. The impact location was at the middle span of the center sheet.

The results for this test were as follows:

- a) The permanent deformation of the panel did not present evidence of torsion as was observed in the first test as shown in Figure 3-15.
- b) The impacted sheet did not loose the encasing provided by the top end support.
- c) At mid span, the permanent deformation ranged between 7 ½ to 8 inches. This impact could cause damage to protected fenestration in a real situation.
- d) One of the clips attached to the lower support was lost. The others clips were not affected.
- e) The panel behavior in terms of deflection was similar to a simple beam under a concentrated load at mid span.

The results obtained from both tests showed that the air cannon can be used to evaluate the effect of windborne debris acting against of storm shutter panels. Parameters like missile velocity, missile characteristics (small or large), and the location and angle of impact caused by the missile can be evaluated with the proposed impact setup. Finally, it was demonstrated that the impact set up can be used in the execution of a complete testing program of storm shutters that will be discussed in Chapter IV.



Figure 3-15. Permanent deformation at middle span

Chapter IV

Guidelines for Testing and Approval of Storm Shutters and Panels

4.1 Introduction

This chapter presents the first draft of guidelines developed for testing and approval of storm protection shutter and panels in Puerto Rico. The main objective of the guidelines was to develop a scientific reference for manufacturers and customers that will be incorporated in their procedures of production and selection of storm protection. The tests proposed include the application of uniform static pressure, repetitive pressure and impact load tests.

The uniform static pressure will be applied in such a manner that the pressure and suction effects produced by the wind during a hurricane will be obtained. Due to the fact that the path of motion of a fluid (air) will change over the surface of the shutter, repetitive pressure tests must be performed to account for this phenomenon.

As was mentioned in previous chapters, one of the most dangerous agents during the pass of a hurricane are the windborne debris. Those can produce serious damages to the storm shutters protections. The impact test can simulate this event, giving results for deformations and effects in capacities of the systems.

Windstorm damage experiences have revealed that windows and other structural roof elements may be strong enough for windstorm-exerted wind pressures but are not able to

preserve the integrity of the building envelop when impacted by windborne debris. Minor (et al., 1972) concluded that post impact behavior is as important as pre impact strength if the preservation of the building envelop is concerned. This argument serves as a basis for the protocols for testing hurricane resistance products wherein debris impacts are followed by cycles of pressures representing wind gusts (ASTM, 1997).

The tests were developed to represent conditions that are likely to occur in a hurricane: debris impact followed by cycles of pressures created by direction-changing of hurricane wind gusts.

4.2 Proposed Guidelines for Testing and Approval Storm Shutters and Panels

A. Test Specimens and Installation

A.1 Test Specimens

A.1.1 Test specimens consist of all parts contained on the assembly of storm shutters or panels systems. Those parts must be of the same size, using the same materials, methods of constructions and methods of attachment as recommended by the manufacturer.

A.1.2 The number of storm panels in the system must be established according to the opening size to be evaluated.

A.2 Installation

A.2.1 Test specimens must be fit to a rigid structure that will be able to create the site conditions such as: opening size to be covered and base material connection. The

- rigid structure must be built taking in consideration that it has to be capable of resisting the test loads without affecting the performance of the specimen tested.
- A.2.2 The outdoor side of the specimen shall face the higher pressure side for positive pressure and the indoor side of the specimens shall face the higher pressure side of negative pressure.
- A.2.3 The number, spacing and type of connectors must be established according to the manufacturer instructions.
- A.2.4 A deflection measuring system will be attached to the specimens at the maximum points of deflection. The system shall measure the deflections within a tolerance of 0.01 of an inch.
- A.2.4.1 The permissible deflection for shutters at its maximum point of deflection will correspond to a value equal to $SPAN / 30$.

B. Required Tests

B.1 Missile Impact

- B.1.1 *Scope* - Test procedures to determine resistance of storm shutters and panels to hurricane windborne debris shall be performed according to this section.
- B.1.2 *Large missile impact test*
- B.1.2.1 This test applies to shutters and panels to be installed at location up to and including 30 feet in elevation from ground surface.
- B.1.2.2 The large missile will consist of a piece of wood with nominal dimensions of 2" x 4". The weight of the missile must be 9 pounds and have a length of not less than 7 feet and not more than 9 feet. It may be propelled through a cannon as described in section B.1.2.4.

B.1.2.3 Each specimen must receive two impacts. The first impact shall be located at the center of the specimen, or the weakest area of the specimen near the center, and the second impact shall be located at the corner of the specimen 6 inches from the supporting members.

B.1.2.4 The large missile cannon will use compressed air or springs to propel the large missile. The cannon must be capable of producing the missile impact velocity of 50 ft/s (34 mph). For the compressed air cannon the principal components are: an air compressor, a release valve, a barrel, a pressure gauge, a support base and a velocity reading system. The barrel shall consist of a 4-inch inside diameter pipe and be at least as long as the missile. The cannon has to be mounted on a support base in a manner that the desired target location at the specimens may be hit. The distance from the end of the cannon to the specimens must be at least 9 feet plus the length of the missile.

B.1.3 *Small missile impact test*

B.1.3.1 This test applies to shutters and panels to be installed at locations above 30 feet in height from ground surface. The small missile test may not be used if the effects on shutter and panels are less severe compared to the large missile test.

B.1.3.2 The small missile test consists of a cluster of gravel with a nominal diameter range between 0.5 inches to 0.75 inches, weighing approximately 0.0044 pounds (2grams). It must be propelled through cannon as described in section B.1.3.4.

B.1.3.3 Each specimen will receive thirty (30) small missile impacts. The first ten are distributed over an area of two (2) square foot located at the center of the specimen or the weakest area of the specimen near the center. The second ten

(10) will be distributed over an area of two (2) square foot located at the center of the long dimension of the specimen near the edge. The third ten (10) will be distributed over an area of two square foot located at the corner of the specimen.

B.1.3.4 The small missile cannon will use compressed air or springs to propel the small missile. The cannon must be capable of producing the missile impact velocity of 80 ft/s (54.5 mph). For the compressed air cannon the principal components are the same as the large air cannon. The barrel shall consist of a 2-inch inside pipe.

B.2 Uniform Static Air Pressure Test

B.2.1. *Scope* - Test procedures for determining resistance to wind forces of storm shutters and panels must be performed according to this section as determined in Chapter VI of the ASCE Standard, ASCE (2006), “Minimum Design Loads for Buildings and Other Structures”, ASCE 7-05.

B.2.2 The device used for the application of load shall have the capacity to obtain the load magnitude calculated on section B.2.3.

B.2.3 The test load is calculated using the equation 6-2 given in the ASCE Standard, ASCE 7-05. See Table 4-1.

B.2.4 Factors such as: adjustment for building height and exposure (λ), topographic effect, (K_{zt}), importance (I), and simplify design wind pressure (p_{s30}); must be used according to the ASCE Standard, ASCE 7-05. Those factors shall comply with the site conditions where the specimens will be installed.

Table 4-1. Test loads, based on ASCE Standard, ASCE (2006).

| Height from ground elevation (ft) | Net Design pressure (p_{net30}) Positive* (lb/ft ²) | Net Design pressure (p_{net30}) Negative* (lb/ft ²) | Importance Factor, I | Wind pressure based on Exposure Categories | | | | | |
|-----------------------------------|---|---|----------------------|--|--------------------------------|--------------------------------|--------------------------------|--------------------------------|--------------------------------|
| | | | | B | | C | | D | |
| | | | | Positive (lb/ft ²) | Negative (lb/ft ²) | Positive (lb/ft ²) | Negative (lb/ft ²) | Positive (lb/ft ²) | Negative (lb/ft ²) |
| 0 - 15 | 33.9 | -42.7 | 1 | 33.9 | -42.7 | 41.0 | -51.7 | 49.8 | -62.8 |
| | | | 1.15 | 39.0 | -49.1 | 47.2 | -59.4 | 57.3 | -72.2 |
| 20 | 33.9 | -42.7 | 1 | 33.9 | -42.7 | 43.7 | -55.1 | 52.5 | -66.2 |
| | | | 1.15 | 39.0 | -49.1 | 50.3 | -63.3 | 60.4 | -76.1 |
| 25 | 33.9 | -42.7 | 1 | 33.9 | -42.7 | 45.8 | -57.6 | 54.6 | -68.7 |
| | | | 1.15 | 39.0 | -49.1 | 52.6 | -66.3 | 62.8 | -79.1 |
| 30 | 33.9 | -42.7 | 1 | 33.9 | -42.7 | 47.5 | -59.8 | 56.3 | -70.9 |
| | | | 1.15 | 39.0 | -49.1 | 54.6 | -68.7 | 64.7 | -81.5 |
| 35 | 33.9 | -42.7 | 1 | 35.6 | -44.8 | 49.2 | -61.9 | 57.6 | -72.6 |
| | | | 1.15 | 40.9 | -51.6 | 56.5 | -71.2 | 66.3 | -83.5 |
| 40 | 33.9 | -42.7 | 1 | 37.0 | -46.5 | 50.5 | -63.6 | 59.0 | -74.3 |
| | | | 1.15 | 42.5 | -53.5 | 58.1 | -73.2 | 67.8 | -85.4 |
| 45 | 33.9 | -42.7 | 1 | 38.0 | -47.8 | 51.9 | -65.3 | 60.3 | -76.0 |
| | | | 1.15 | 43.7 | -55.0 | 59.6 | -75.1 | 69.4 | -87.4 |
| 50 | 33.9 | -42.7 | 1 | 39.3 | -49.5 | 52.9 | -66.6 | 61.4 | -77.3 |
| | | | 1.15 | 45.2 | -57.0 | 60.8 | -76.6 | 70.6 | -88.9 |
| 55 | 33.9 | -42.7 | 1 | 40.3 | -50.8 | 53.9 | -67.9 | 62.4 | -78.6 |
| | | | 1.15 | 46.4 | -58.4 | 62.0 | -78.1 | 71.7 | -90.4 |
| 60 | 33.9 | -42.7 | 1 | 41.4 | -52.1 | 54.9 | -69.2 | 63.4 | -79.8 |
| | | | 1.15 | 47.6 | -59.9 | 63.2 | -79.6 | 72.9 | -91.8 |

* Net design wind pressure (p_{net30}) calculated for an effective wind area of 50 ft².

B.2.5 Application of load

B.2.5.1 Apply the load with any device that can sustain a uniform static pressure for a minimum time period of one minute.

B.2.5.2 Release the load and record all readings after a recovery period of not less than 1 minute and no more than 5 minutes.

B.2.5.3 The static pressure test must be done for pressure and suction.

B.3 Repetitive Uniform Air Pressure Test

B.3.1. *Scope* - Test procedures for determining resistance to repetitive wind forces of storm shutters and panels shall be performed according to this section.

B.3.2 The device used for the application of load must be able to apply the repetitive loads to specimens specified on Table 4-2.

Table 4-2. Repetitive Pressure Loading

| Pressure | | Suction | |
|--------------------------------|-------------------|--------------------------------|-------------------|
| Range | No. of Repetition | Range | No. of Repetition |
| 0.2 P_{max} to 0.5 P_{max} | 3500 | 0.5 P_{max} to 1.0 P_{max} | 50 |
| 0.0 P_{max} to 0.6 P_{max} | 300 | 0.5 P_{max} to 0.8 P_{max} | 1050 |
| 0.5 P_{max} to 0.8 P_{max} | 600 | 0.0 P_{max} to 0.6 P_{max} | 50 |
| 0.3 P_{max} to 1.0 P_{max} | 100 | 0.2 P_{max} to 0.5 P_{max} | 3350 |

Note: P_{max} denotes maximum design load in pressure or in suction in accordance with Table 4-1.

C. Information to be reported

- C.1 Date of the test.
- C.2 Information of person or entity requiring of the test.
- C.3 Information of the specimen (manufacturer, material, dimensions, model type, condition prior to testing and any other pertinent information).
- C.4 Drawings of the specimens showing section profiles, panel arrangements, system of attachments, and any other pertinent construction details.
- C.5 Maximum deflection recorded and description of the system used to make such determination.
- C.6 Permanent deflection and description of the location where it occurred.
- C.7 Maximum positive and negative pressures used in the test.
- C.8 Locations of impacts on test specimens.
- C.9 Description of large and small missiles such as: velocities, weight and length.
- C.10 Observations and recommendations.

Chapter V

Analytical Study of Storm Shutters Behavior due to Impact Loads

5.1 Introduction

This chapter describes the different steps necessary to define an analytical model that will represent a storm shutter assembly. Based on the physical characteristics of a tested assembly a model was developed to simulate the dynamic impact event that occurred during the test. These characteristics were defined as parameters and incorporated into the model. A general purposed finite element code ABAQUS (Hibbit, Karlson & Sorensen, 1997) was used to perform the structural analysis.

The current study has found that the storm shutter assembly tends to vibrate as a respond to the impact load. The panels showed a series of oscillations that make difficult to establish the final results of the event. Thus a frequency analysis was performed to introduce damping into the model.

The accuracy of the results was influenced by the size of the meshes and type of element used in the analysis. A convergence analysis was carried out to define the total number of elements that provided the best results. A total of five meshes were evaluated in the current study. In addition, three models were developed using the shell elements provided by ABAQUS.

Finally, a model consisting of three panels was analyzed to validate its results with the ones obtained on the tested assembly.

5.2 Definition of Storm Shutter System

The first step to develop the proposed model is to establish the most relevant parameters that will be used to represent the real behavior of the system. Information related to the material and physical properties, boundary conditions and geometric configuration of panels is used to develop an analytical model using ABAQUS (Hibbit, Karlson & Sorensen, 1997). The shutter assembly used on Test #1 was selected to represent a real system as described on Chapter III. The required parameters to perform the initial modeling process were based on it.

5.2.1 Panel Material

A survey was carried out to establish the most typical material used in the fabrication of storm shutters panels. It was found that aluminum alloys and galvanized steel are the most commonly used materials for this purpose. Some characteristics such as light weight, structural capacity, easy handling and storage, and low fabrication costs, are the primary considerations that manufacturers use to prefer those materials.

Test 1 was performed with aluminum panels based on allow 3003-H14. Table 5.1 shows some of the material and physical properties which define the panels used in the tested assembly. A stress-strain curve based in the mechanical properties of aluminum allows

3003-H14 was developed to consider the non-linear behavior of the material during the simulation.

Table 5.1. Mechanical and physical properties for aluminum panels.

| Parameter | Description |
|---------------------------|---------------------------|
| Aluminum Alloy | 3003-H14 |
| Density | 0.0986 lb/in ³ |
| Thickness | 0.0630 in |
| Modulus of Elasticity | 10,000.00 ksi |
| Tensile Yield Strength | 21,000.00 psi |
| Ultimate Tensile Strength | 22,000.00 psi |
| Poisson Ratio | 0.33 |
| Length | 7'-2" |
| Thickness | 0.063" |

One of the constraints imposed by ABAQUS is the use of true values versus engineering values. The engineering stress-strain curve does not give a true indication of the deformation of the metal because it is based in the original cross section during the deformation process (Boyer, 1987). However, if constancy of volume and an homogeneous distribution of strain are assumed, one will express the true stress, σ , and true strain, ε , in terms of engineering values, by:

$$\sigma = \frac{P}{A_0}(e + 1) = s(e + 1) \quad (5.1)$$

$$\varepsilon = \ln(e + 1) \quad (5.2)$$

where:

e = average linear strain, in/in

P = axial load, lb

A_0 = original cross-section, in²

s = engineering stress, lb/in²

Both equations should be used until the onset of necking. Beyond the maximum load, the true stress and strain should be determined from actual cross section area. The stress-strain curve necessary to define the material model under analysis is shown in Figure 5.1.

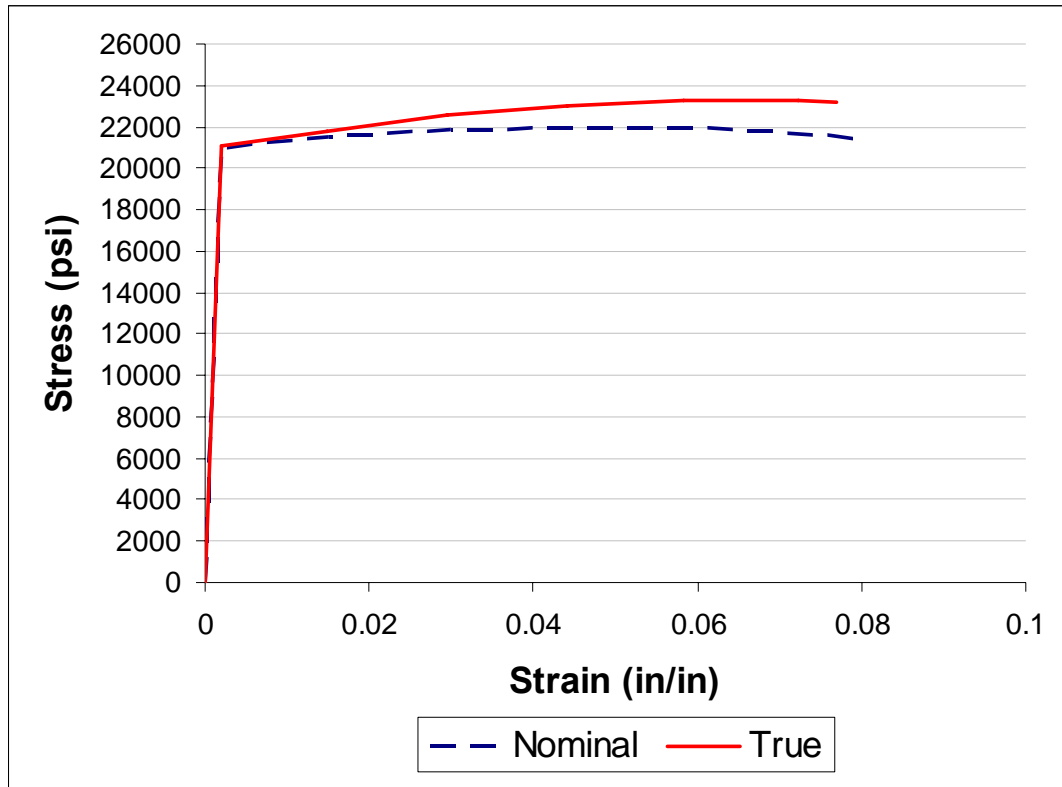


Figure 5-1. Aluminum 3003-H14 Stress-Strain Curve

In tri-dimensional states is necessary to define a surface based on the stresses combination whose produce the yielding of the material. ABAQUS use the Von Mises yield surface as the plasticity criteria during the analysis. Based on the defined stress-strain curve and Mises plasticity criteria, ABAQUS modify the stiffness matrix during the analysis to consider the plastic flow of the material.

5.2.2 Boundary Conditions

Typical storm shutter supports consists in the attachment of two aluminum beam sections at the opening edges of the wall to be covered. Once the aluminum sections are fixed to the wall, the storm panels are added to the system fixing both edges as shown in Figure 5-2. The upper edge is located inside the header or U type channel of the assembly. Once the upper edge is inside, the panel is prevented of moving out of the plane due to the contact provided by two sides of the channel. However the in-plane direction the panel is free to move. For modeling purposes, a representation of this condition is developed by using a roller support at the upper edge of the panel. A more complex definition of boundary condition is explained in Chapter VI.

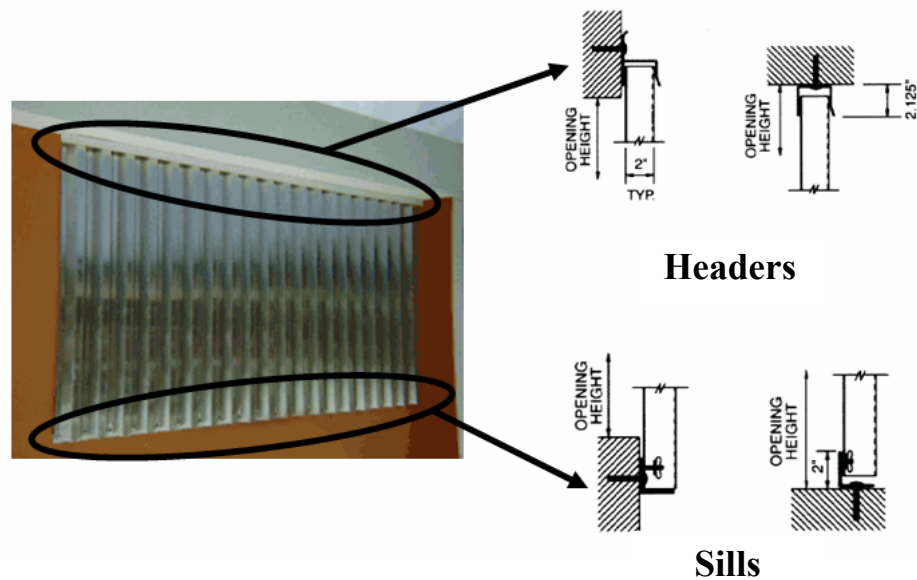
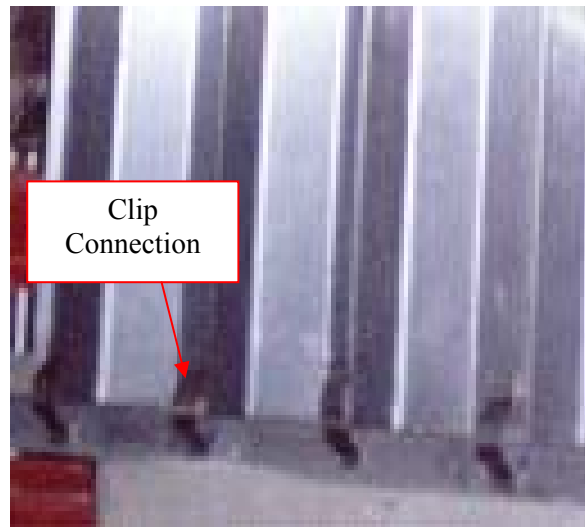


Figure 5-2. Typical Storm Shutters Assembly

In the case of the lower edge, the typical panels are attached to the system using clips as in Test 1, or bolts, washers and wing nuts as shown in Figure 5-3. For modeling purposes

a pin support is used to restrain any lateral displacement and facilitate a free rotation at the restrained zone. This condition represents the type of support used in the protection of doors. The aluminum section (angle) is connected to the floor such that the edge of the panels can be free to rotate same as a pin support.



(a)



(b)

Figure 5-3. Typical lower edge attachments devices: a) metal clips b) wing nuts and washers

5.2.3 Cross section

Each manufacturer may suggest a different geometrical configuration for the panels. The configuration or cross section has an effect in the physical behavior of the panel, especially in the moment of inertia affecting its structural capacity. Figure 5-4 shows the cross section of panels used on Test 1. For reference purpose the cross section have been called CST#1.

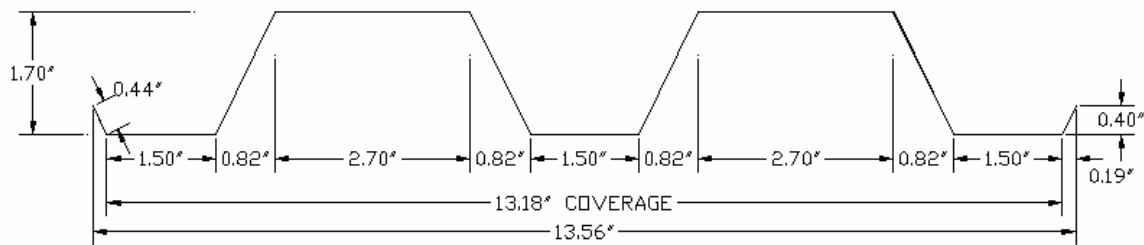


Figure 5-4. Cross section "CST#1" of shutter panels used on Test 1

5.2.4 Contact Interactions

The application of load to the system under investigation consists in establishing contact zones that transfer the forces produced by the windborne impact. ABAQUS (Hibbit, Karlson & Sorensen, 1997) has the capability of including special algorithms to account for the effect of contact interactions between surfaces. Three contact zones or contact pairs are specified in the simulation. Contact pairs are surfaces of bodies that could potentially be in contact. For a hard contact, a node on one surface is constrained without penetrating the other surface. The node with constrain is on the slave surface and the surface with which it

interacts is called the master surface. The nodes on the master surface can in principle penetrate the slave surface as can be the case of the missile.

As was mentioned above, three situations of contact pair are defined in the analysis. The first contact pair is the contact between the missile and the selected panel area to be impacted. Based in the physical behavior of this interaction, the missile is defined as the master surface and the panel as the slave surface as shown in Figure 5-5. The second contact pair is the contact produced between the storm panel edges in the assembly. As a standard procedure and previously mentioned on Chapter III, the panels are installed so that one of its edges is supported by the following panel, while the other one is free as shown in Figure 5-6. In this case, the definition of master-slave interaction is based in the level of mesh refinement. As a simple rule, the master surface is assigned to the finest mesh.

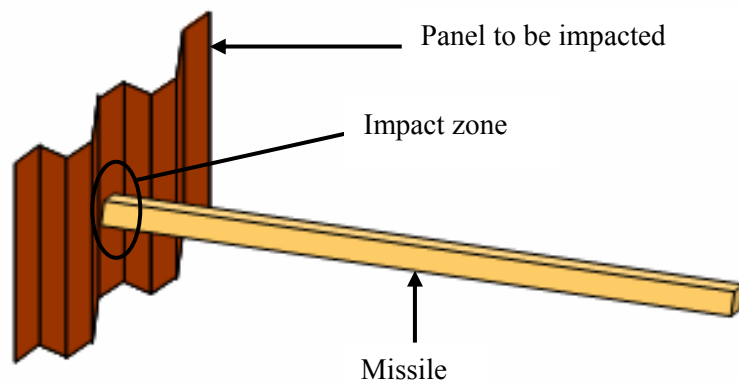


Figure 5-5. Contact pair between missile and panel

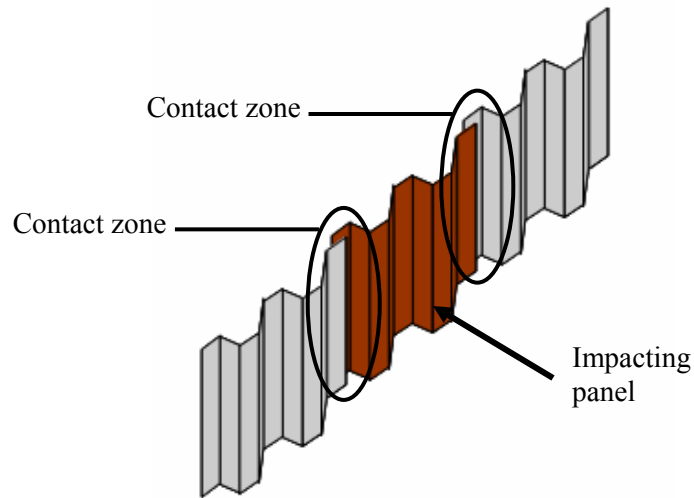


Figure 5-6. Contact pair between panels

The third contact pair is the contact produced between the upper edge zone of the panels and the header channel. As mentioned before, the upper edge of the sheets are embedded into the header channels such any out of plane movement is restrained. Therefore, surface contact is produced as the upper edge of the sheets move against the walls of the channel as a result of the applied impact load as shown in Figure 5-7. This contact pair was introduced in the more complex models.

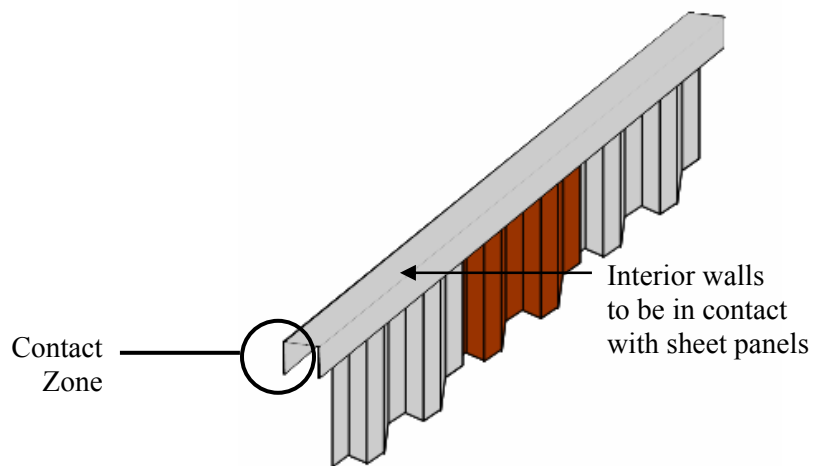


Figure 5-7. Contact pair between header and panels

5.2.5 Windborne definition

Many international authorities have developed a series of protocols oriented to testing storm shutters (ASTM, 1997). One of these protocols refers to the impact load test. The protocols include the definition of related materials, testing procedures, and testing facility requirements. As a testing material the protocols suggest the use of a 2”x 4” piece of wood as the most characteristic windborne debris material. A weight of 9 lb is established to perform the impact load test. The missile shall have a length of not less than 7 feet and not more than 9 feet. Nine feet length has been used for our study based in a specific mass density value as shown in Figure 5-8. Table 5-2 summarizes the physical and mechanical properties of the missile used in the model.



Figure 5-8. Missile used on Test 1

The protocols also indicate that the missile velocity to carry out the impact test shall be 50 ft/s (34.1 mph). This value and others are specified as relevant parameters to be considered as discussed on Chapter #6.

Table 5.2. Windborne Debris or Missile properties.

| Properties | Description |
|-------------------|--------------------------|
| Cross section | 2" x 4" |
| Length | 9' - 0" |
| Weight | 9 lb |
| Mass density | 0.013 lb/in ³ |

5.3 Model Generation

Once the most relevant parameters have been defined the next step is to incorporate these into the general purpose finite element code, ABAQUS. The geometry of the model is defined by organizing it into parts, which are positioned relative to one another in an assembly. For each part, the corresponding parameters are assigned according to its purpose into the model.

5.3.1 Model Assembly

The model under investigation consists of the assembly of three parts which are shown in Figure 5-9 to Figure 5-11. The storm shutter panels are defined by creating a part which is copied according to the number of panels to be evaluated. Another part, the missile, is created and copied once. The last part, the top header, is created as a series of connected flat plates which represent the header walls. Therefore, this part requires to be copied

according to the required length to fit the number of panels in the assembly. All characteristics (such as material and section definitions) indicated for a part becomes characteristic for each instance of that part. In ABAQUS (Hibbit, Karlson & Sorensen, 1997) copies of each part are called instances.

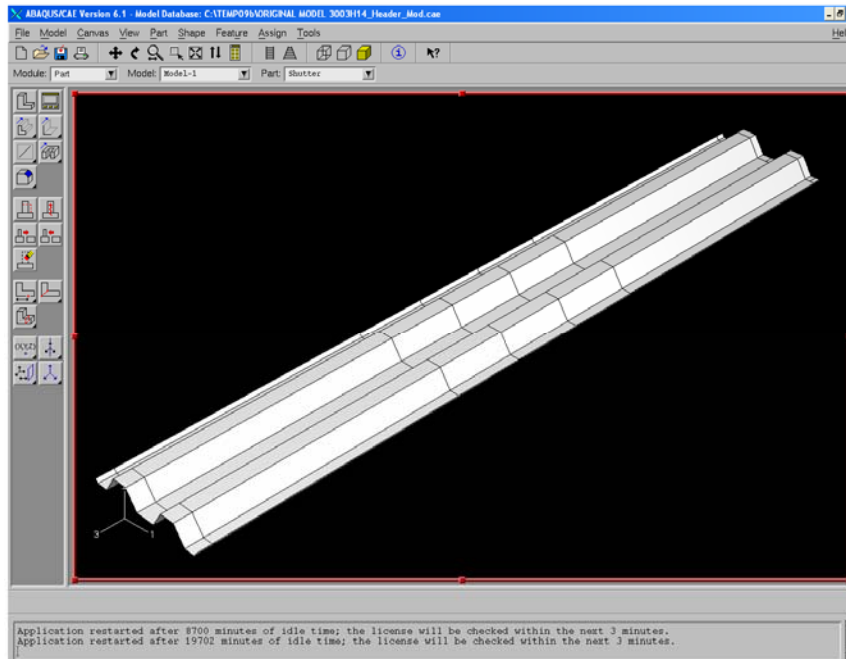


Figure 5-9. Screen showing in ABAQUS the part related to shutter panel

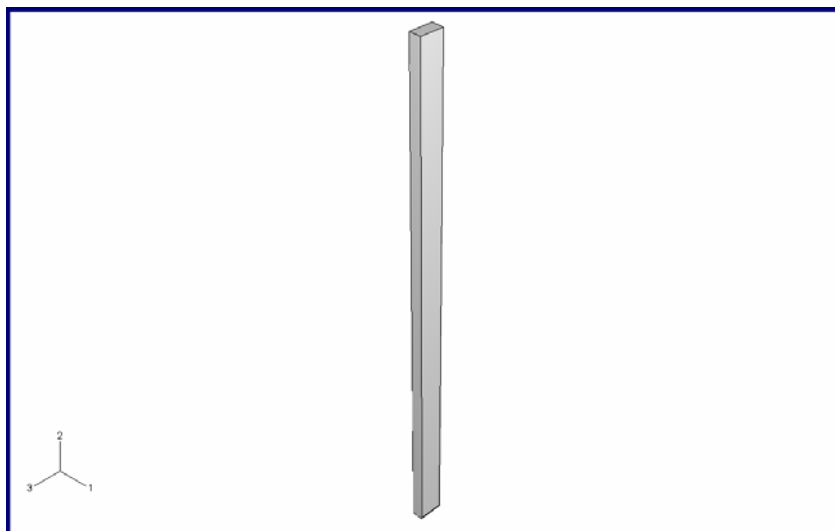


Figure 5-10. Part related to missile

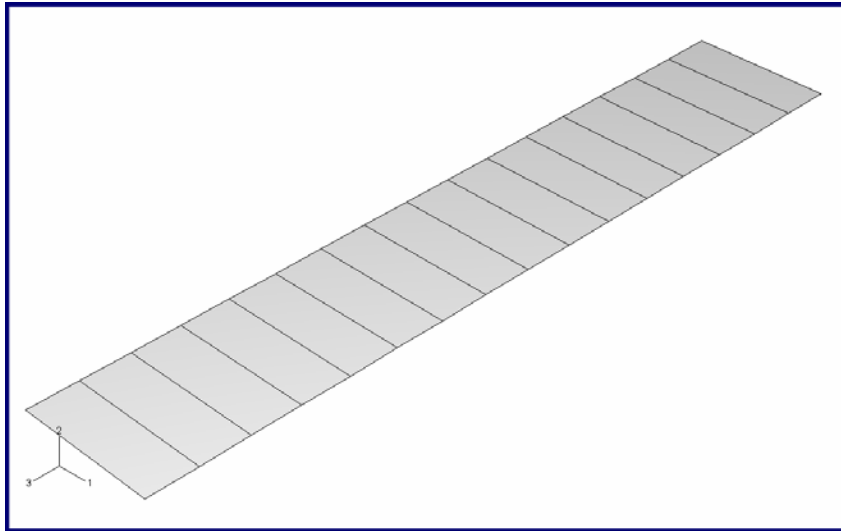


Figure 5-11. Part related to top header walls

Once the instances are positioned, some of them require to be partitioned. Partitions are used to specify points, edges and zones where parameters like boundary conditions, contact interactions and output request are required. Figure 5-12 and Table 5.3 shows the different partitions developed on the instance related to the shutter panels to be impacted.

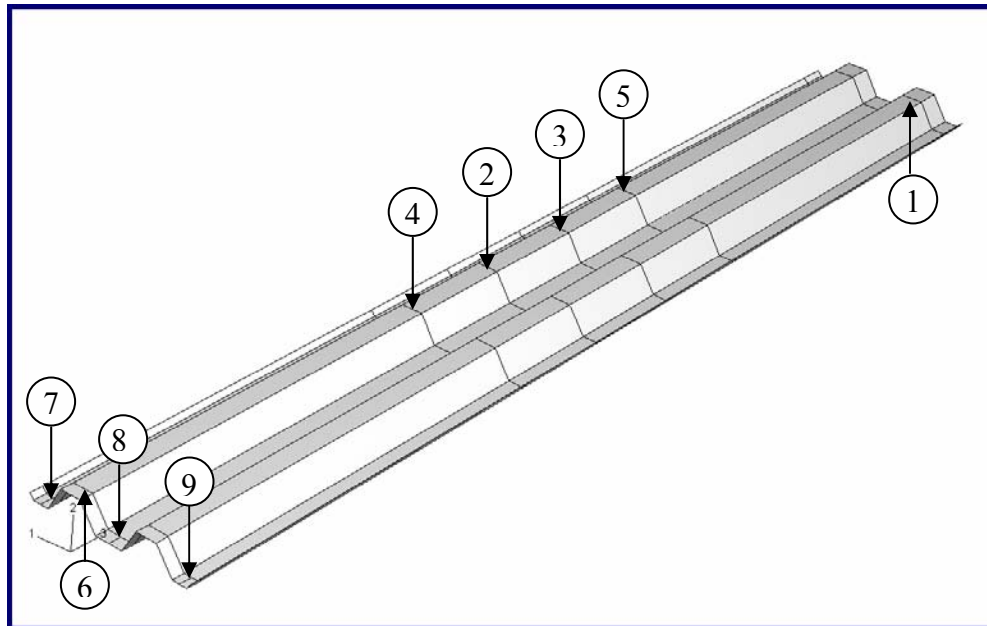


Figure 5-12. Partitions on the part related to shutter panel

Table 5.3. Partitions used on part related to shutter panel.

| Partition | Location | Description |
|------------------|---------------------|--|
| 1 | 2" from top edge | To provide the required zone such that contact surfaces related to top header and panels interaction are defined. |
| 2 | 6" above mid span | To provide the required area such tha contact surfaces related to missile and shutter intaraction are defined. To define a zone for a more dense meshing and output request. |
| 3 | 6" below mid span | To provide the required area such tha contact surfaces related to missile and shutter intaraction are defined. To define a zone for a more dense meshing and output request. |
| 4 | 15" above mid span | To provide a transition zone for element size adjustment between the defined zone by partitions 2 or 3 and the rest of the mesh. |
| 5 | 15" below mid span | To provide a transition zone for element size adjustment between the defined zone by patitions 2 or 3 and the rest of the mesh. |
| 6 | 1" from lower edge | To establish boundary conditions at lower edge with partitions #7, #8, and #9. |
| 7 | mid width of valley | To establish boundary conditions at lower edge (interception point with partition #6). |
| 8 | mid width of valley | To establish boundary conditions at lower edge (interception point with partition #6). |
| 9 | mid width of valley | To establish boundary conditions at lower edge (interception point with partition #6). |

Not all partitions are used in the model. For example, the part used to define shutter panels is instanced or copied according to the total of panels used in the system. Therefore, for instances that are not subjected to a direct impact load, partitions #2, #3, #4 and #5 are not used in the analysis.

In a typical assembly such as Test 1, adjacent panels provide some support only at one edge. Based in this argument, a simple model of two panels is used to represent this condition. Only instances related to shutter and missile components are incorporated as

initial step for modeling process. Figure 5-13 shows the instances which represents the proposed model.

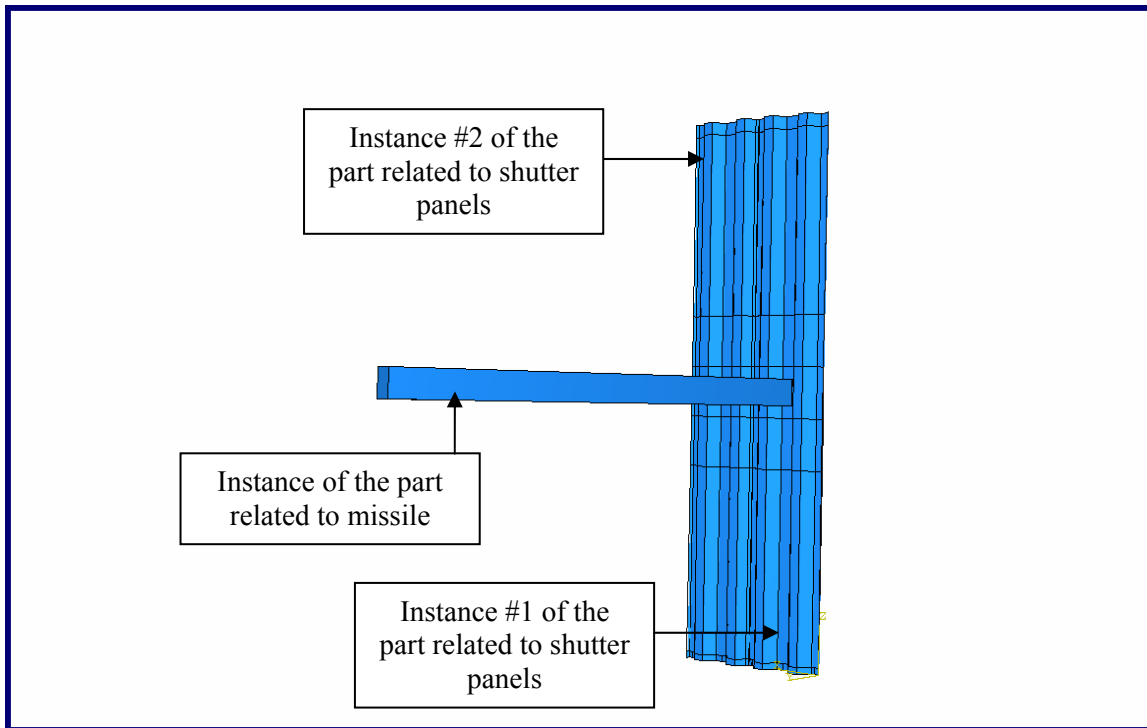


Figure 5-13 Instances used in the model.

5.3.2 Meshing

The panels are modeled with two finite element meshes, as shown Figure 5-14. The only difference between them is the number of elements used in each mesh generation. Other parameters are the same. As only one panel is subject to the missile impact, a high degree of refinement is required. A fine mesh provides more accurate results that are necessary due to the dynamic nature that define our simulation as further explained.

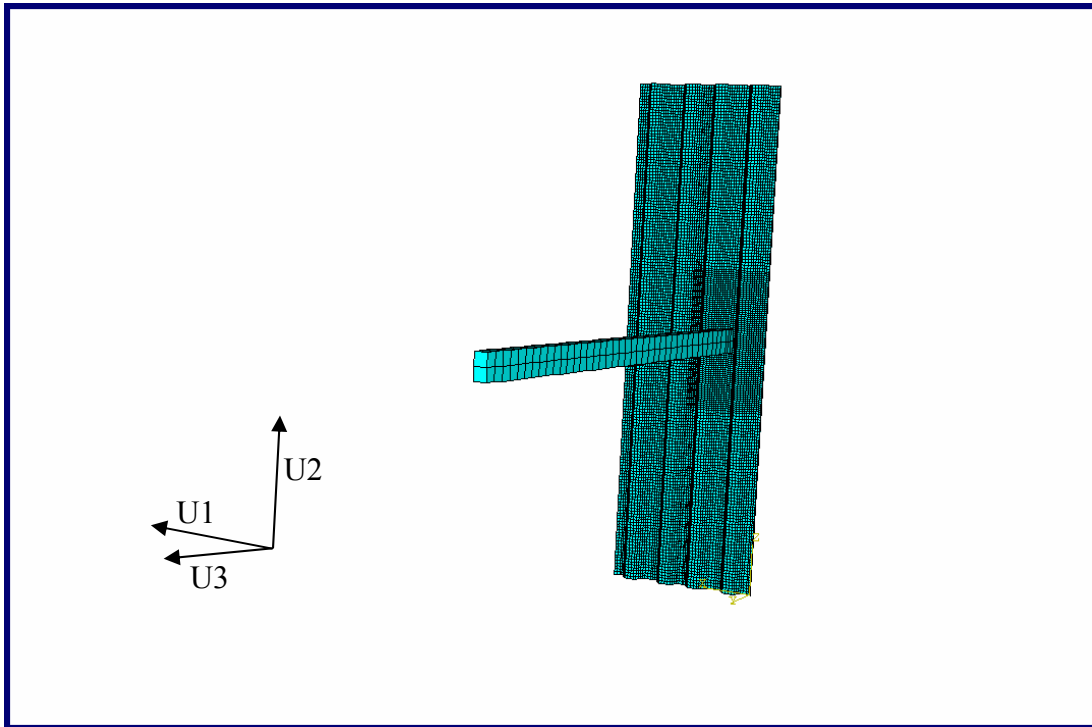


Figure 5-14. Example of Finite Element Mesh

In terms of the missile, a mesh consisting of hexahedral (“brick”) elements named C3D8R are used to obtain the necessary stiffness and mass transfer to the system by the impact action. The missile was located at an initial distance of 0.5 inches from the panel surface to be impacted as shown Figure 5-15. As the analysis of the missile behavior is not part of the study, the specified distance reduce the number of iterations required to perform the simulation.

During the mesh generation the number of elements is specified for every instance included in the model. For our study, the instance related to the panel to be impacted required a more dense mesh at the impact zone. As a result, a larger number of elements are contained in this zone than the rest of the mesh.

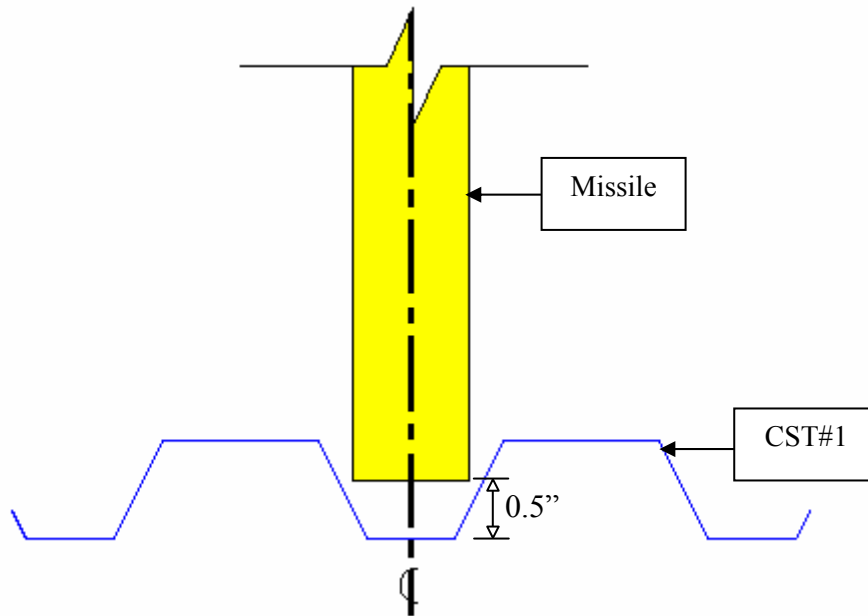


Figure 5-15. Initial missile location from impact zone

For each instance a maximum aspect ratio of 2:1 was used as a criterion to establish the size of the elements. Regardless of the degree of refinement required at specific zones the criterion was used for the complete mesh.

It's well known that in finite element analysis, the computational time and the accuracy of the results are influenced by the total elements used in the meshing generation. ABAQUS (Hibbit, Karlson & Sorensen, 1997) provides some techniques to establish the number of elements to be used for every instance. One of them is the creation of subdivision points called seeds as shown in Figure 5-16. Seeds are located along the instance edges to indicate where the corner nodes of the elements should be located. As the number of seeds is increased a higher degree of refinement is obtained during the mesh generation. Once the seeds are established a mesh is automatically created by ABAQUS. At this point a

verification of the aspect ratio of the elements is performed to comply with the defined criteria as it was previously explained. If the criterion is not satisfied then the mesh and seeds for the instance are removed and the process is repeated.

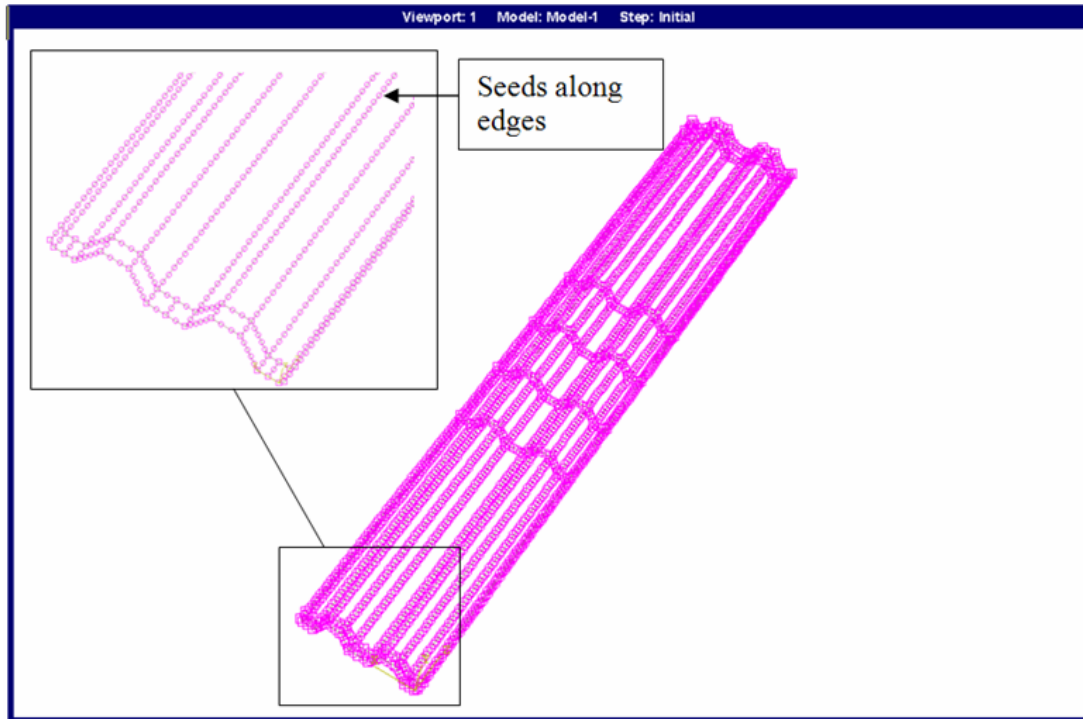


Figure 5-16. Seeds generation along instance edges

5.3.2.1 Frequency Analysis

In performing nonlinear analysis, it is appropriate to define a proportional damping matrix for the initial elastic state of the system and to assume that this damping property remains constant during the response even though the stiffness may change and cause hysteretic energy losses in addition to the viscous damping losses. A simple way to

formulate a proportional damping matrix is to make it proportional to either the mass or the stiffness matrix. ABAQUS provides “Rayleigh” damping for this purpose.

Rayleigh (Clough and Penzien, 1975) proposed the following relation, where two coefficients or matrix proportions are given by

$$\zeta_n = \frac{a_o}{2\omega_n} + \frac{a_1\omega_n}{2} \quad (5.3)$$

where:

a_o, a_1 = damping factors or proportionality factors

ζ_n = damping ratio for the n^{th} mode.

ω_n = natural frequency for the n^{th} mode.

If the damping ratios associated with different frequencies are known or assumed, then the two damping factors a_o and a_1 can be evaluated by the solution of simultaneous equations based in the Rayleigh relation (equation 5.3). Assuming that the same damping ratio applies to both frequencies, the proportionality factors are given by a simplified relation

$$\begin{Bmatrix} a_o \\ a_1 \end{Bmatrix} = \frac{2\zeta}{\omega_m + \omega_n} \begin{Bmatrix} \omega_m\omega_n \\ 1.0 \end{Bmatrix} \quad (5.4)$$

where ω_m typically is taken as the fundamental frequency of the system and ω_n is set among the higher frequencies of the modes that contribute significantly to the dynamic response.

Assuming a damping ratio in the first (ζ_1) and third (ζ_3) modes as 2 % of critical and performing a frequency analysis of the system, proportionality factors were obtain as shown in Table 5.4.

Table 5.4. Proportionality factors for a damped system.

| First Mode ω_m (rad/sec) | Frequency Third Mode ω_n (rad/sec) | Proportionality Factors | |
|------------------------------------|---|----------------------------|----------|
| | | a_o | a_l |
| 169.23 | 408.08 | 4.78 | 6.93E-05 |

Once the proportionality factors are obtained, the next step is to determine the system response to the introduction of critical damping. Two simulations were developed based on the proposed model and the different parameters already discussed. The only difference was the use of 2% of critical damping in one of them. Both simulations used the same finite element mesh. A time increment of 0.10 micro-seconds was established as the Δt to obtain the solution for an event of approximately 1.2 seconds with a missile velocity of 51.7 mph.

A free vibration behavior of the impact panel was obtained for the system without damping. As the panel continues its vibrations, the different oscillations make it difficult to define the permanent deformation at the end of the event. Meanwhile, the simulation containing 2% of critical damping showed a dissipation of the energy such that the permanent deformation would be defined as shown in Figure 5-17. Both simulations required a high computational time (114 hours) to obtain a solution in which the oscillations would be minimized. An event of 1.2 seconds was not enough to obtain a steady state of the panel.

The remaining simulations in our study were based on a shorter duration event. An event of 0.2 seconds was enough to obtain a good approximation of the permanent deformation of the impacted panel. In Chapter VI proportionality factor values are obtained and included in each model as part of the material properties under evaluation.

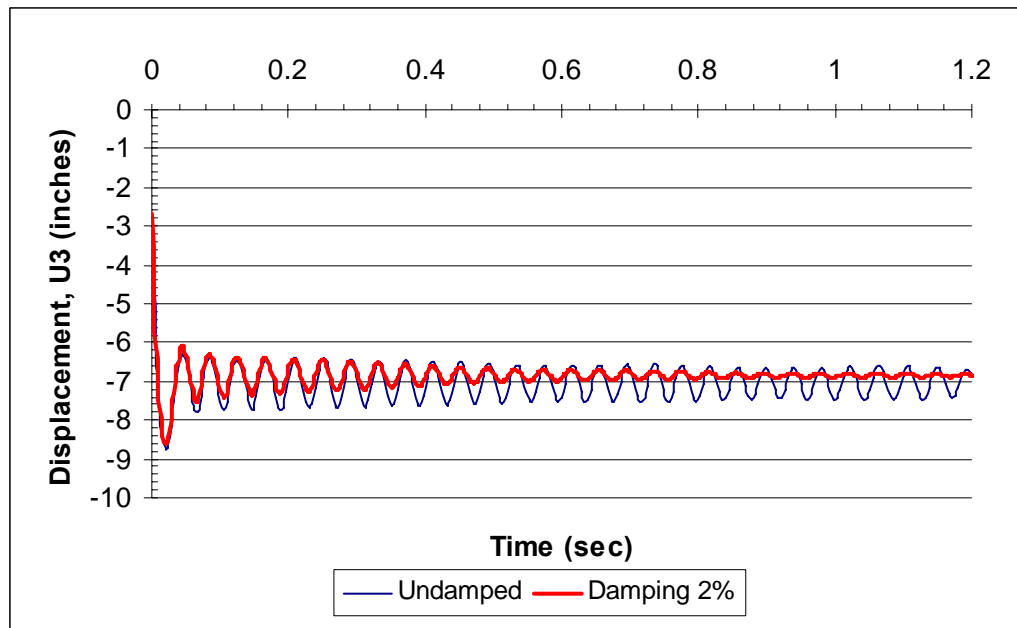


Figure 5-17. Effect of critical damping in main panel displacements

5.3.2.2 Convergence Analysis

A convergence analysis was developed to define the degree of refinement required for proposed model. For this purpose five simulations or cases were studied. The cases were defined using the same parameters. Only the number of elements used on the main panel varied for each case. A time increment of 0.10 micro-seconds was established as the Δt to obtain the solution for an event of approximately 0.20 seconds with a missile velocity of 51.7 mph. Shell finite elements named S4RS were used due to the reduction in computational time that provides their usage as is explained in section 5.3.3.

The first case consisted of generating two identical meshes to represent both panels as shown in Figure 5-18. A total of 6,817 elements were used for each mesh. The average element size (AES) for each element was 0.5 square inch.

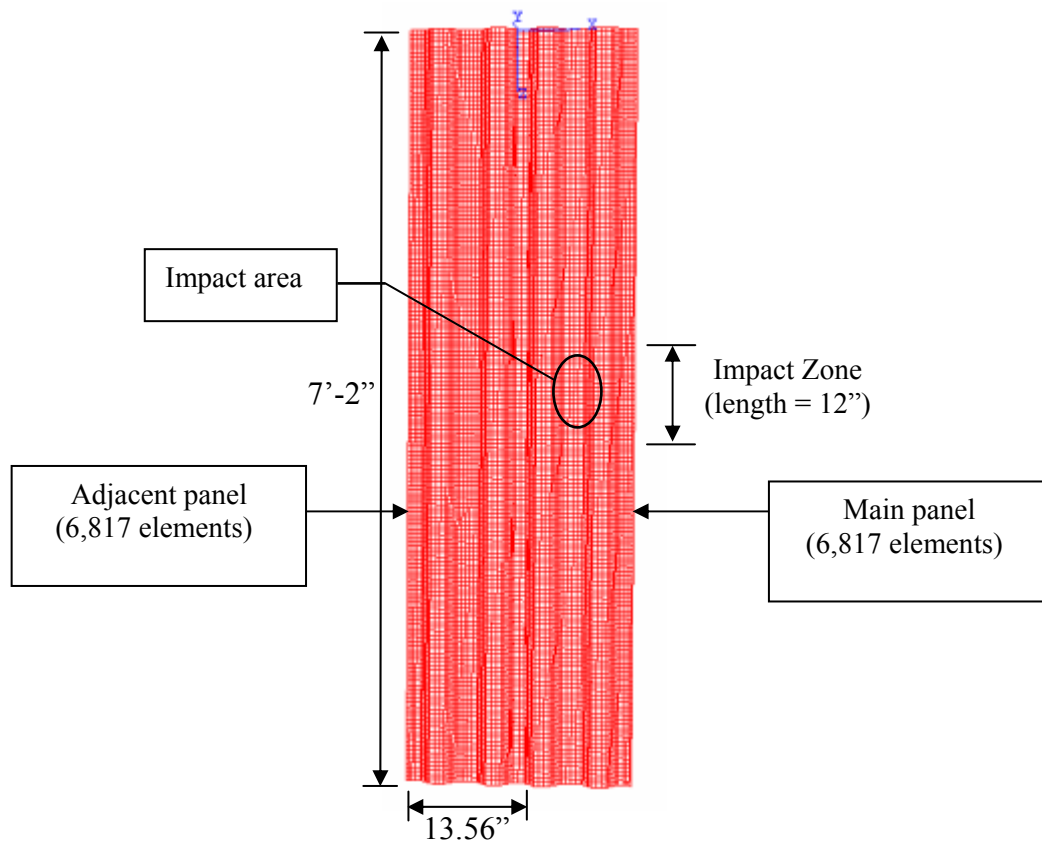


Figure 5-18. Model meshes used on Case #1

The second case consisted of defining a more dense area at the impact zone as shown in Figure 5-19. Therefore, a larger number of elements were required compared with the mesh used on the adjacent panel. At the impact area the AES was 0.35 square inch. For the rest of the mesh and the adjacent panel the AES was 0.50 square inch. A total of 8,973 elements were used on the main panel mesh. The number of elements for the adjacent panel mesh remained unchanged.

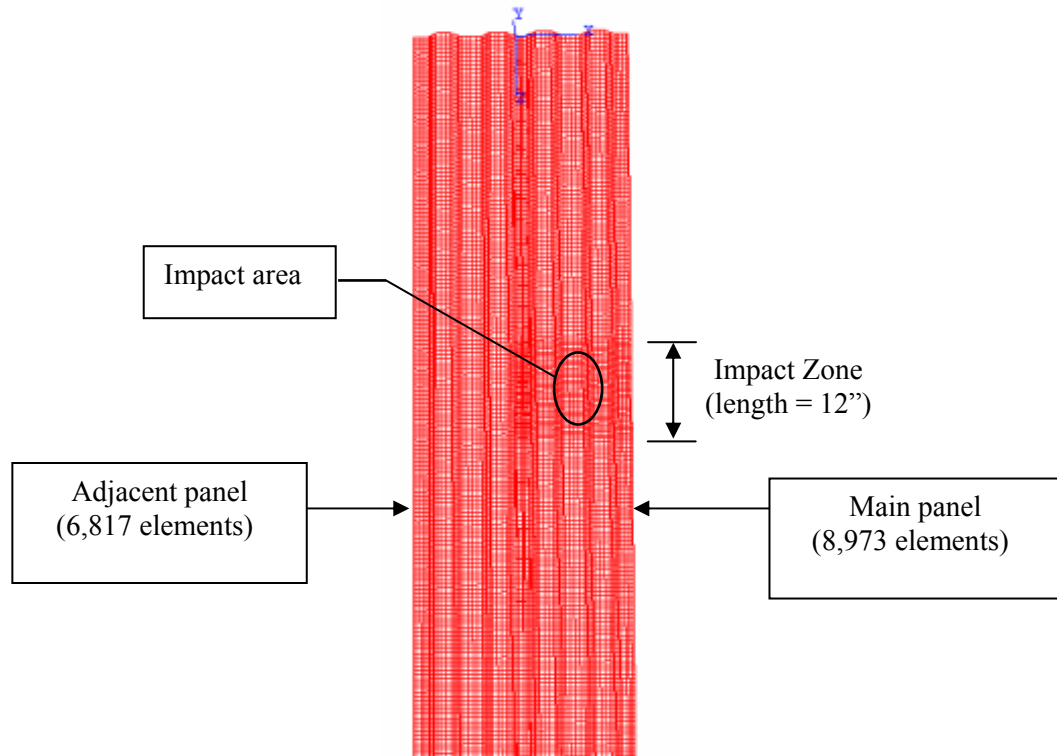


Figure 5-19. Model meshes used on Case #2

As a relevant decrease on element size was expected for the rest of the study, transition zones were added to the main instance. The use of transition zones facilitated the use of smaller size elements at the impact region avoiding any possible distortion failure for the rest of the mesh. Two zones were located at both sides of the impact area.

The third case consisted of defining a more dense area at the impact zone equal to the previous case. However, due to the defined AES, it required the use of transition zones as shown in Figure 5-20. At the impact area, for transition zones and the rest of the mesh, the AES was 0.20, 0.30, and 0.50 square inch, respectively. A total of 18,888 elements were

used on the main panel mesh. The number of elements for the adjacent panel mesh remained unchanged.

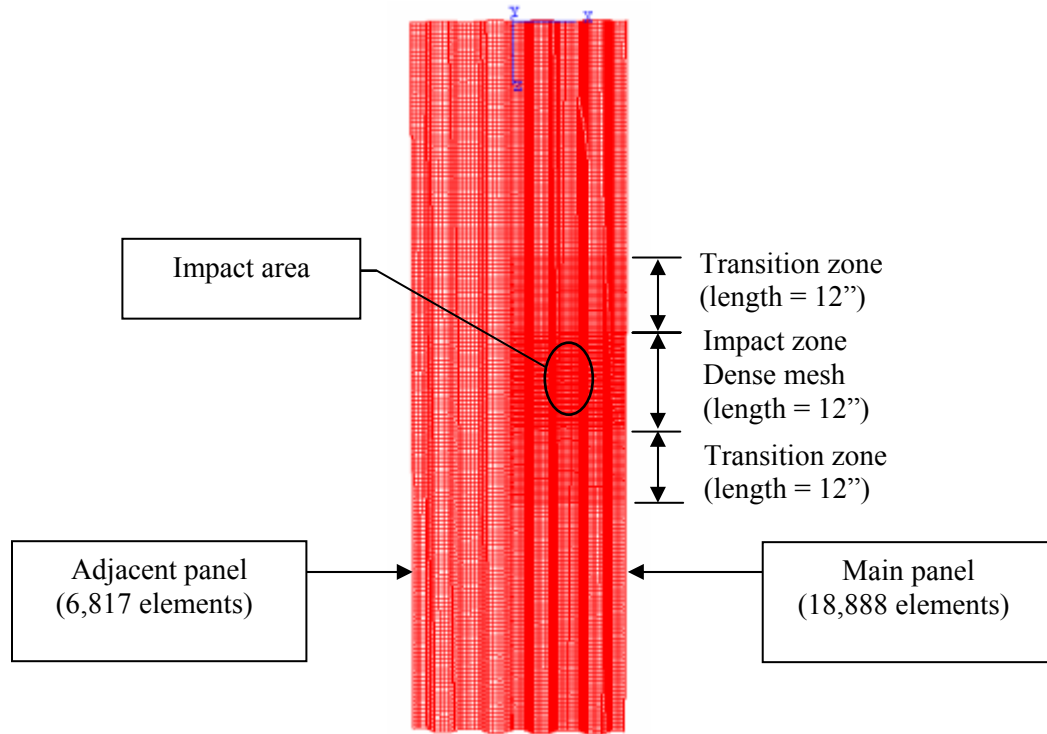


Figure 5-20. Model meshes used on Case #3

For the fourth case, a similar meshing arrangement as the third case was used. The only difference between both cases was the number of elements used for each region as shown in Figure 5-21. At the impact area, transition zones and rest for the mesh the AES was 0.20, 0.25, and 0.30 square inch, respectively.

For the fifth and last case, a smaller size of elements was used in comparison with the other simulations. As a result, the highest degree of refinement was evaluated for the main panel as shown in Figure 5-22. A mesh with an AES of 0.20 square inch was used.

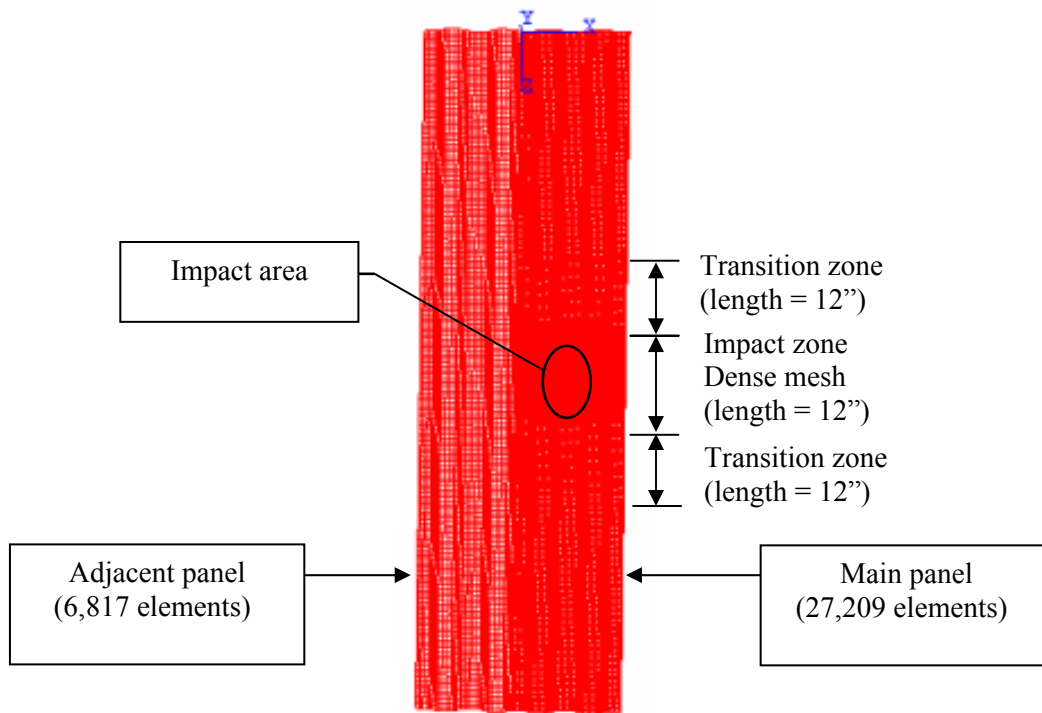


Figure 5-21. Model meshes used on Case #4

A sequence of deformation was observed for all cases as the missile impacted the main panel. First, the missile touches the main panel at the specified location and a process of a missile desacceleration begins. The kinematics energy of the missile is lost as the panels absorbed it producing a displacement of the section until a maximum value is reached. At this value the missile discontinued its movement against the panel as shown in Figure 5-23.

The missile begins a process of rebounding taking a reverse trajectory moving out of the plane of the system. The panels begin a vibration process with a series of oscillations as the storage energy is dissipated. This vibration behavior was evident during the rest of the simulation.

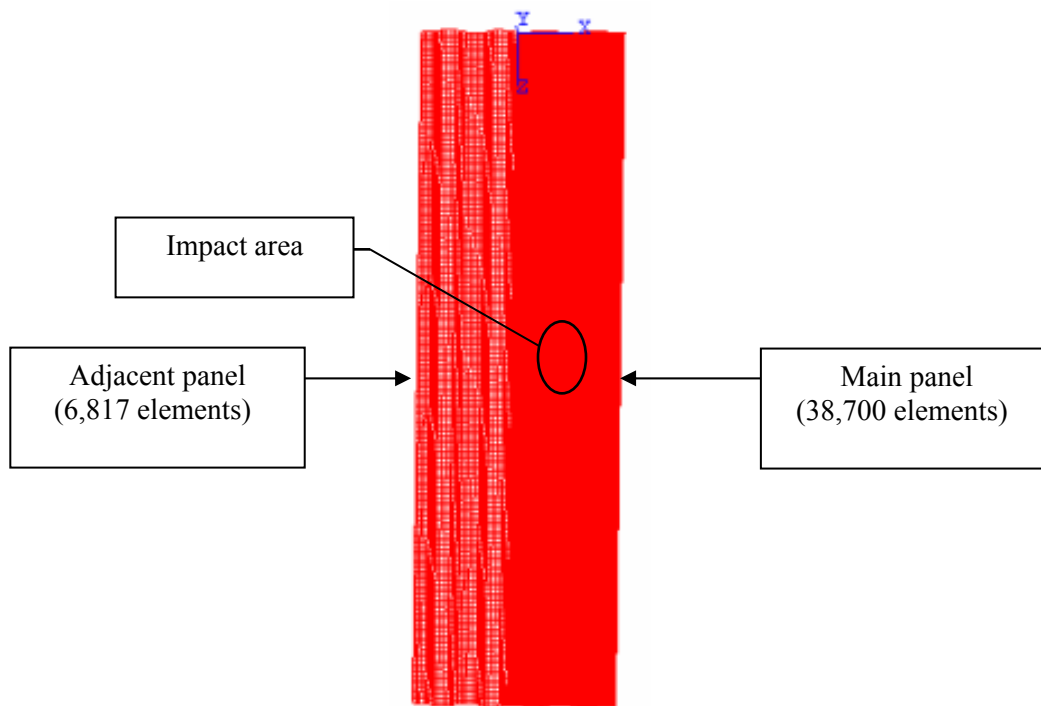


Figure 5-22. Model meshes used on Case #5

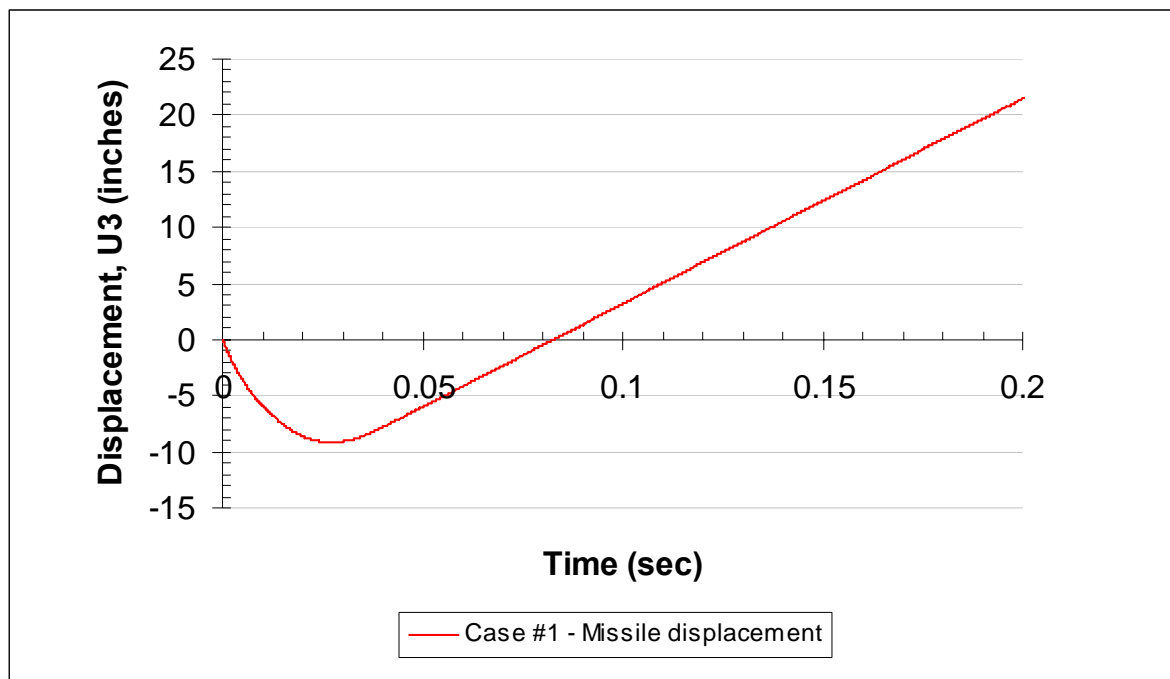


Figure 5-23. Missile displacement obtained in Case #1

Finally, a permanent deformation of the main panel is achieved. Figure 5-24 shows a typical simulation sequence of deformation as the solution for the complete event is obtained.

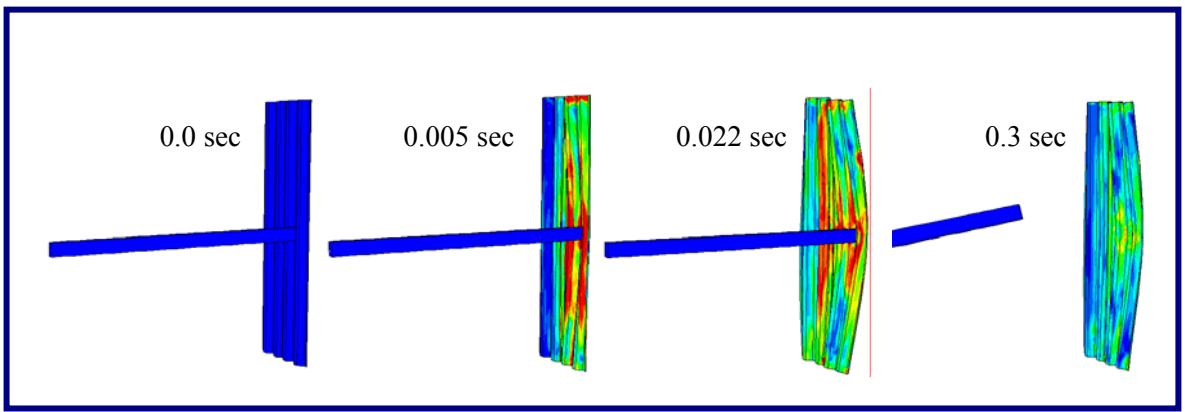


Figure 5-24. Impact Simulation Sequence

The maximum and permanent deformation values were obtained for each case as shown in Figure 5-25 and summarized in Table 5.5.

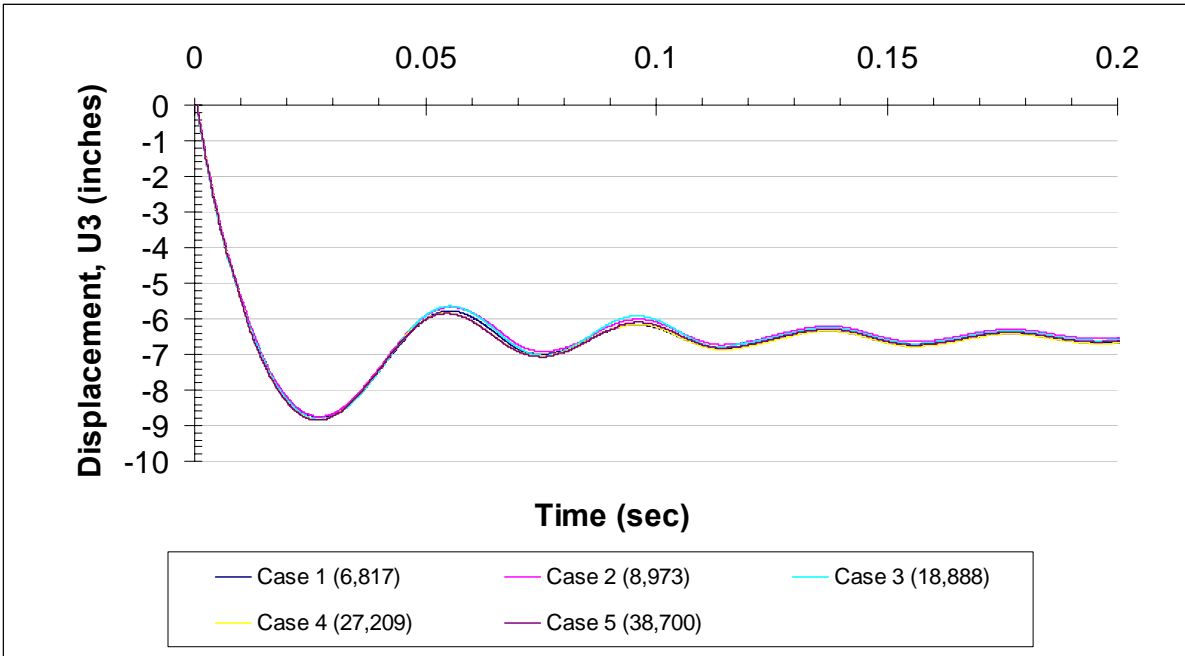


Figure 5-25. Convergence Analysis Results for Five Cases

Table 5.5. Summary of values obtained from the convergence analysis

| Case | No. of elements | | Maximum displacement U3 (inch) | Permanent displacement U3 (inch) | Required Run-time (hrs) | $\frac{\Delta U3_{max}}{\Delta Time Req.}$ |
|------|-----------------|----------------|--------------------------------|----------------------------------|-------------------------|--|
| | Main panel | Adjacent Panel | | | | |
| 1 | 6,817 | 6,817 | 8.68 | 6.57 | 22.0 | - |
| 2 | 8,973 | 6,817 | 8.75 | 6.55 | 35.0 | 0.0055 |
| 3 | 18,888 | 6,817 | 8.82 | 6.60 | 51.5 | 0.0043 |
| 4 | 27,709 | 6,817 | 8.84 | 6.68 | 75.0 | 0.0009 |
| 5 | 38,700 | 6,817 | 8.85 | 6.63 | 101.0 | 0.0003 |

The maximum deflection obtained at the main panel was 8.85 inches. In terms of the permanent deformation a value of 6.68 inches was obtained. However, a value of 6.61 inches was obtained if an average permanent deformation value is calculated among the studied cases. It is important to note that a measured value of 6.5 inches was recorded as the permanent deformation of the panel used on Test 1 as was mentioned in Chapter III. This average value is only 1.5% greater than the real value observed. Therefore, it can be concluded that the proposed model can be used as a simple representation of the shutter system to investigate its behavior under impact loads.

The results showed a tendency to reduce the difference between them when a mesh with a number of elements equal or greater than Case #3 was used as shows Figure 5-26. Only, a difference of 0.0009 was obtained between Case #3 and Case#4. Case #3 established the starting point to obtain a stable solution in the analysis. The slope of the curve tends to become flat from this point. Therefore, convergence was reached based on the number of finite elements used to define the impact panel mesh.

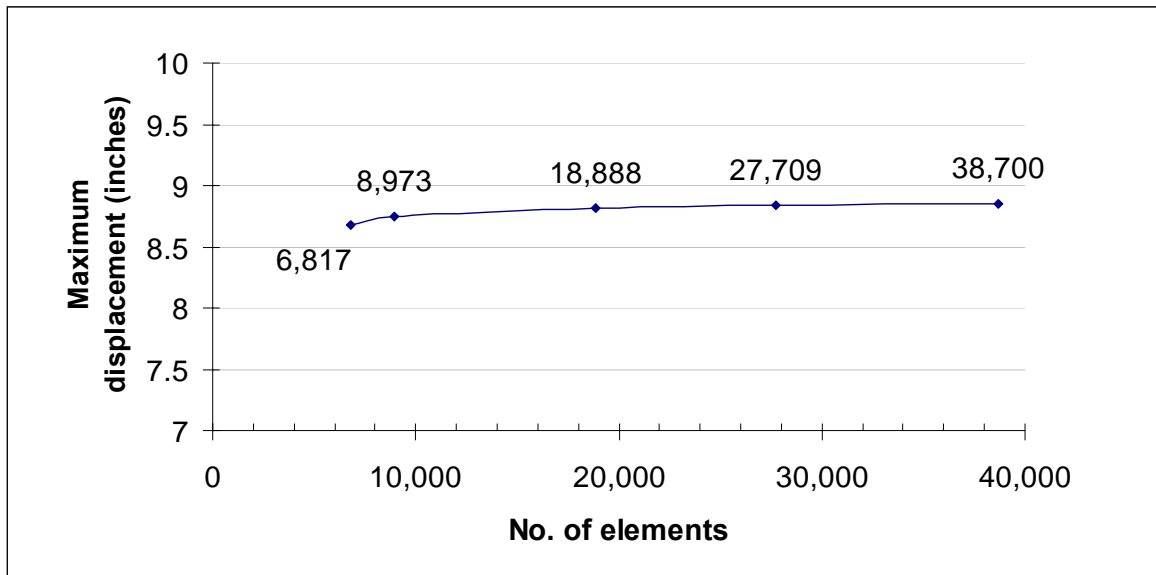


Figure 5-26. Maximum deformation vs. number of elements

In addition, Case #3 values were close to the cases with the highest degree of refinement but the computational time required to be performed was less. Based on these arguments, Case #3 was selected to define the meshing generation criteria for future models.

5.3.3 Shell finite elements

Storm panels are thin in comparison with their span. Shell elements are used to model structures in which one dimension, the thickness, is significantly smaller than other dimensions. Conventional shell elements use this condition to discretize a body by defining the geometry at a reference surface. In this case the thickness is defined through the section property definition.

ABAQUS provides a shell element library that is used according to the modeling purpose and the element formulations. Stress and deformation theory, strain and

displacement relationships, degrees of freedoms and numerical integration methods are some of the relevant aspects to be considered in the selection of finite elements.

Permanent deformations of panels are expected as a result of impact loads. Therefore, a nonlinear dynamic analysis is required to simulate the behavior of shutters under the effect of missile loads. Based on material properties as stress–strain curves, constitutive relationship is established such that non linearity of material is evaluated. In terms of kinematics formulations, ABAQUS (Hibbit, Karlson & Sorensen, 1997) provides some alternatives that are included in the shell element formulation. Table 5.6 shows a summary of the most relevant aspects of shell elements that are available in ABAQUS to perform a dynamic analysis.

Table 5.6. Shell finite elements

| Element Name | Number of nodes | Degrees of Freedom | Formulation |
|---------------------|------------------------|---------------------------|---|
| S4RS | 4 | 6 | small - strain formulation with large rotations |
| S4RSW | 4 | 6 | small - strain formulation with large rotations and warping effects |
| S4R | 4 | 6 | large - strain formulation with large rotations |

Storm shutter panels will experience a high membrane action during the applied loads under scope. In fact, panels are expected to suffer large deformations due to the nonlinearity behavior during the analysis. Thus, large strain formulation seems to be recommended. However, each formulation has a significant effect on the time required to complete the analysis.

As previously mentioned, the convergence analysis was developed using small-strain shell elements. The small-strain shell elements in ABAQUS use a Mindlin-Reissner type of flexural theory that includes transverse shear and are based on a corotational velocity-strain formulation described by Belytschko (et al., 1984). A corotational finite element formulation reduces the complexities of nonlinear mechanics by embedding a local coordinate system in each element at the sampling point of that element. By expressing the element kinematics in a local coordinate frame, the number of computations is reduced substantially. Therefore, the corotational velocity-strain formulation provides significant speed advantages in explicit time integration software, where element computations can dominate during the overall solution process.

S4RS and S4RW are small-strain shell elements based in the Belytschko formulation. S4RS element was developed to obtain a convergent and stable element with the minimum number of computations. Because of the emphasis on speed, a few simplifications were made in formulating the equations for the S4RS elements. Although the S4RS element performs very well in most practical applications, it has one major weakness. It can perform poorly when is distorted. Otherwise, S4RSW element was formulated with additional terms added to the strain-displacement equations.

S4R shell elements account for finite membrane strains and arbitrarily large rotations; therefore, they are suitable for large-strain analysis. As small-strain elements, S4R elements use reduced (lower-order) integration to form the element stiffness. The mass matrix and distributed loadings are still integrated exactly. Reduced integration usually provides more accurate results and significantly reduces running time, especially in three dimensions.

A comparative analysis was performed to study the additional kinematics formulations provided by ABAQUS. Based on the proposed model, two new simulations were developed containing S4RW and S4R shell elements. The effect of different kinematics formulations and the measure of the computational time required to perform the analysis was studied for each one. The only difference between the simulations was the shell element assigned to the model. The meshing arrangement for both simulations was based in the meshing criteria established as a result of the convergence analysis discussed in the previous section.

The maximum and permanent deformations for the main panel were slightly affected by the use of S4RW shell elements. However, a significant increase in both results was obtained under the use of S4R shell elements. Figure 5-27 and Table 5-7, shows the results obtained as the proposed model is defined with different shells elements available in ABAQUS.

It is important to note that high levels of load are applied to the panel in a short period of time. This situation tends to produce a distortion behavior of the elements which are located at the impact zone and the edges of the panel. From previous analysis, it was found that the distortion of elements is minimized when a well defined mesh is used to perform the simulation.

However, as S4RS elements are based in a kinematics formulation which do not responds very well to warping behavior and some errors can be induced in the final results. Meanwhile, S4RW was developed to cover this weakness of S4RS. These arguments explain the reduction in the results obtained between the uses of small-strain shell elements.

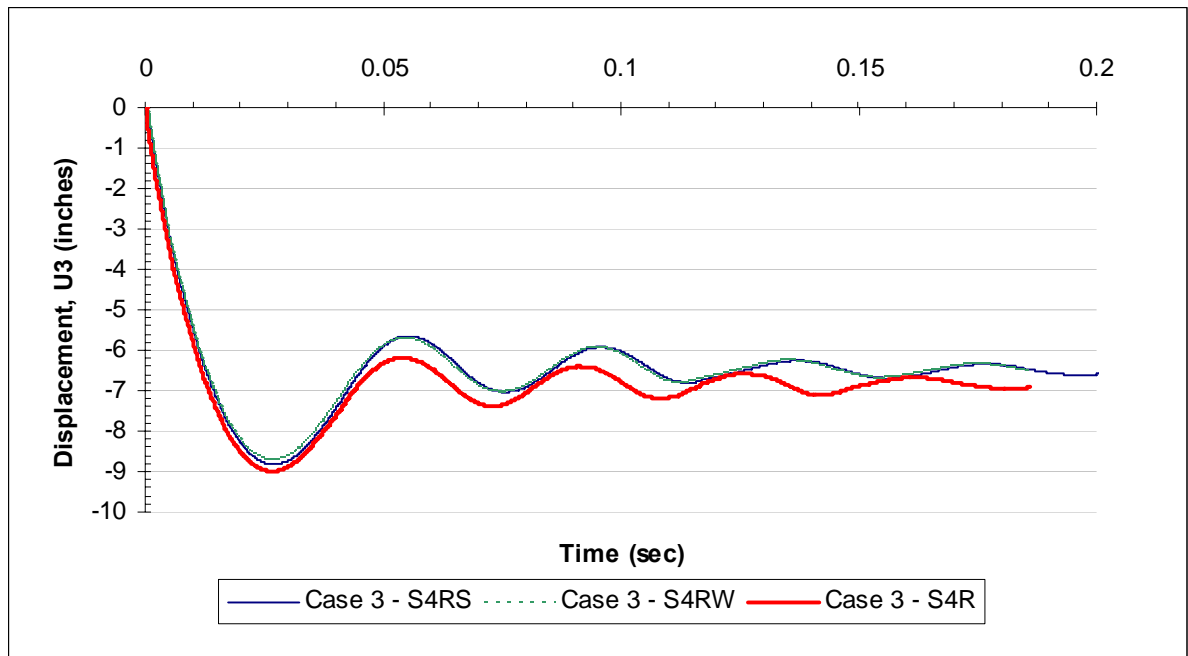


Figure 5-27. Main panel displacement for different shell elements

It was evident that the non lineal behavior presented in our study required the use of higher order formulations as provided by S4R shell elements. The results showed an increase of 0.26 inches in the maximum and permanent deformations of the panel.

Table 5.7. Summary of values obtained for different shell elements

| Shell Element | Maximum displacement U3 (inch) | Permanent displacement U3 (inch) | Required Run-time (hrs) |
|---------------|--------------------------------|----------------------------------|-------------------------|
| S4RS | 8.82 | 6.60 | 51.50 |
| S4RW | 8.71 | 6.59 | 57.25 |
| S4R | 8.99 | 6.85 | 80.25 |

It was found that S4R elements modified the panel respond further than the maximum deflection point. The oscillations of the panel presented a different rate of decay in

comparison to the other cases. In addition, the maximum strain acting at the impact area was obtained to compare the degree of deformation acting in the impacted panel. Table 5.8 shows the maximum strain acting at the mid-surface of the shell elements based on small-strain and large strain formulation models.

Table 5.8. Maximum strain values obtained for different kinematics formulation

| Shell Element | Maximum Strain (in / in) |
|---------------|--------------------------|
| S4RS | 0.047 |
| S4R | 0.072 |

The results showed that the use of large-strain formulation elements, S4R, obtained strain values approximately 65% greater than small-strain formulation elements, S4RS. Although, the boundary conditions used in the model allow a large deformation of the impact panel, the nonlinear behavior required the use of a kinematics formulation to account a high degree of deformation as provided by S4R elements.

As expected, S4R elements increased the computational time by approximately 28.75 hours in comparison with the other cases. It was demonstrated that higher order formulations required extra computational effort to obtain the numerical solutions. However, the nonlinear behavior treatment in the model is an important aspect to consider no matter the computational time required to perform the analysis. Therefore, S4R elements were used in subsequent studies.

5.4 Model Validation

In previous sections, a simple model was developed to simulate a shutter panel assembly used on Test 1, as mentioned in Chapter III. Two panels were used to simplify the model and reduce the numerical calculations required to obtain the solutions. Although the model was able to produce a modeling criterion for future analysis, a more complex model was developed for validation purposes. Thus, a third panel was added to the model. All other model characteristics remained the same. Following the installation sequence of panels, the third panel was located such that one of its lateral edges would be over the main panel. Figure 5-28 shows the three panel's model used in the analysis.

The maximum deflection obtained at the main panel was 8.47 inches. In terms of the permanent deformation a value of 6.37 inches was obtained. Thus, the results were lower than the obtained values from the two panel model as shown in Figure 5-29. Notice that the third panel reduced the response of the main panel. In the previous model the main panel had an unsupported edge that could vibrate without any constrain. Now, this condition was interrupted with the third panel in the assembly. The oscillation of each panel produced an intermittent contact between their edges. These contacts reduced the displacement of each panel. In addition, the third panel restrained the rotation of the upper edge of the main panel due to the contact between them at the support area.

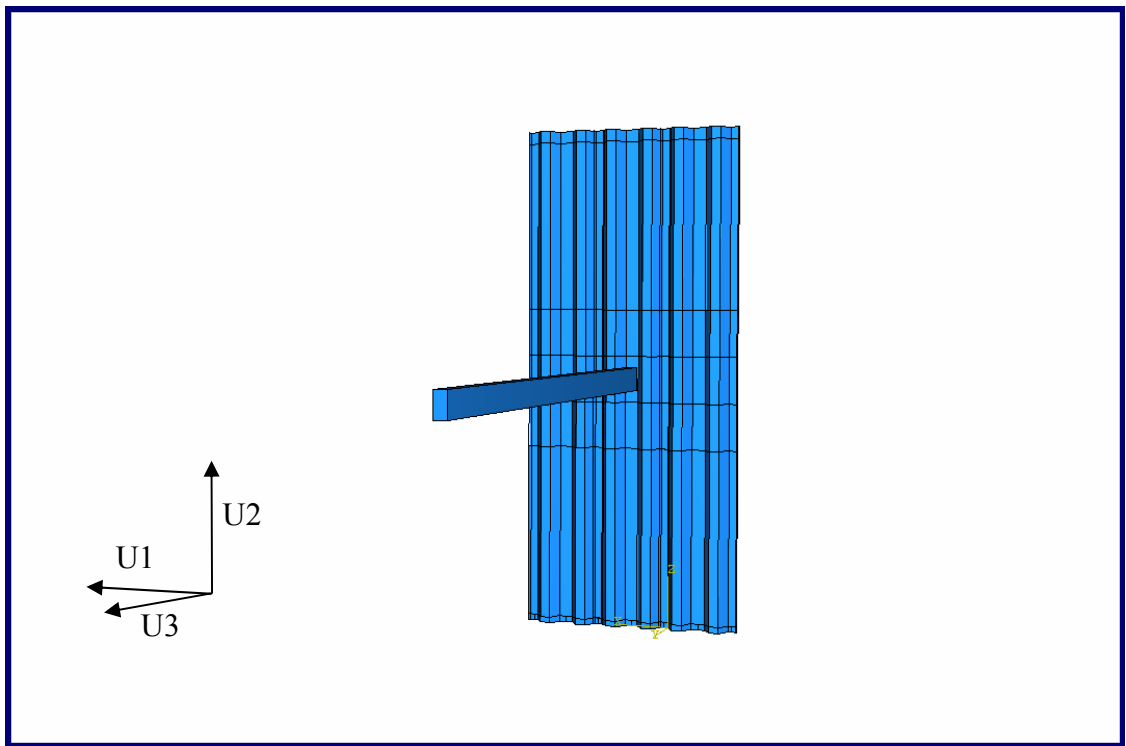


Figure 5-28. Three panel's model

The permanent deformation obtained shows a slight difference of 1.98% in comparison to the measured value on Test 1. It is important to know that on Test 1, the assembly suffered a failure at the lower support. The attachment of the system was lost due to an excessive deformation experienced by some clamps. Therefore, the system was exposed to obtain larger displacements in its response.

Therefore, it has been demonstrated that the proposed model can be a simple tool to evaluate the performance of a storm shutter assembly under impact loads. The established parameters and the procedure to incorporate them into general purpose software, ABAQUS, defined the analytical approach to be followed in the development of the simulation. The

maximum and permanent values obtained from the model were satisfactory in comparison with results in Test 1.

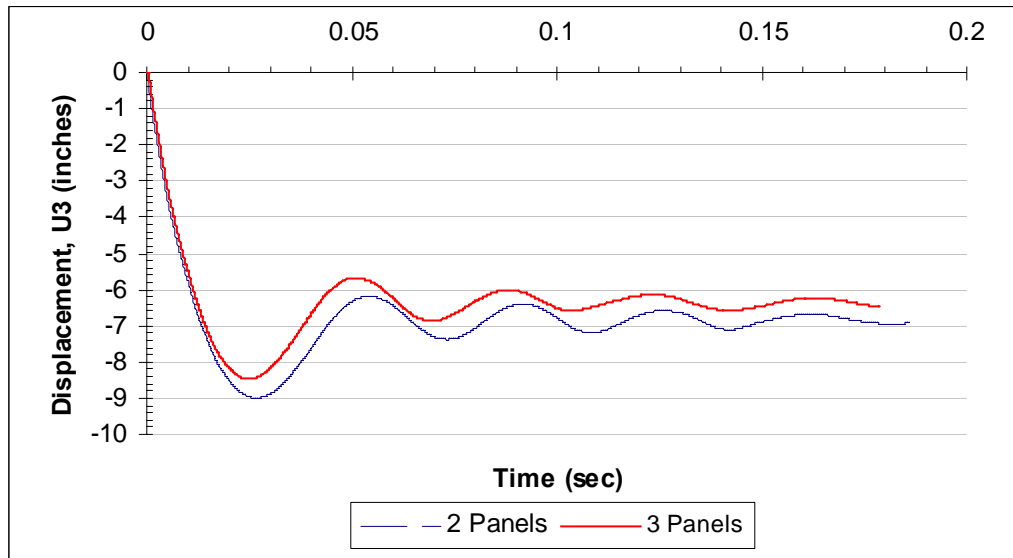


Figure 5-29. Main panel deformation for two and three panel's model

5.5 Discussion of Results

It has been demonstrated that a model consisting of two panels can be used as a simple tool to obtain approximate values of maximum and permanent deformations of the impacted panel. Also, the consideration of the upper and lower panel attachments as roller and pinned connections simplified the modeling process avoiding the use of complex modeling techniques to define the boundary conditions of the system. However, the vibration of the panels required the use of proportionality factors to incorporate critical damping to the system. Proportionality factors were obtained by performing a frequency analysis. ABAQUS provides the option to perform frequency analyses by solving the

eigenvalues problem. Therefore, the purpose of this analysis was to obtain the natural frequencies of the panel for the first and third vibration modes. Assuming 2% of critical damping, the proportionality factors were calculated based on the Rayleigh relations, previously described. A damped system provided a better visualization of the permanent deformation of the impacted panel. Also, it was showed that the panels dissipated the impacted energy of the missile in a shorter period of time. However, the panels continued their vibration behavior at the end of the 1.2 seconds event. It can be concluded that approximated permanent deformations can be calculated using simulation events in the range of 0.15 to 0.30 seconds. This range of time reduced the computational time by approximately three (3) days in comparison with the simulations of 1.2 seconds. The permanent deformations were obtained using the average between maximum and minimum values in the final frequency cycle at the end of the event. This procedure was used for subsequent analyses in the current study.

It was showed that the number of finite elements used in the models affected the accuracy of the results obtained. The maximum displacement of the impact panel increased as a higher degree of refinement at the impact zone of the panel was used. The permanent deformation values showed a random tendency of variation. It is important to note that panels were still vibrating at the end of the event. It was observed that panels required more time to dissipate the energy affecting the calculation of the permanent values. A slight difference was obtained.

In terms of the number of elements to be used in the models, it showed a reduction in the difference between the studied cases when a total of 18,880 elements or greater were used

in the impact panel mesh. This number of finite elements was used as a minimum value to achieve the degree of refinement required in the models.

It was found that different types of shell elements affected the obtained results as well as the computational time required to perform the analyses. S4RS and S4RW shell elements are based on similar kinematics formulations. However, the maximum displacement and permanent deformation values obtained using both type of shell elements were not the same. It was expected that distortion of elements will be produced due to the level of load applied to the system. As mentioned before, S4RS shell elements were not formulated to respond to this behavior. As a result, some errors can be induced in the obtained results. Otherwise, S4RW were formulated to be used in problems involving the possibility of high degree of distortions. This situation explained the difference of the obtained results between the small-strain elements used in the models.

Meanwhile, S4R shell elements were formulated with large-strain formulation with large rotations. The use of S4R increased the maximum displacement and permanent deformation values when compared to ones obtained with S4RS and S4RW shell elements. In addition, the use of S4R showed an increase of the maximum strains acting at the impact area compared with S4RS elements. Therefore, S4R shell elements were selected to be used on the subsequent models of the current study.

The use of a third panel in the assembly was evaluated when an additional instance of the part related to shutter panels was incorporated into the model. The objective was to validate the proposed model based on a better representation of the real assembly used on Test 1. The new instance was located above the impact panel following the typical sequence of panel installation. The impacted panel improved its response obtaining a reduction in the

maximum and permanent deformation compared to the values obtained from previous analyses. It was found that the contact between the third panel and the impacted panel provided an additional support to the assembly. As the impacted panel tried to rotate as a response to the applied loads, the third panel restrained the rotation of its edges due to the contact between them during the simulation. The total deformation of the impacted panel was reduced obtaining similar results to the values measured on Test #1 validating the proposed model.

Taking in consideration all this factors, the use of proportionality factors to incorporate critical damping into the model, a minimum of 18,880 finite elements to generate the impact panel mesh and the selection of S4R shell elements defined the modeling criteria to study the behavior of storm shutter panels using an analytical approach as developed in the current study.

Chapter VI

Parametric Study of Storm Shutters due to Impact Loads

6.1 Introduction

Chapter V demonstrated that a computer simulation can be used to represent the effect of windborne debris on storm shutter systems. A model generation criteria was defined based on different approaches in terms of formulations and assumptions. However, it was demonstrated that the results obtained from the model are very sensitive to any modification in the parameters used in the model generation.

This chapter describes the effect of different parameters in the model. Parameters like geometrical configuration of panels, material, and boundary conditions are explained. Values of permanent and maximum deformations and stresses to determine the most detrimental behavior of the storm shutter assembly were evaluated by means of parametric studies.

6.2 Parametric Study

Two steps were used to perform the parametric study. The first step was to develop a simple model to represent the storm shutter behavior similar to the one used on Chapter V. For reference purpose this model was named Base Case. Thus, the results obtained from the Base Case model would be used as reference to investigate the effect of different parameters in the system. The second step was to establish the most important parameters that will affect the behavior of storm shutter systems under impact loads. Surveys were realized to obtain the required information among shutter manufacturers in Puerto Rico and United States. Each manufacturer suggests its own design consisting in the use of specific material and cross section. This argument explains the variety of storm shutter systems available in the industry. Therefore, material and cross section of panels were defined as relevant parameters for our study. In addition, parameters like number of panels, boundary conditions and missile conditions will influence the response of the shutter systems.

The proposed parameters were incorporated to the Base Case model such that new models were defined to evaluate each parameter. Values of maximum and permanent deformation and stress of the impact panel were obtained according to the parameter under investigation and compared with the results obtained from the Base Case model.

6.2.1 Base Case Model

A simple model was defined as a reference model in the parametric study. Table 6-1 shows the physical characteristics and configuration used to define the model. Notice that

the model was basically the same as Case #3 used in Chapter V. However, a different cross section was used to represent the shutter panels. This was obtained by one of the major and more accessible local supplier of storm shutters as shown in Figure 6-1. In addition the missile velocity was defined as 50 mph.

Table 6.1 Description of Base Case model.

| Model Components | Characteristics | Description |
|-------------------------|---|--|
| Assembly | No. of Panels Top Support Lower Support Meshing Finite Element | 2 Roller Pinned Case #3* S4R |
| Panels | Length of Panels Material Thickness | 84" Aluminum Alloy, 3003 H14 0.063" |
| Missile | Weight Cross Section Length Material Mass Density Velocity Location | 9 lbs 2"x 4" 84" Wood (Southern Pine) 0.13 lb/in ³ 50 mph Center of Middle Span |

* Meshing generation defined in Chapter V

As mentioned earlier, different models were created based on the Base Case model. The difference between models was the substitution of the specific parameter to be analyzed.

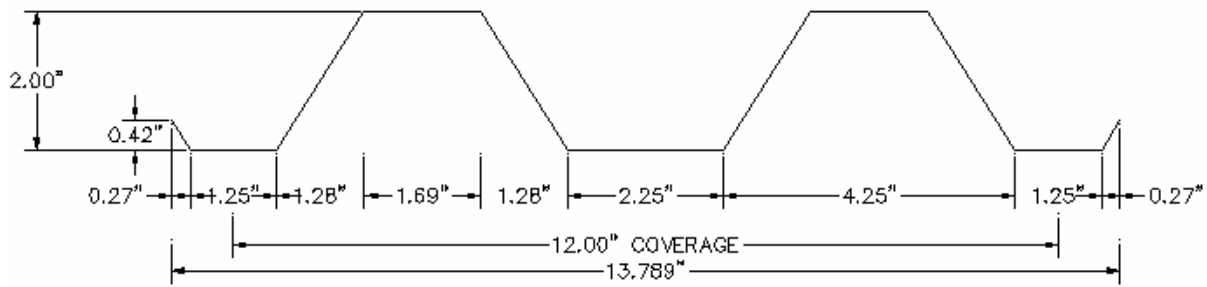


Figure 6-1. Cross section used in Base Case model

6.2.2 Effect of Panel Material

A survey was carried out to establish the most typical material used in the fabrication of storm shutters panels in Puerto Rico and United States. It was found that aluminum alloys and galvanized steel are the most commonly used materials for this purpose. It is important to know that galvanized panels have half of the thickness of the aluminum panels. The gage or thickness used for galvanized panels corresponds to the manufacture requirement of providing a lightweight product at the moment of the assembly installation. The mechanical and physical properties of these materials are used to represent the material in the proposed models, as shown Table 6.2.

Stress-strain curves based in the mechanical properties of each material are presented in Figures 6.2 to 6.6. Notice that for each material, two curves were defined to consider the use of true values instead of engineering values. ABAQUS (Hibbit, Karlson & Sorensen, 1997) imposed this constrain as it was explained in Chapter V.

Table 6.2 Mechanical and physical properties of typical materials used in the storm panels fabrication (MatWeb, 2009).

| Property | Aluminum Alloys | | | | Galvanized Steel, A446 Gr. 40 |
|---------------------------------|-----------------|----------|----------|---------|-------------------------------|
| | 3003-H14* | 3004-H34 | 5052-H32 | 6063-T6 | |
| Density (lb/in ³) | 0.0986 | 0.0983 | 0.0968 | 0.0975 | 0.2840 |
| Modulus of Elasticity (ksi) | 10,000 | 10,000 | 10,200 | 10,000 | 29,000 |
| Tensile Yield Strength (psi) | 21,000 | 29,000 | 28,000 | 31,000 | 34,800 |
| Ultimate Tensile Strength (psi) | 22,000 | 35,000 | 33,000 | 35,000 | 51,900 |
| Poisson Ratio | 0.33 | 0.35 | 0.33 | 0.33 | 0.28 |

* Aluminum alloy used on Base Case model.

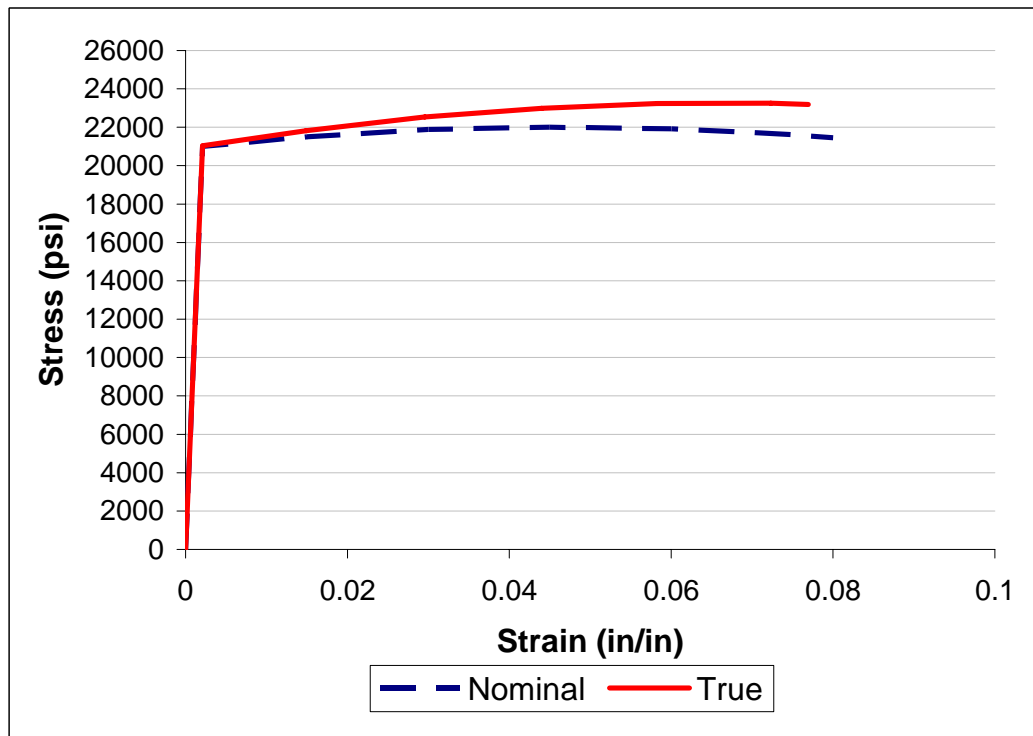


Figure 6-2. Aluminum 3003 H14 Stress-Strain Curve. Material used in Base Case model.

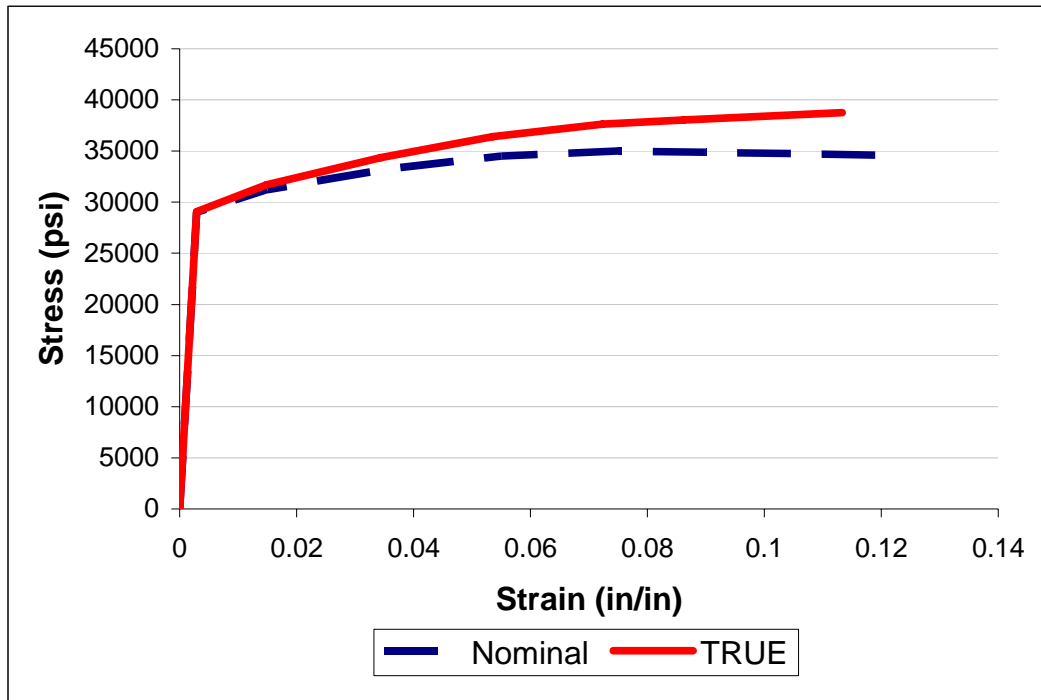


Figure 6-3. Aluminum 3004-H34 Stress-Strain Curve

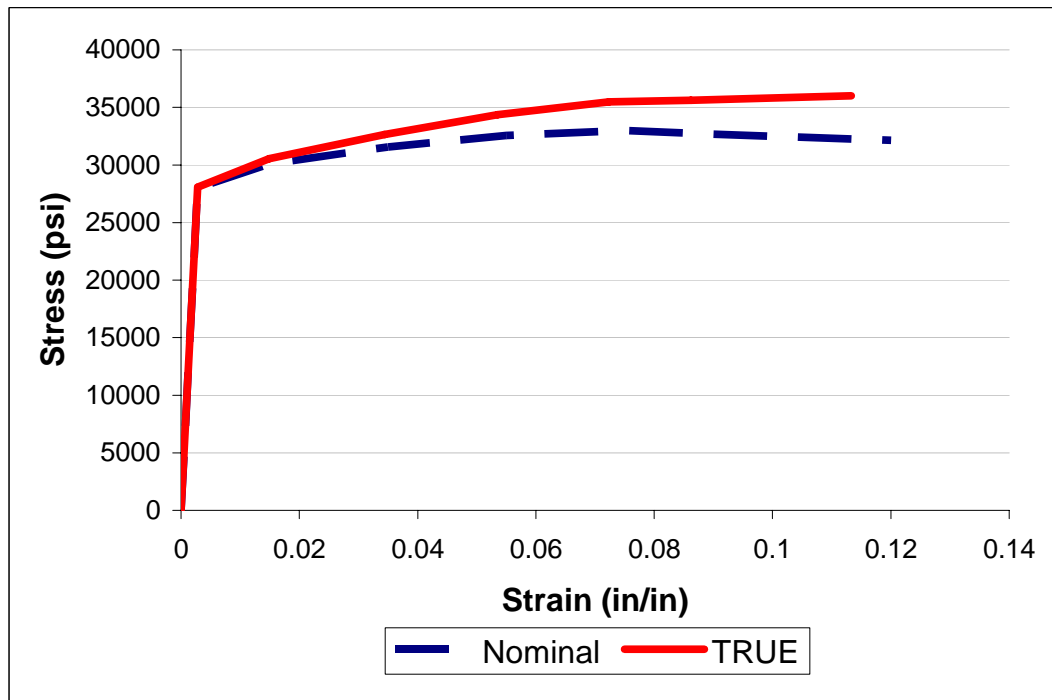


Figure 6-4. Aluminum 5052-H32 Stress-Strain Curve

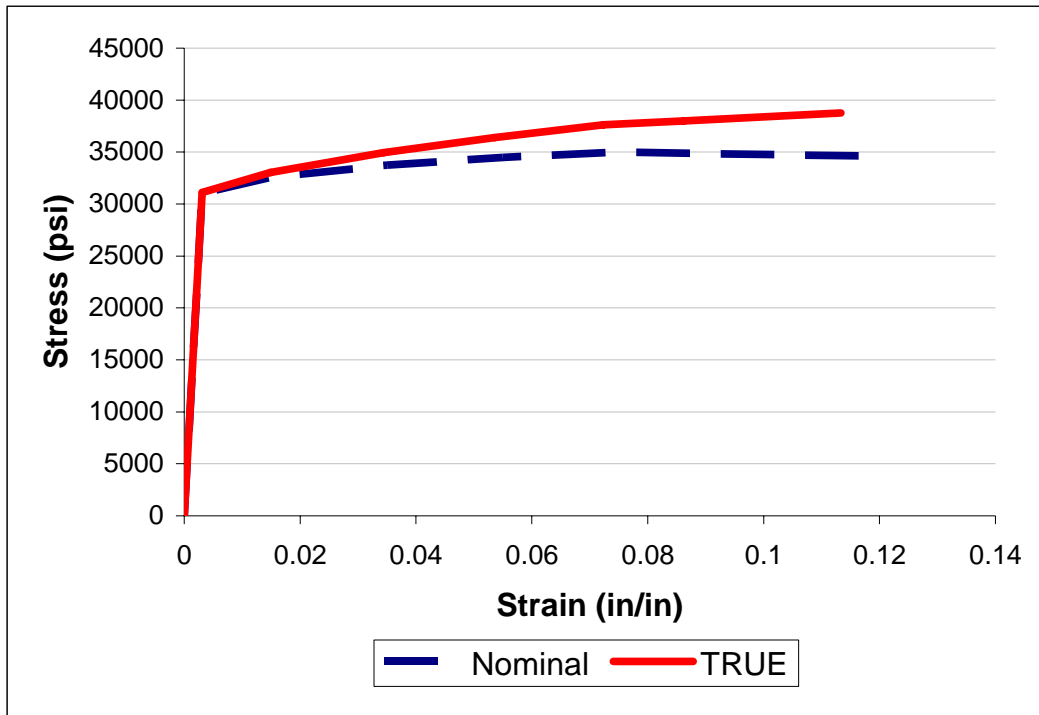


Figure 6-5. Aluminum 6063-T6 Stress-Strain Curve

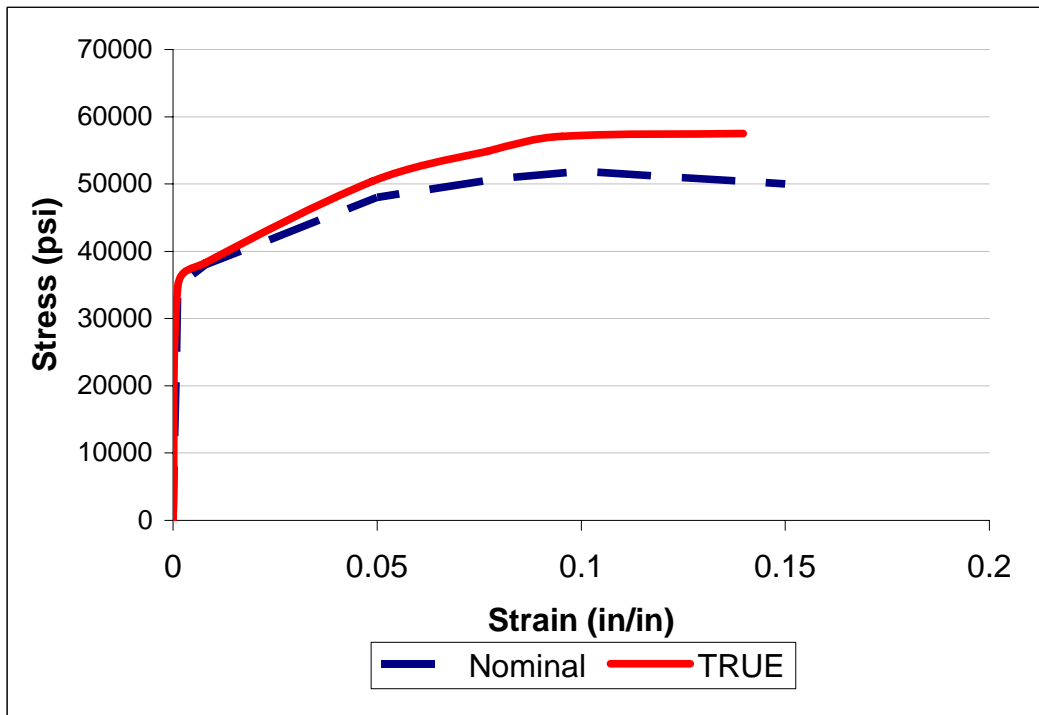


Figure 6-6. Galvanized ASTM A446, Gr. Stress-Strain Curve

A total of four models were generated based on the Base Case model to study the established materials. The only difference between the models was the parameters related to the material properties of the panels. A frequency analysis was evaluated for each model such that 2% of critical damping was introduced to the analysis as shown in Table 6.3. A total of 19,252 and 6,945 shell finite elements, S4R, were used to develop the impact panel and adjacent panel meshes, respectively.

Table 6.3 Proportionality factors for damped systems in the evaluation of panel materials

| Material | Frequency First Mode ω_m (rad/sec) | Frequency Third Mode ω_n (rad/sec) | Proportional Factors | |
|------------|---|---|-------------------------|---------|
| | | | a_o | a_1 |
| 3003 H14 | 131.36 | 237.22 | 4.565 | 0.00015 |
| 3004 H34 | 131.57 | 238.31 | 4.578 | 0.00015 |
| 5052 H32 | 131.44 | 237.76 | 4.571 | 0.00015 |
| 6063 T6 | 131.54 | 238.23 | 4.576 | 0.00015 |
| Galv.Steel | 105.66 | 175.98 | 3.565 | 0.00019 |

Figure 6.7 to 6.11 shows the maximum and permanent deformation of the impacted panel obtained for each material. The results showed that the storm shutter assembly behavior was similar for all materials. A maximum deformation was achieved at the early stage of the event. Then the system began to vibrate as the energy tried to dissipate. However, the maximum deformation values occurred at different times in the event and varied in magnitude for each material as shown in Figure 6.12. Also permanent deformation values varied in magnitude. Table 6.4 summarizes the values of maximum and permanent deformation obtained for each material.

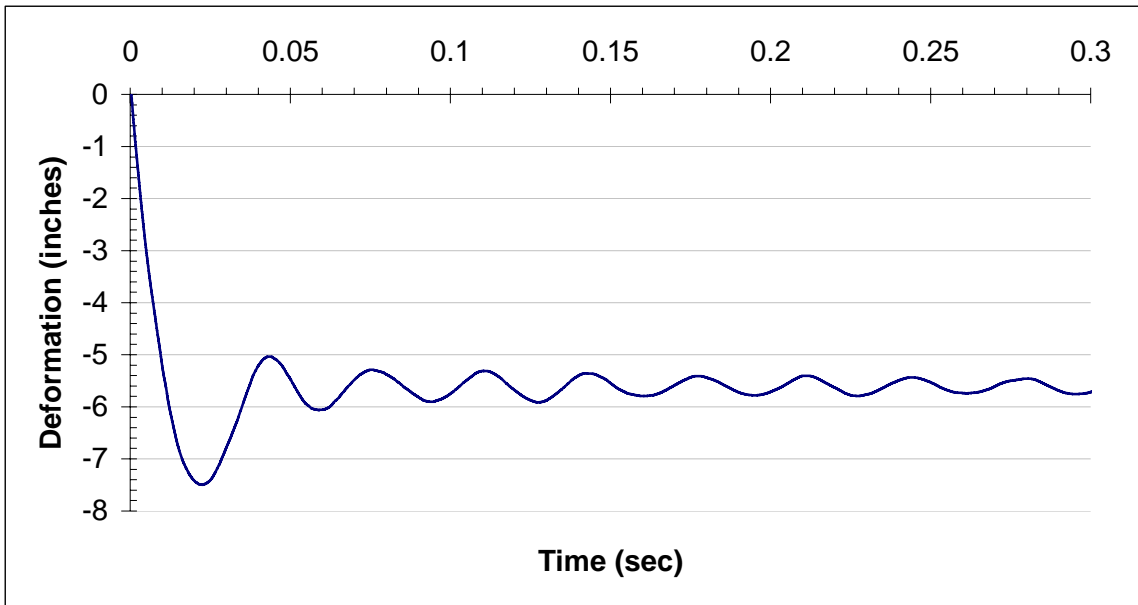


Figure 6-7. Maximum and permanent deformation for Aluminum Alloy 3003-H14

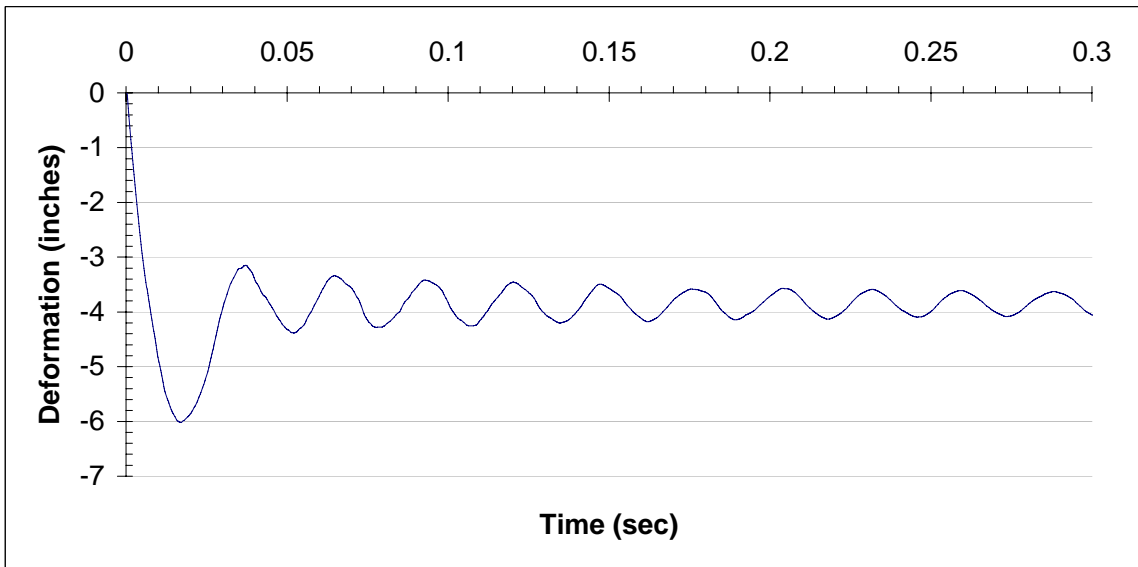


Figure 6-8. Maximum and permanent deformation for Aluminum Alloy 3004-H34

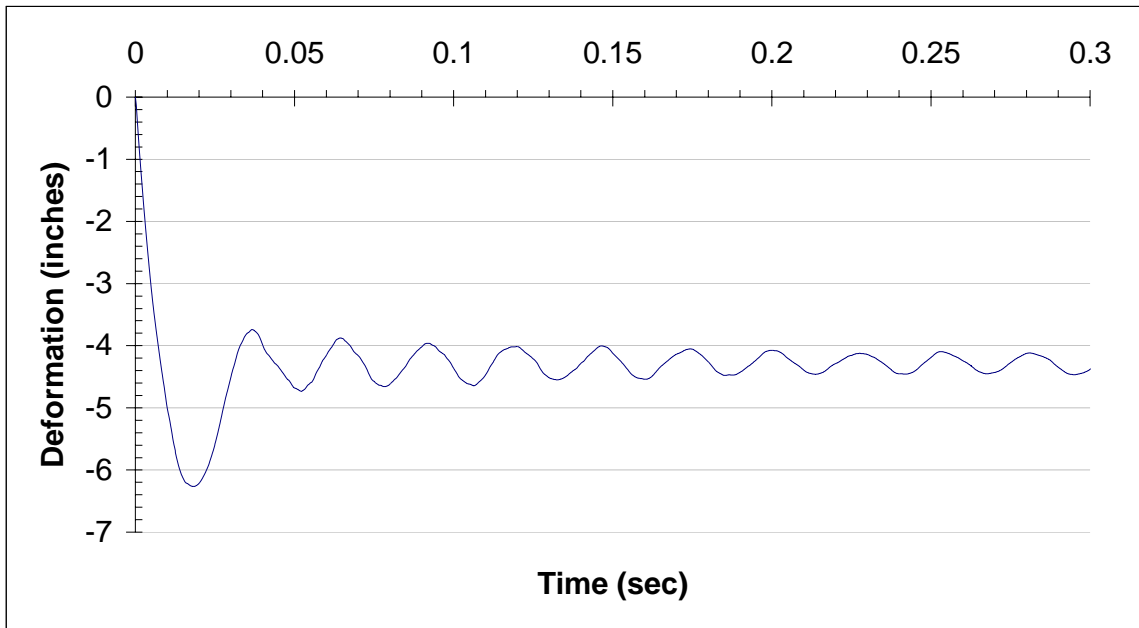


Figure 6-9. Maximum and permanent deformation for Aluminum Alloy 5052-H32

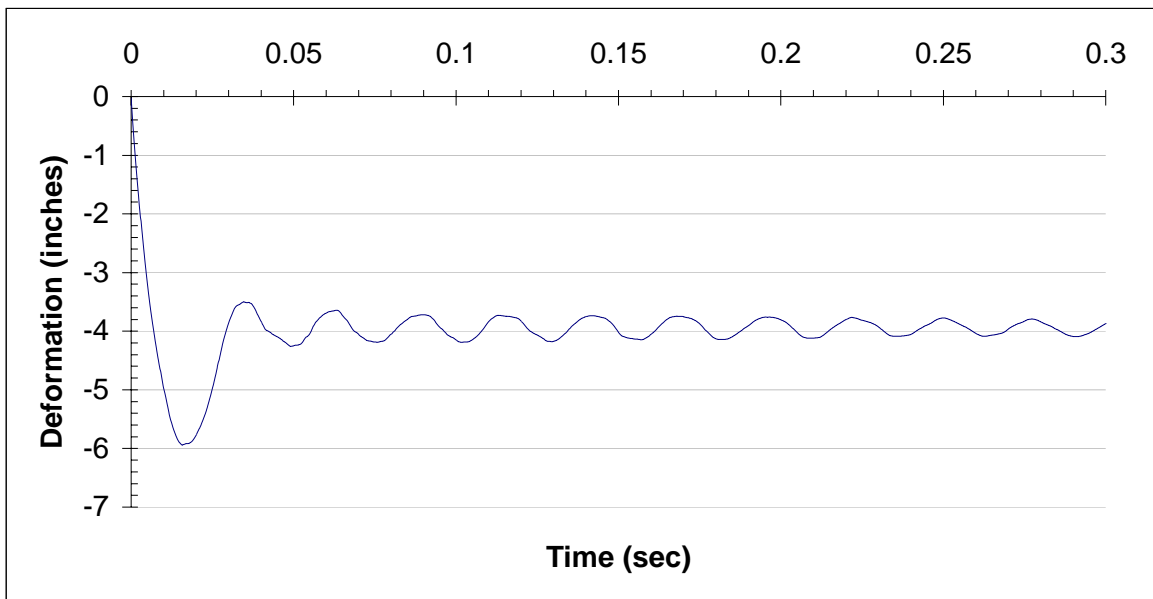


Figure 6-10. Maximum and permanent deformation for Aluminum Alloy 6063-T6

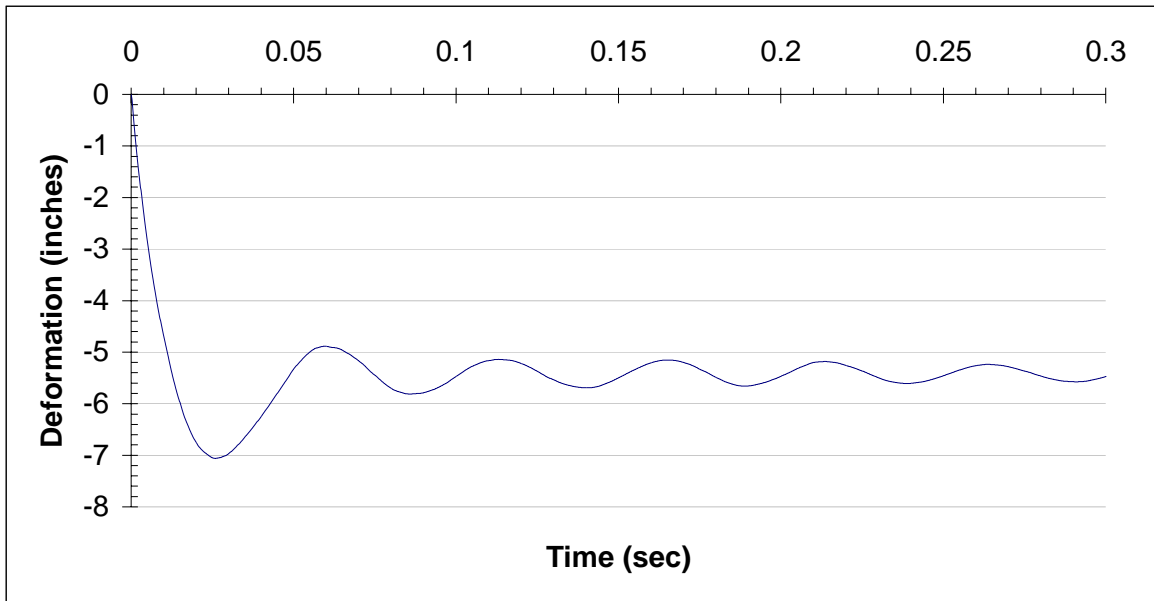


Figure 6-11. Maximum and permanent deformation for Galvanized Steel 446, Gr.40

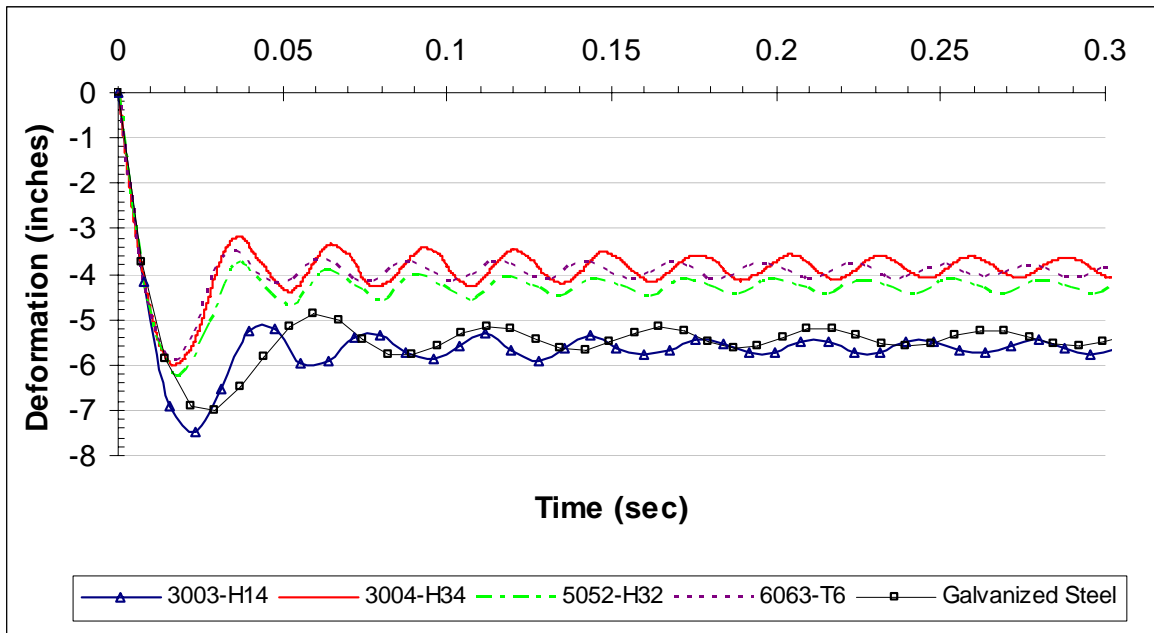


Figure 6-12. Maximum and permanent deformations of impact panel obtained for different materials

Table 6.4 Maximum and permanent deformation obtained varying the panel's material

| Material | Maximum Displacement | | Permanent Deformation Value (in) |
|------------------|----------------------|-------------|----------------------------------|
| | Value (in) | Time (sec)* | |
| 3003-H14 | 7.49 | 0.023 | 5.70 |
| 3004-H34 | 6.02 | 0.017 | 3.87 |
| 5052-H32 | 6.27 | 0.018 | 4.35 |
| 6063-T6 | 5.98 | 0.016 | 4.02 |
| Galvanized Steel | 7.06 | 0.026 | 5.51 |

* Time of occurrence for maximum deformation

The best overall shutter panel response was obtained for Aluminum Alloy 3004-H34 followed by 6063-T6. In fact, according to local manufacturers 3004-H34 is the most used Aluminum Alloy for the fabrication of aluminum panels in the local industry. Also Aluminum Alloy 3004-H34 has replaced the use of Aluminum Alloy 3003-H14. This argument shows the tendency of the industry to improve their products using more efficient materials. From the results, Aluminum Alloy 3003-H14 allowed the impacted panel to get the largest deformation in comparison with the other material. Thus the worst response from the panels was achieved using this material.

As mentioned earlier, galvanized steel panels are fabricated with half of the thickness used in aluminum panels. A value of 0.039 inches was used to define the thickness of the panels. For this reason galvanized steel panels had a weaker response compared to aluminum alloys panels.

It was found that high levels of stress occur on specific locations of the impact panel. It was clear that a high concentration of stress was expected to occur at the impact area.

However, higher stresses were obtained at the lower connection and the top of the ridge of the cross section near the impact zone. Figure 6-13 shows the three zones in which the higher level of stress were obtained.

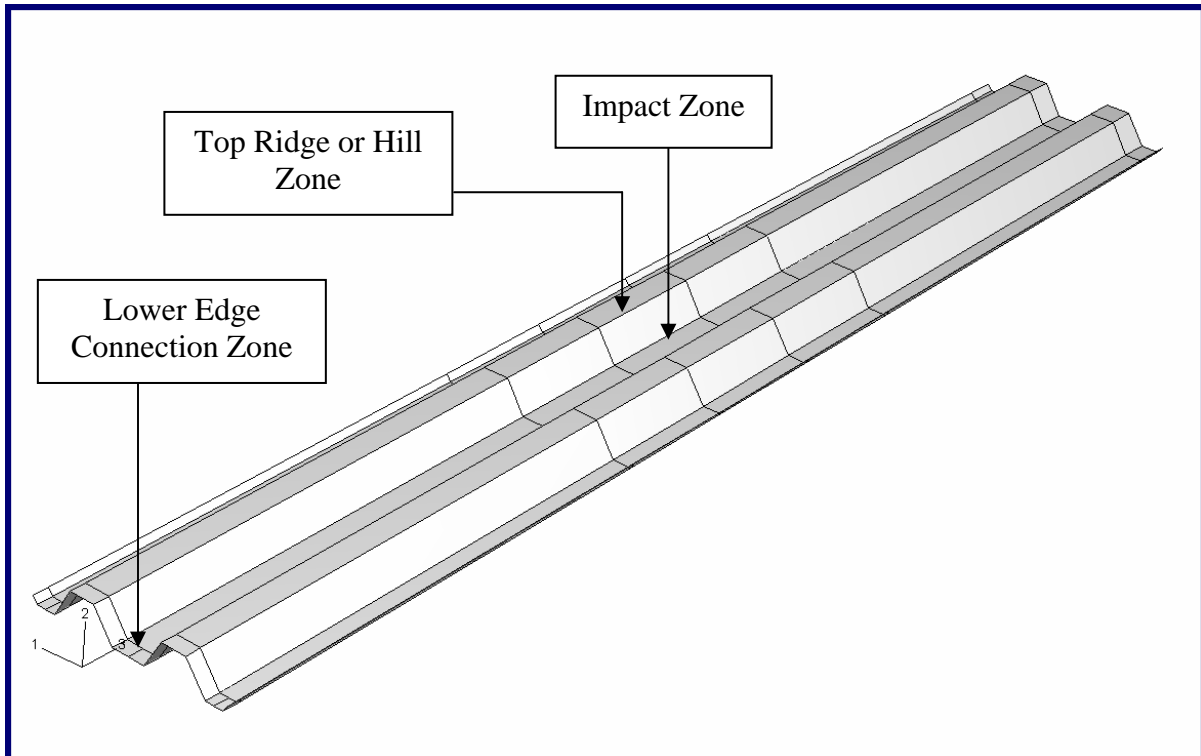
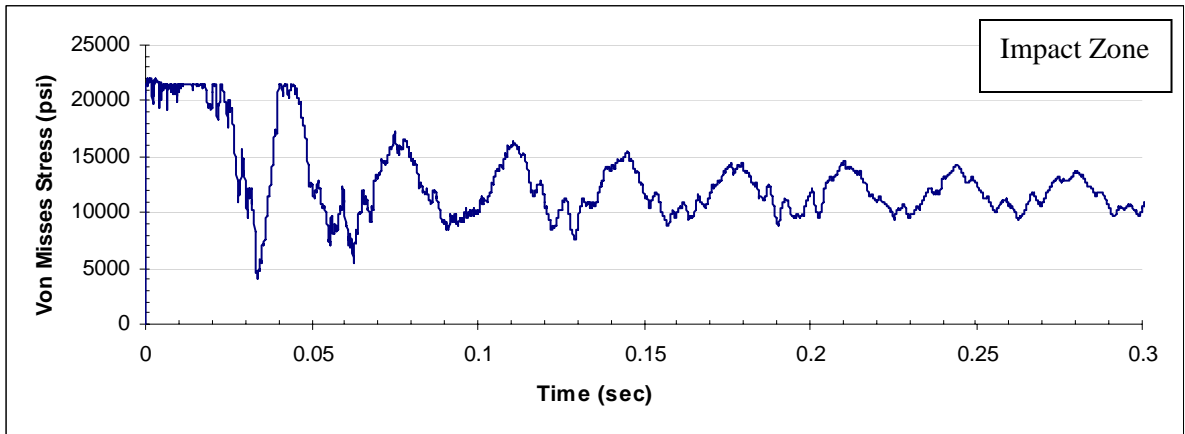
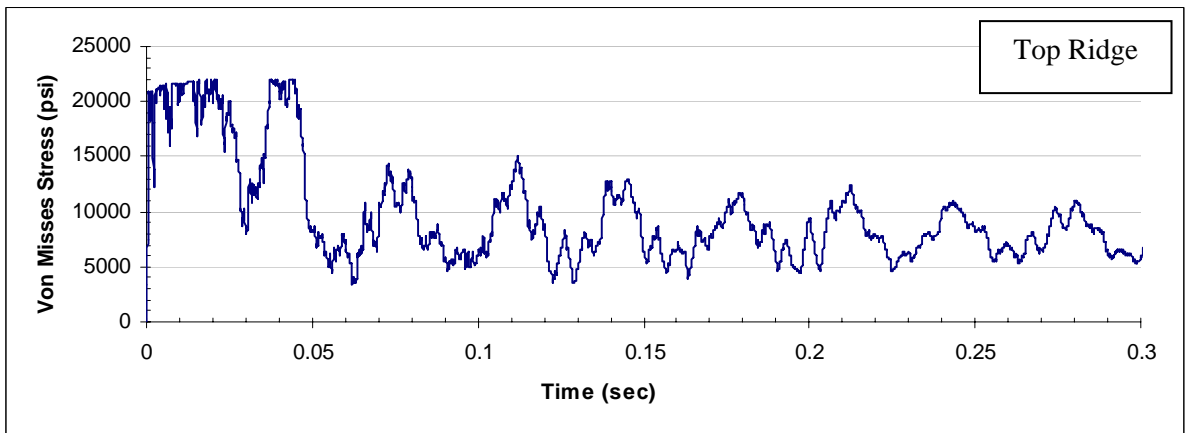


Figure 6-13. High stress level zones on the impact panel

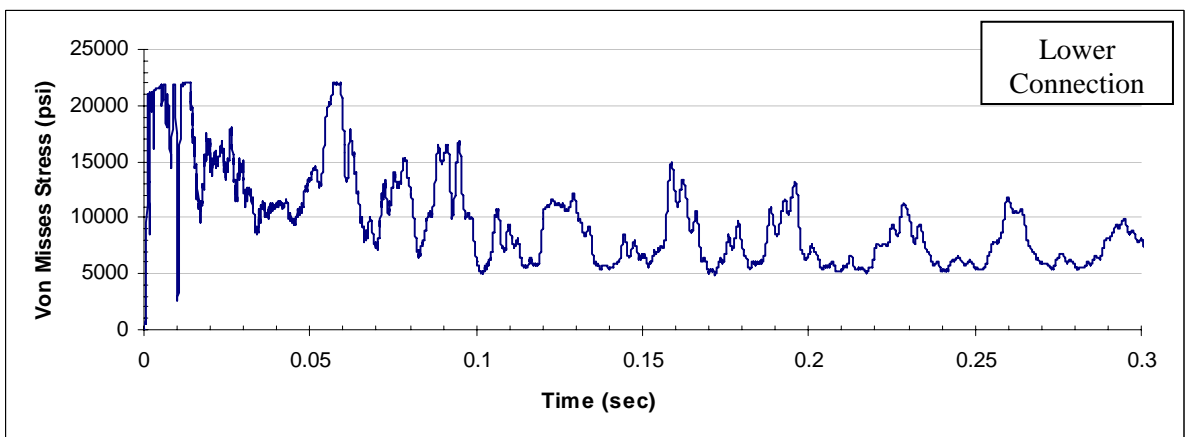
Figure 6.14 to 6.18 shows the maximum stresses obtained for each material. These values were based on the Von Mises failure criteria as provided by ABAQUS. Every critical zone reached the maximum stress values at different times. With the exception of Base Case model (Aluminum Alloy 3003-H14), the models showed that the maximum values were reached in a similar sequence throughout the established zones.



(a)

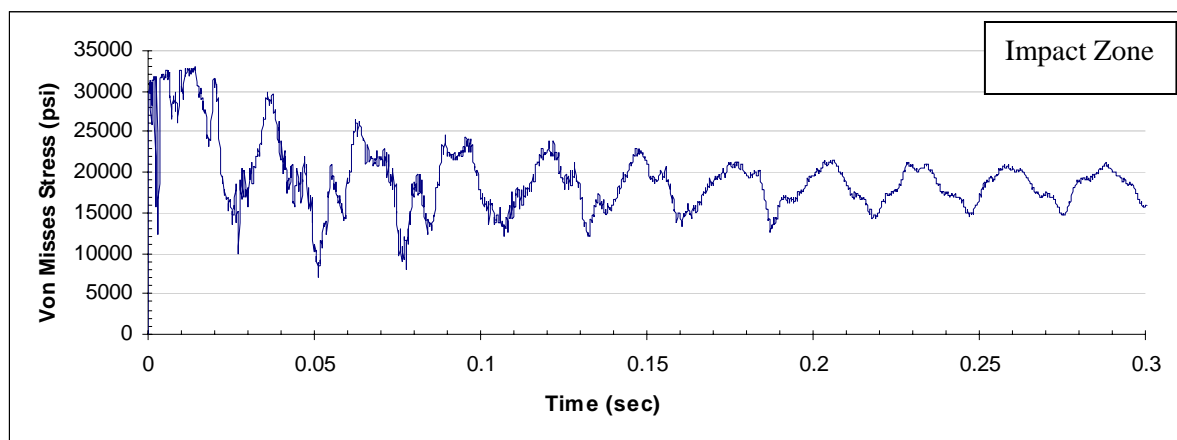


(b)

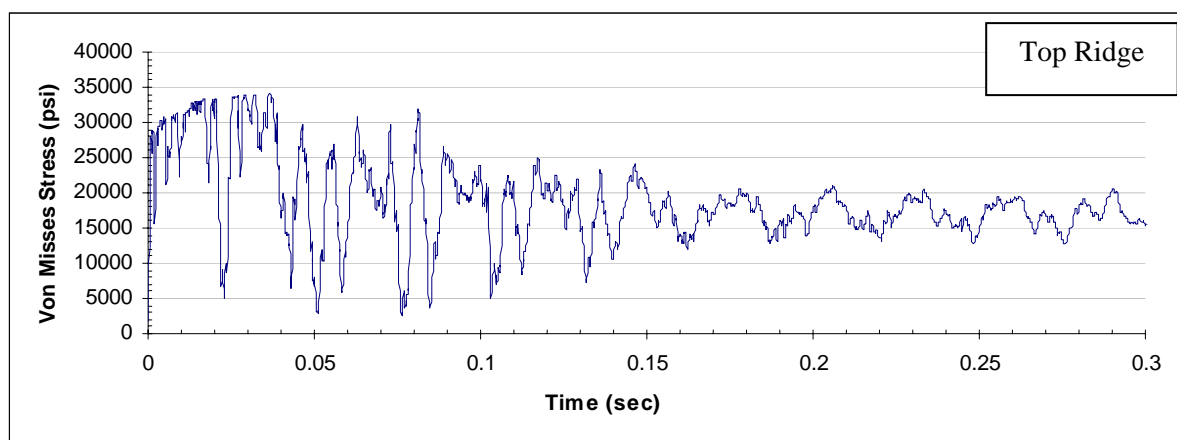


(c)

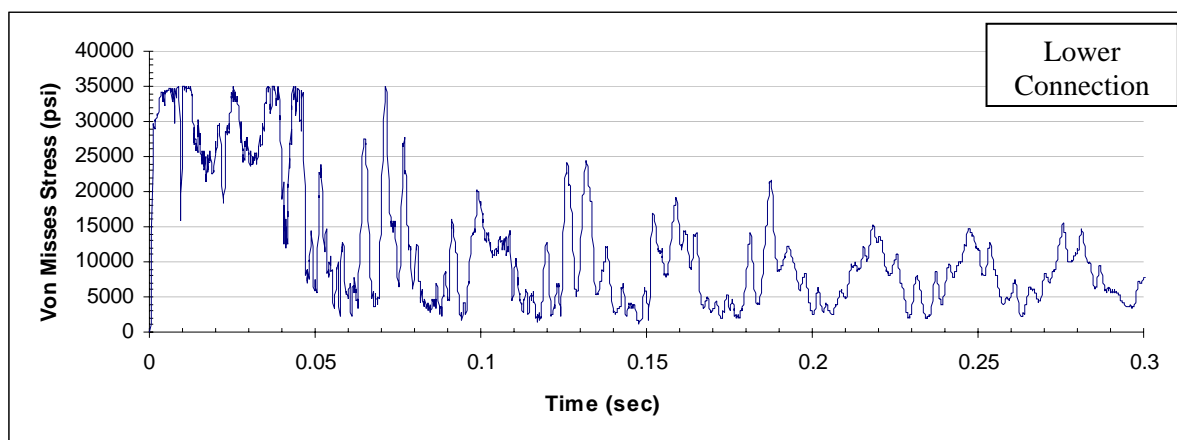
Figure 6-14. Maximum Von Mises stresses for Aluminum Alloy 3003-H14 acting at (a) impact zone (b) top ridge and (c) lower edge connection.



(a)

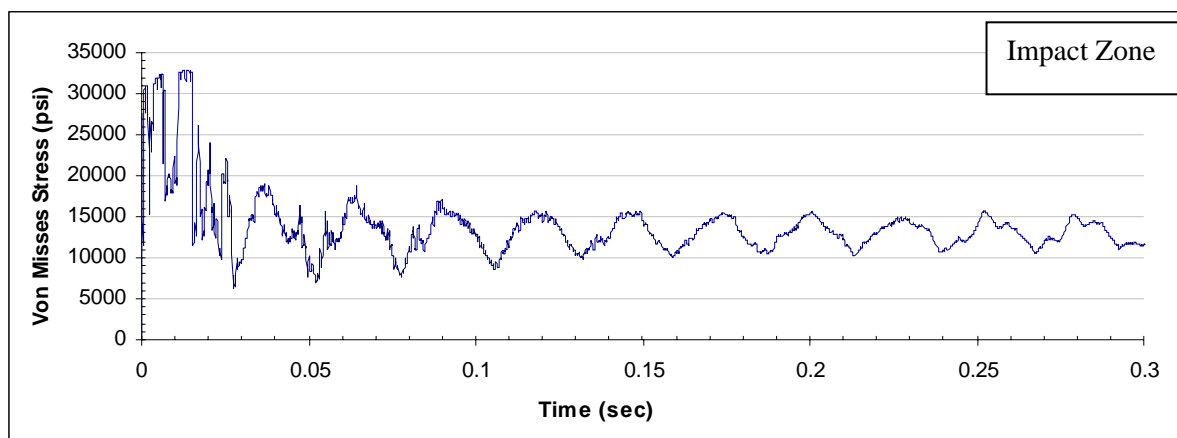


(b)

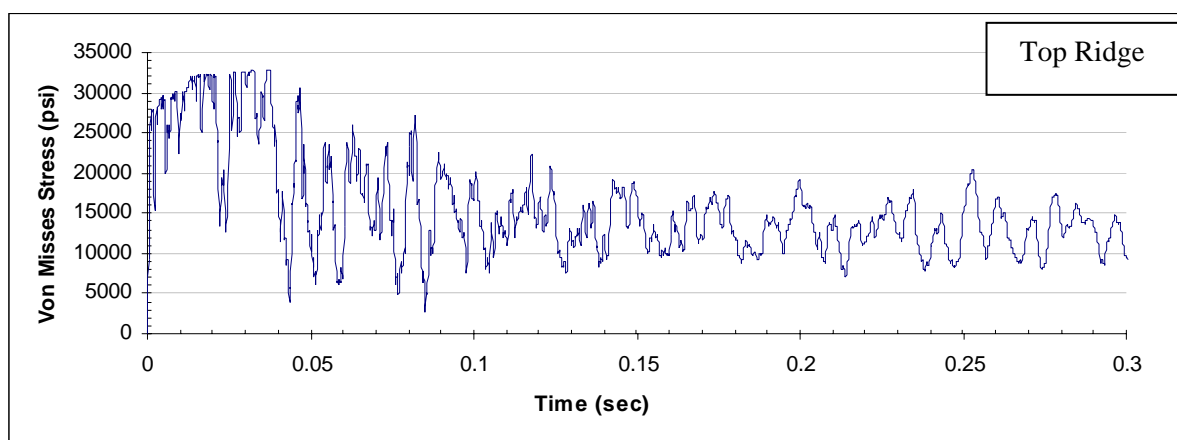


(c)

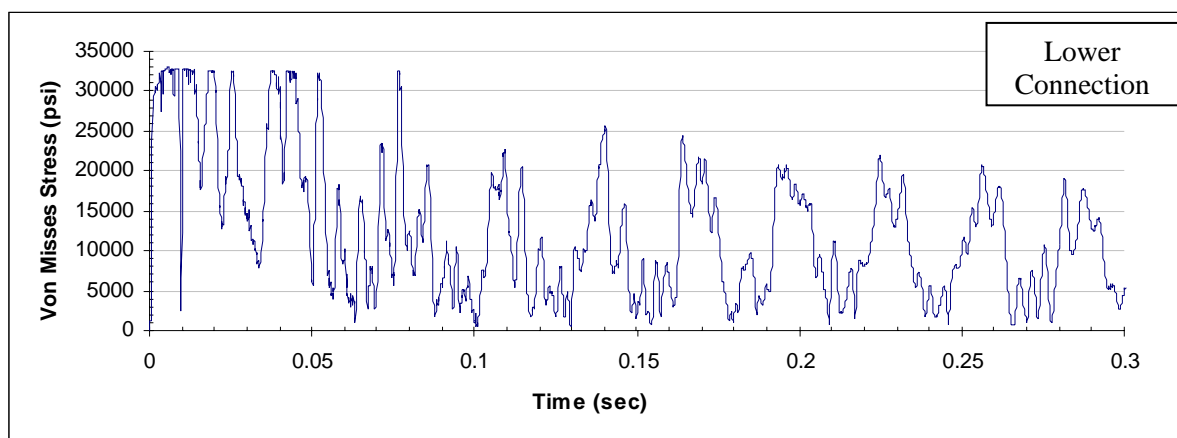
Figure 6-15. Maximum Von Mises stresses for Aluminum Alloy 3004-H34 acting at (a) impact zone (b) top ridge and (c) lower edge connection.



(a)

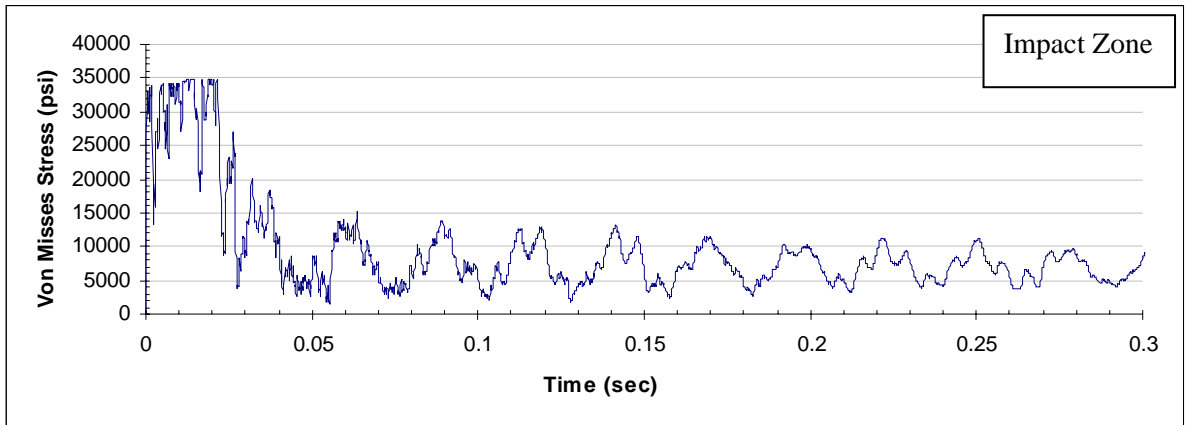


(b)

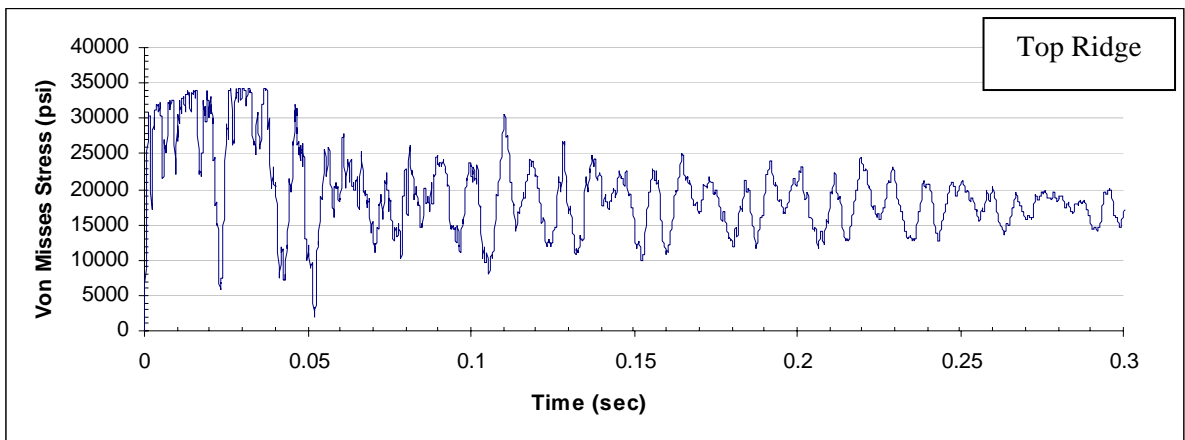


(c)

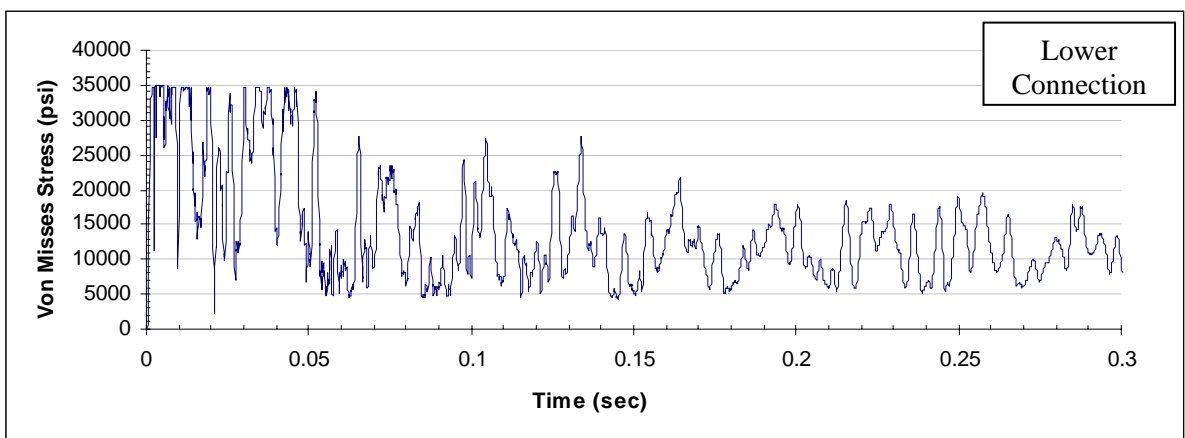
Figure 6-16. Maximum Von Mises stresses for Aluminum Alloy 5052-H32 acting at (a) impact zone (b) top ridge and (c) lower edge connection.



(a)

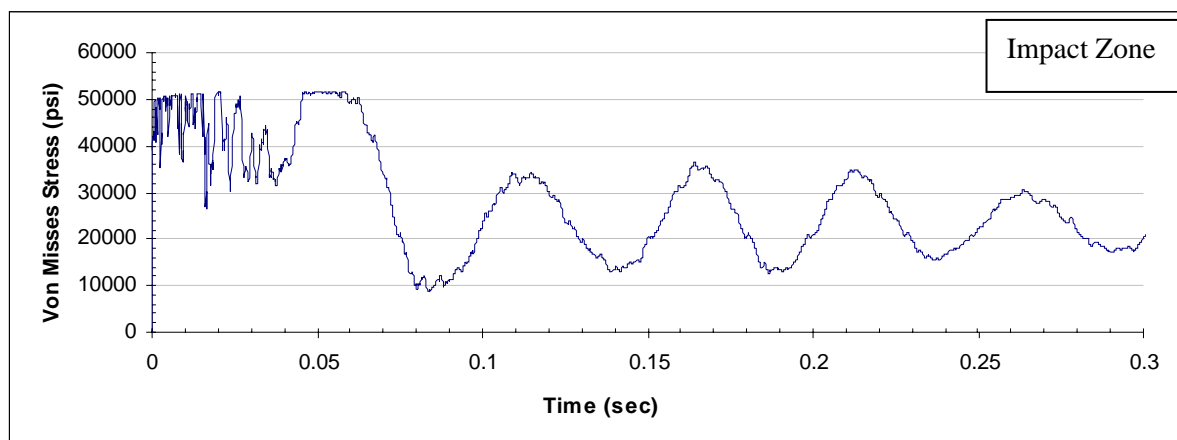


(b)

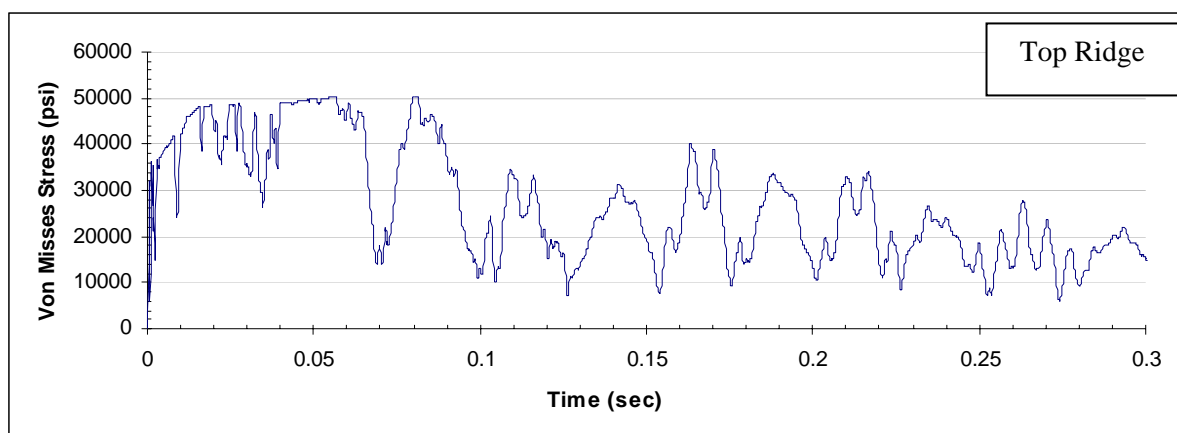


(c)

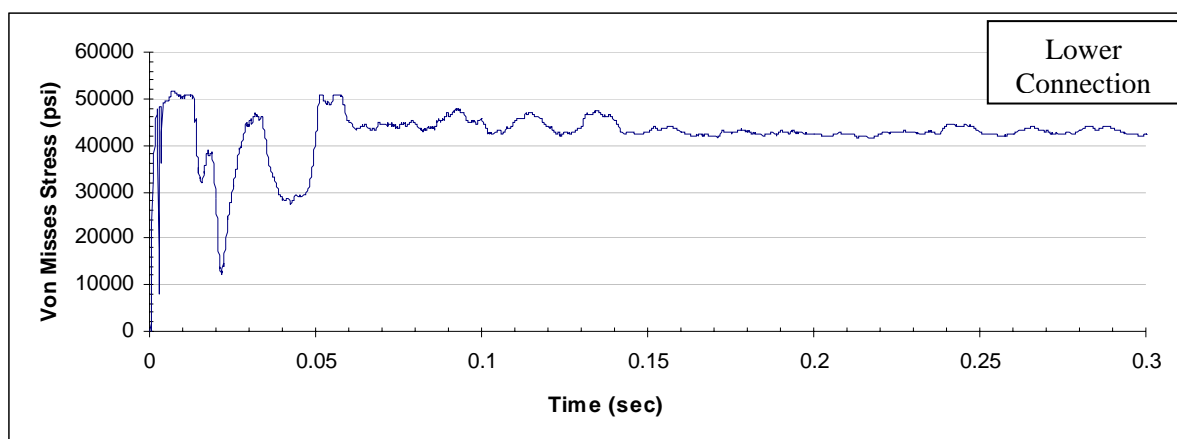
Figure 6-17. Maximum Von Mises stresses for Aluminum Alloy 6063-T6 acting at (a) impact zone (b) top ridge and (c) lower edge connection.



(a)



(b)



(c)

Figure 6-18. Maximum Von Mises stresses for Galvanized Steel, ASTM A446, Gr. 40 acting at (a) impact zone (b) top ridge and (c) lower edge connection.

The first zone to reach the maximum values was the zone surrounding the lower edge connection. The second zone was the impact region followed by the zone defined by the top ridge of the cross section. For the first and second zones only, a slight difference was obtained between the maximum values. Table 6.5 summarizes the obtained results showing the time of occurrence of the maximum values for each zone.

Based on the stress strain relation of each material, the impact load produced a level of stress larger than the ultimate stress without reaching failure. It is important to note that the panels were free to displace in the in-plane direction. Therefore, the panels could achieve enough deformation to dissipate the impact load and avoid any rupture of the material. This situation was observed in all materials.

Table 6.5 Maximum Von Mises stresses acting at different zones of the impacted panel. Values obtained for different panel materials.

| High Stress Zones | 3003-H14 | | 3004-H34 | | 5052-H32 | | 6063-T6 | | Galvanized Steel, Gr.40 | |
|-------------------|------------------|------------|------------------|------------|------------------|------------|------------------|------------|-------------------------|------------|
| | Max. Value (psi) | Time (sec) | Max. Value (psi) | Time (sec) |
| Impact | 21,983 | 0.001 | 32,987 | 0.014 | 32,932 | 0.013 | 34,918 | 0.013 | 51,521 | 0.059 |
| Top Ridge | 21,929 | 0.045 | 34,065 | 0.037 | 32,770 | 0.037 | 34,242 | 0.037 | 50,259 | 0.081 |
| Lower Connection | 21,983 | 0.014 | 34,940 | 0.012 | 32,932 | 0.006 | 34,918 | 0.003 | 51,693 | 0.007 |

Notice that for Aluminum Alloy 3003-H14, the maximum stress at the impact zone occurred in the shortest time of the analysis. Only 0.001 seconds were necessary to reach this maximum value. Aluminum Alloy 3003-H14 is constituted by a stress–strain relationship with an ultimate stress of 22,000 psi. Meanwhile, values of ultimate stress

greater than 30,000 psi are defined by other materials. Therefore, the impacted panel based on 3003-H14 could not distribute its internal forces in the same way as the other panel materials due to its limitation of stress capacity. It was evident that when the impacted panel initiated a deformation process its internal forces were distributed from the impact load location to the edge supports. Thus high stress concentrations were generated around the lower support. It was found that these stresses occurred simultaneously with the ones produced at the impact zone. However, due to the reduced stress capacity of 3003-H14, this behavior was not achieved. Once the impact load was applied to the system the impacted panel reached its maximum value automatically.

6.2.3 Effect of Geometrical Configuration

The geometrical configuration of the system is defined by the cross section and the number of panels used in the assembly. Storm panels are fabricated by a cold form process in which the manufacturer suggests the final shape of the panels. Typically, a machine consisting of a series of metal rollers is used as the equipment to bring the shape of the panels as shown in Figure 6-19. At the beginning of the process flat sheets of metal are cut to the desired length of the panels. Then, the flat sheets are set into the machine and pass through the rollers. The shape of the rollers is imposed to the sheet by the application of a high level of pressure. The desired shape is obtained at the end of the process.

In terms of the number of panels, it is established according to the area to be protected by the storm shutter system. Therefore, a number of panel's representative for this condition is established as a parameter for our study.



Figure 6-19. Equipment used in the storm shutter panel's fabrication (JA, 2008)

6.2.3.1 Cross Sections

Each manufacturer suggests different cross sections for the panels. The cross section affects the physical behavior of the panel, especially in the moment of inertia affecting its structural capacity. Based on this fact, a survey was carried out to establish the most typical or representative cross sections used in the fabrication of storm shutters panels in United States (MDC, 2009) and Puerto Rico. A total of twenty seven (27) shutter designs from different manufacturers were compared in terms of their cross sections. Figure 6-20 shows a scaled plot providing a better visualization of how the proposed shutter cross sections differ for each manufacturer. Each schematic cross section was located in the graph such that its center coincides with the other ones. Drawings corresponding to each shutter as well as information related to material and thicknesses are included in Appendix A.

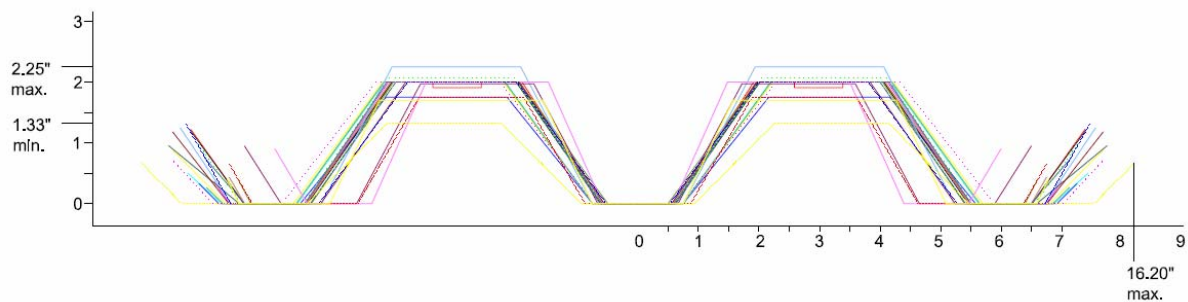


Figure 6-20. Variation of twenty seven (27) cross sections of shutter panels

It was found that height and overall width of panels are the most significant differences between the shutters. The height of shutters varied between 1.33 to 2.25 inches. In terms of the overall width panels varied between 12 to 16.36 inches. In addition to the information provided by the survey, the selected cross sections used in the models were based on the following considerations:

1. It is representative of available shutters in the local industry.
2. It is easily found by local consumers. For this reason, the cross sections correspond to the ones available in the most known or main hardware stores of the locality.
3. The cross section must be different from the others such that it will represent a not typical case.

Finally, four cross sections were selected to represent the typical shutters panels in the study. For reference purpose, the cross sections have been called CS#1, CS#2, CS#3, and CS#4 as shown in Figure 6-21 to Figure 6-24. Table 6.6 describes relevant characteristics of the selected cross sections and shows the number of finite elements used to model the storm shutter panels. It is important to note that S4R shell finite elements were used in the models.

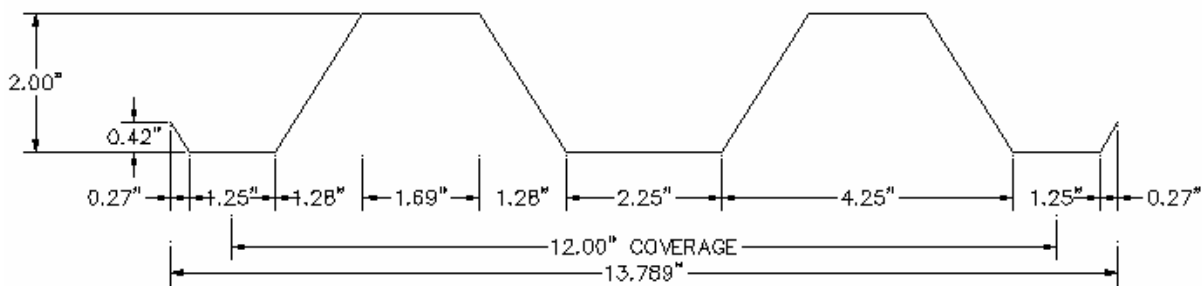


Figure 6-21. Cross Section CS#1. Cross section used in Base Case model.

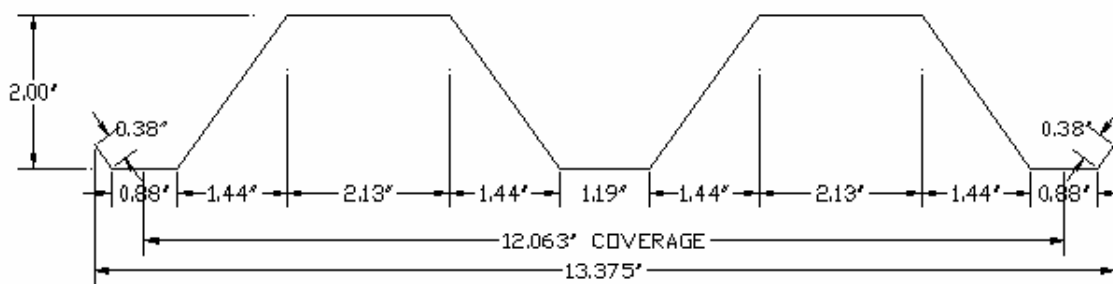


Figure 6-22. Cross Section CS#2

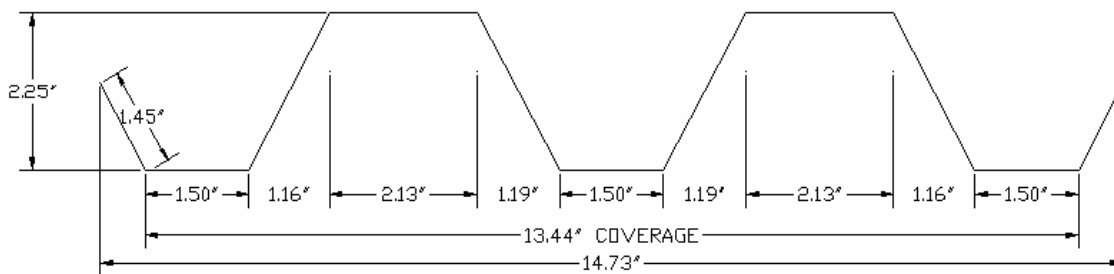


Figure 6-23. Cross Section CS#3

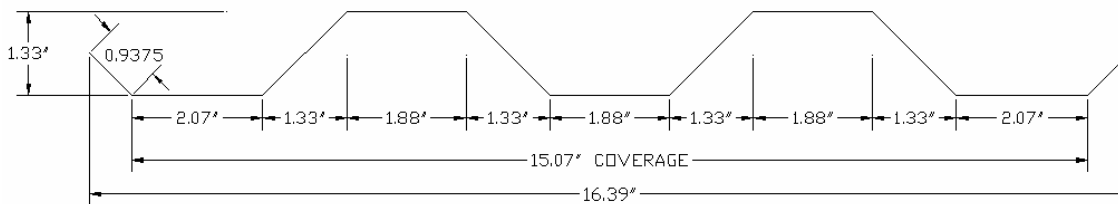


Figure 6-24. Cross Section CS#4

Table 6.6 Cross sections used on the parametric study

| Cross Sections | Remarks | No. of Finite Elements | |
|----------------|--|------------------------|----------------|
| | | Impact Panel | Adjacent Panel |
| CS#1* | Cross section available by one of the important local shutter supplier. Cross section used as base case. | 19,252 | 6,945 |
| CS#2 | Cross section available by another important local shutter supplier. | 19,521 | 7,121 |
| CS#3 | Cross section with higher height profile. | 21,145 | 7,866 |
| CS#4 | Cross section with lower height profile. | 18,658 | 6,621 |

* Base Case model

As previously mentioned, a frequency analysis was evaluated for each model such that 2% of critical damping was introduced to the analysis. Table 6.7 shows the proportionality factors obtained in each model.

Table 6.7 Proportionality factors for damped systems in the evaluation of panel cross sections

| Cross Sections | Frequency First Mode ω_m (rad/sec) | Frequency Third Mode ω_n (rad/sec) | Proportional Factors | |
|----------------|--|--|----------------------|---------|
| | | | a_o | a_1 |
| CS#1* | 131.36 | 237.22 | 4.57 | 0.00015 |
| CS#2 | 131.48 | 234.24 | 4.55 | 0.00015 |
| CS#3 | 130.53 | 229.65 | 4.49 | 0.00015 |
| CS#4 | 132.42 | 239.48 | 4.60 | 0.00015 |

* Base Case model

Figures 6.25 to 6.28 show the maximum and permanent deformation of the impact panel obtained from each cross section. It is found that the panels with a profile of higher height obtained the best response of the analysis. That was the case of CS#3 where its profile is 0.25 inches higher than CS#1 and CS#2 and 0.92 inches higher than CS#4. A high height

profile provides more moment of inertia to the panels. Thus, panels fabricated with these profiles result in more stiffness to the system. In contrast, a lower profile as CS#4 obtained the weakest performance of the analysis as shown in Figure 6-29. Table 6.8 summarizes the results obtained according to the studied cross sections.

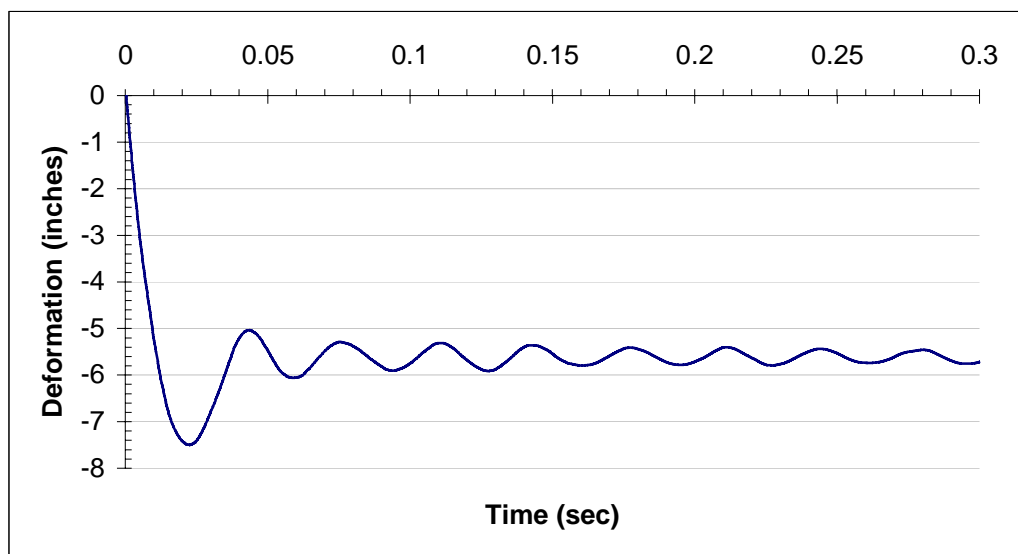


Figure 6-25. Maximum and permanent deformation for CS#1

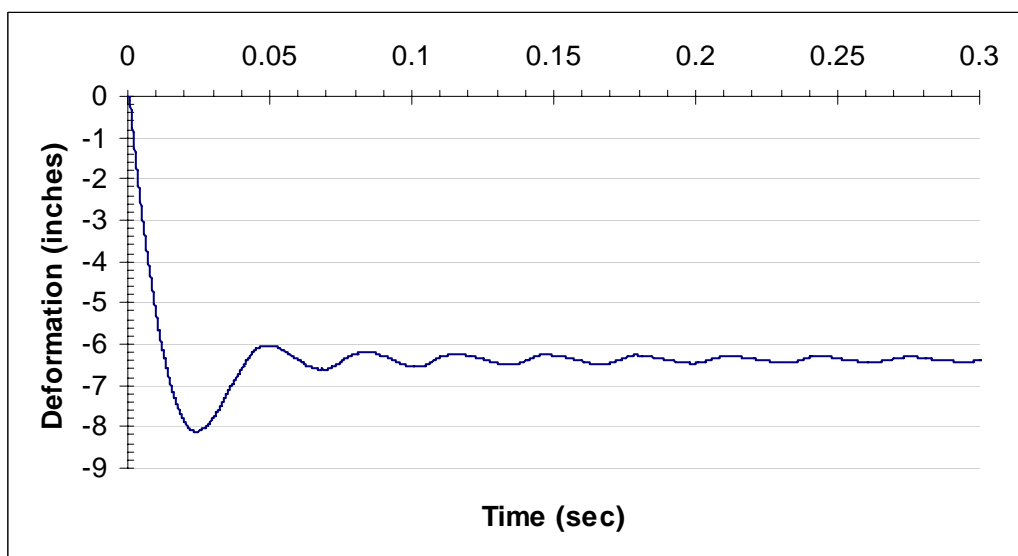


Figure 6-26. Maximum and permanent deformation for CS#2

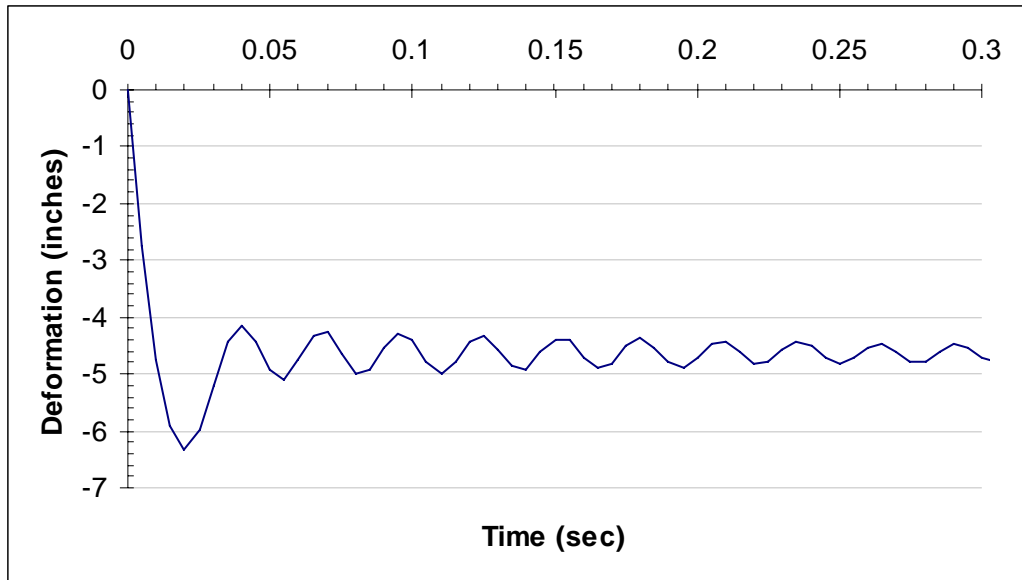


Figure 6-27. Maximum and permanent deformation for CS#3

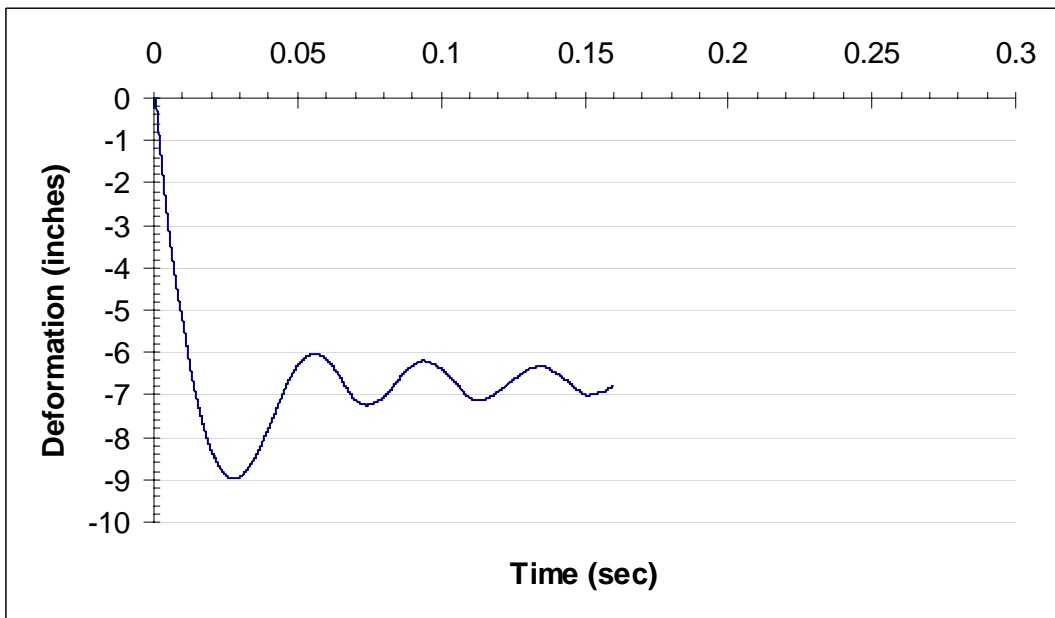


Figure 6-28. Maximum and permanent deformation for CS#4

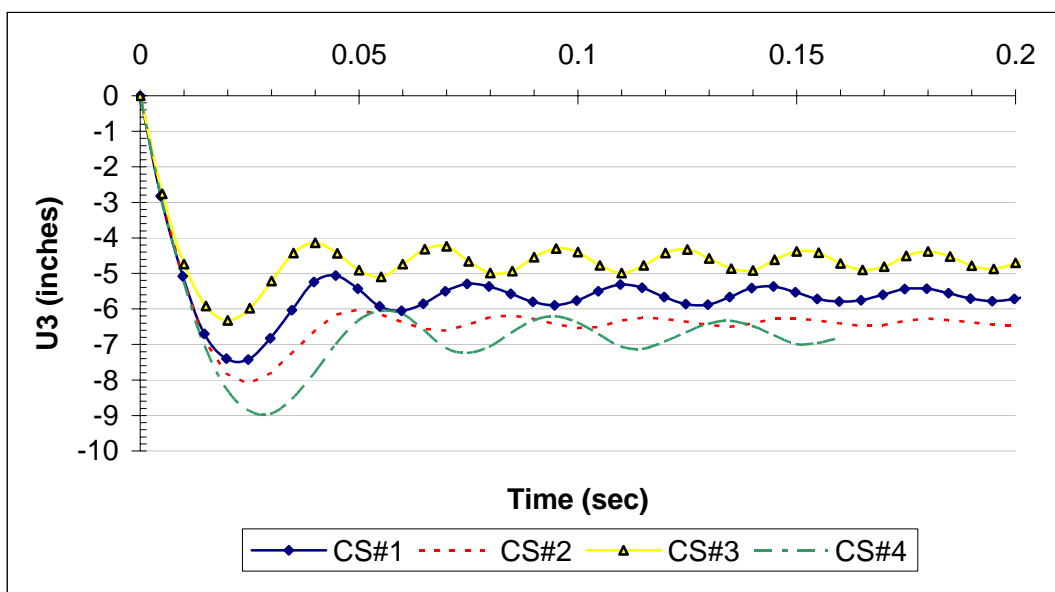


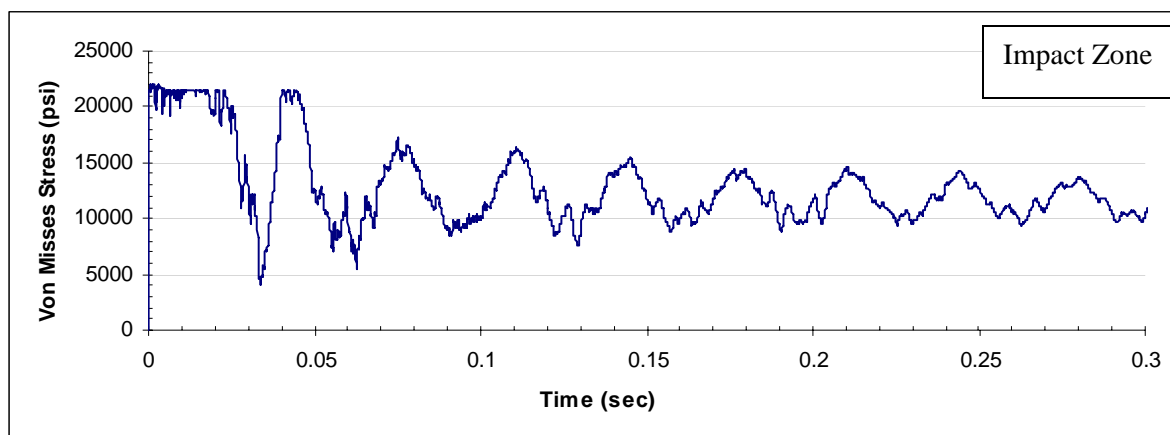
Figure 6-29. Maximum and permanent deformations of impact panel obtained for different cross sections

Table 6.8 Maximum and permanent deformation obtained varying the panel cross sections.

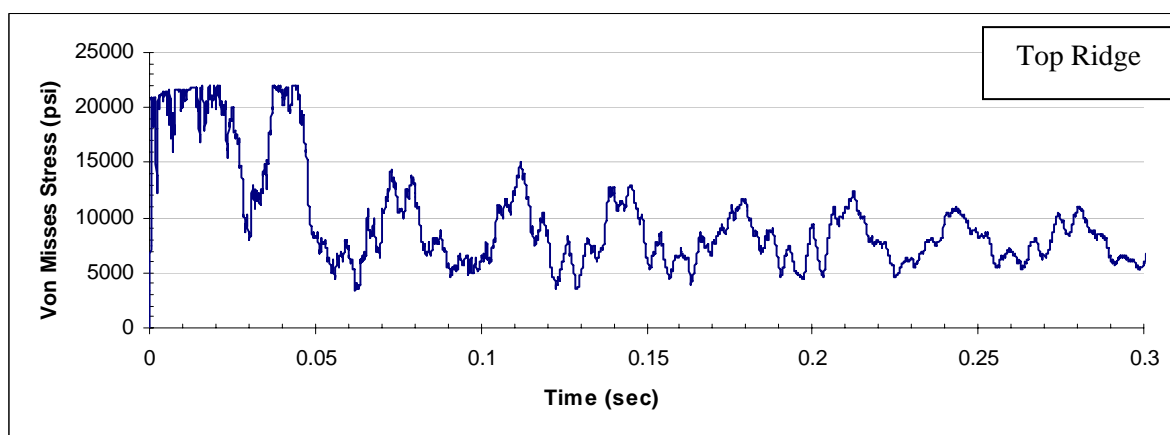
| Cross Sections | Maximum Displacement | | Permanent Deformation Value (in) |
|----------------|----------------------|------------|----------------------------------|
| | Value (in) | Time (sec) | |
| CS#1* | 7.49 | 0.023 | 5.70 |
| CS#2 | 8.12 | 0.024 | 6.42 |
| CS#3 | 6.32 | 0.020 | 4.72 |
| CS#4 | 8.98 | 0.027 | 6.80 |

* Base Case model

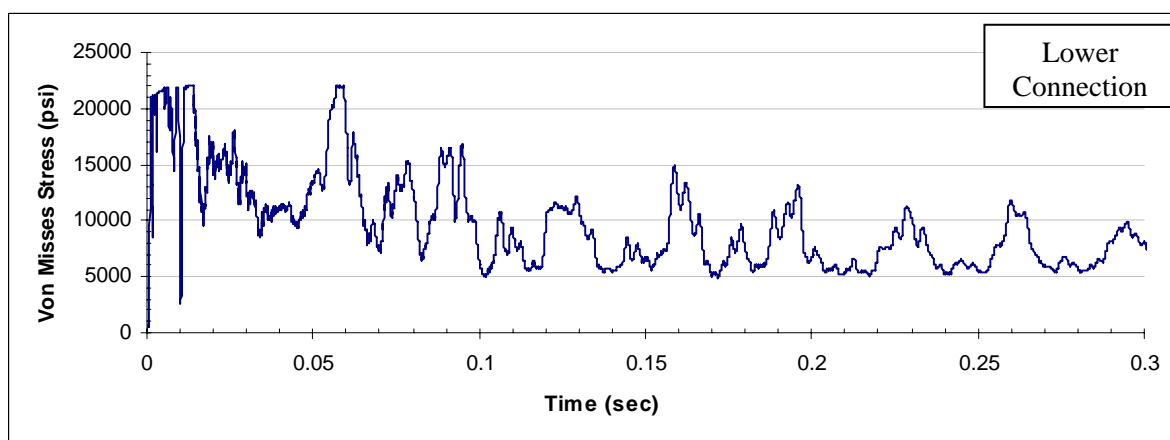
In previous parameter evaluation, the models showed that the maximum values were reached in a sequence through the established zones as shown in Figure 6-30 to Figure 6-33. Table 6.9 summarizes the obtained results showing the time of occurrence of the maximum values for each zone.



(a)

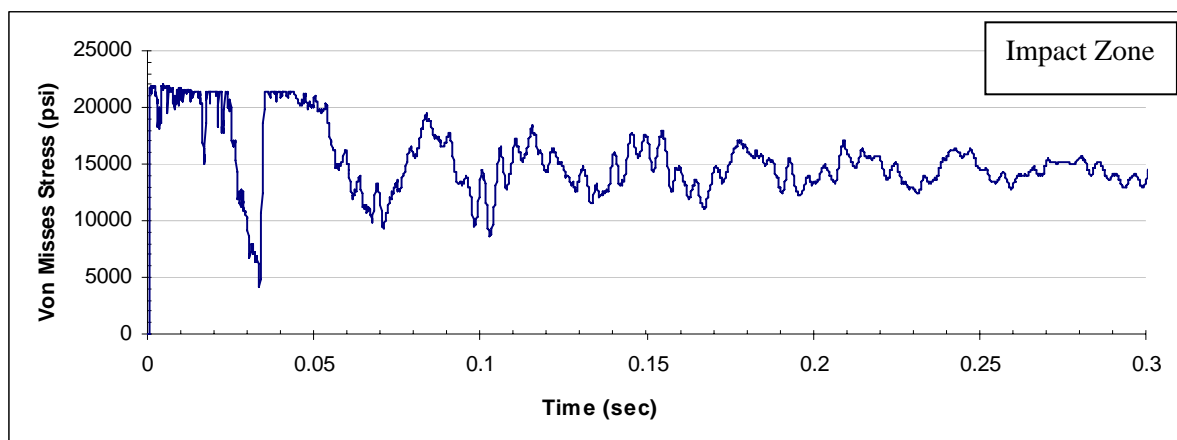


(b)

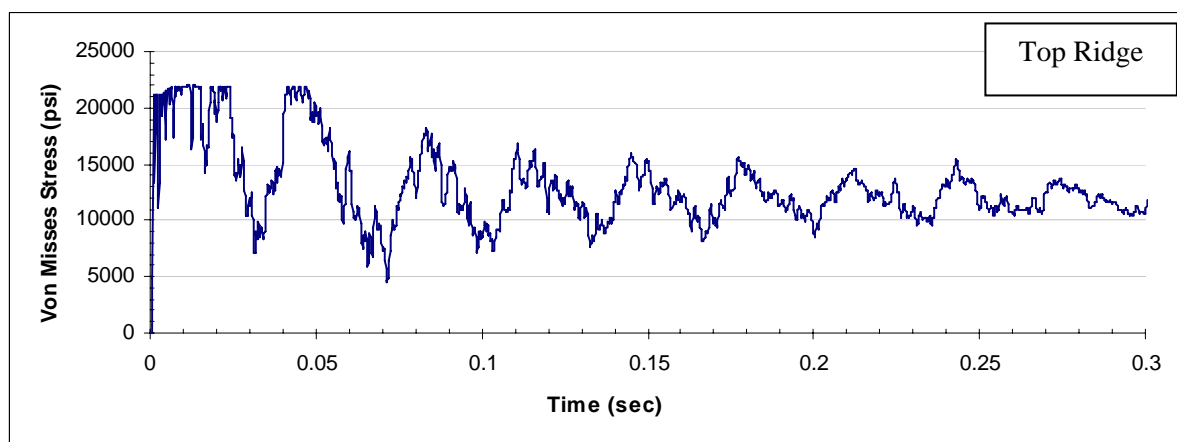


(c)

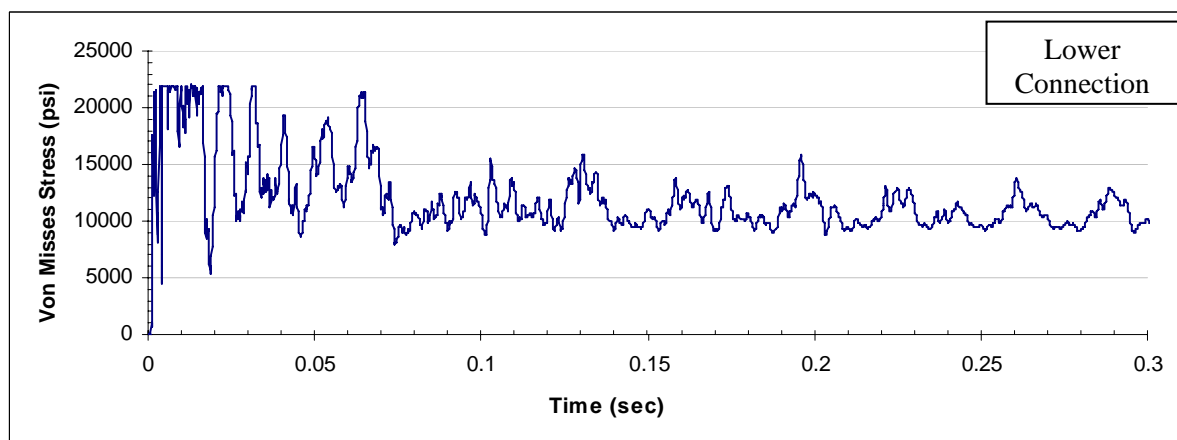
Figure 6-30. Maximum Von Mises stresses for CS#1 acting at (a) impact zone (b) top ridge and (c) lower edge connection.



(a)

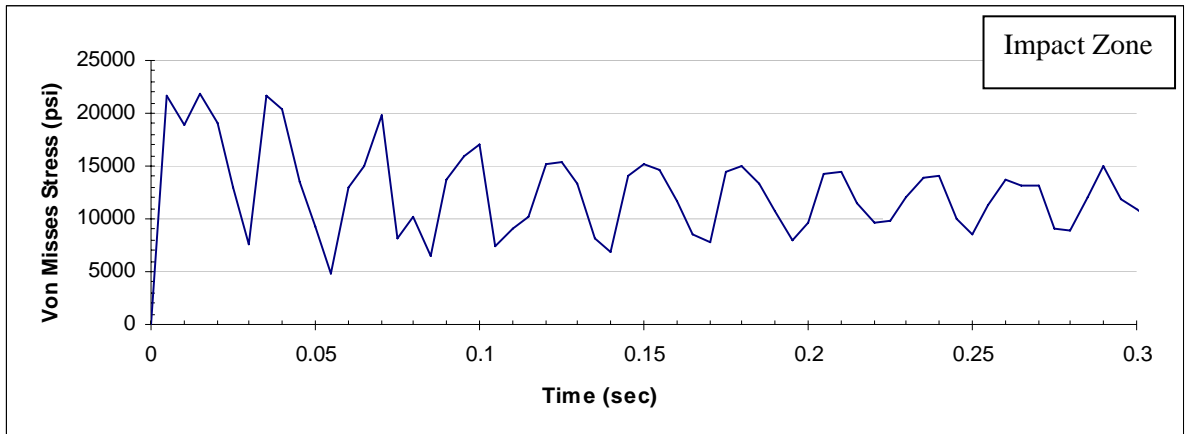


(b)

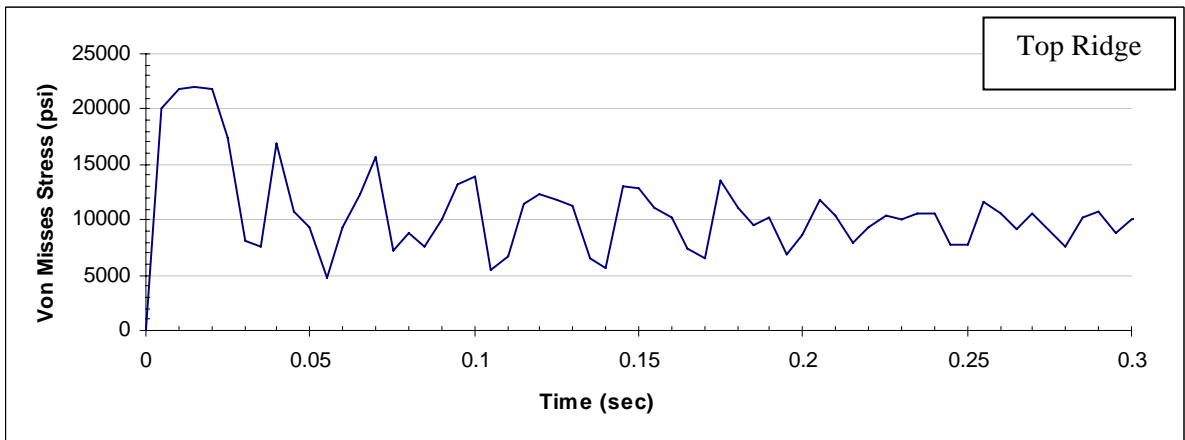


(c)

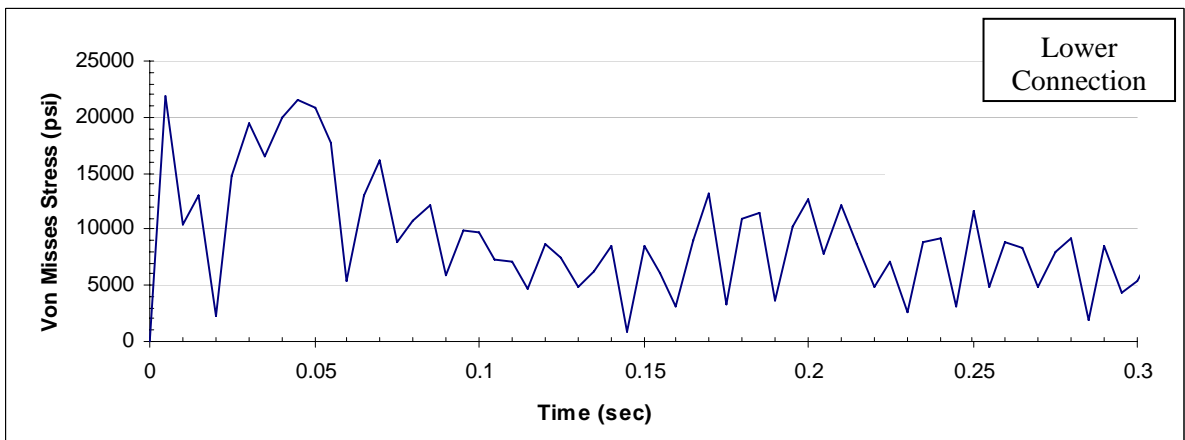
Figure 6-31. Maximum Von Mises stresses for CS #2 acting at (a) impact zone (b) top ridge and (c) lower edge connection



(a)

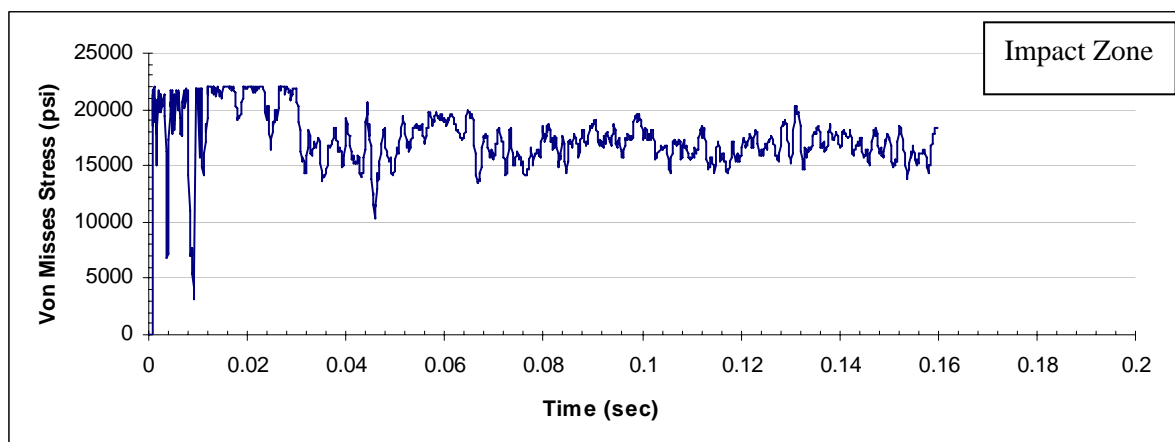


(b)

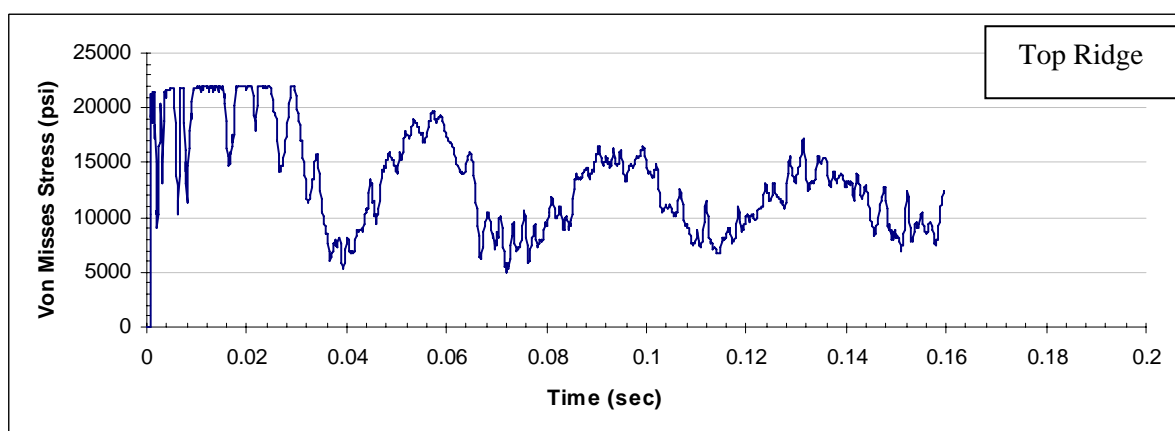


(c)

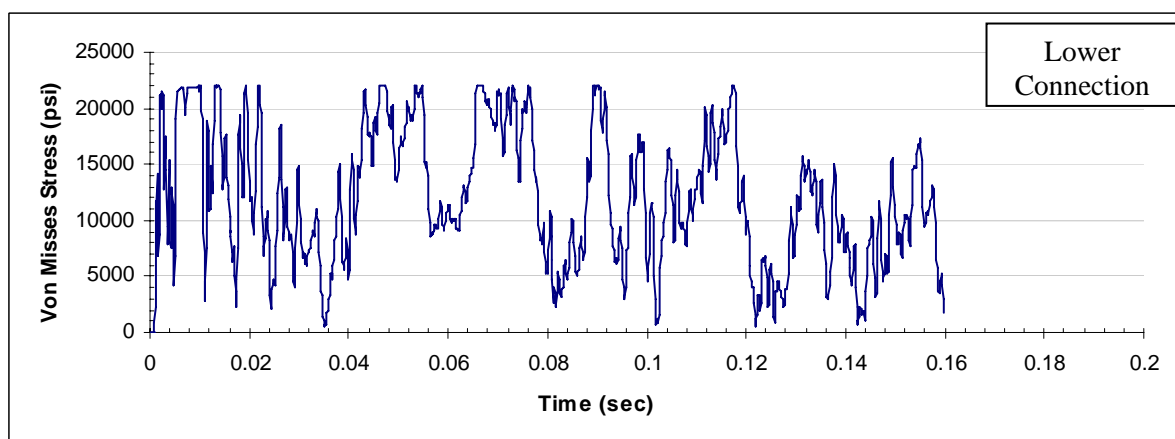
Figure 6-32. Maximum Von Mises stresses for CS #3 acting at (a) impact zone (b) top ridge and (c) lower edge connection



(a)



(b)



(c)

Figure 6-33. Maximum Von Mises stresses for CS #4 acting at (a) impact zone (b) top ridge and (c) lower edge connection

The maximum stresses occurred first at the impact zone for CS#1, CS#2 and CS#4. It is important to note that all the cross sections were evaluated using the Base Case model material (Aluminum Alloy 3003-H14). As mentioned earlier, this material showed this sequence behavior. It was concluded that CS#3 improved the panel material performance due to its high height profile. The other cross sections were designed with a lower height profile in comparison with CS#3. Thus, these panels showed a similar sequence as the Base Case model.

Table 6.9 Maximum Von Mises stresses acting at different zones of the impacted panel. Values obtained for different panel cross sections.

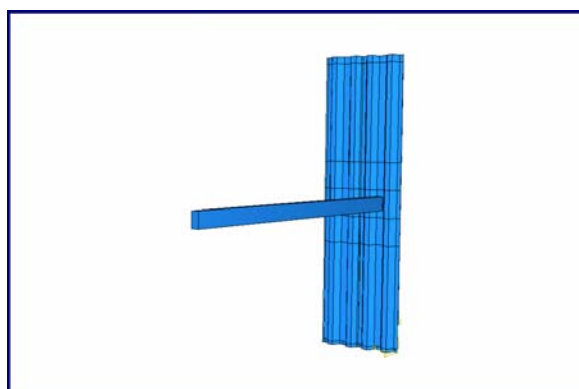
| High Stress Zones | CS#1* | | CS#2 | | CS#3 | | CS#4 | |
|-------------------|------------------|------------|------------------|------------|------------------|------------|------------------|------------|
| | Max. Value (psi) | Time (sec) |
| Impact | 21,983 | 0.001 | 21,984 | 0.005 | 21,914 | 0.015 | 21,984 | 0.001 |
| Top Ridge | 21,929 | 0.045 | 21,983 | 0.013 | 21,980 | 0.015 | 21,984 | 0.021 |
| Lower Connection | 21,983 | 0.014 | 21,984 | 0.013 | 21,983 | 0.005 | 21,984 | 0.066 |

* Base Case model

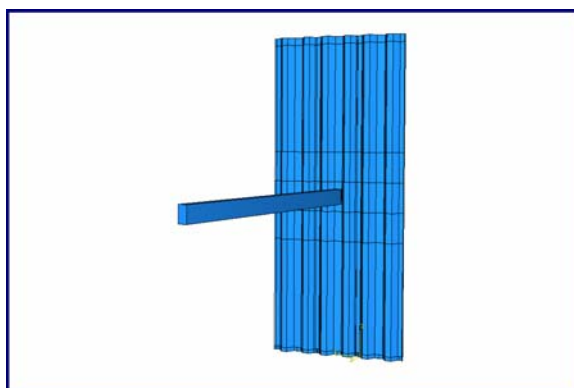
6.2.3.2 Number of Panels

In Chapter II, it was mentioned that typical window panels used in local residential buildings require an opening wall of 5'-0" height by 5'-0" wide. Based on these dimensions, shutter manufacturer's recommend a storm shutter's assembly consisting of five panels of 7'-0" height. Therefore, a total of five panels were used as the maximum number of panels to be evaluated in the parametric study. Assemblies consisting of two (Base Case model), three

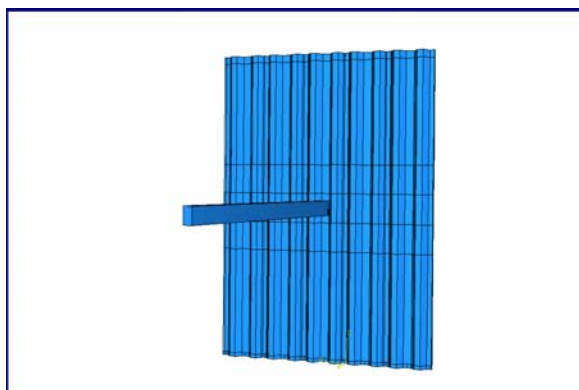
and five panels were evaluated as shown in Figure 6-34. For modeling purposes, all panels were located according to the installation sequence suggested by shutter manufacturers and used on Test 1 as mentioned in Chapter III.



(a)



(b)



(c)

Figure 6-34. Storm shutter model defined with: (a) two panels (b) three panels (c) five panels

The maximum and permanent deformations of the impacted panel were obtained for each model as shown in Figure 6-35 and Figure 6-37. As the number of panels increased, the response of the system showed an improvement. In comparison with the Base Case model (two panel's model), the maximum deformation of the impacted panel was reduced by 0.56 inches and 0.75 inches for using three and five panels in the assembly respectively as shown in Figure 6-39. Table 6-10 not only summarizes the obtained values but also shows how the times of occurrence for the maximum values decreased as panels were added to system.

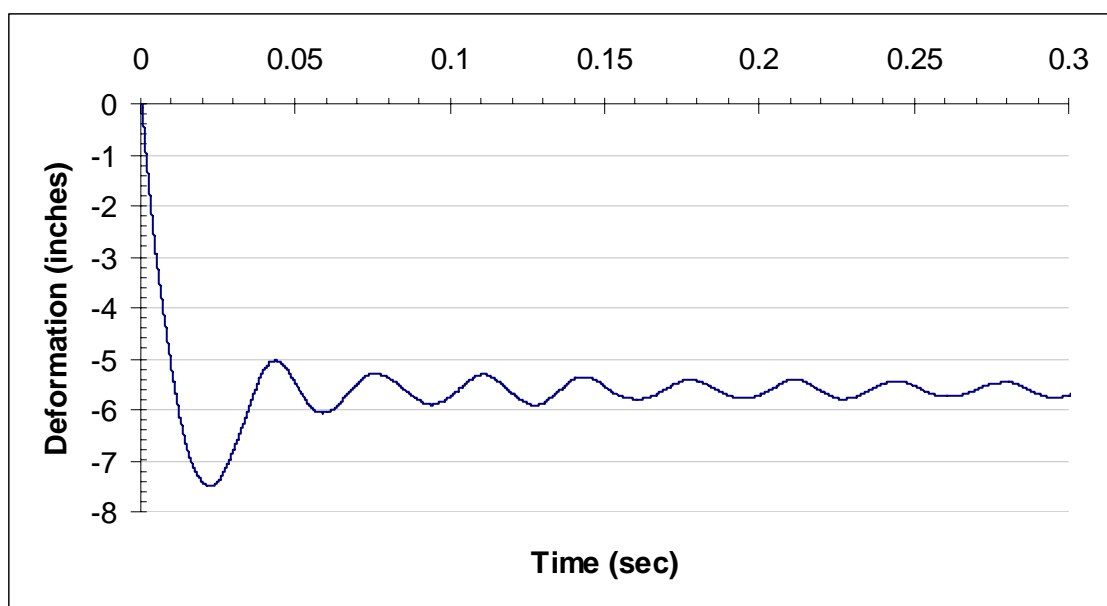


Figure 6-35. Maximum and permanent deformation using two panels

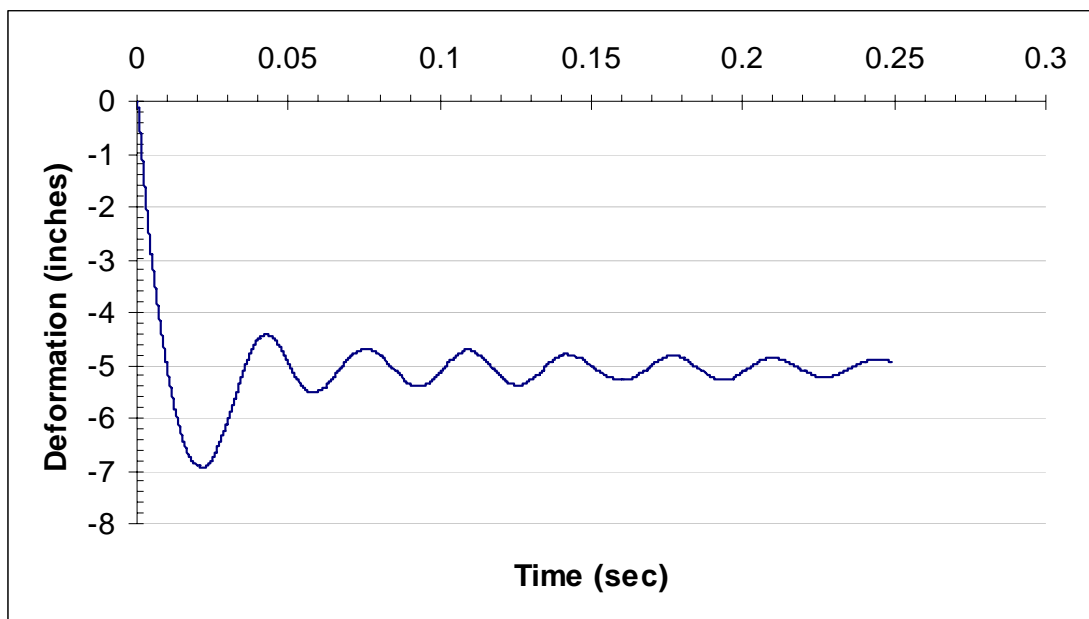


Figure 6-36. Maximum and permanent deformation using three panels

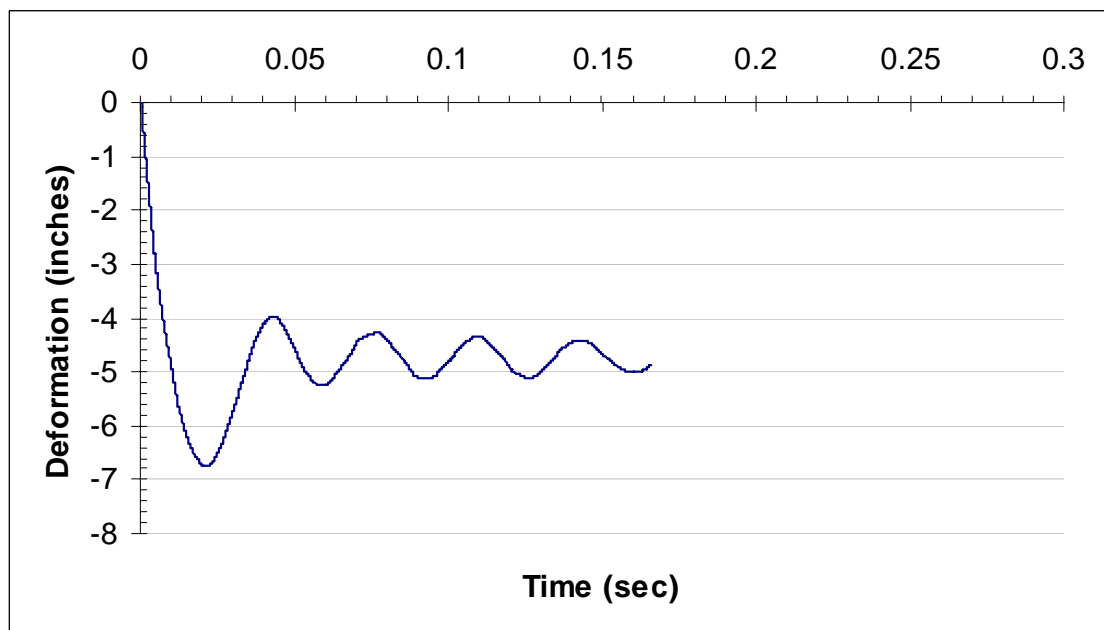


Figure 6-37. Maximum and permanent deformation using five panels

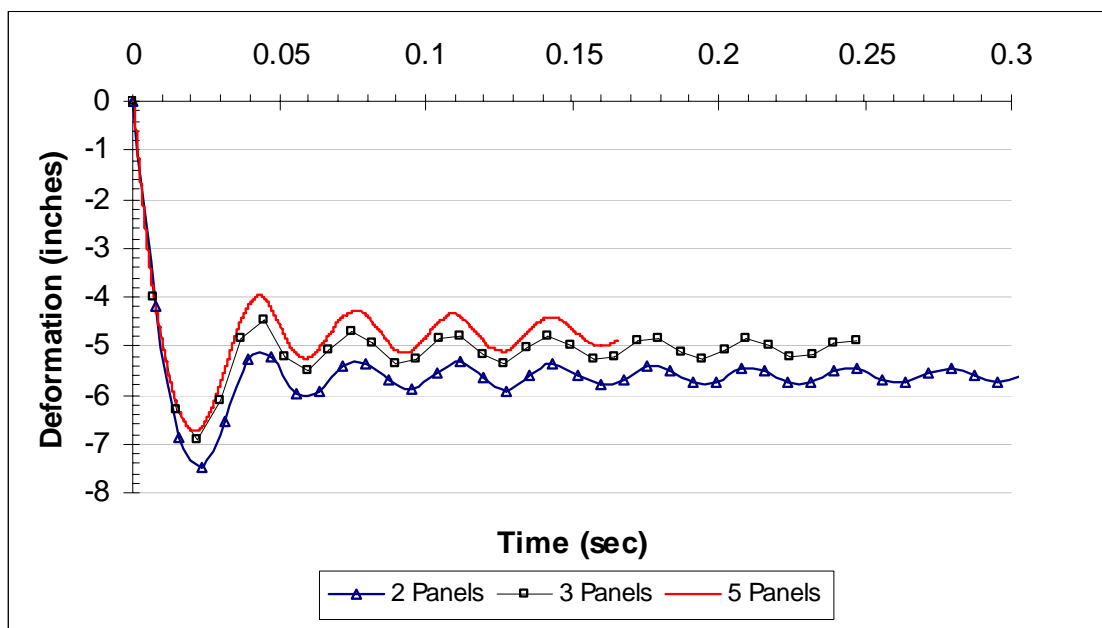


Figure 6-38. Maximum and permanent deformation varying the number of panels

Table 6.10 Maximum and permanent deformation obtained varying the number of panels in the assembly.

| Number of Panels | Maximum Displacement | | Permanent Deformation Value (in) |
|------------------|----------------------|------------|----------------------------------|
| | Value (in) | Time (sec) | |
| 2 * | 7.49 | 0.023 | 5.70 |
| 3 | 6.93 | 0.022 | 5.05 |
| 5 | 6.75 | 0.021 | 4.85 |

* Base Case model

It was observed that the presence of the third panel in the assembly reduced the upper edge rotation of the impacted panel during the simulation as shown in Figure 6-39. Thus, the impacted panel decreased its deformation in comparison with the assembly of two panels

(Base Case model). This behavior continued its improvement as more panels were added to the assembly.

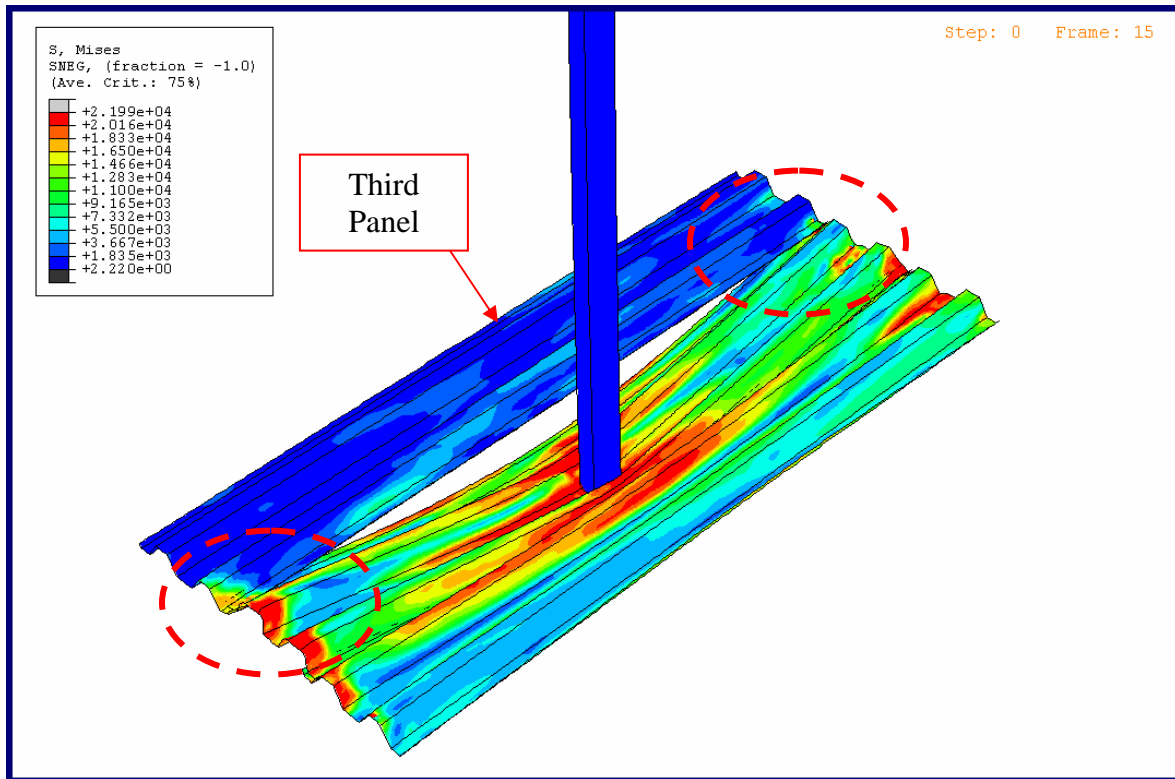
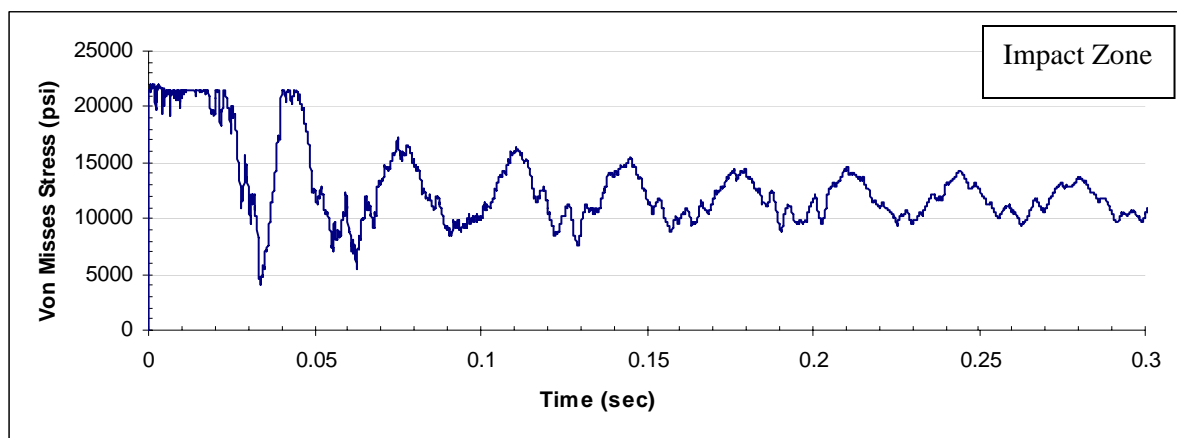
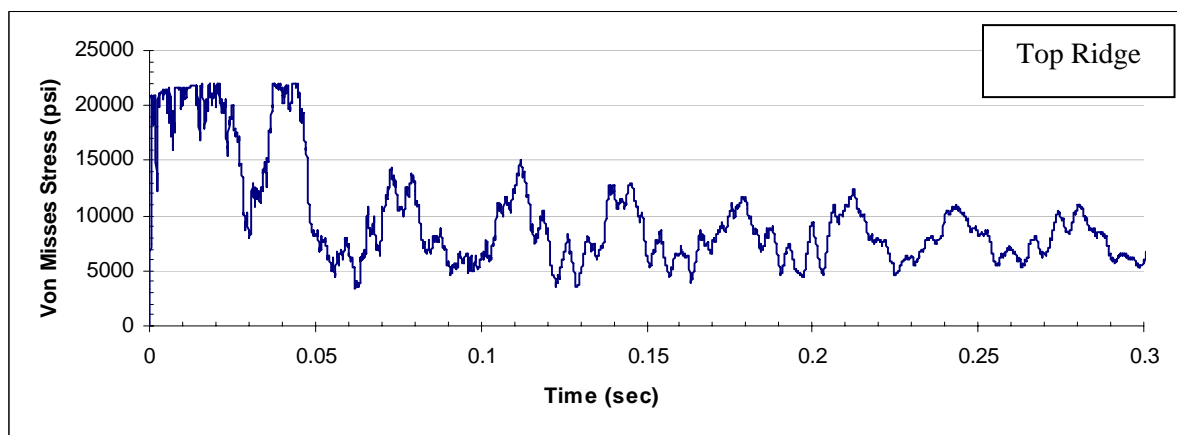


Figure 6-39. Reduction of the upper edge rotation of the impacted panel due to the contact with the third panel

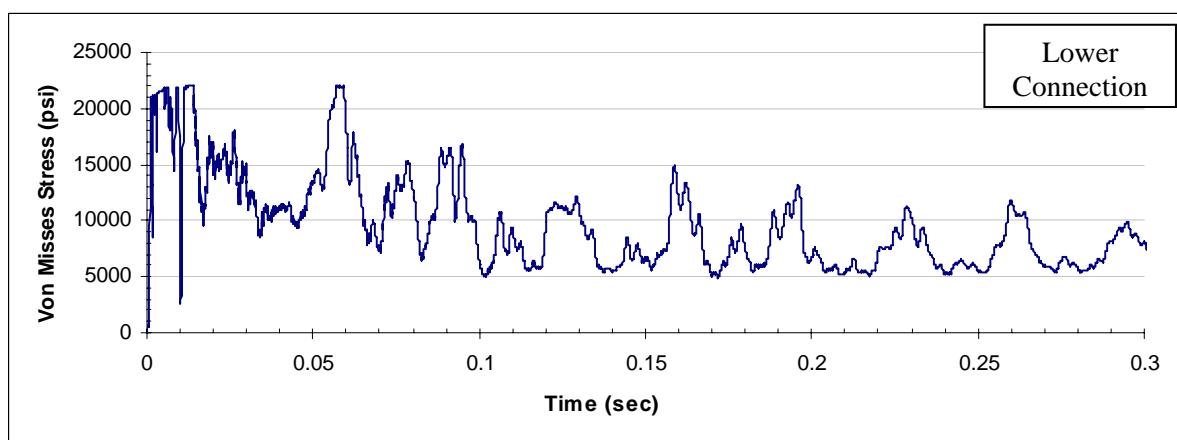
The maximum stresses acting in the impact panels changed its sequence of occurrence as additional panels were used in the system as shown in Figure 6-40 and Figure 6-42. Table 6-11 shows that the maximum stress occurred at the lower edge connection zone where the system becomes stronger by the use of more panels. It was concluded that the panel material behavior was forced to change.



(a)

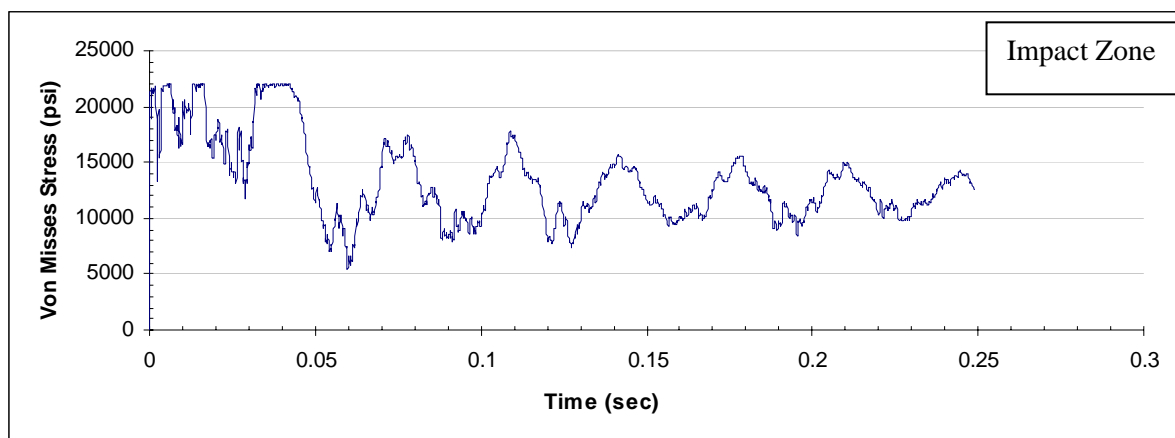


(b)

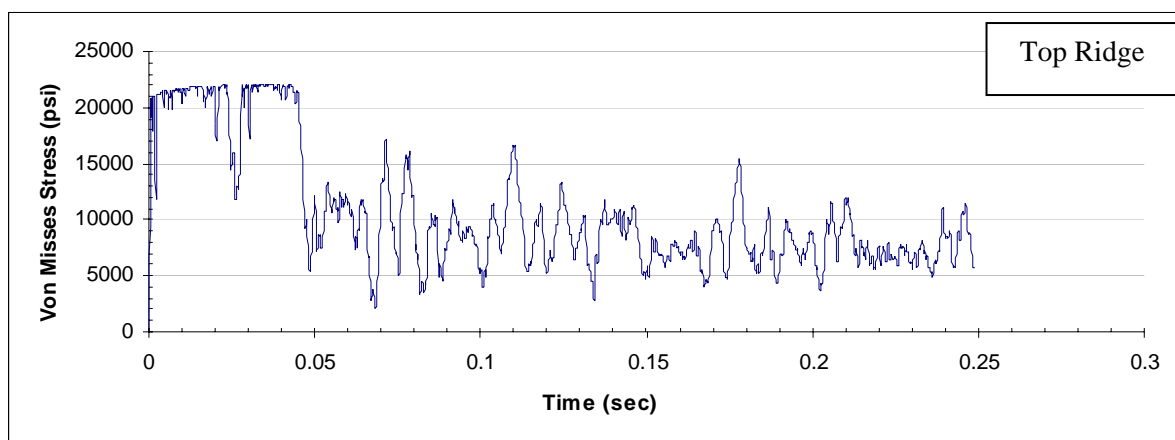


(c)

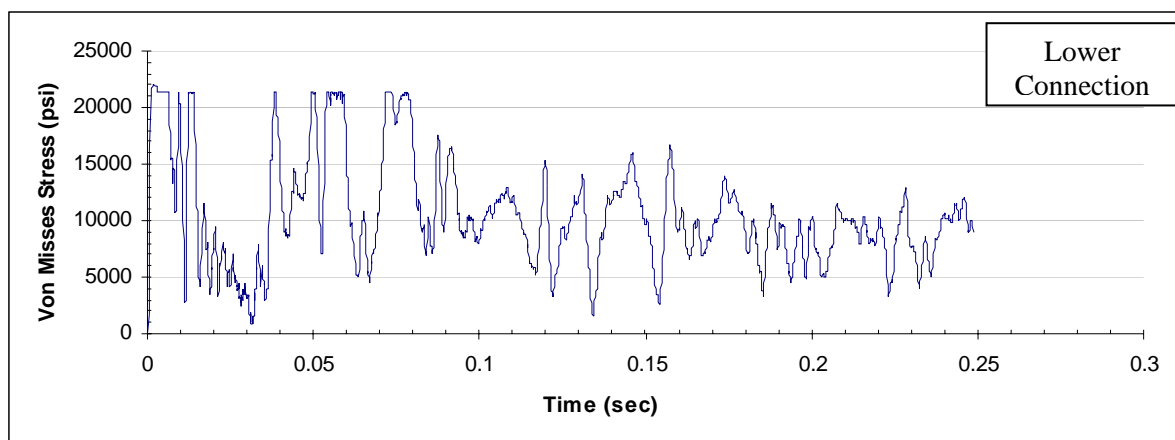
Figure 6-40. Maximum Von Mises stresses for a two panel's model acting at (a) impact zone (b) top ridge and (c) lower edge connection.



(a)

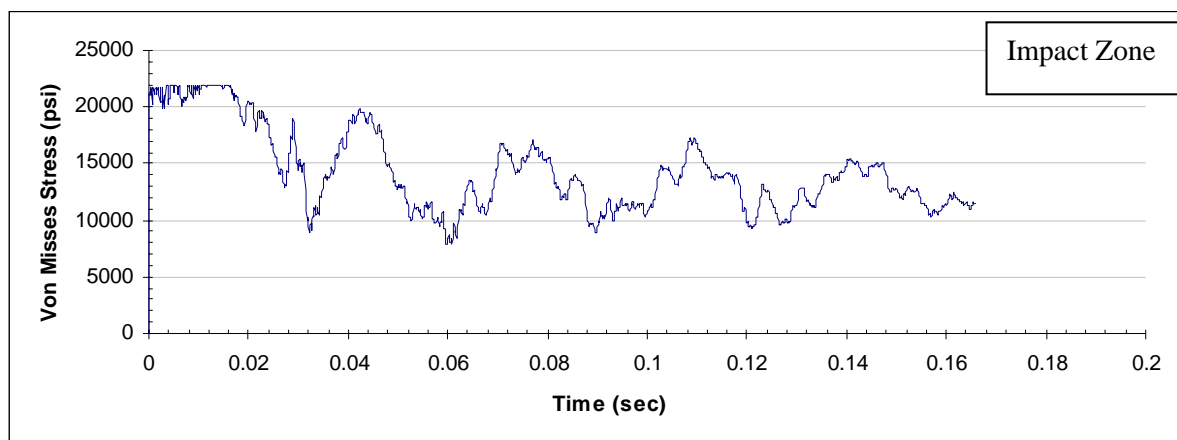


(b)

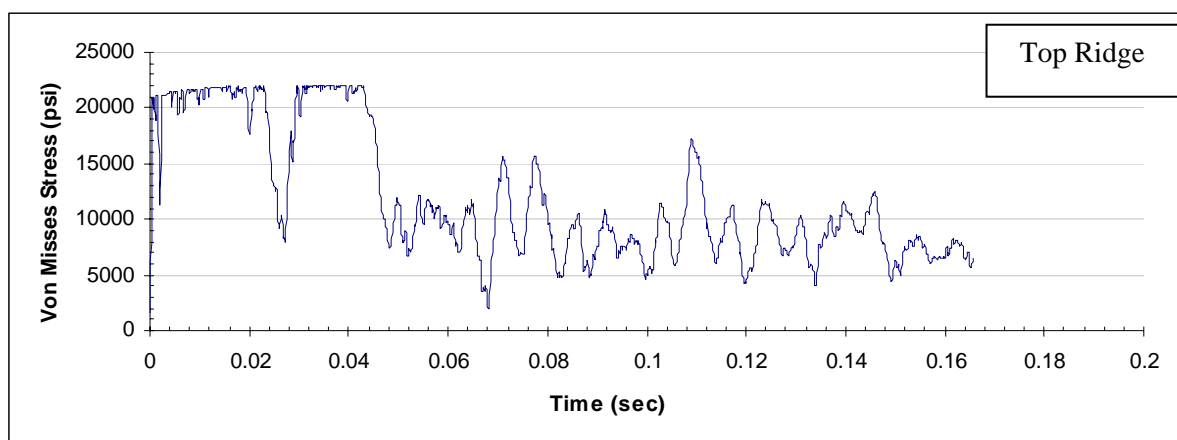


(c)

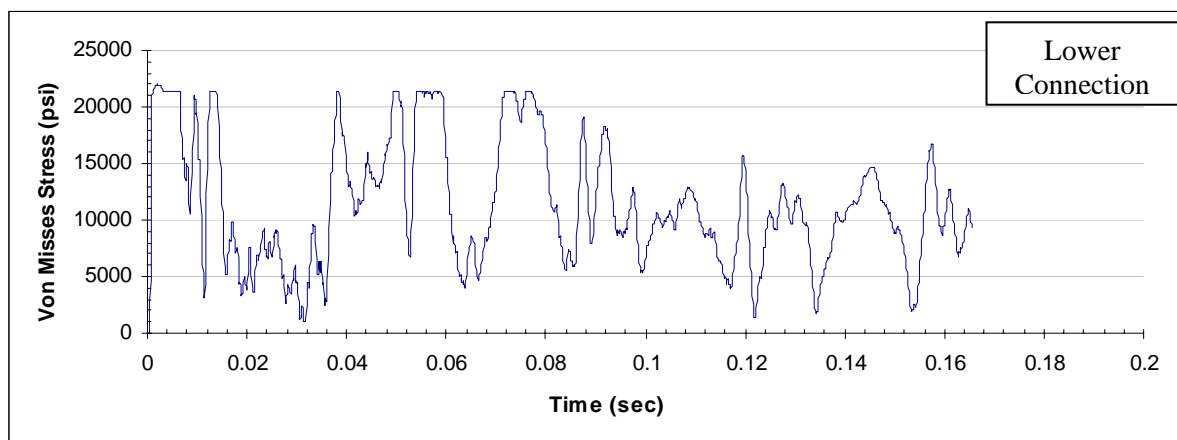
Figure 6-41. Maximum Von Mises stresses for a three panel's model acting at (a) impact zone (b) top ridge and (c) lower edge connection.



(a)



(b)



(c)

Figure 6-42. Maximum Von Mises stresses for a five panel's model acting at (a) impact zone (b) top ridge and (c) lower edge connection

Table 6.11 Maximum Von Mises stresses acting at different zones of the impacted panel. Values obtained for different number of panels in the assembly.

| High Stress Zones | Two Panels* | | Three Panels | | Five Panels | |
|-------------------|------------------|------------|------------------|------------|------------------|------------|
| | Max. Value (psi) | Time (sec) | Max. Value (psi) | Time (sec) | Max. Value (psi) | Time (sec) |
| Impact | 21,983 | 0.001 | 21,984 | 0.035 | 21,984 | 0.013 |
| Top Ridge | 21,929 | 0.045 | 21,984 | 0.036 | 21,983 | 0.043 |
| Lower Connection | 21,983 | 0.014 | 21,984 | 0.002 | 21,984 | 0.002 |

* Base Case model

6.2.4 Effect of Boundary Conditions

Three physical mechanisms defined the existing boundary conditions of a typical storm shutter system. The first mechanism is produced by the contact between panels in the assembly. The installation sequence for shutter panels provides that one edge of each panel can be supported by the edge of adjacent panels. As the impact load is applied at one panel, the support of each adjacent panel contributes to minimize the resulting displacement not only for the impacted panel but all the system. As mentioned earlier, this physical mechanism is considered as a contact interaction between panels. It was applied in every model of the study.

The second mechanism is the support provided by two aluminum sections that are used to connect the upper and lower edges of the panels. In Chapter V, these support sections were defined as simple constraints imposed on certain nodes in the model. A pinned connection was used to represent the bolts and nuts that fixed the panels to the lower support.

Meanwhile, a roller connection was used at the upper edge of the panels as it tends to rotate inside the top header. However, some displacement and rotation of the upper edge would be reduced when it makes contact with the top header walls.

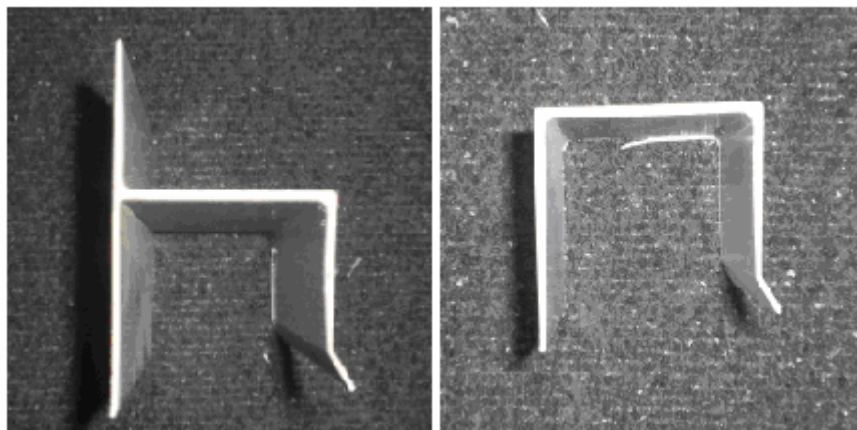
Three parameters were evaluated to obtain the response of the system due to the variations in the degree of freedom of the upper edges of the panels.

1. Free rotation and in-plane displacements. The upper edge of panels rotated without any restriction as was previously assumed. This condition was used in the analysis of previous parameters.
2. Partially rotation and in-plane displacements. This case considered the presence of a top header in the system. Therefore, a more sophisticated definition of this boundary condition was required in the model. The top header walls were modeled as two surfaces located above and below the upper edge of the panels. Typically, top headers are fabricated using an extruded section of 6063-T6 aluminum alloy of 0.094 inches thick and the cross section shown in Figure 6-43. Thus, the surfaces were defined according to these material and physical properties in the model.
3. Free rotation without in-plane displacements. A pinned connection was used in the upper edges. This condition represented the effect of using the same kind of support for both edges.

The third mechanism is the support provided by vertical edges of the opening wall to be covered by the system. This support occurs only in one direction as the first and last panels of the assembly move against the opening edges as a response of the system to applied loads.

h – header

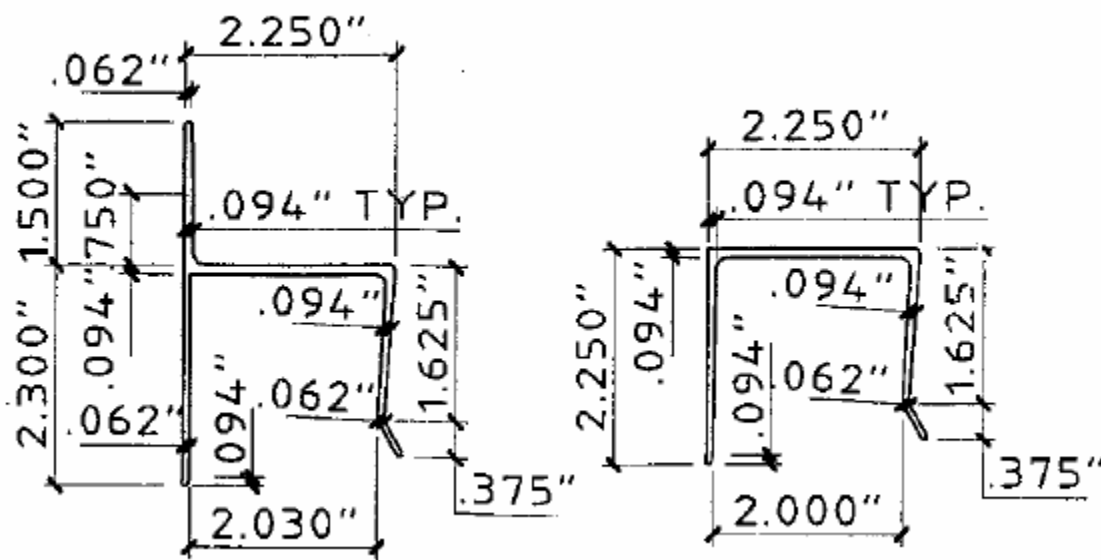
U- Channel header



(a)

h – header

U- Channel header



(b)

Figure 6-43. Typical top headers (a) cross sections (b) dimensions

However, special attention was given to the intermediate panels. Intermediate panels will experience greater displacements than edge panels. This argument is based on the fact that intermediate panels are related only to mechanism #1 and #2. Thus, intermediate panels are allowed to displace without any constraint at its span. It is important to mention that the objective of this study is to analyze the most detrimental behavior of the shutters. Therefore, this last mechanism was not considered in the parametric study.

Minor changes were made to the Base Case model to consider the use of a pinned connection at the upper edge of the panel. However, a more complex modification was necessary to include a top header in the Base Case model.

As mentioned earlier, two surfaces were located 0.05 inches (above and below) from the upper edge of the panels as shown in Figure 6-44. Shell elements with a thickness of 0.093 inches were used to define the surfaces.

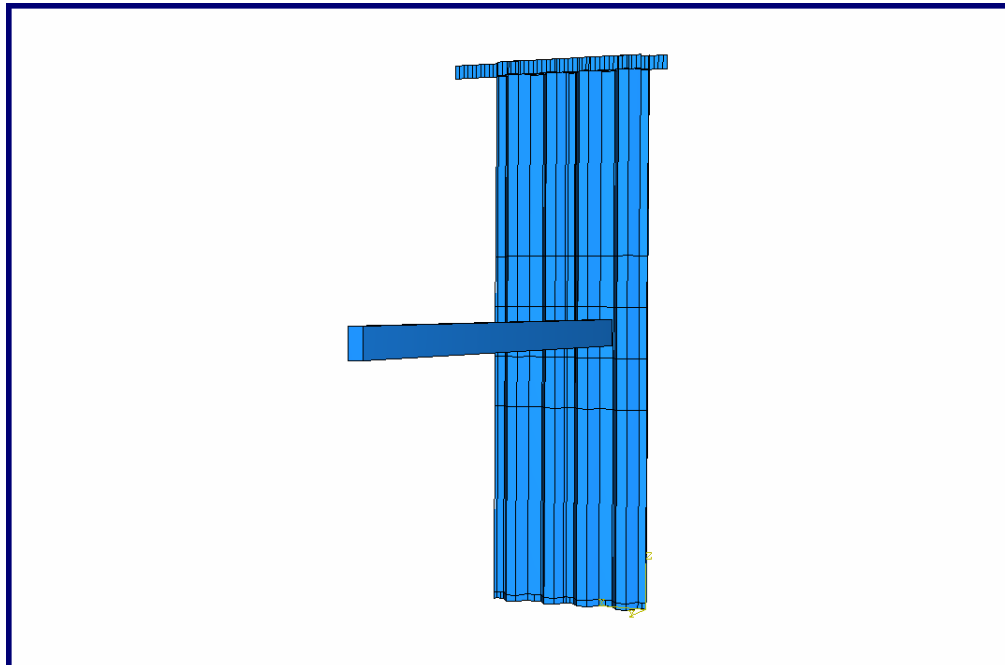


Figure 6-44. Top header model

In the previous analysis it was observed that the panels vibrate as they responded to the missile impact. It means that contact must be generated between the panels and the headers. Therefore, additional contact interaction zones were defined in the Base Case model. A total of nine (9) contact interaction zone were used according to the number of hills and valleys of the two panels that were in contact to the surfaces.

Figure 6-45 to 6-47 shows the maximum and permanent deformation obtained at the impact panel for each type of support. The best response of the system was achieved for the pinned support model as shown in Figure 6-48. As the panel was not able to displace in the in-plane direction the resulting deformation was decreased 1.13 inches compared to the Base Case model. Also, it was observed that the amplitude of the oscillations was minimized resulting in a more clearly permanent deformation behavior. Table 6-12 shows the maximum and permanent deformation of the impact panel obtained for different type of top edge supports.

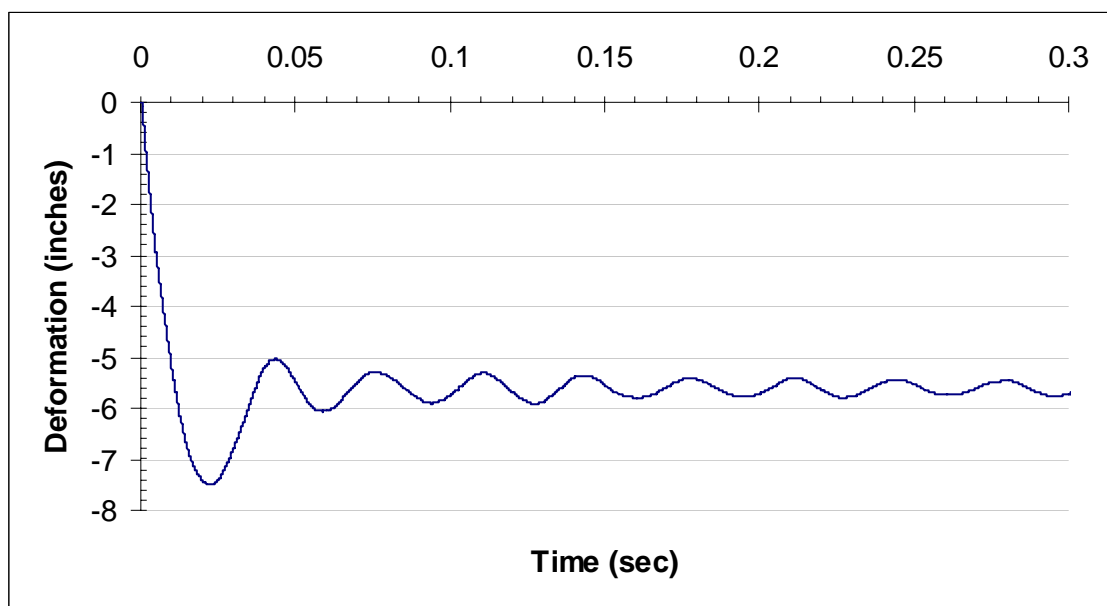


Figure 6-45. Maximum and permanent deformation of the impact panel when its top edge was supported by a roller connection

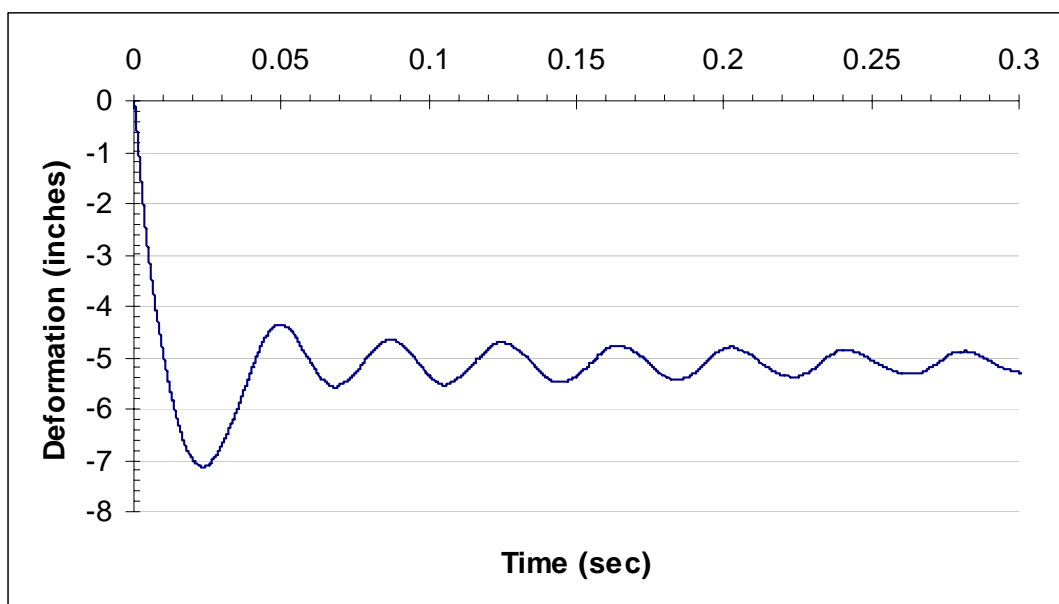


Figure 6-46. Maximum and permanent deformation of the impact panel when its top edge was supported by the top header

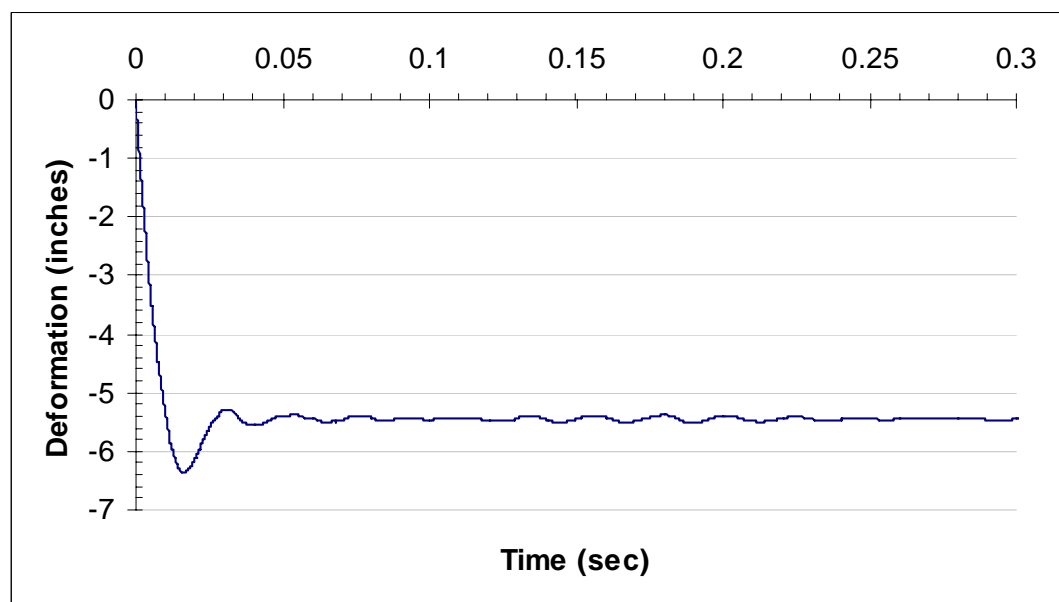


Figure 6-47. Maximum and permanent deformation of the impact panel when its top edge was supported by a pinned connection

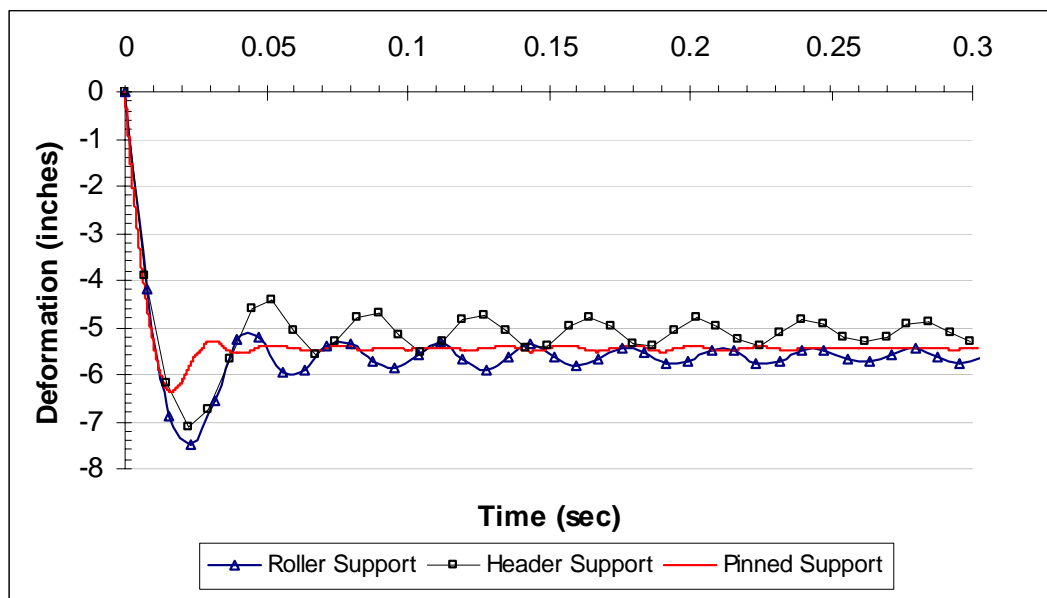


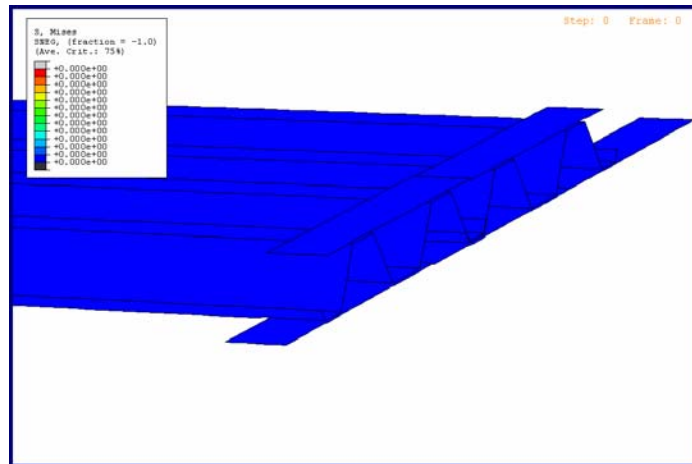
Figure 6-48. Maximum and permanent deformation varying the type of the top edge support

Table 6.12 Maximum and permanent deformation obtained varying the type of the upper support.

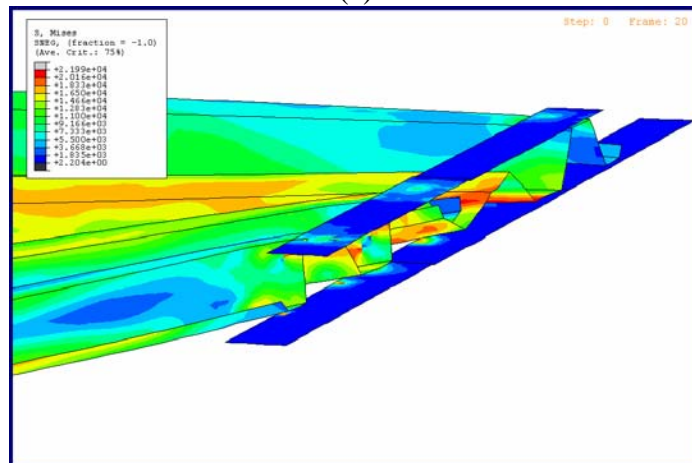
| Top Edge Support | Maximum Displacement | | Permanent Deformation Value (in) |
|------------------|----------------------|------------|----------------------------------|
| | Value (in) | Time (sec) | |
| Roller * | 7.49 | 0.023 | 5.70 |
| Header | 7.14 | 0.024 | 5.23 |
| Pinned | 6.36 | 0.016 | 5.45 |

* Base Case model

Although the best response of the system was obtained for the pinned support the top header model improved to the model too. The interior walls of the header restrained the rotation of the impact panel. Figure 6-49 shows that the upper edge tried to rotate but it was limited due to the contact produced with the upper and lower surfaces. As a result the maximum displacement was 0.35 inches less than the Base Case model.



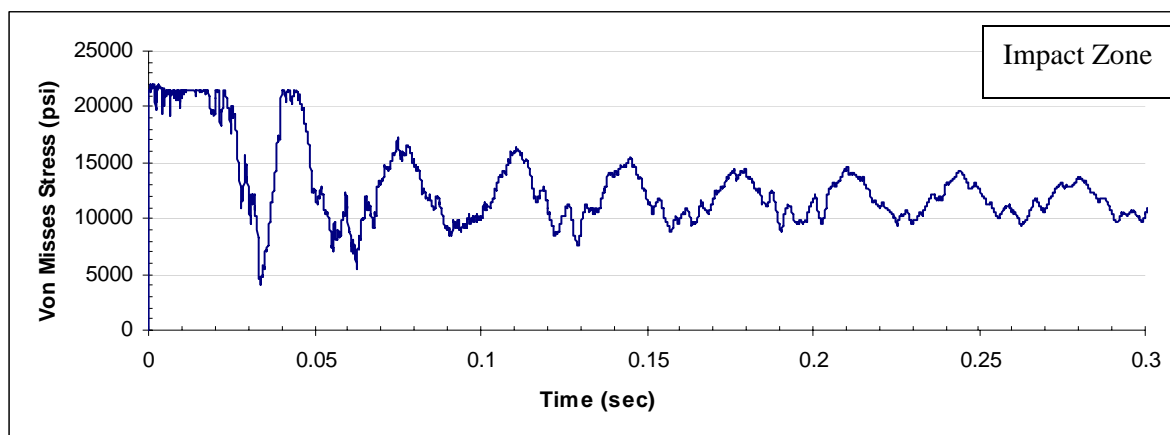
(a)



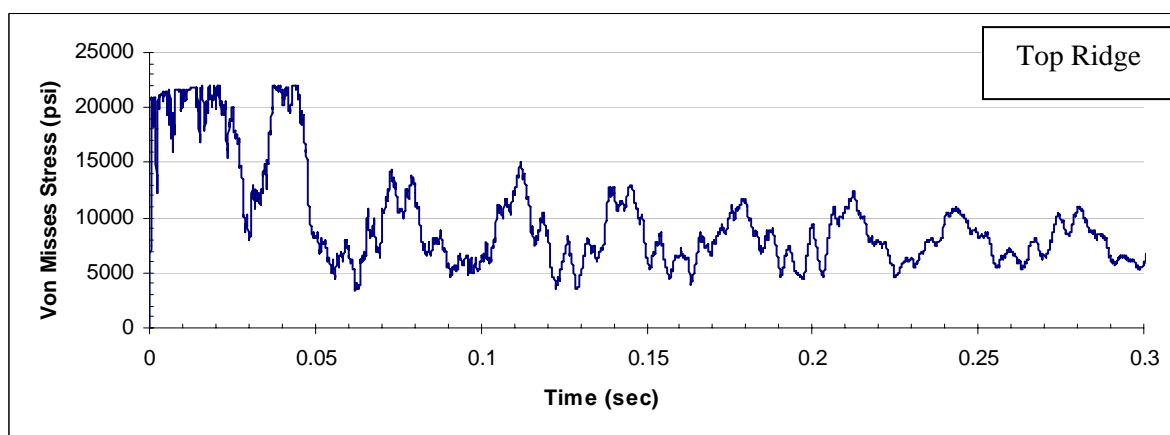
(b)

Figure 6-49. Panel edge rotation inside the top header: (a) zero rotation previous to the applied load, $t = 0.0$ sec. (b) panel rotation constrained by the contact with the inside walls of the top header, maximum rotation at $t = 0.027$ sec.

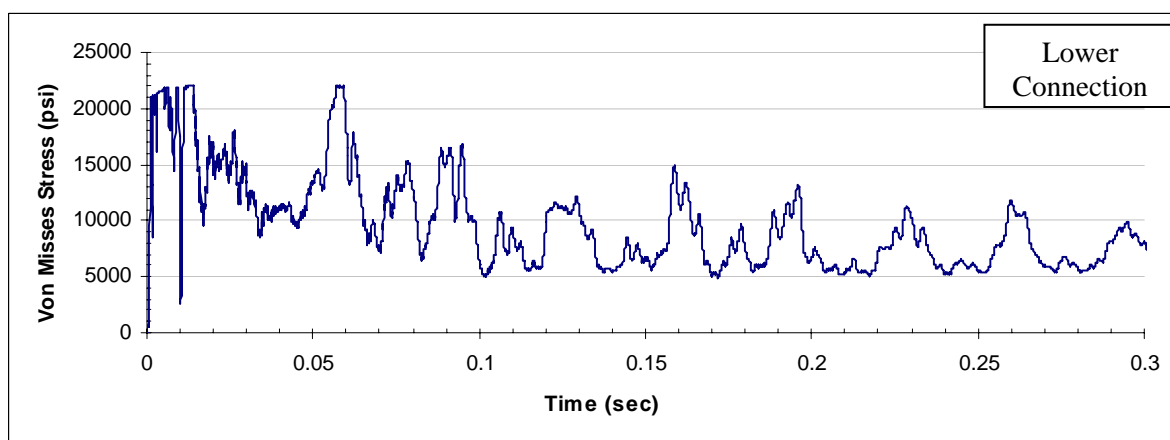
The maximum stress zones experienced similar levels of stress as shown in Figure 6-50 and 6-52. However, the stresses were reached first at the lower connection zone for the pinned support model in comparison with the others. The restriction of in-plane displacements imposed by the pinned support tended to generate more tension in the lower area (valleys) of the panel profile. As a result the panels become more rigid such that the distribution of stress was concentrated at the supports. Table 6-13 summarizes the maximum stresses obtained for each model.



(a)

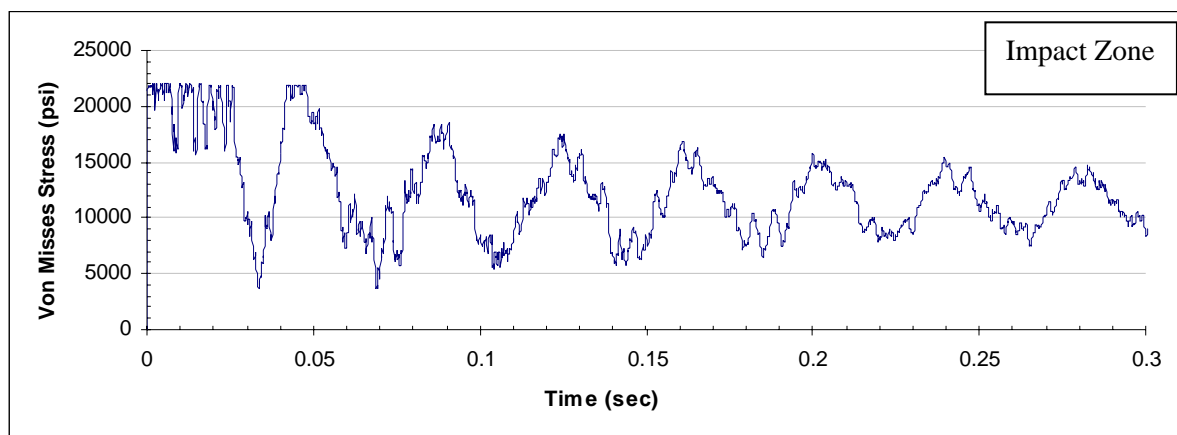


(b)

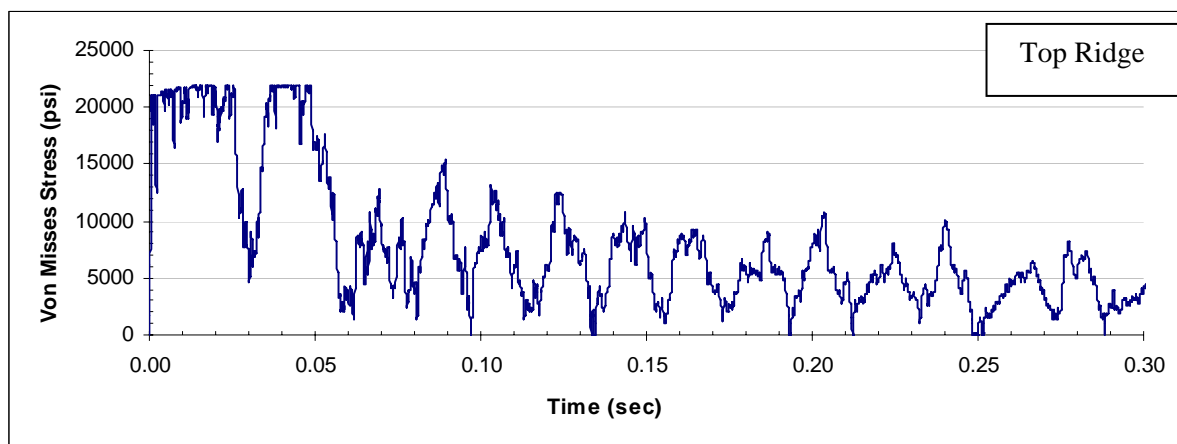


(c)

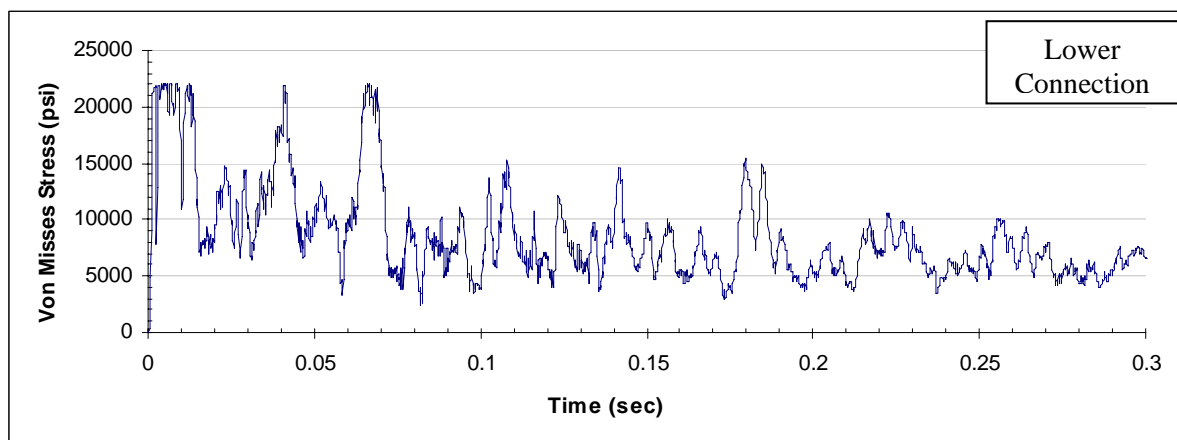
Figure 6-50. Maximum Von Mises stresses for a top roller support model acting at (a) impact zone (b) top ridge and (c) lower edge connection



(a)

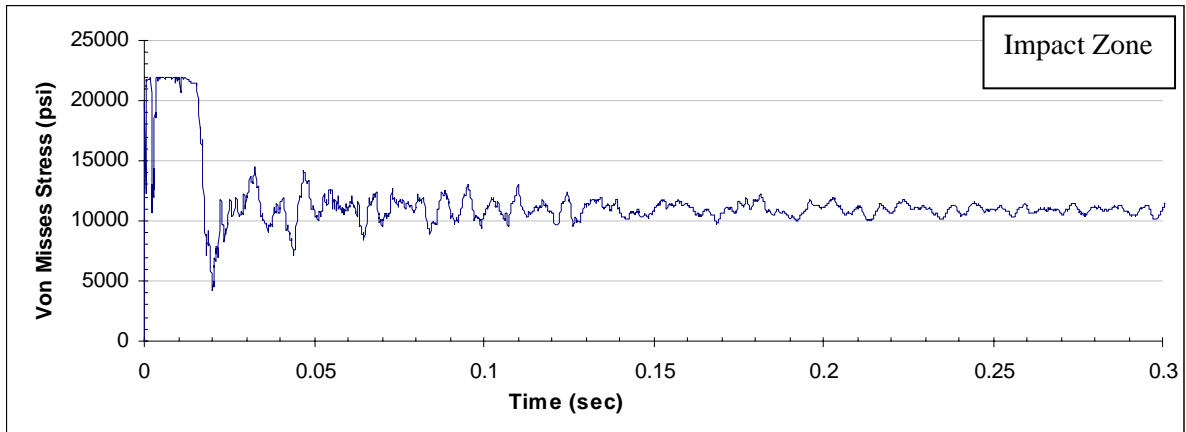


(b)

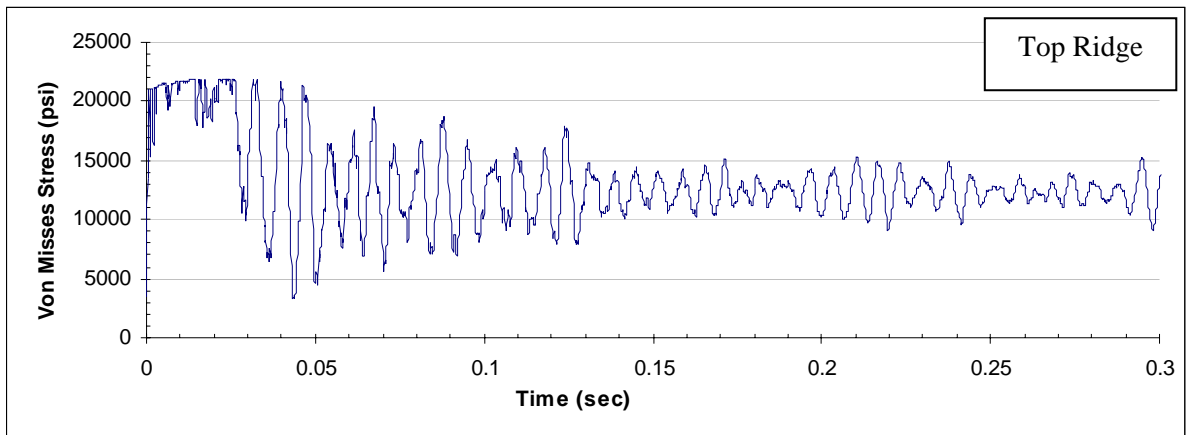


(c)

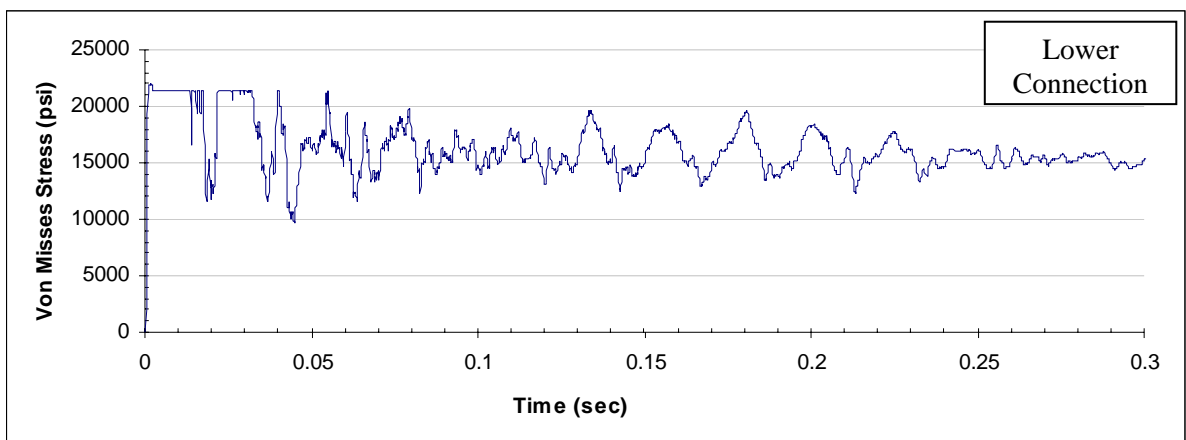
Figure 6-51. Maximum Von Mises stresses for a top header model acting at (a) impact zone (b) top ridge and (c) lower edge connection



(a)



(b)



(c)

Figure 6-52. Maximum Von Mises stresses for a top pinned support model acting at (a) impact zone (b) top ridge and (c) lower edge connection

Table 6.13 Maximum Von Mises stresses acting at different zones of the impacted panel. Values obtained for different type of upper edge supports.

| High Stress Zones | Type of top edge support | | | | | |
|-------------------|--------------------------|------------|------------------|------------|------------------|------------|
| | Roller * | | Header | | Pinned | |
| | Max. Value (psi) | Time (sec) | Max. Value (psi) | Time (sec) | Max. Value (psi) | Time (sec) |
| Impact | 21,983 | 0.001 | 21,983 | 0.005 | 21,984 | 0.006 |
| Top Ridge | 21,929 | 0.045 | 21,984 | 0.042 | 21,926 | 0.033 |
| Lower Connection | 21,983 | 0.014 | 21,984 | 0.007 | 21,984 | 0.002 |

* Base Case model

6.2.5 Effect of Missile Velocity

As previously mentioned, the missile behavior is not considered in this investigation. Although large number of impact test have been performed to decide the required strength of windstorm resistance products to resist impact debris (eg., McDonald, 1990; Minor, 1994; McDonald, 1999), in practice the properties and velocities of windborne debris are uncertain. Twisdale (1988) concluded that the only viable approach to missile behavior is computer simulations. Since 1970, only few articles related to this topic had been developed. Holmes (2003) compared the topic of windborne debris as “the unforgotten load”.

However, the performance of a shutter assembly depends on the missile velocity in which it will be impacted. Therefore, an arbitrary range of missile velocities between 25 mph and 75 mph were proposed to this study. In this range, the velocity value specified on

protocols for testing shutters was analyzed. The proportionality factors of the Base Case model were used to consider damping in the system.

Figures 6-53 to 6-56 and Table 6-14 show the maximum and permanent deformation of the impact panel as it was impacted by the missile at different velocities. It was expected that the resulting deformations of the impacted panel would increase due to the proposed variation in the velocity of the missile as shown in Figure 6-57. However, it was showed that the integrity of the assembly was affected for a velocity greater than 50 mph. At 0.01 sec of the event, the impacted panel lost the edge support provided by the adjacent panel as shown in Figure 6-58. At this time, the impacted panel begun to deform very fast until it reached the maximum value permitted by the edge supports.

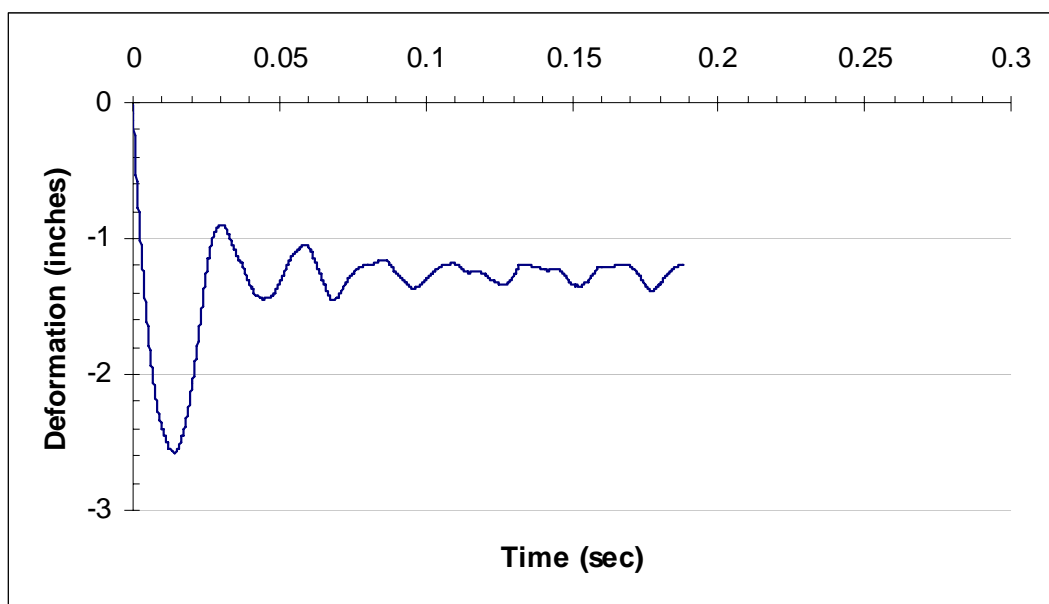


Figure 6-53. Maximum and permanent deformation of the impact panels with a missile velocity of 25 mph.

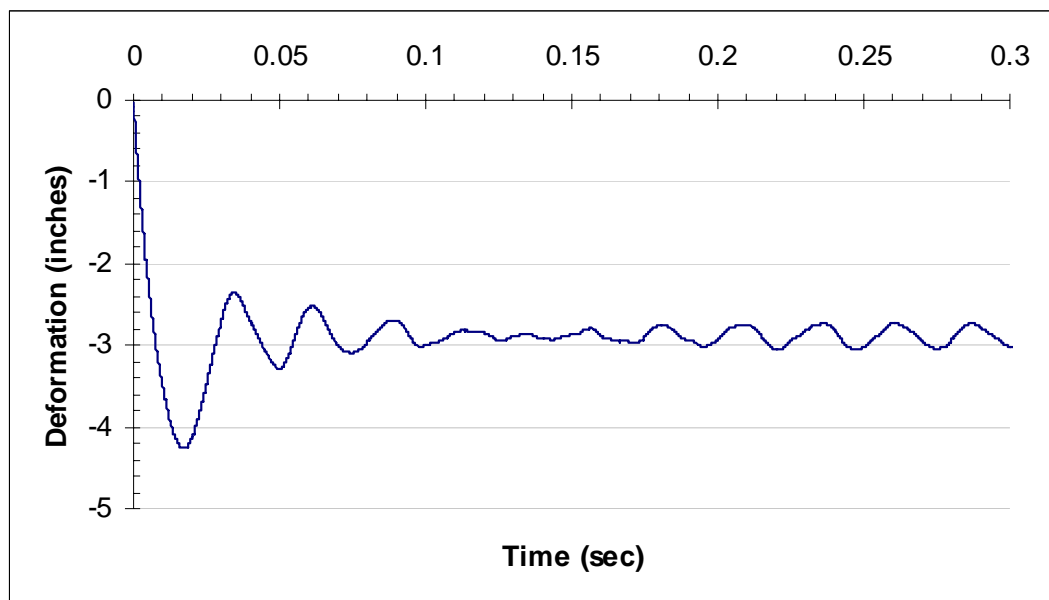


Figure 6-54. Maximum and permanent deformation of the impact panels with a missile velocity of 34.1 mph. Missile velocity defined in protocols of testing.

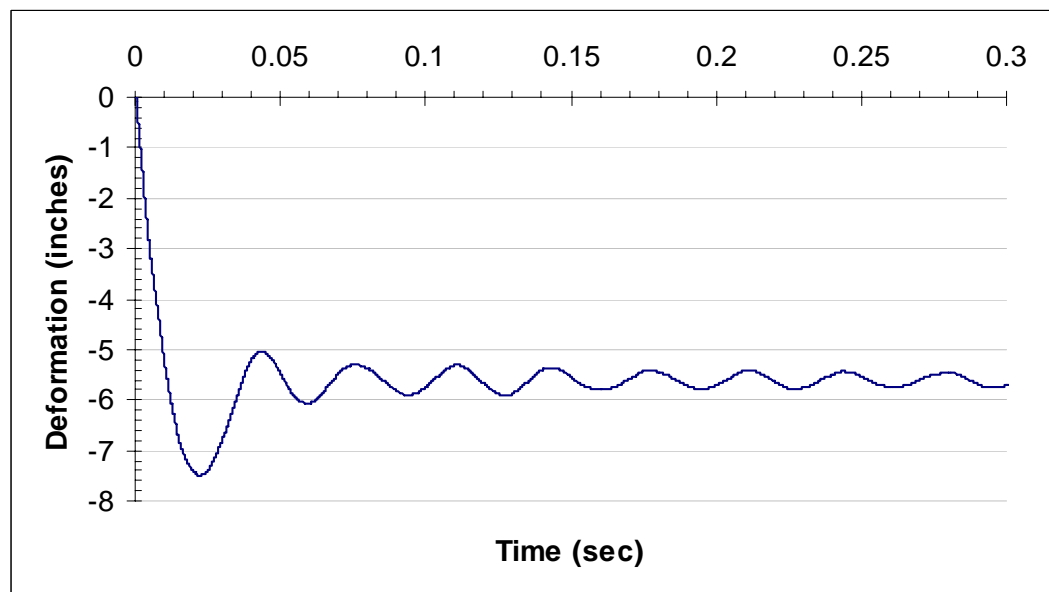


Figure 6-55. Maximum and permanent deformation of the impact panels with a missile velocity of 50 mph. Missile velocity defined in Base Case model.

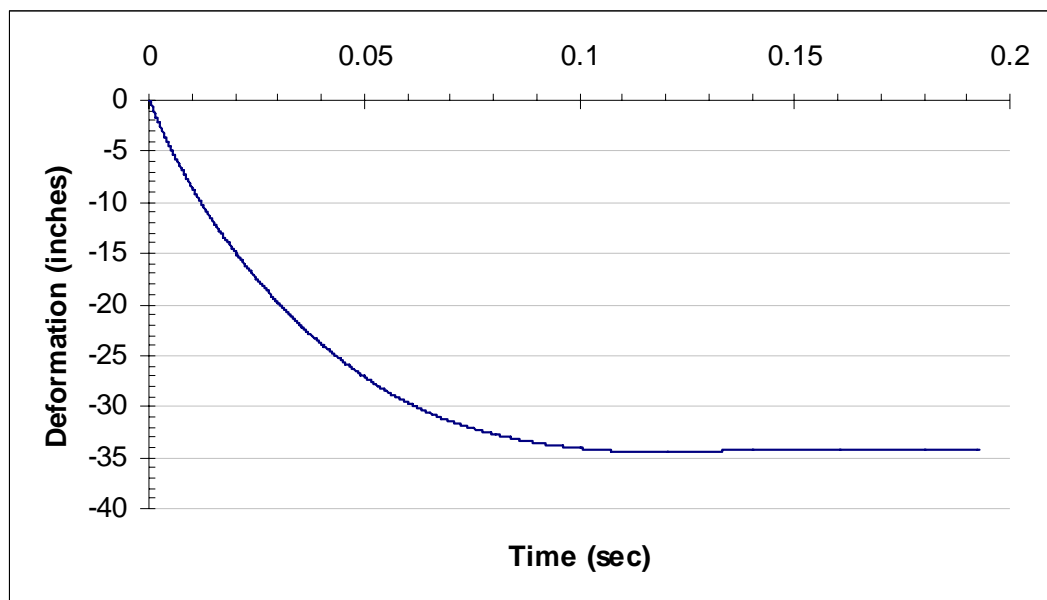


Figure 6-56. Maximum and permanent deformation of the impact panels with a missile velocity of 75 mph.

Table 6.14 Maximum and permanent deformation obtained varying the missile velocity

| Missile Velocity (mph) | Maximum Displacement | | Permanent Deformation Value (in) |
|------------------------|----------------------|------------|----------------------------------|
| | Value (in) | Time (sec) | |
| 25.0 | 2.58 | 0.014 | 1.30 |
| 34.1 | 4.26 | 0.017 | 2.88 |
| 50 * | 7.49 | 0.023 | 5.70 |
| 75.0 | 34.48 | 0.119 | 34.48 |

* Base Case model

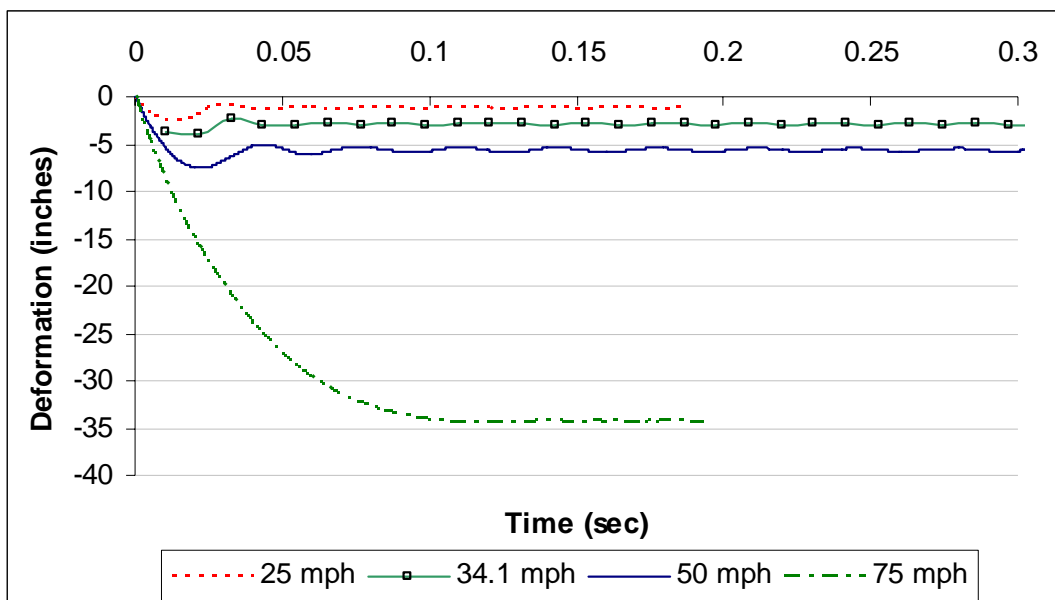


Figure 6-57. Maximum and permanent deformation of the impact panel varying the missile velocity

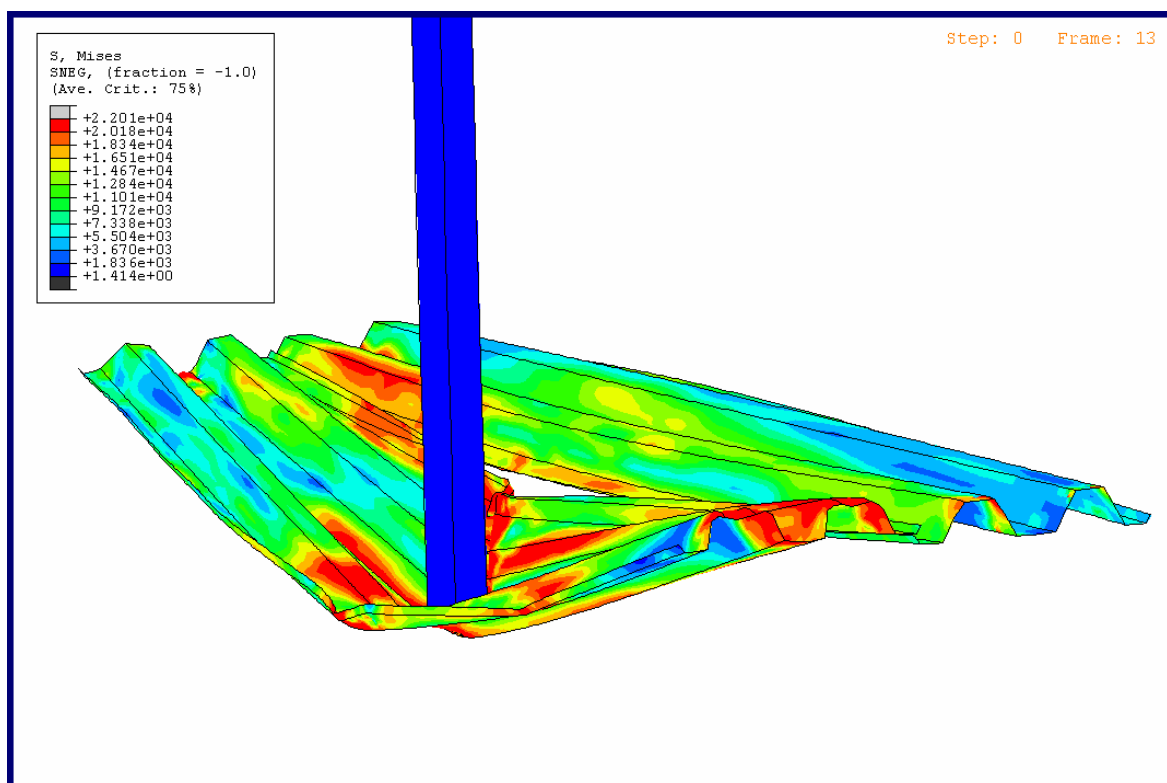


Figure 6-58. Main panel lost the edge support provided by the adjacent panel for 75 mph missile velocity. The lost occurred at 0.01 sec of the event.

It was expected that for a missile velocity of 75 mph some ruptures would be detected in analysis. As mentioned earlier, an excessive displacement of the impacted panel at the upper boundary condition was obtained. As the panel is free to move due to the roller support the panel will be able to deform as the distance between the two edges is reduced as shown in Figure 6-59. This situation provided to the panel enough time to dissipate the energy without any rupture of the material.

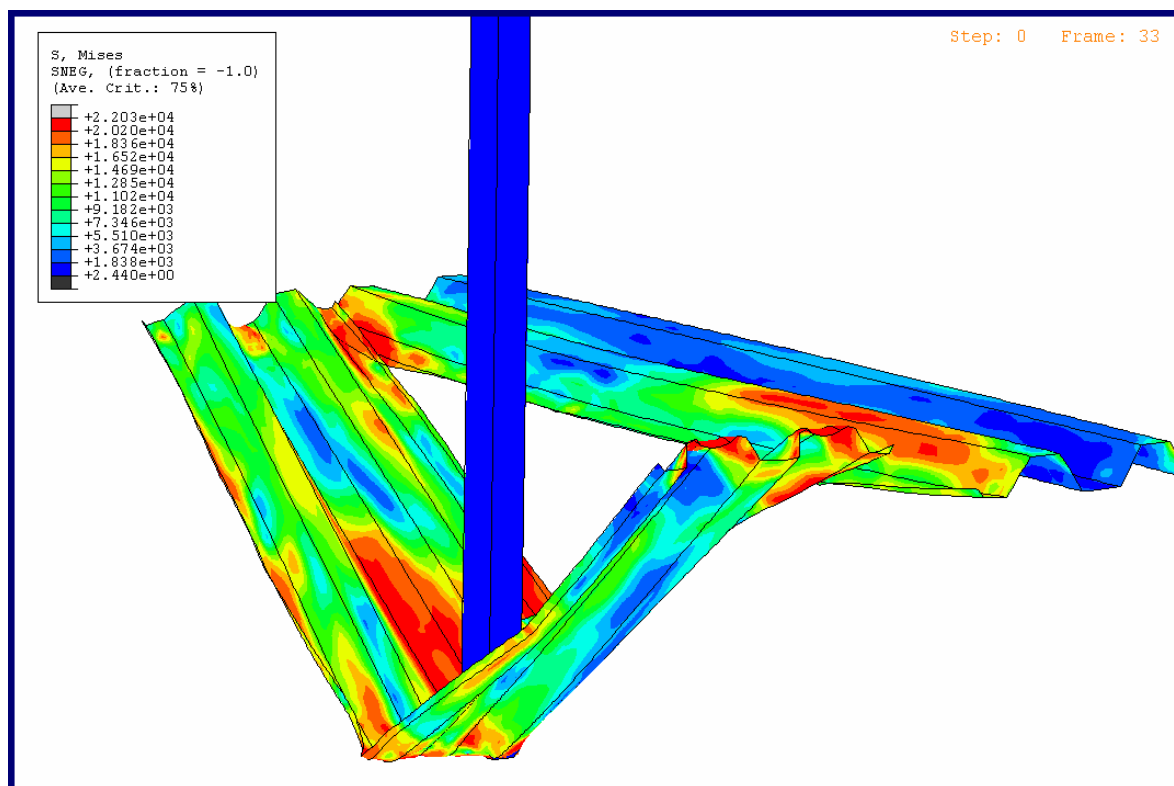
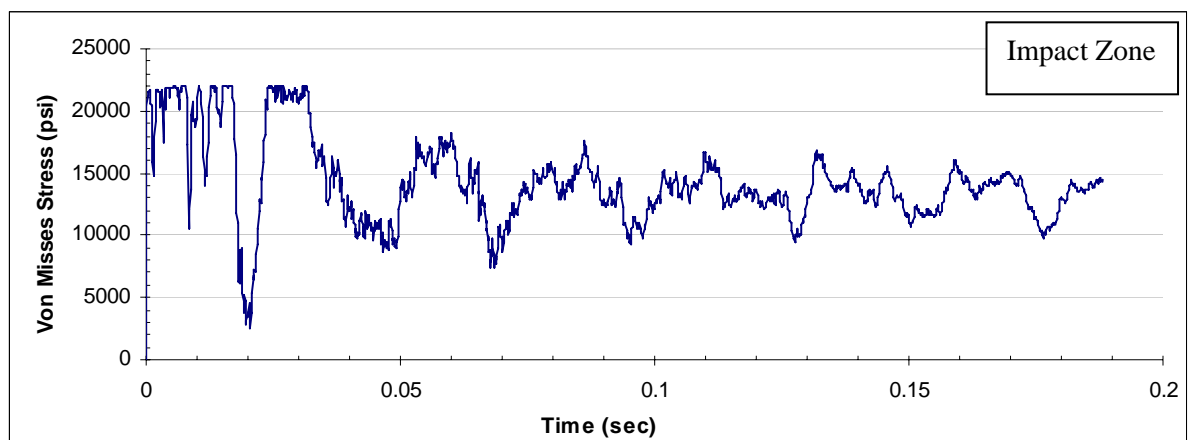
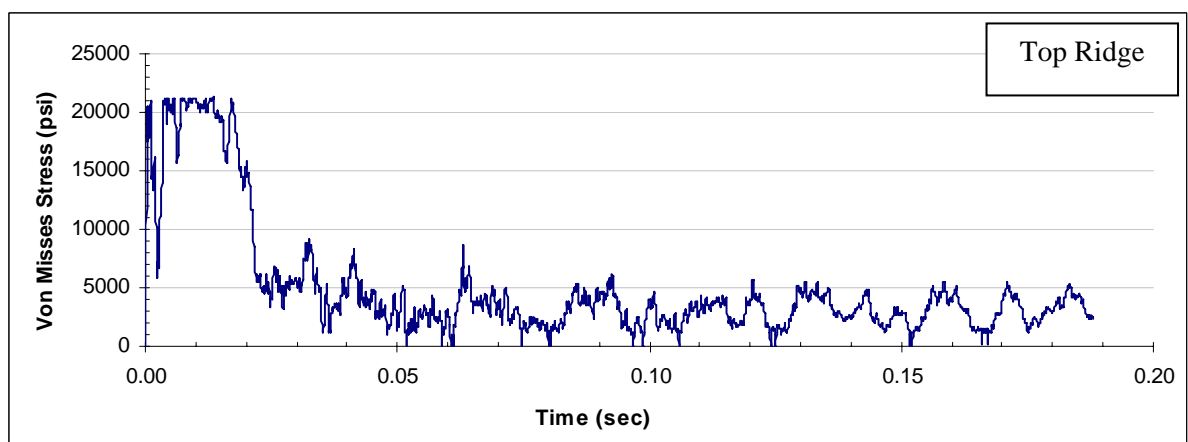


Figure 6-59. An excessive deformation of the main panel avoids any possible failure of the panel material.

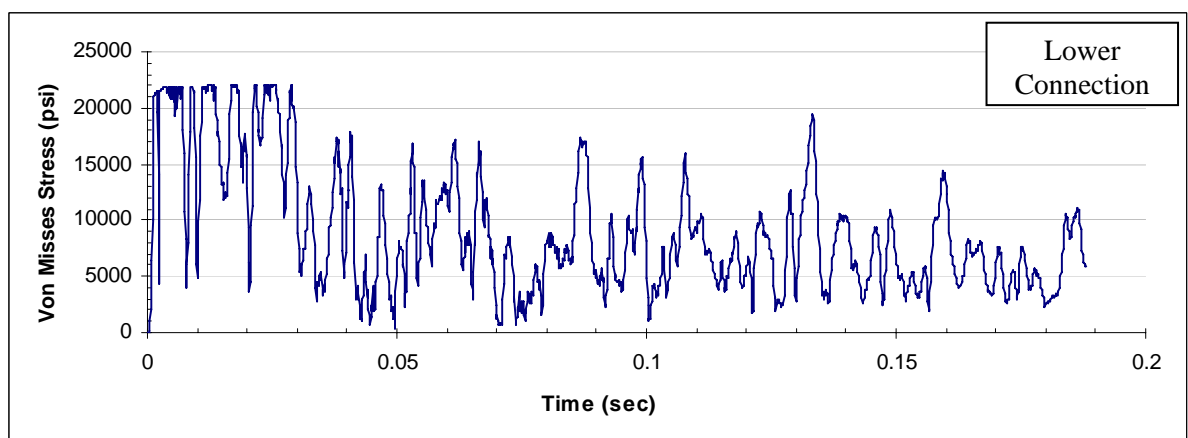
For all the studied velocities, the ultimate stress of the material was reached without rupture as shown in Figure 6-60 to Figure 6-63.



(a)

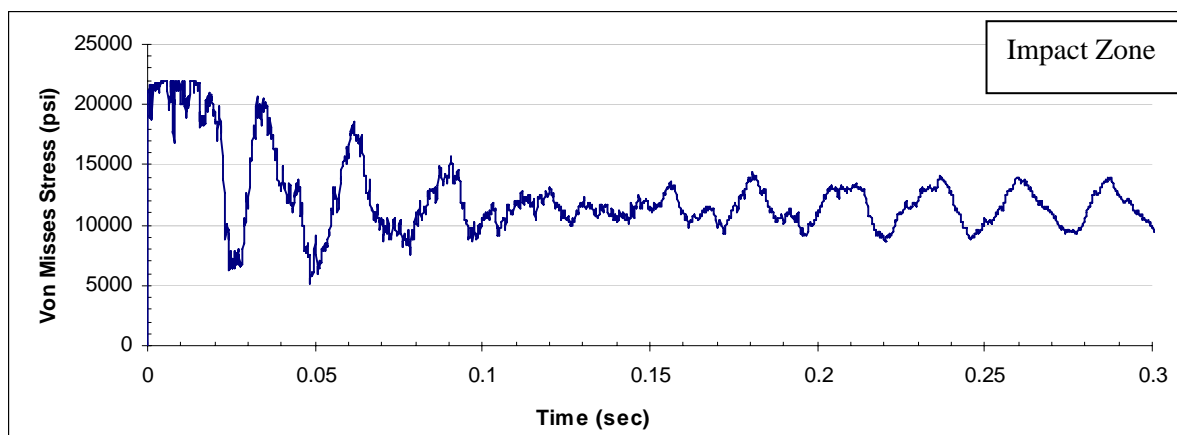


(b)

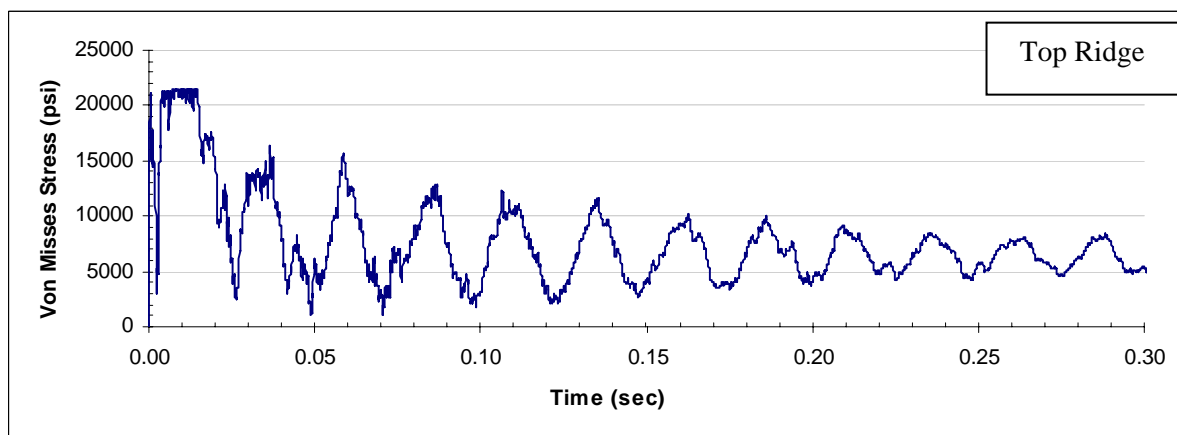


(c)

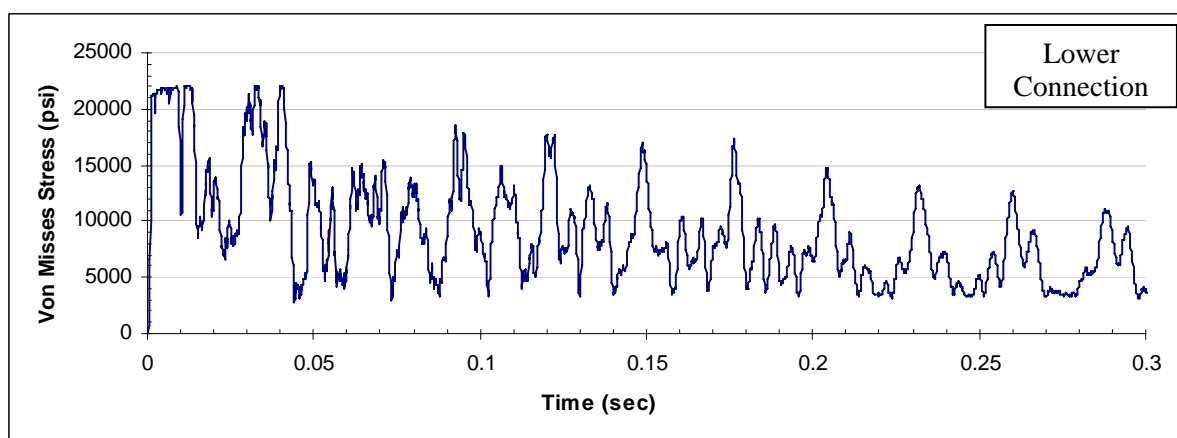
Figure 6-60. Maximum Von Mises stresses for a missile velocity of 25 mph acting at (a) impact zone (b) top ridge and (c) lower edge connection



(a)

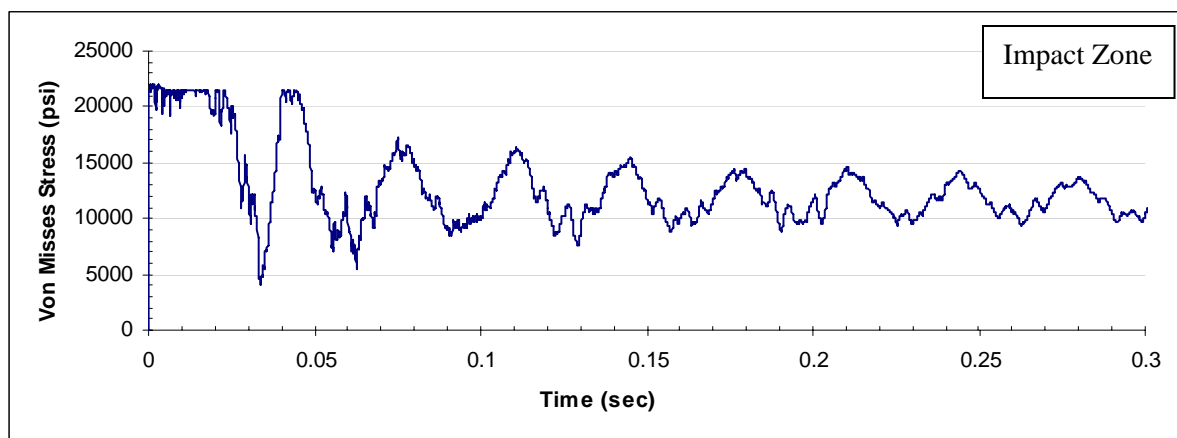


(b)

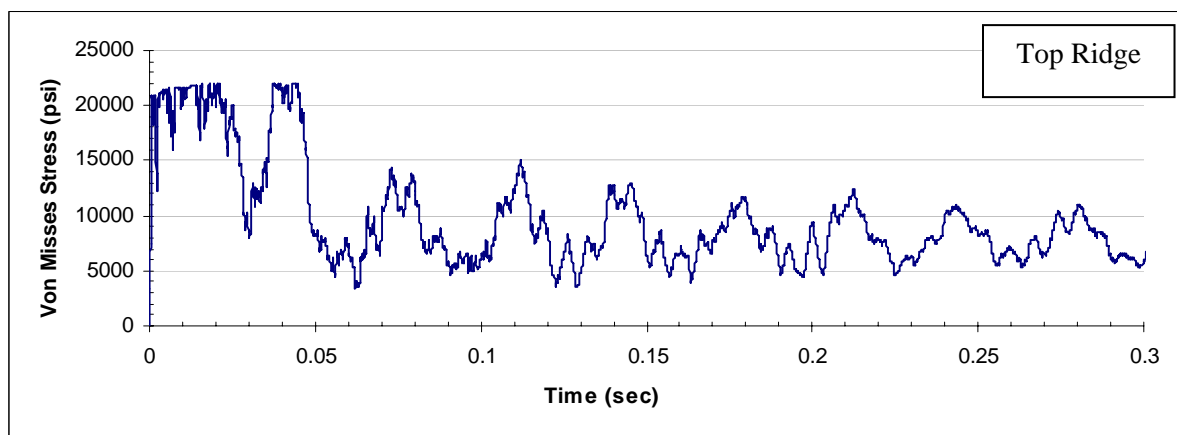


(c)

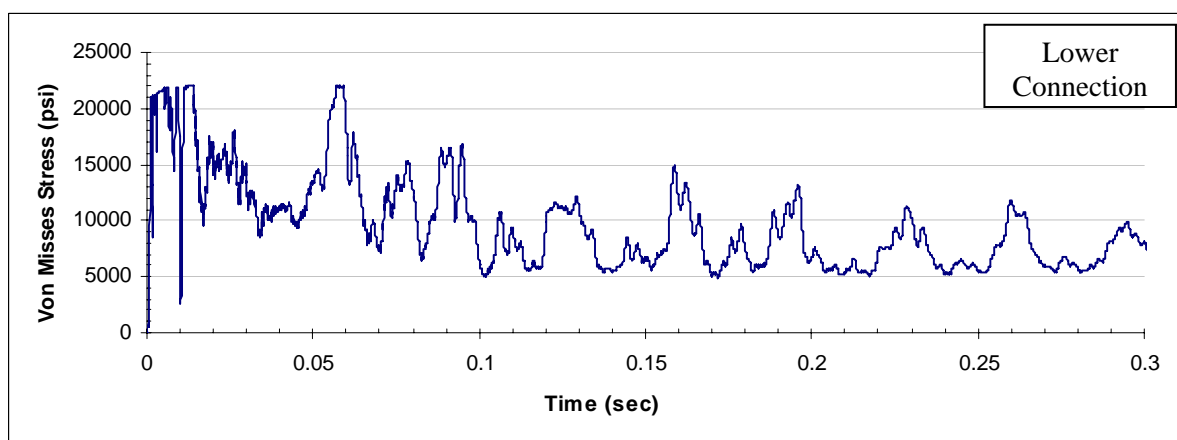
Figure 6-61. Maximum Von Mises stresses for a missile velocity of 34.1 mph acting at (a) impact zone (b) top ridge and (c) lower edge connection



(a)

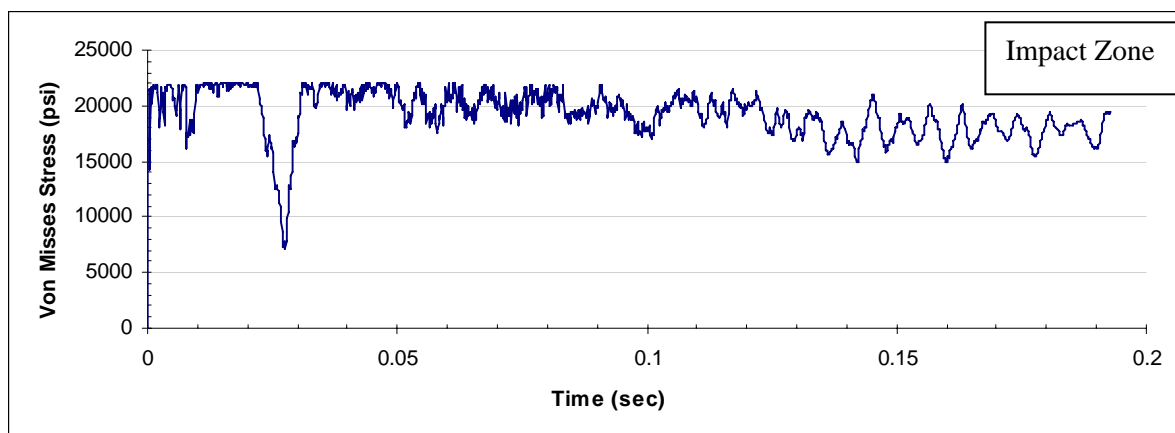


(b)

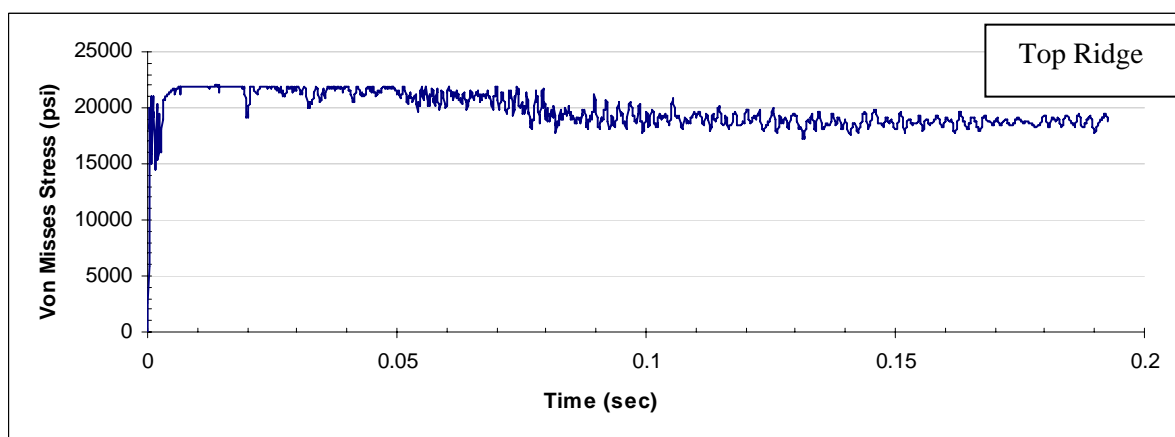


(c)

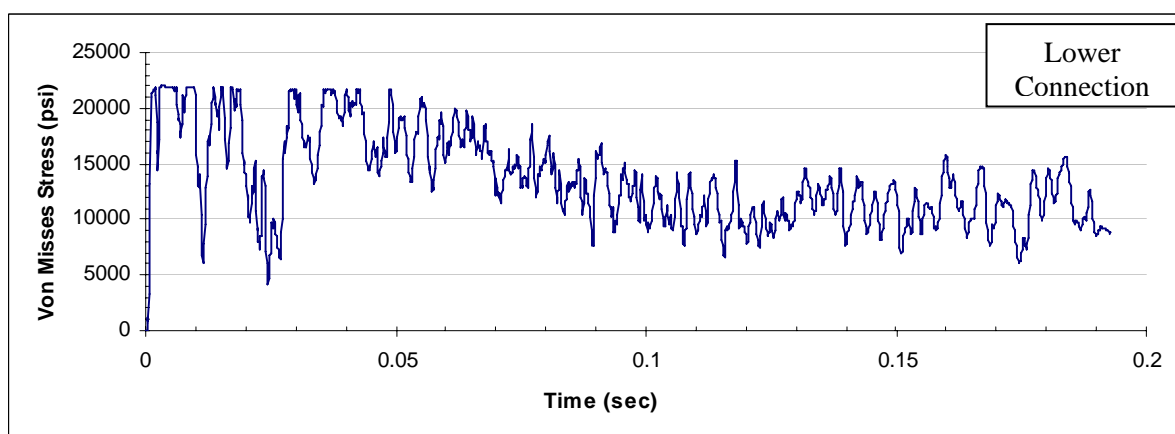
Figure 6-62. Maximum Von Mises stresses for a missile velocity of 50 mph acting at (a) impact zone (b) top ridge and (c) lower edge connection



(a)



(b)



(c)

Figure 6-63. Maximum Von Mises stresses for a missile velocity of 75 mph acting at (a) impact zone (b) top ridge and (c) lower edge connection

The material properties and the reduced thickness of the panels produced a nonlinear behavior for all velocity levels. Table 6.15 summarizes the obtained results showing the time of occurrence of the maximum values for each zone.

Table 6.15 Maximum Von Mises stresses acting at different zones of the impacted panel. Values obtained for different missile velocities.

| High Stress Zones | 25 mph | | 34.1mph | | 50 mph * | | 75 mph | |
|-------------------|------------------|------------|------------------|------------|------------------|------------|------------------|------------|
| | Max. Value (psi) | Time (sec) |
| Impact | 21,964 | 0.016 | 21,984 | 0.008 | 21,983 | 0.001 | 21,988 | 0.020 |
| Top Ridge | 21,252 | 0.018 | 21,566 | 0.015 | 21,929 | 0.045 | 21,984 | 0.014 |
| Lower Connection | 21,992 | 0.025 | 21,984 | 0.041 | 21,983 | 0.014 | 21,983 | 0.003 |

* Base Case model

The sequence of occurrence for maximum stress varied according to the missile velocity. For velocities under 50 mph the maximum values occurred first at the impact and top ridge zone. This sequence is representative of the material used in the analysis. However, with a missile velocity greater than 50 mph, the first zone of occurrence of maximum values was the lower connection zone.

6.2.6 Effect of Impact Location

As the missile velocity, the exact location that windborne debris will impact any target is unpredictable. However, guidelines for testing storm shutter panels suggest three impact locations to evaluate the performance of the systems. The impact locations defined

by the guidelines are based on evaluating not only the response of panels but to consider the performance of the assembly connections during the tests. For this reason, impacts are required to be evaluated near the lower edges of the panels. The studies of the assembly connections were not considered in the analysis of the current study. Therefore, only impacts located at the center span of the panel were defined. Two impacts were analyzed at the middle span of the panels. The first was the established for all previous analysis (located at the middle center of the panel just over the valley section). The second was located at the right center of the panel just over the hill section.

The impact over the hill generates a deformation process very different to the other cases already mentioned. As the load is applied to the hill and the lateral sides connected to it, a buckling process begins due to the excessive compression stress in the zone. The deformed section becomes flat and the panel tends to rotate or twist so that it will accommodate to the new configuration. The missile tends to slip over the surface until it reaches the edge of the panel. At the edge of the panel, the missile continues its displacement until the panel does not restrain it. This panel behavior is shown as a sequence of deformations in Figure 6-64 to Figure 6-68.

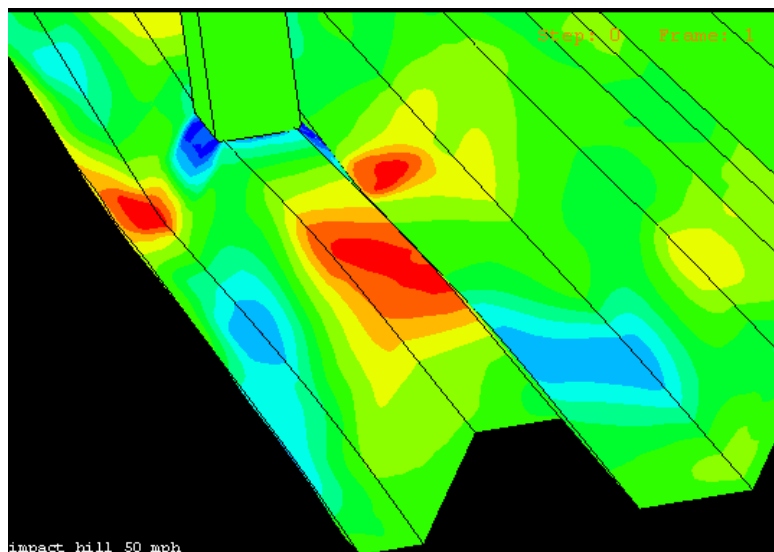


Figure 6-64. Impact missile over the hill at 0.001 sec

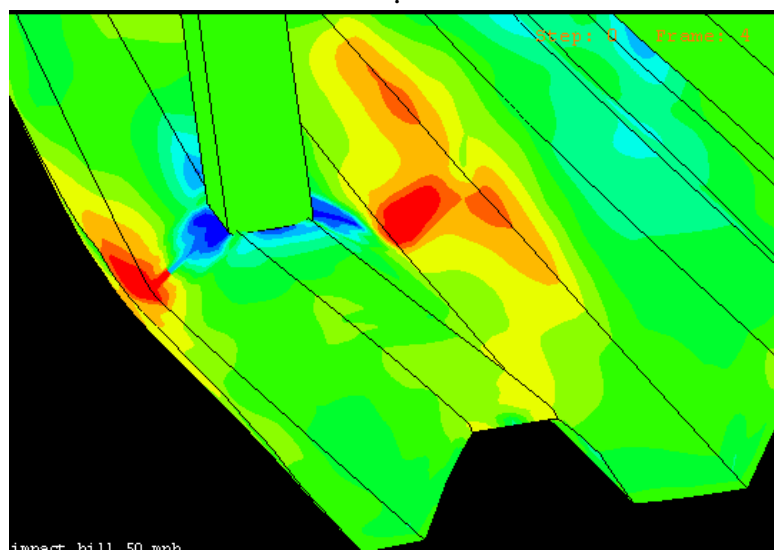


Figure 6-65. Impact missile over the hill at 0.004 sec

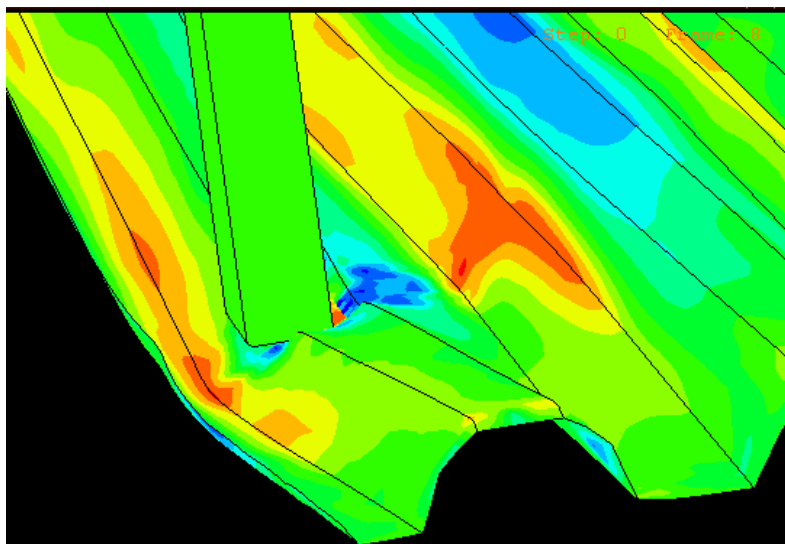


Figure 6-66. Impact missile over the hill at 0.008 sec

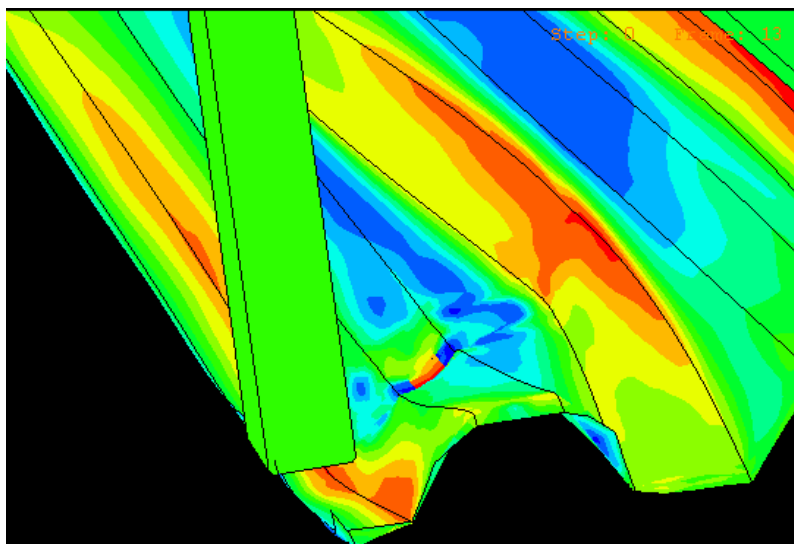


Figure 6-67. Impact missile over the hill at 0.013 sec

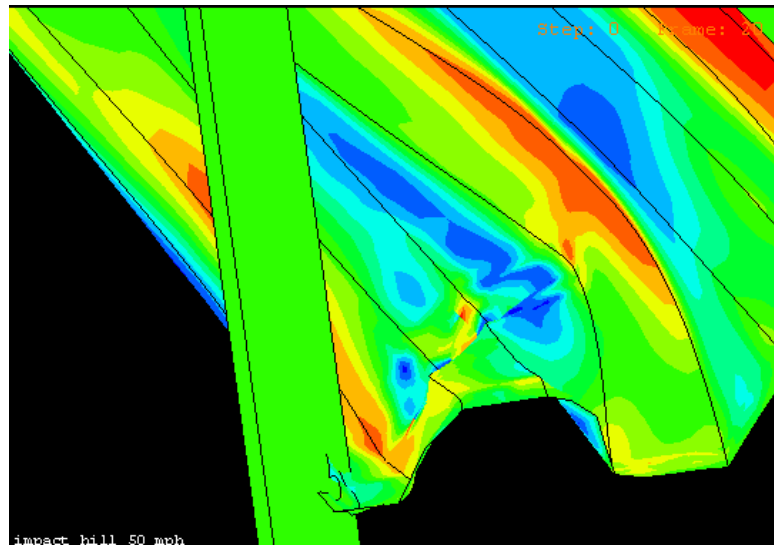


Figure 6-68. Impact missile over the hill at 0.022 sec

6.3 Discussion of Results

It has been showed that the response of storm shutter panels subjected to impact loads can be affected by the type of materials used in their fabrication. The use of aluminum alloy 3003-H14 obtained the worst performance compared to the other aluminum alloys panels evaluated in the current study. In contrast, aluminum alloys 3004-H34 and 6063-T6 improved the capacity of the panels obtaining the best results in the analyses. Both aluminum alloys shows similar stress-strain relationships with higher level of stress than 3003-H14.

The results showed the development of high stress zones in the panels during the event. A total of three zones were identified for all the studied cases. The zones were called based on the location where the maximum stresses were obtained. It was found that the

maximum stresses followed a sequence of occurrence depending on the stiffness of the system. For aluminum alloy 3003-H14, the maximum stress values were obtained at the impacted zone. The reduced capacity of this material affected the load distribution in the panel avoiding the transfer of forces to the support connection area. Notice that impact of the missile occurred at mid span of the panel. Meanwhile, the maximum stresses were developed first at the lower connection zone for the other aluminum alloys. It was concluded that the capacity of the material to sustain high level of stresses controls the sequence of occurrence of maximum stress values.

Four cross sections were evaluated to obtain the effect of its variation on the behavior of storm panels. The obtained results showed that the cross section with the highest height profile, CS#3, produced the best response on the panels. A high profile resulted in a greater moment of inertia for the panels. As a result, an increase of stiffness was gained providing more capacity to the panels. The maximum displacement and permanent deformation values were reduced compared to the other profiles. For CS#3, the maximum stresses occurred first at the lower connection zone. This behavior was similar to the one showed by the stronger materials as mentioned before.

As the number of panels was increased into to the system, an improvement in the response of the impacted panel was obtained. A greater number of panels provided to the assembly additional supports that limited the degree of freedom of the panels. During the deformation process of the panels it was observed that panels tried to restrained the rotation of the adjacent panels in the assembly. As a result, a reduction in the maximum displacement and permanent deformation of the impacted panel was obtained. Also, the contact between the lateral edges of panels provided an additional support that reduced the amplitude of the

vibrations produced as a response to the applied load. The maximum stresses occurred first at the lower connection zone for a number of panels greater than two. Once again, this behavior was typical for systems in which their stiffness had been improved.

The use of top header as upper edge support restrained the rotation of the panels. As a result a reduction of the maximum displacement and permanent deformation of the impacted panel was obtained. However, the best response of the impact panel to the variation of boundary condition was obtained when the top connection was defined as a pinned connection. The pinned connection restrained the in-plane displacements of the panels generating tension forces in the lower section of the panel's profile. As a result, the panels became more rigid reducing their out of plane displacements and concentrating the maximum stresses at the support connection zones.

It was found that the integrity of storm shutter assembly was affected due to the impact missile for velocities greater than 50 mph. The lateral edge support provided by the adjacent panel was lost due to the high level of load induced in the system. An excessive deformation of the impacted panel was obtained. This process of deformation provided the panel enough time to dissipate the energy without any rupture of the material. For all the studied velocities a nonlinear behavior in the impacted panels was observed. Also, the ultimate stress of the material was reached without ruptures.

As the missile velocity, the location in which windborne debris will impact the storm shutter panels is uncertain. For this reason, a simulation to study the behavior of panels under missile impact located other than the center of the panel was performed. The selected location was the middle center of the panel just over the hill or ridge section. It was observed that the behavior of the impact panel was different compared to the previous analyses. The

impacted panel tended to rotate due to eccentricity of the applied load. Also, the cross section deformed until its original shape was lost. As the ridge section became flat, the missile tended to slip over its surface passing near the edge of the panel. It is important to note that the studied assembly consisted of two panels. Thus, the missile can be displaced without any restriction. Therefore, any protected element by the storm shutters will be damaged by a direct impact of the missile.

Chapter VII

Summary, Conclusions and Recommendations

7.1 Introduction

In the first part of this investigation a system for storm shutter testing devices was designed and assembled in the Structural Laboratory of the Civil Engineering and Surveying Department of the University of Puerto Rico at Mayagüez. In addition the proposed guidelines for testing and approval of storm protection shutter and panels in Puerto Rico was developed in accordance with local building code. Two storm shutter specimens were tested according to the guidelines for testing to validate the performance of the testing facility. An analytical study was performed to model the behavior of the test assembly. For this, a general purpose finite element code ABAQUS was used. Important characteristics modeled were material, cross sections, dimensions and supports were obtained from the tested panels. The results of the analyses were compared with values measured during the tests. Also a computational modeling technique was defined for further analysis. The most critical behavior for shutter panel subjected to impact was studied by means of parametric studies. Sets of tables were prepared such that the readers will understand the response of shutter assemblies to the variation of different parameters.

7.2 Storm Shutter Testing Facilities

The storm shutter testing facility was the first one developed in Puerto Rico. The testing facility provides particular devices which can be used to follow the procedures established in protocols for storm shutters testing. The devices were designed to facilitate their use during a test. The following conclusions can be drawn related to the testing facility:

1. The proposed pressure setup can be used to obtain a very good approximation of the capacity of the specimens using a very simple testing device.
2. The use of an hydraulic actuator is a very common equipment that can be used to apply the required force to recreate the acting pressure on the system. The use of a personal computer connected to the actuator gave the opportunity to control the equipment such that any type of load-time application can be tested.
3. The rigid frame permits a realistic connection behavior of the storm shutter system due to the installation of the exact materials (concrete or wood) where the typical system is attached. This fact will generate a reliable source of data about the capacity and behavior of the system connections.
4. Different sizes of panel systems can be installed due to the flexibility of the rigid frame to adjust the height of its test base supports (horizontal beams) according to the opening dimensions to be covered.
5. The proposed air cannon can be used to evaluate the effect of windborne debris acting against storm shutter panels. Parameters like: missile velocity, missile characteristics (small or large) and the location and angle of impact can be evaluated with the proposed impact setup.

It is recognized that the testing facilities can be used to evaluate construction materials other than the storm shutter systems. The Civil Engineering and Surveying Department of the University of Puerto Rico at Mayagüez have been using the pressure set up to develop new research related to structural elements subjected to extreme wind loads (Avilés, 2006; García, 2007; García, 2008). Elements like steel desk panels and their connection components had been installed and tested using the pressure set up obtaining satisfactory results.

Once the testing facility was established the first draft of guidelines for testing storm shutter panels for Puerto Rico was developed to comply with the local building codes. It is important to note that these guidelines correspond to the reality of the local construction industry. Local materials, typical elements to be protected, wind loads expected to occur on our zone and others were used as the principal source of information to establish each step to be followed in the testing of shutter panels.

The proposed guidelines can be used as the first step to start a process of legislation to establish a process to certify local products instead of using foreign certification providers.

7.3 Modeling of Storm Shutter Panels

The modeling process started with the definition of parameters that represent real storm shutter assemblies. Information related to dimensions, type of connections, panel material, profiles and missile characteristics were obtained from the specimens tested during the validation process of the testing facilities previously mentioned. The information was

summarized as specific parameters that were used to generate the different component of the models.

A general purpose finite element code, ABAQUS, was used to perform the proposed analysis. ABAQUS provided the capacity to perform dynamic simulations representative of the impact load that typical shutter panels will be exposed during an extreme wind event. Also, the nonlinear behavior of the panels was considered such that excessive and permanent deformations were obtained. ABAQUS performed this type of analysis based on the stress – strain relationship of the materials and the kinematics formulation of the finite elements used in the analysis.

A simple model consisting of two panels was used to represent the specimens tested during the validation of the testing facilities. To ensure the accuracy of the results two analysis were performed. The first analysis consisted on the determination of the number of finite elements necessities to develop the meshes of the model. It was realized by means of a convergence analysis. A special attention was given to the impact panel. Thus, a total of five meshes were evaluated to define the required degree of refinement of the impact panel mesh. Only the number of elements contained in each mesh makes them different from the others. The results showed a slight variation as the number of elements was increased. However, a mesh containing a total of 18,888 elements showed similar results in comparison with the other meshes of higher number of elements but with less computational time. It was concluded that meshes generated with this level of refinement were enough for the development of further models.

The second analysis was the evaluation of different kinematics formulations according to the finite elements. ABAQUS has an extensive element library to provide a

powerful set of tools for solving many different problems. In our study, shell finite elements were used based on the physical characteristics of the panels in which their thickness is significantly smaller than the other dimensions. Notice that each finite element is formulated to consider certain level of deformation according to the kinematics formulation used to define it.

Three different type of shell elements were compared to select the one that will represent the behavior of the panels. The first element, S4RS, considered a small-strain formulation with large rotations. The second element, S4RW, is formulated similar than the first element but additional terms were added to its strain displacement equations such that warping can be considered. That last element, S4R, considered a large-strain formulation with large rotations.

Three models were developed to incorporate each type of elements. The meshing generation was based on the previous analysis. It was found that the use of each element affected the final results of the analysis. The model formed with elements consisting in large – strain formulation with large rotations (S4R) showed the most similar results in comparison with the values measured during the testing of the specimens. Also, it was found that the computational time required to perform the analysis was increased as higher order element formulations were used. As mentioned earlier, the tested specimens showed permanent deformations as the result of the impact load. Therefore, it was concluded that shell element consisting in large – strain deformation with large rotations must be used no matter the time required to complete the analysis. The results obtained from the two analyses established the modeling criteria used in the development of the parametric study described in Chapter VI.

7.4 Parametric Study

A parametric study was performed to understand the most detrimental behavior of storm shutter panels under impact loads. The first step was to establish the parameters that will affect the response of the panels due to their variation in a typical assembly. Some parameters like cross sections and panel materials were obtained from a survey. The others simply consisted in the variation of its use in the model.

A model called Base Case was developed. The purpose of the Base Case model was to obtain some results based on specific parameters. These results were compared with the ones obtained by the models containing other parameters. New models were generated for each parameter under study. The following results can be drawn related to the parametric study:

1. A nonlinear behavior occurred in all the cases considered. Based in the stress-strain relations assumed, the yield stress values were exceeded resulting in a permanent deformation of the panels.
2. Failure of the material was not achieved in any case. The flexibility of the typical assembly to allow the free displacement of the upper edge of the panel avoids any possibility of failure by punching shear of the missile at the impact area. The energy induced in the system will be dissipated via an excessive deformation of the panel.
3. The tendency of the industry to improve their products was evidenced when models containing different aluminum alloys were compared. The model developed with Aluminum Alloy 3003-H14 panels obtained the worst results. It is recognized that Aluminum Alloy 3003-H14 was the most used aluminum alloy by manufacturers a few

years ago. Now, the most common is Aluminum Alloy 3004-H34 which obtained the best overall results.

4. Galvanized steel displays similar structural behavior than the aluminum alloy panel. However, its thickness is too thin and a suggestion to use these panels with a larger thickness than the ones evaluated will improve their response significantly in comparison with the aluminum panels.
5. The zones surrounding the impact area, the lower central connection and the central ridge of the cross section showed the highest concentration of stresses in comparison with the rest of the panel. The stresses presented an order or sequence of occurrence as they were generated in the impacted panel during the event. It was found that the maximum stress occurred first at the impact zone for flexible assemblies. Otherwise, the central connection zone reached the maximum stress values first when a more rigid assembly was analyzed.
6. The use of different boundary conditions and a change in the geometrical configuration produced an improvement in the behavior of the panels specifically with respect to the expected deformation. Additional panels provided support to free edges and high height cross sections increased the moment of inertia of the panels. As a result, a reduction of deformation is obtained at maximum values and during the vibration period of the system. However, the use of five panels showed that the contribution of panels that are located at edges of the system is reduced.
7. The use of a pinned connection to represent the main supports of the panels obtained the best response in the study. The pinned connection controlled the deformation of the impacted panel as both edges were restrained to displace in the in-plane direction.

However, the reduction in deformation was not sufficient to prevent damage due to the direct contact of the panels to the element to be protected. This argument is based on the fact that typically, residential windows are installed in the middle width of 5 to 6 inches walls. Thus, a distance between 2 to 3 inches defined the center of the protected element. All the evaluated cases exceeded these measures.

8. Modeling the top header was a good representation of the assembly used in Test 1 in terms of defining its components. However, the permanent deformation was less than the value obtained during the test. It is important to note that the tested system suffered a support loss as some clips that were damaged and released from the system. During the simulation, support conditions were not affected. As a result, the stiffness of system remained stable during the event.
9. The most detrimental behavior was produced when the impact is located out of the center of the panel when two panels are used in the assembly. The geometric non-linearity results in a direct impact of the missile to the element to be protected. As one side of the panel is not prevented from displacement, the change in the geometry causes relocation in the missile trajectory such that the panel does not offer any resistance, allowing a direct contact of the missile with the elements to be protected.

7.5 Recommendations

The flexibility offered by the testing facility allows the testing of different storm protection products other than storm shutter panels. Storm shutters like rolling, accordion and swing louvers type (Bahamas or Colonial) can be installed and tested to comply with the

established regulations. As a result, new research can be developed to study the behavior of these storm shutter systems subjected to impact loads.

It is recommended to the University of Puerto Rico at Mayagüez to obtain a patent of the testing equipment to guarantee the authenticity of different devices created as part of this investigation.

The proposed guidelines for testing and approval of storm shutters and panels can be revised to include some additional information related to test procedures, passing or failing criteria based on the specimens to be tested, development of notice of acceptance, etc. The revised version can be used as a first step for establishing local guidelines by regulatory agencies.

This investigation showed that the analytical approach is an alternative to study storm shutter panels under the effect of windborne debris. The angle and location of missile impact, external components to provide more strength to the system, new materials, and others are just a few parameters to be considered for future works. The development of models to represent the storm shutter assemblies is a complementary tool considering the high cost of materials employed during testing programs. The considerable amount of computational time and model development complexities are factors to be considered.

References

AISC (1994). "Manual of Steel Construction." 2nd Edition, American Institute of Steel Construction, Inc., Vol.1 & 2.

ARPE (1999). "Amendments to UBC-97 Volumes 1, 2 and 3." Puerto Rico Building Code 1999, Regulation and Permits Administration, ARPE, PR.

ASCE (2006). "Minimum design loads for buildings and other structures." ASCE 7-05, American Society of Civil Engineers, Reston, Va.

ASTM (1997). "Standard test method for performance of exterior windows, curtains walls, doors, and storm shutters impacted by missile(s) and exposed to cyclic pressure differentials." ASTM E 1887-97, American Society and Testing Materials.

Avilés, D. (2006). "On Improving the Performance of Wood-Zinc Roof Systems." Ph.D. Thesis, Department of Civil Engineering, University of Puerto Rico at Mayagüez.

Belytschko, T., J. I. Lin, and C. S. Tsay, (1984). "Explicit Algorithms for the Nonlinear Dynamics of Shells." Computer Methods in Applied Mechanics and Engineering, vol. 43, pp. 251–276.

Borges, A., López, R., and Zapata, R. (1997). "Guidelines for testing and approval of storm protection shutter and panels." Report submitted to Federal Emergency Management Agency, FEMA.

Borges, A., López, R., and Zapata, R. (2006). "Testing of storm shutter panels." Fourth LACCEI International Latin American and Caribbean Conference for Engineering and Technology.

Boyer, H. E. (1987). *Atlas of Stress-Strain Curves*, ASM International, Ohio.

Clough, R. W. and Penzien, J. (1975). *Dynamics of Structures*, McGraw-Hill, New York, 1975.

Colegio de Ingenieros y Agrimensores de Puerto Rico (CIAPR), Defensa Civil Estatal de Puerto Rico, and Federal Emergency Management Agency (FEMA), (1996). "Huracanes en Puerto Rico: Guía de mitigación de daños." pp. 19-24.

Dade County (1992). "Building code evaluation task force final report." Metro Dade County Building Evaluation Task Force, Dade County, Miami.

Dade County, (1994a). Protocol PA 201-94, "Impact Test Procedures." pp. 1-9, Dade County, Miami.

Dade County, (1994b). Protocol PA 202-94, "Criteria for testing impact and non impact resistant building envelop components using uniform static air pressure." pp. 1-9, Dade County, Miami.

Dade County, (1994c). Protocol PA 203-94, "Criteria for testing products subject to cyclic wind pressure loading." pp. 1-8, Dade County, Miami.

Federal Emergency Management Agency (FEMA), (1992). "Building performance: Hurricane Andrew in Florida." Federal Insurance Administration, FEMA, Washington, D.C.

Federal Emergency Management Agency (FEMA), (1998). Section 404 Hazard Mitigation Grant Program, FEMA 1068-DR-PR. The project number PR 0007.

García, R. (2007). "Development of Hurricane Based Fragility Curves For Wood-Zinc Houses in Puerto Rico." Ph.D. Thesis, Department of Civil Engineering, University of Puerto Rico at Mayagüez.

García, A.J. (2008). “Estimación de daños producidos por viento en edificaciones industriales.” MSCE Thesis, Department of Civil Engineering, University of Puerto Rico at Mayagüez.

Hattis, D.B. (1996). “Progress of the ASTM standard on fenestration relative to windstorms and its relationship to building codes.” Proceedings of the Conference of Natural Disaster Reduction, ASCE, pp. 119-120.

Hattis, D.B. (2006). “Standards Governing Glazing Design in Hurricanes Regions.” Journal of Architectural Engineering, ASCE, Vol. 12, No.3, pp. 108-115.

Hibbit, Karlson & Sorensen (1997). “ABAQUS/User Manual.” Version 5.7, Hibbit, Karlson & Sorensen, Inc., Pawtucket, RI, USA.

Holmes, J.D. (2003). “Emerging issues in wind engineering.” Proceedings of the Eleventh International Conference on Wind Engineering (11ICWE), Lubbock, Texas, June 2-5, 2003.

International Conference of Building Officials (ICBO), (1997). Uniform Building Code, Whittier, California.

Jordan’s Aluminum (JA) (2008). “Hurricane & Security Shutters.”
<http://www.stormsecure.com> (Jordan’s Aluminum Inc., Hollywood, FL.).

MatWeb (2009). “MatWeb, Your Source for Materials Information,”
<http://www.matweb.com> (Christiansburg, VA: MatWeb).

McDonald, J. R. (1976). “Tornado-generated missiles and their effects.” Proceeding of the Symposium on Tornados: Assessment of Knowledge and Implication for Man, Texas Tech University, Lubbock, Texas, June 22-24, 1976.

McDonald, J.R. (1990). "Impact resistance of common building materials to tornado missiles." *Journal of Wind Engineering and Industrial Aerodynamics*, pp. 717-742.

McDonald, J.R. (1999). "Windborne debris impacts on metal walls and their implications." *Journal of Wind Engineering into the 21st Century*, Larsen, Larose & Livesey (eds), Balkema, Rotterdam, ISBN 90 5809 059 0, 1443-1449.

Metropolitan Dade County (MDC), (2009). "Product Control", http://www.miamidade.gov/buildingcode/pc_app.asp.html (Building Code Compliance Office, Metropolitan Dade County, Miami).

Minor, J.E. (1994). "Windborne debris and the building envelope." *Journal of Wind Engineering and Industrial Aerodynamics*, Vol. 53, pp. 207-227.

Minor, J.E. (2005). "Lessons learned from failures of the building envelop in windstorms." *Journal of Architectural Engineering*, Vol. 11, No. 1, March 1, 2005.

Minor, J.E., Mehta, K.C. and McDonald, J.R. (1972). "Failures of structure due to extreme winds." *ASCE, Journal of Structural Engineering*, Vol. 98, pp. 2455-2471.

Puerto Rico Building Code (PRBC), (1987). "Reglamento Número 7", Puerto Rico Planning Board.

South Florida Building Code (SFBC), (1994). Metropolitan Dade County edition of the South Florida Building Code, Metropolitan Dade County, Miami.

Sparks, P. R., Schiff, S. D., and Reinhold, T.A. (1994). "Wind damage to envelopes of houses and consequence insurance losses." *Journal of Wind Engineering and Industrial Aerodynamics*, Vol. 53, pp. 145-155.

Rodríguez L. (1995). Personal communication.

Twisdale, L.A., (1988). "Probability of facility damage from extreme wind effects." *Journal of the Structural Division*, Vol. 114, No. 10, ASCE, pp. 2190.

Wills, J.A.B., Lee, B.E., and Wyatt, T.A. (2002). "A model of wind-borne debris damage." *Journal of Wind Engineering and Industrial Aerodynamics*, 90, pp. 555-565.

Wind Engineering Research Council (WERC), (1992). "Preliminary observations of WERC post disaster team." WERC, College Station, Tex.

Appendix A

Storm Shutter Profiles

A survey was realized to study actual designs of storm panels used in the industry. A total of twenty seven (27) cross sections were identified according to different local and foreign manufacturers. Part of the information was obtained through a data base provided by the Dade County (MDC, 2009) as shown in Figure A.1 to A.24. Meanwhile, a field survey was carried out such that information of three major local storm panels' suppliers was included in the investigation as shown in Figure A.25 to A.27.

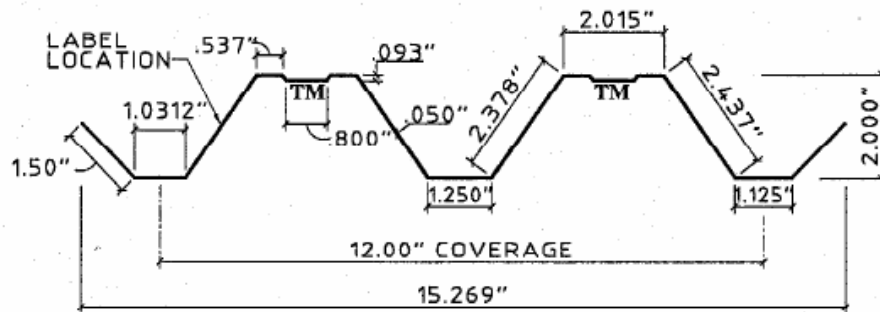


Figure A.1 Storm Shutter Cross Section #1. Aluminum 3004-H34 or 5052-H32, Thickness of 0.050".

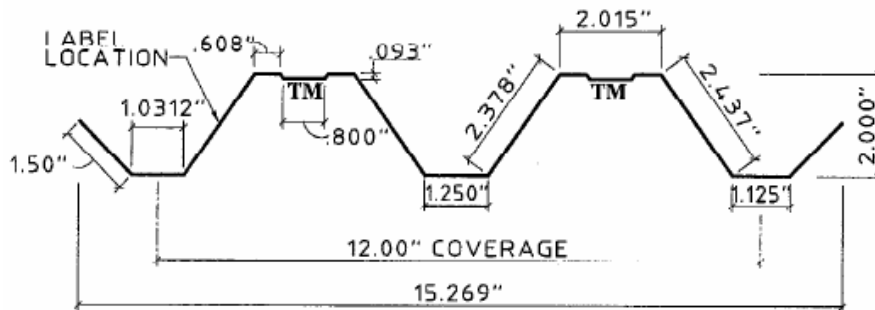


Figure A.2 Storm Shutter Cross Section #2. Aluminum 3004-H34 or 5052-H32, Thickness of 0.063".

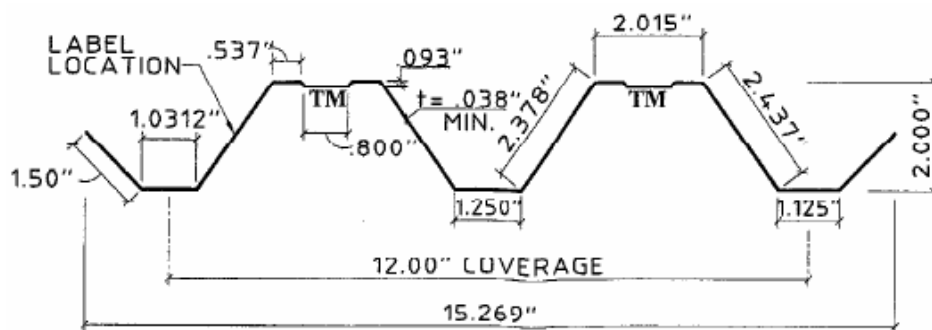


Figure A.3 Storm Shutter Cross Section #3. Galvanized Steel, ASTM A446, Grade 40, Thickness of 0.038”.

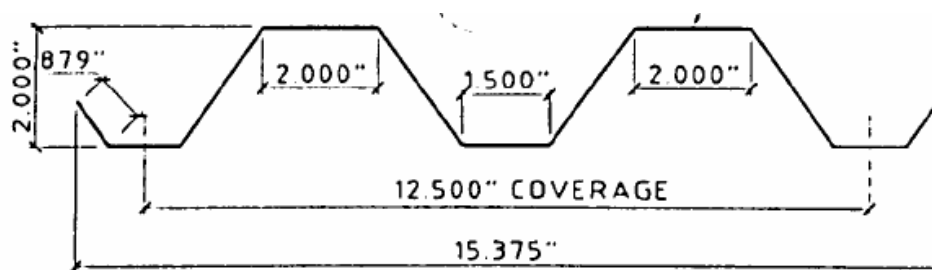


Figure A.4 Storm Shutter Cross Section #4. Aluminum 5052-H32, Thickness of 0.050”.

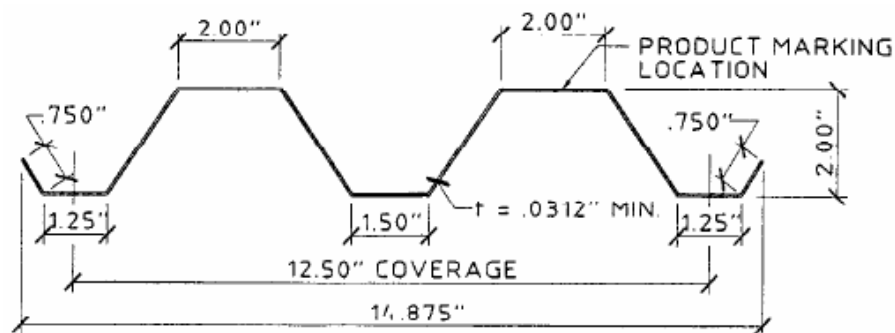


Figure A.5 Storm Shutter Cross Section #5. Galvanized Steel, ASTM A653, Grade 80, Thickness of 0.0312”.

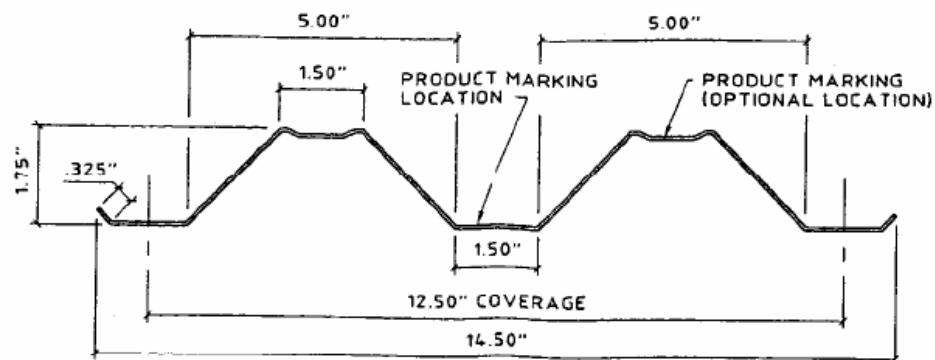


Figure A.6 Storm Shutter Cross Section #6. Aluminum 3004-H34, Thickness of 0.060".

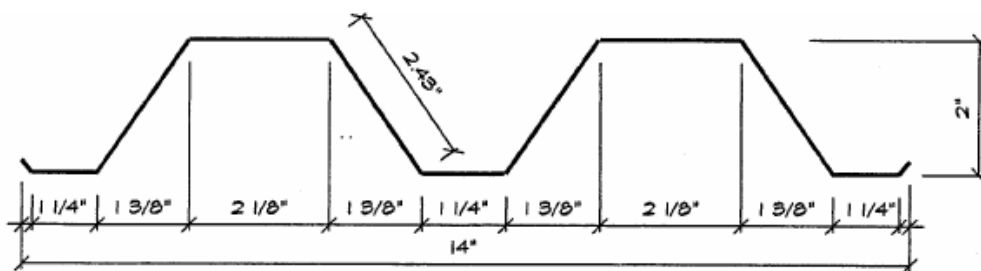


Figure A.7 Storm Shutter Cross Section #7. Aluminum 5052-H32, Thickness of 0.063".

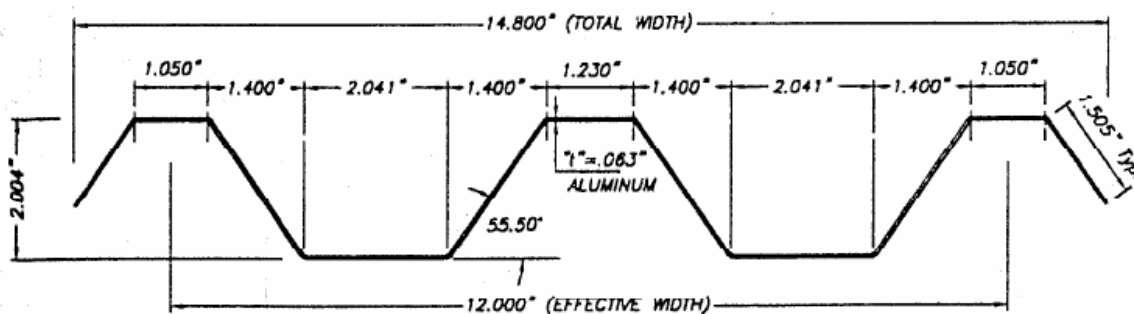


Figure A.8 Storm Shutter Cross Section #8. Aluminum 5052-H32, Thickness of 0.063".

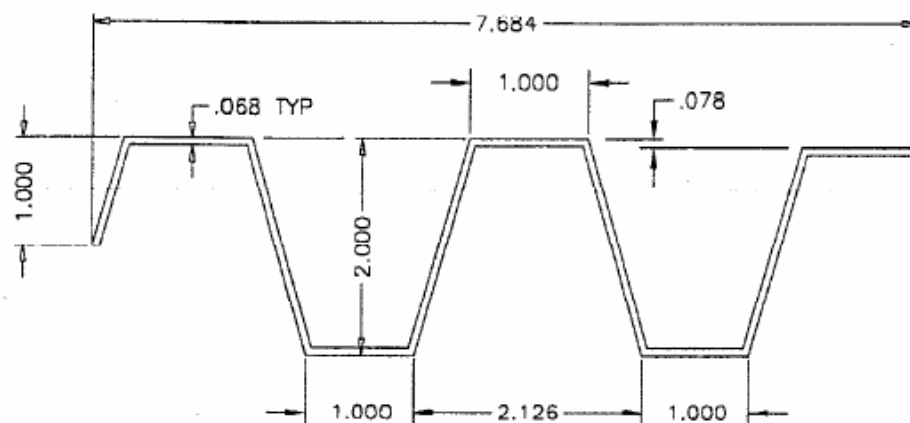


Figure A.9 Storm Shutter Cross Section #9. Aluminum 6063-T6, Thickness of 0.068”.

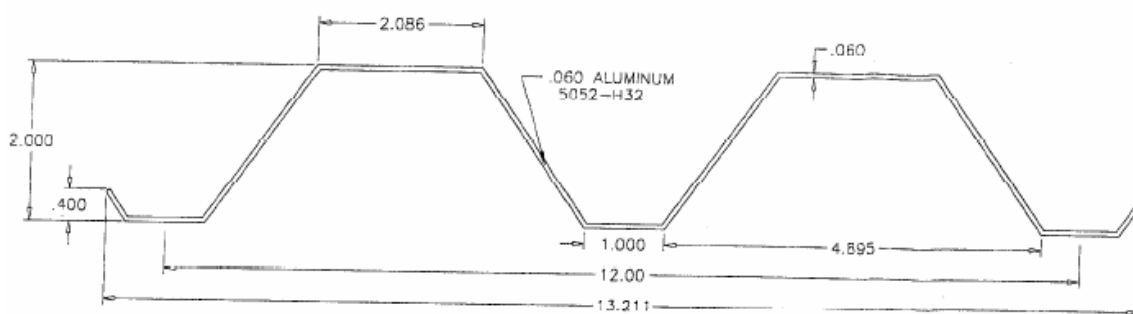


Figure A.10 Storm Shutter Cross Section #10. Aluminum 3004-H34 or 5052-H32, Thickness of 0.060”.

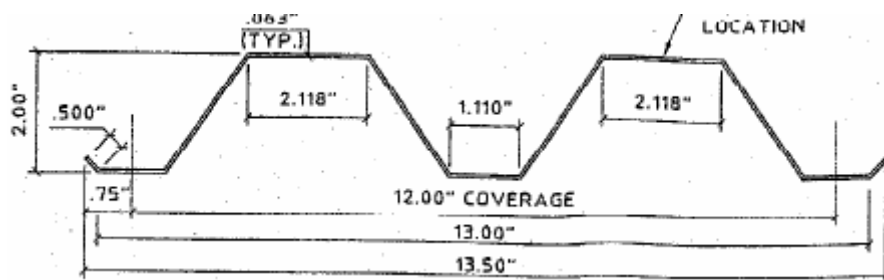


Figure A.11 Storm Shutter Cross Section #11. Aluminum 5052-H32, Thickness of 0.063”.

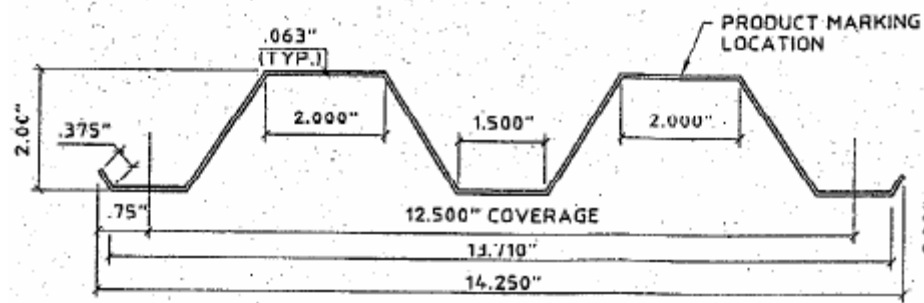


Figure A.12 Storm Shutter Cross Section #12. Aluminum 5052-H32, Thickness of 0.063”.

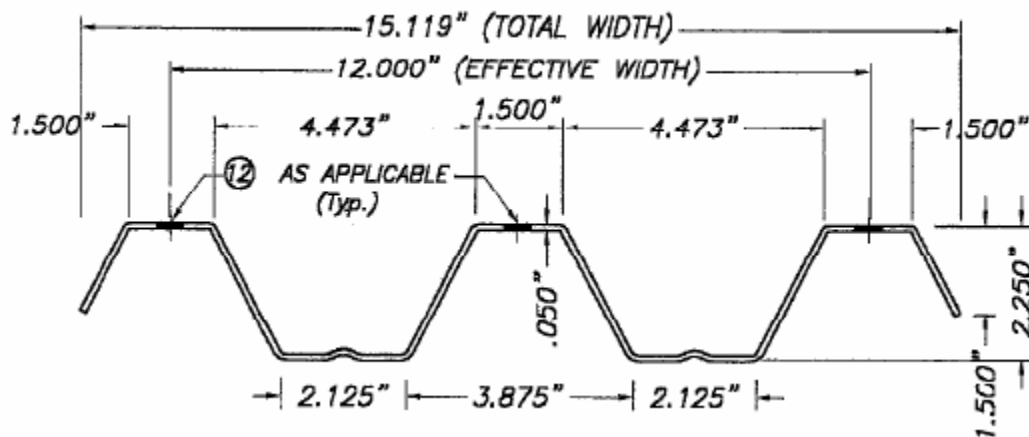


Figure A.13 Storm Shutter Cross Section #10. Aluminum 3004-H34 or 5052-H32, Thickness of 0.050”.

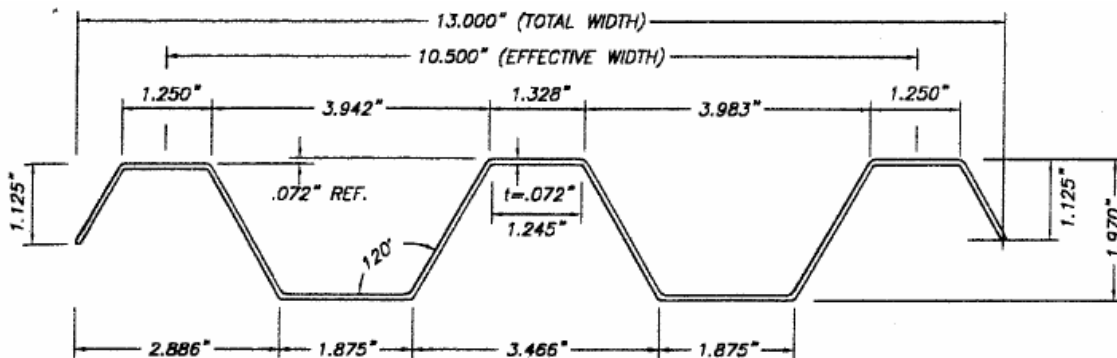


Figure A.14 Storm Shutter Cross Section #14. Aluminum 6063-T6, Thickness of 0.072”.

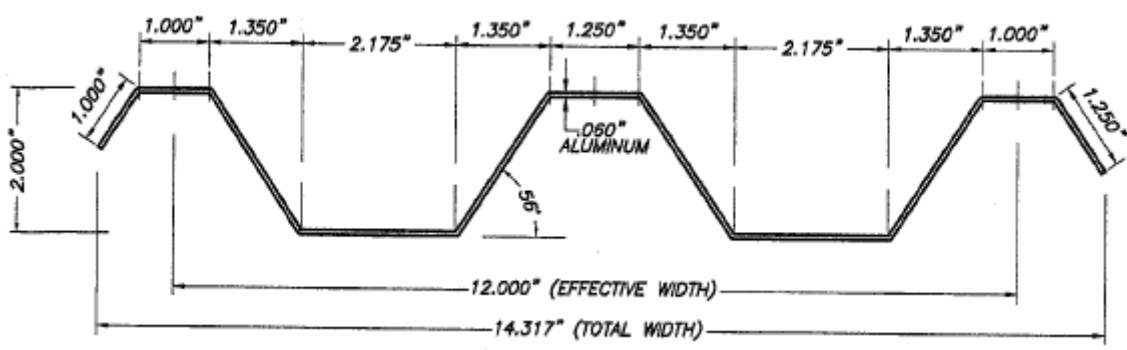


Figure A.15 Storm Shutter Cross Section #15. Aluminum 5052-H32, Thickness of 0.060".

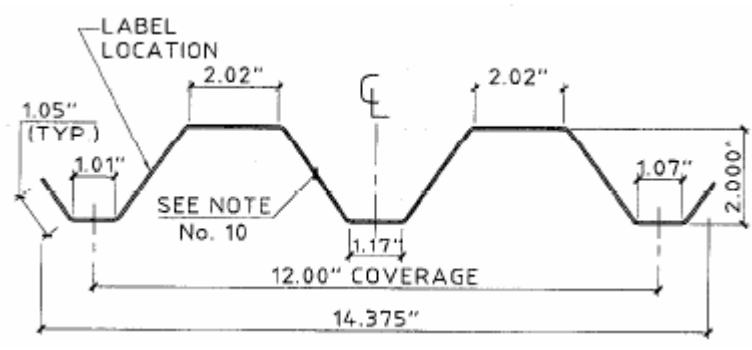


Figure A.16 Storm Shutter Cross Section #16. Aluminum 3004-H34 or 5052-H32, Thickness of 0.0615".

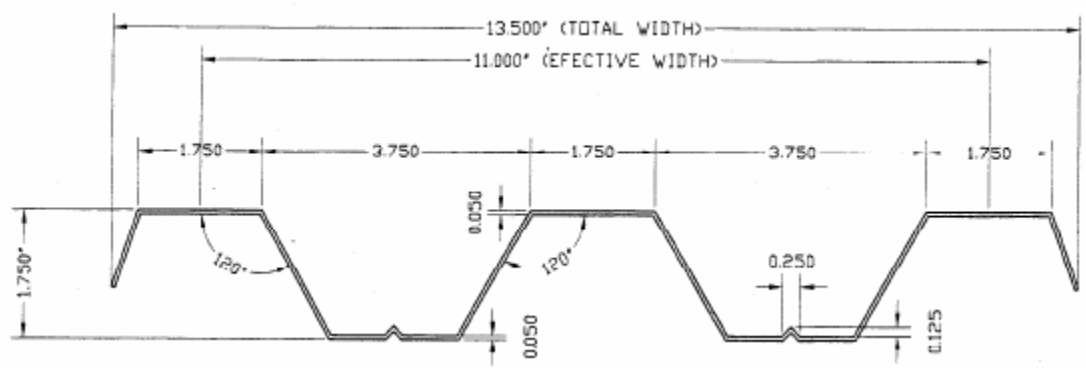


Figure A.17 Storm Shutter Cross Section #17. Aluminum 5052-H32, Thickness of 0.050”.

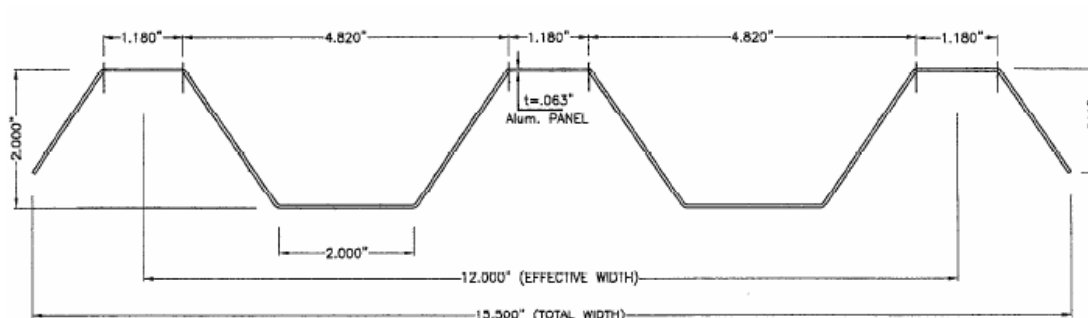


Figure A.18 Storm Shutter Cross Section #18. Aluminum 5052-H32, Thickness of 0.063”.

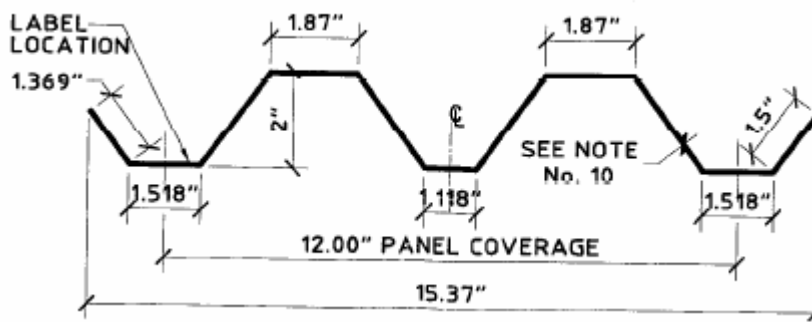


Figure A.19 Storm Shutter Cross Section #19. Aluminum 3004-H34 or 5052-H32, Thickness of 0.063”.

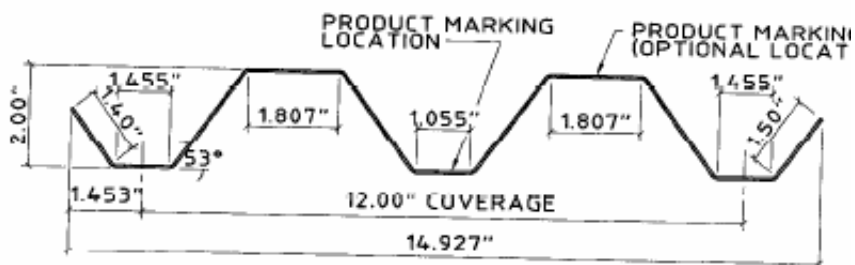


Figure A.20 Storm Shutter Cross Section #20. Aluminum 3004-H34 or 5052-H32, Thickness of 0.063".

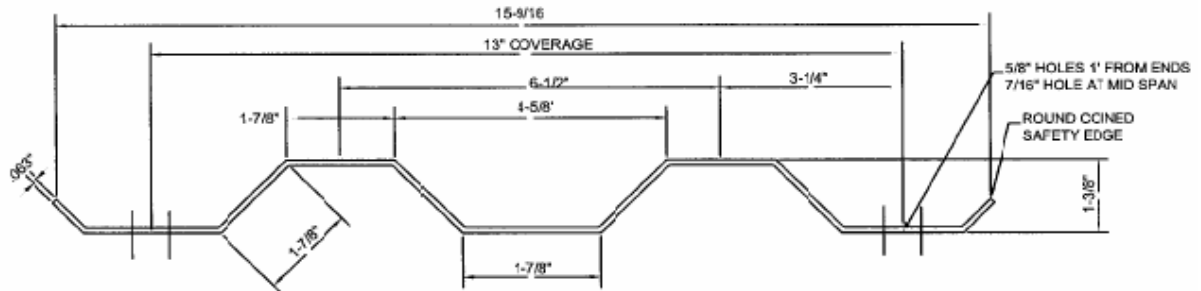


Figure A.21 Storm Shutter Cross Section #21. Aluminum 3004-H34 or 5052-H32, Thickness of 0.063".

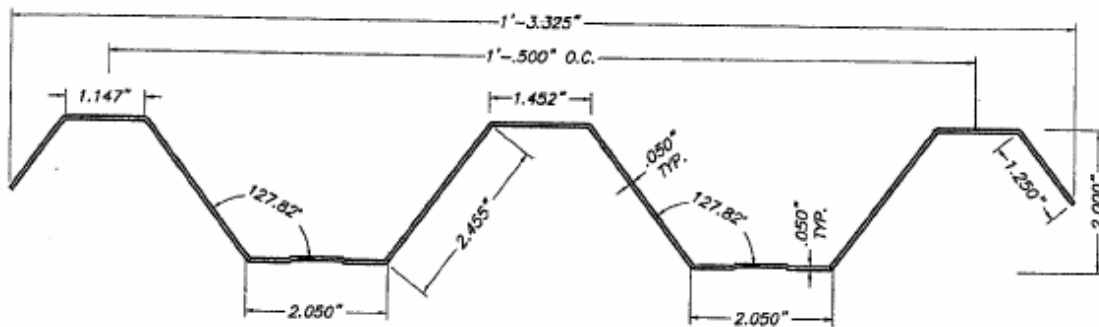


Figure A.22 Storm Shutter Cross Section #22. Aluminum 3004-H34, Thickness of 0.050".

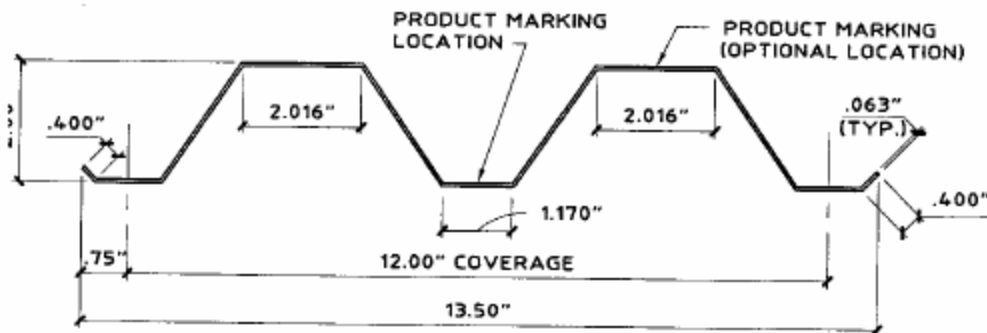


Figure A.23 Storm Shutter Cross Section #23. Aluminum 5052-H32, Thickness of 0.063".

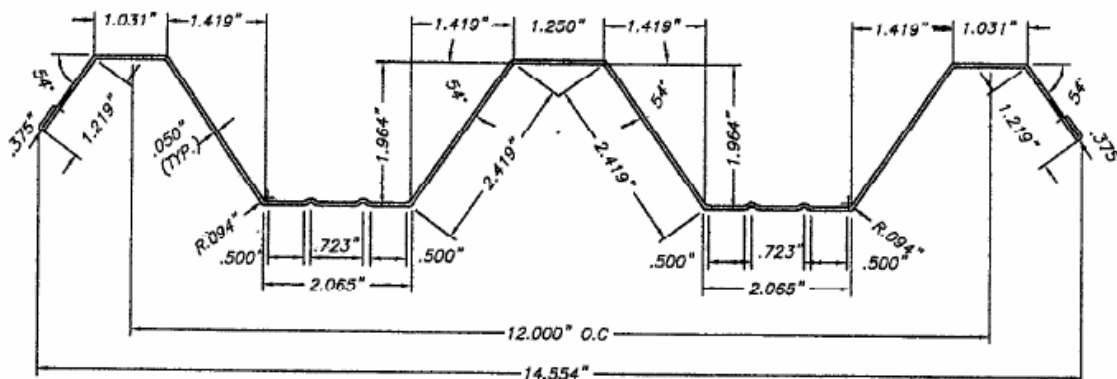


Figure A.24 Storm Shutter Cross Section #24. Aluminum 5052-H32, Thickness of 0.063".

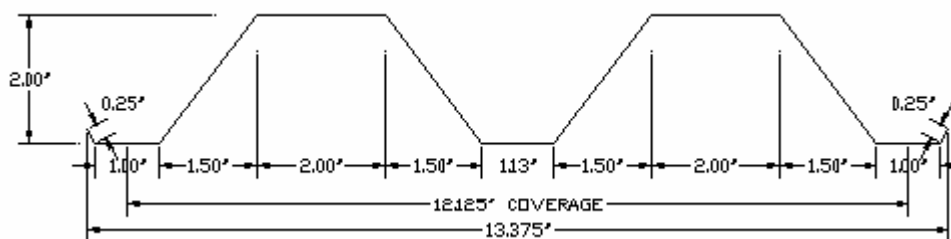


Figure A.25 Storm Shutter Cross Section #25 (Local Supplier #1). Aluminum 3034-H34, Thickness of 0.063".

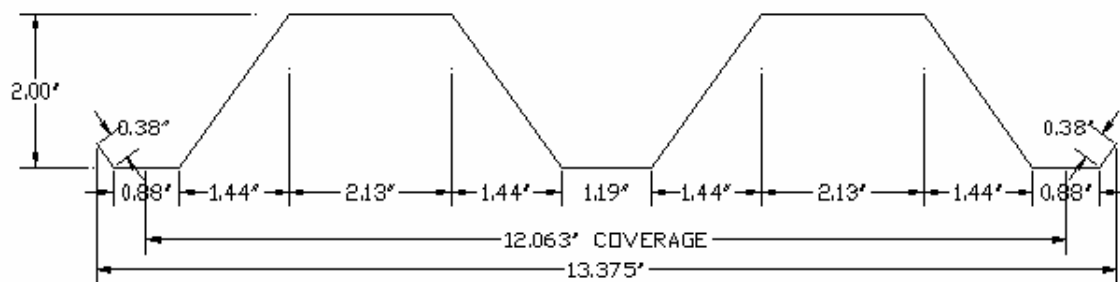


Figure A.26 Storm Shutter Cross Section #26 (Local Supplier #2). Aluminum 3034-H34, Thickness of 0.063".

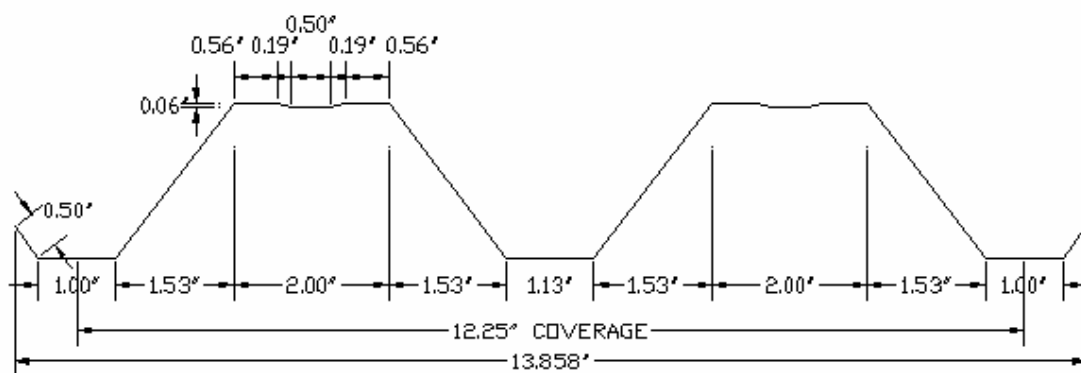


Figure A.27 Storm Shutter Cross Section #27 (Local Supplier #3). Aluminum 3034-H34, Thickness of 0.063".